National Library
of Canada

Bibliothèque nationale
du Canada

Canadian Theses Service

Service des thèses canadiennes

Ottawa, Canada
K1A 0N4

NOTICE

The quality of this microform is heavily dependent upon the quality of the original thesis submitted for microfilming. Every effort has been made to ensure the highest quality of reproduction possible.

If pages are missing, contact the university which granted the degree.

Some pages may have indistinct print especially if the original pages were typed with a poor typewriter ribbon or if the university sent us an inferior photocopy.

Reproduction in full or in part of this microform is governed by the Canadian Copyright Act, R.S.C. 1970, c. C-30, and subsequent amendments.

AVIS

La qualité de cette microforme dépend grandement de la qualité de la thèse soumise au microfilmage. Nous avons tout fait pour assurer une qualité supérieure de reproduction.

S'il manque des pages, veuillez communiquer avec l'université qui a conféré le grade.

La qualité d'impression de certaines pages peut laisser à désirer, surtout si les pages originales ont été dactylographiées à l'aide d'un ruban usé ou si l'université nous a fait parvenir une photocopie de qualité inférieure.

La reproduction, même partielle, de cette microforme est soumise à la Loi canadienne sur le droit d'auteur, SRC 1970, c. C-30, et ses amendements subséquents.

NL-339 (r. 88/04) c

Canada

UNIVERSITY OF ALBERTA

A DISTRIBUTED NUMERICAL MODEL FOR WATERSHED HYDROLOGY

by

Md. Abdus SABUR ©

A THESIS
SUBMITTED TO THE FACULTY OF GRADUATE STUDIES AND RESEARCH
IN PARTIAL FULFILLMENT OF THE REQUIREMENTS FOR THE DEGREE
OF
DOCTOR OF PHILOSOPHY

DEPARTMENT OF CIVIL ENGINEERING

EDMONTON, ALBERTA

FALL 1990

National Library
of Canada

Bibliothèque nationale
du Canada

Canadian Theses Service

Service des thèses canadiennes

Ottawa, Canada
K1A 0N4

The author has granted an irrevocable non-exclusive licence allowing the National Library of Canada to reproduce, loan, distribute or sell copies of his/her thesis by any means and in any form or format, making this thesis available to interested persons.

The author retains ownership of the copyright in his/her thesis. Neither the thesis nor substantial extracts from it may be printed or otherwise reproduced without his/her permission.

L'auteur a accordé une licence irrévocable et non exclusive permettant à la Bibliothèque nationale du Canada de reproduire, prêter, distribuer ou vendre des copies de sa thèse de quelque manière et sous quelque forme que ce soit pour mettre des exemplaires de cette thèse à la disposition des personnes intéressées.

L'auteur conserve la propriété du droit d'auteur qui protège sa thèse. Ni la thèse ni des extraits substantiels de celle-ci ne doivent être imprimés ou autrement reproduits sans son autorisation.

ISBN 0-315-65014-1

UNIVERSITY OF ALBERTA

RELEASE FORM

NAME OF AUTHOR Md. Abdus SABUR

TITLE OF THESIS A DISTRIBUTED NUMERICAL MODEL FOR WATERSHED HYDROLOGY

DEGREE FOR WHICH THESIS WAS PRESENTED DOCTOR OF PHILOSOPHY

YEAR THIS DEGREE GRANTED FALL 1990

Permission is hereby granted to THE UNIVERSITY OF ALBERTA LIBRARY to reproduce single copies of this thesis and to lend or sell such copies for private, scholarly or scientific research purposes only.

The author reserves other publication rights, and neither the thesis nor extensive extracts from it may be printed or otherwise reproduced without the author's written permission.

(Signed) Md. Abdus Sabur

PERMANENT ADDRESS:
Village: Pakhimara
Post Office: Tarakandi
District: Jamalpur
BANGLADESH

DATED .May. .24,... ... 1990

THE UNIVERSITY OF ALBERTA

FACULTY OF GRADUATE STUDIES AND RESEARCH

The undersigned certify that they have read, and recommend to the Faculty of Graduate Studies and Research, for acceptance, a thesis entitled "A DISTRIBUTED NUMERICAL MODEL FOR WATERSHED HYDROLOGY" submitted by Md. Abdus SABUR in partial fulfilment of the requirements for the degree of DOCTOR OF PHILOSOPHY.

Jac-P. Verschuren

Supervisor

D. W. Murray — D W Murray

P. M. Steffler

D. S. Chanasyk — DS Chanasyk

Stephen J. Burges
External Examiner

DATE ...May 24......... 1990

ABSTRACT

Hydrologic modeling allows the prediction of the impact of changes within the watershed (e.g. in meteorological, morphological, geological or pedological conditions) on soil moisture and streamflow, or the development of practical watershed management prescriptions for improved water resources utilization in a specified river basin.

Although numerous models exist, few are capable of handling the distributed nature of changes and their impacts. Furthermore, existing models cannot be rigorously applied to watersheds of low relief in which surface slopes are small and sometimes interrupted by extensive local depressions. Infiltration and evapotranspiration are the dominant hydrological processes in such watersheds and in most existing models, these processes are given cursory treatment.

The objective of this treatise is to develop and asses a hydrological model from the physical perspective. The model is a distributed type so that wide variation in conditions within the watershed can be simulated.

To apply the model the watershed is considered in segments, these segments being sub-basins bounded at the top by a water divide, at the base by a stream and at the sides by lines drawn normal to the contours. The required inputs for each segment are precipitation and other meteorological data necessary to calculate potential evapotranspiration, the

nature and extent of vegetation, and soil hydraulic properties.

The partial differential equation for vertical, single-phase, unsaturated flow of water in soils is used as the mathematical model governing infiltration, groundwater recharge and evapotranspiration. The kinematic and diffusion wave approximations to the equation of unsteady surface flow are used for modeling the overland flow and the flow in the channel network. The Dupuit-Forchheimer equation is used to model the saturated flow. The control volume formulation is used to obtain the solution of these equations for realistic initial and boundary conditions. The solution of the unsaturated flow, the overland flow, and the groundwater flow equations are coupled with channel flow equation to form a runoff model for the watershed. Since computer cost is a limiting factor in numerical modeling, Fourier analysis has been used to minimize computational time. The model is tested by comparison with data from the Spring Creek experimental watershed in Alberta, Canada.

ACKNOWLEDGEMENTS

The author wishes to express his appreciation to his supervisors Professor Jac P. Verschuren and Dr. Peter M. Steffler for their suggestions and guidance provided throughout the course of the work.

The author will remain indebted to Professor N. Rajaratnam, Professor A. W. Peterson and Professor R. Gerard for their support and encouragement. The constructive criticisms and suggestions for improvement extended by the examination committee are highly valued.

Sincere appreciation is expressed to Mr. M. Jasek and Mr. S. Lovell for their assistance in collecting and processing soil samples from the Spring Creek watershed. A special thank you is extended to Professor D. S. Chanasyk for his helpful advice concerning different aspects of soils and for letting the author use his soil physics laboratory. The assistance and help of Ms. Kelly Ostermann of the soil physics laboratory (U of A) is gratefully acknowledged.

Finally the author is obliged to the staff of the Hydrology and Water Survey branches of Alberta Environment for providing precipitation and discharge data and other necessary information on the Spring Creek watershed.

TABLE OF CONTENTS

Chapter Page

1 Watershed Models 1

- 1.1 Introduction 2
- 1.2 The Concepts of the Conceptual Models 6
- 1.3 Modeling Approaches 12
  - 1.3.1 Lumped catchment models 12
  - 1.3.2 Distributed catchment models 19
- 1.4 On the Present Approach 23
  - 1.4.1 Outline of the model 24
- 1.5 On the Solution Methods 29

2 Unsaturated Flow Model 41

- 2.1 Soil and Moisture 42
- 2.2 Infiltration 45
  - 2.2.1 Mathematical models of infiltration 46
  - 2.2.2 Moisture flow equations 50
  - 2.2.3 Boundary conditions 53
  - 2.2.4 Hydraulic properties of the soil 55
  - 2.2.5 Solution of flow equation 62
  - 2.2.6 Finite difference formulation 65
  - 2.2.7 Some applications of the F-D solutions 78
- 2.3 Evaporation 87
  - 2.3.1 Meteorological conditions 90

2.3.2 Transport mechanism 91
2.3.3 Combination equation 98
2.3.4 Actual evaporation (AE) 103
2.3.5 Models for AE 111
2.3.6 Present approach 113

3 Saturated Flow Model 118
3.1. Groundwater 119
3.2 Flow Equations 120
3.2.1 Boundary conditions 125
3.2.2 Solution methods 126
3.2.3 Numerical formulation 130
3.3 Solution of Example Problem 135

4 Overland Flow Model 139
4.1 Overland Flow 140
4.2 Flow Equation 141
4.2.1 Boundary conditions 143
4.2.2 Solution techniques 144
4.3 Numerical Formulation of K-W Equation 144
4.4 Solution of Example Problem 148

5 Channel Network Flow Model 150
5.1 Channel Routing 151
5.2 Flow Equations 151
5.2.1 Diffusion wave equation 154
5.3 Boundary Conditions 156

5.3.1 Compatibility at internal junctions 156
5.3.2 At the external junctions 160
5.4 Initial Conditions 160
5.5 Solution of the Channel Flow Equations 161
5.5.1 Numerical formulation 162
5.5.2 Coefficient matrix 170
5.5.3 Evaluation of partial derivatives 173
5.6 Solution of Example Problems 174

6 Analysis of the Numerical Techniques 186
6.1 On the Accuracy of the Solution 187
6.2 Consistency 187
6.3 Stability 188
6.4 Convergence 195
6.4.1 Amplification ratio 196
6.4.2 Space time discretization 212
6.5 Mass Conservation 233

7 Application to the Spring Creek Watershed 236
7.1 Introduction 237
7.2 The Spring Creek Basin 237
7.3 Measurements Of the Model Parameters 241
7.3.1 Soil properties 241
7.3.2 Channel and overland flow parameters 259
7.3.3 Other parameters 260
7.4 Application of the Unsaturated Flow Model 262
7.5 Simulation of Discharge Hydrograph 269

7.5.1 Spatial variability of the inputs 269
7.5.2 Discretization of the watershed 272
7.5.3 Assembling the model 273
7.6 Application of the Model to a Sub-basin 282
7.7 Extension of the Model to the Entire Basin 299

8 Finale 312
8.1 Conclusions 313

REFERENCES — 315

LIST OF TABLES

Table Page

1-1 Factors affecting watershed response 4

2-1 Water holding capacity of different soils 43

2-2 Review of numerical solutions of unsaturated flow problems 64

2-3 Computational informations 80

2-4 Computational time requirements 84

5-1 Order of magnitude of terms in St. Venant equation 155

5-2 Channel characteristics of example network-1 180

5-3 Channel characteristics of example network-2 180

7-1 Model parameters 242

7-2 Classification of the soils of Spring Creek 249

7-3 Comparison of hydraulic properties 257

7-4 Soil parameters of the Spring Creek watershed 258

7-5 Approximate channel characteristics 259

7-6 Approximate values of available water capacity and drainable porosity 260

7-7 Meteorological elements used to define the upper boundary conditions 265

LIST OF FIGURES

Figure		Page
1-1	Hydrological processes modeled in this study	26
1-2	F-D grid for eqn.[1-1] with distance x and time t	36
1-3	Forward and backward characteristic directions of channel flow equations in the solution domain x, t	36
2-1	Relation between permanent wilting percentage, field capacity, etc.	44
2-2	Soil moisture characteristic (Spring Creek)	57
2-3	F-D grid in the z-t plane showing location of grid points and counter, n, j	67
2-4	Comparison of solutions	81
2-5	Comparison of numerical solution with experimental data	83
2-6	Infiltration into Yolo light clay	85
2-7	Cumulative infiltration into Yolo light clay	85
2-8	Potential distribution after 34 days of infiltration	86
2-9	The relationship of the ratio PE/AE	110
2-10	Schematized soil-plant-atmosphere continuum	115
3-1	Similarity between drainage ditch and stream channel	121
3-2	Schematized saturated flow domain	128

3-3 Falling water table 128

3-4 Discretization of flow domain 131

3-5 Computed water table location and discharge 138

4-1 Space-time-grid system for F-D approximations using the box method 145

4-2 Comparison of simulated and observed overland flow 149

5-1 Definition sketch of a channel element 153

5-2 Channel network of Spring Creek watershed 157

5-3 Definition sketch of control volume 163

5-4 Discretization of channel network 164

5-5 Space-time-grid system for F-D approximation 166

5-6 Storage junction-11 168

5-7 The arrays of the coefficient matrix 172

5-8 Example network-1 (Yen and Akan, 1976) 177

5-9 Example network-2 (Joliffe, 1984) 178

5-10a Computed discharge at the end of branch-1 181

5-10b Discharge at the end of branch-3 182

5-10c Computed depth at junction-3 183

5-11a Computed depth at junctions 1 and 8 184

5-11b Input to the network-2 185

6-1a Amplification ratio with $C_r = 1.0$ and $\omega = 0.5$ 199

6-1b Celerity ratio with $C_r = 1.0$ and $\omega = 0.5$ 200

6-2a Amplification ratio with $C_r = 5.0$ and $\omega = 0.5$ 201

6-2b Celerity ratio with $C_r = 5.0$ and $\omega = 0.5$ 202

6-3a Amplification ratio with $C_r = 1.0$ and $\omega = 0.6$ 203
6-3b Celerity ratio with $C_r = 1.0$ and $\omega = 0.6$ 204
6-4a Amplification ratio with $C_r = 5.0$ and $\omega = 0.6$ 205
6-4b Celerity ratio with $C_r = 5.0$ and $\omega = 0.6$ 206
6-5a Amplification ratio with $C_r = 1.0$ and $\omega = 1.0$ 207
6-5b Celerity ratio with $C_r = 1.0$ and $\omega = 1.0$ 208
6-6a Amplification ratio with $C_r = 5.0$ and $\omega = 1.0$ 209
6-6b Celerity ratio with $C_r = 5.0$ and $\omega = 1.0$ 210
6-7a Amplification ratio for the box method 213
6-1b Celerity ratio for the box method 214
6-8 Wave forms in soil moisture profiles 217
6-9 A linear system 217
6-10 Overland flow response to a unit pulse 220
6-11 Mass balance error of the overland flow computation 221
6-12 Energy spectrum of the overland flow 222
6-13 Channel response to a pulse input 223
6-14 Energy spectrum of channel response 224
6-15 Hydraulic properties of soil-C of Spring Creek 226
6-16 Evaluation of derivatives for unsaturated flow case 228
6-17 Effect of discretization on discharge 231

6-18 Effect of discretization on mass balance 232

7-1 Location map of the Spring Creek watershed 238

7-2 Spring Creek watershed: land systems 240

7-3 Moisture characteristic curves of the sampled soils 244

7-4a Variation of soil characteristics with depth 245

7-4b Spatial variation of soil characteristics 246

7-5 Particle size distribution 248

7-6 Hydraulic conductivities: comparison of measured and calculated values 251

7-7 Determination of Brooks-Corey parameters 253

7-8 Determination of saturation and residual moisture content 254

7-9 The Brooks-Corey curves of Spring Creek soils 256

7-10a Simulated and observed soil moisture content 267

7-10b Simulated runoff, evapotranspiration and infiltration 268

7-11 Distance vs correlation coefficients of the potential evaporation estimates 271

7-12 Discretization of the watershed 274

7-13 Model representation of the profile of sloping surface divided into columns 275

7-14 Coupling element to the channel 279

7-15 Synchronization of the model segments 281

7-16 The Horse Creek sub-basin 283

7-17a Water table movement 285

7-17b Actual nonuniform distribution of

groundwater recharge 286
7-17c Assumed uniform distribution of groundwater recharge 286
7-18 Contaminated solution of outflow hydrograph 289
7-19 Effect of discretization 290
7-20 Groundwater outflow from element-5 292
7-21 Fluctuation of water table 293
7-22 Groundwater outflow from Horse Creek 294
7-23 Horse Creek rating curve 296
7-24 Simulated and recorded hydrograph of Horse Creek 297
7-25 Effect of runoff volume 298
7-26 Wolverine Creek rating curve 300
7-27 Rocky Creek rating curve 301
7-28 Bridlebit Creek rating curve 301
7-29 Spring Creek-upper rating curve 302
7-30 Spring Creek rating curve 302
7-31 Simulated and recorded hydrograph of Wolverine Creek 306
7-32 Simulated and recorded hydrograph of Rocky Creek 307
7-33 Simulated and recorded hydrograph of Bridlebit Creek 308
7-34 Simulated and recorded hydrograph of Spring Creek-upper 309
7-35 Simulated and recorded hydrograph of Spring Creek watershed 310

LIST OF PLATES

Plate		Page
2-1	Typical vegetation of Spring Creek watershed	106
7-1	Typical vegetation of the channel system of Spring Creek watershed	261
7-2	Outlet control structure of Bridlebit Creek	303
7-3	Outlet control structure of Spring Creek-upper	303

Chapter 1

Watershed Models

1.1 Introduction

The science of hydrology consists of many components and the physical scale of hydrologic cycle is very large, e.g. water evaporated near the equator may be moved by winds to become precipitation in the temperate zones. However, the scale of hydrological processes in a narrow sense is much smaller. Usually it is possible to isolate on the surface of the earth an area in which the precipitation having contributed to evaporation and storage is eventually returned to the sea through a single channel. That area represents a catchment or watershed or basin within which water is conserved, permitting the balance between incoming and outgoing fluxes.

In a catchment it is possible to distinguish several processes such as (1) the processes of evaporation, transpiration, infiltration and percolation; (2) subsurface flow processes which includes groundwater and unsaturated flows; (3) and the processes of surface runoff including open channel flows. These processes are in turn dependent on the following watershed characteristics such as physiography, vegetation, soils, geology, topography etc.

Physiography: The physical features of the watershed on which precipitation falls influence the rainfall-runoff relationship. Chow (1959) has tabulated these factors. The effects of the factors whose relationships are more or less obvious are shown in the Table 1-1, however, those which are more complex are discussed in the text.

Vegetation: Vegetative cover exerts its influence on runoff and water yields through its infiltration capacity, water storage and detention, and evapotranspiration and interception. In addition to its effects on the soil surface, dense vegetation extracts water from the lower soil layers at a much higher rate than sparse vegetation. Thus a much greater water deficit in the subsoils allows greater infiltration capacity.

Soils: Soils play a significant role in the rainfall-runoff relationship. Vegetative cover, evapotranspiration, soil water storage capacity, and infiltration rate are intimately related to soil properties. Sandy or gravelly soils may have enormous infiltration capacities but low storage capacities, and finer textured soils may have low infiltration capacities with greater storage for comparable soil depths. Coarse-textured soils may have low surface runoff and high groundwater recharge rates. Fine-textured soils tend to yield high surface runoff and low groundwater recharge under similar conditions.

Geology: The geology of a watershed affects soils, topography, land aspects and slopes, vegetation, permeability, and the presence or absence of groundwater aquifers. These factors in turn affect the water yields and the relation of precipitation to them.

Topography: The topography of watersheds affects the efficiency of the channel systems as conveyors of water from the watershed. Topography also affects overland flow velocity, and the amount of depression storage. In cases of flat catchments, detention time and storage is greater than those of steep slope watersheds.

Channel: Channel size, shape, roughness, slope, and densities affect the rainfall-runoff relationship. Any factor in the channel which tend to slow the movement of water acts as storage component and increases the duration of runoff. Any factor in the channel which accelerates the velocity of flow in turn decreases the duration of runoff period. Thus, channels as conveyance systems greatly influence the runoff and water yield from a watershed.

Table 1-1. Factors affecting watershed response (adapted after Chow, 1959).

Factor	Kind of relationship
Size of catchment	Direct
Shape	Affect lag time, time to peak
Slope	Direct proportion to peak yield
Drainage density	Inverse relation
Storage capacity	Duration proportional to storage

It is necessary to (1) manage natural waters as resources for social welfare, environmental protection and economic development and (2) control floods for protection of life, man-made structures, and property. To meet these needs a quantitative relationship between incoming water such as precipitation and catchment water yield such as streamflow is essential. This relationship is important not only to predict when and how much water will be available to cope with, but also to predict the effect of the inevitable interference (due to those activities e.g. construction of different water management structures) with the aforementioned factors which through complicated interactions among themselves determine this quantity and timing of occurrence.

The problem of quantifying river flow from evaporation, rainfall and other factors, mentioned above, occupies a central place in the technology of applied hydrology. Most studies of representative and experimental basins and a large part of the effort of classical hydrology have been directed towards obtaining at least a partial solution of this problem.

Despite the attention which this problem has attracted over many years, the present position is far from satisfactory (Nash, 1983). Many different models of runoff processes are being developed. No single approach has been proved satisfactory in applications to both gauged and ungauged catchments and not all new models represent improvement on previous ones. This a direct reflection of both complexity of the class of system under study and nature of modeling process.

Because of the complexity of the hydrologic processes, hydrologic models developed so far have used more-or-less coarse idealization of hydrologic system. The general categories of approach that have been employed to formulate input-output relations in hydrology are (1) system synthesis, and (2) system analysis.

In system synthesis, a conceptual knowledge of the various physical processes involved in the system is presupposed. Each component process is governed by particular laws, and is linked to the others to form a model of the total system. Such a model is called a conceptual model. Conceptual models may recognize explicitly the points at which system specification is imprecise.

In system analysis, the function or functions describing the overall system operation are determined from concurrent input and output sequence alone, without explicit use or knowledge of the physical laws involved. As a result of such simplification in the design of this type of model, it is expected that the operation of the model will not be error free. In addition such models are not unique, and a great many equivalent formulations are possible.

In the following sections, conceptual models of catchment response are reviewed with special attention to the problems of catchments with limited hydrological data available that will help choose the methodology in this study.

1.2 The Concepts of the Conceptual Models

O'Connell (1988) provided a general review of the rainfall-runoff modeling approaches. An account of distributed modeling of watershed hydrology is given by

Chanasyk (1980). Here, to begin with, the model of Horton (1933, 1939) is considered. Horton (1933, 1939) proposed the concept now known as rainfall excess or effective rainfall to represent rainfall exceeding the infiltration capacity (defined in section 2.2) of the soil and remaining on the surface. After filling the depression storage, additional rainfall excess would travel downslope as overland flow. Infiltrated water was thought to have no immediate contribution to storm discharge in the stream. All the infiltrated water would pass into groundwater and was the sole source of the baseflow part of the hydrograph (Chorley, 1978). If soil conditions were taken as nearly homogeneous over the basin and that, as a first approximation, additional amounts of rainfall excess would contribute linearly to the amount of storm runoff. This model still underlies a great deal of hydrologic methodology although its validity appears to be limited to areas of very low infiltration capacities or very high rainfall intensities (Kirkby and Chorley, 1967).

There is evidence that the response to increasing amount of rainfall excess exhibits nonlinearity at some or all flow stages (Amorocho, 1967b; Pilgrim, 1966; Hewlett et al., 1977; Hewlett, 1982). Hewlett (1961) proposed that this is partly a result of variable soil moisture conditions occurring over the catchment prior to the onset of rainfall. In particular, downslope drainage of soil moisture would lead to generally higher soil moisture content close to the channels. Since infiltration rates tend to decrease with increasing moisture content, overland flow would be expected to occur first close to the channel (Calver et al., 1972). The area contributing overland flow would generally comprise only part of the catchment, and even on a homogeneous soil, would expand and contract depending on rainfall intensity and duration. This variable 'partial contributing area' (Betson, 1964) or 'dynamic watershed concept' (Tennessee Valley Authority, 1965; East China College of Hydraulic Engineering, 1977) was held to account for some at least of the observed nonlinearities in storm runoff production.

Hortonian 'infiltration excess' overland flow does not always occur (Chorley, 1978; Burt, 1989). Even allowing for the effects of swelling of the soil, the packing of the surface by raindrops, the effects of entrapped air and the dislocation of fine particles (Horton, 1933), infiltration capacities of soils, particularly in vegetated humid temperate areas, are often high in comparison with the highest observed rainfall intensities (Kirkby, 1969; Freeze, 1972b). Two interrelated concepts were proposed to account for the production of storm discharge under such conditions; 'saturation excess' overland flow (Kirkby and Chorley, 1967) and 'throughflow' within the soil mass corresponding to the 'subsurface stormflow' of Hursh (1944) and 'interflow' as defined by Hewlett and Hibbert (1967) and 'piston flow' of Anderson and Burt (1982).

When the soil profile becomes completely saturated, saturation excess overland flow will occur (Zaslavsky and

Sinai, 1981; Burt, 1986). Then additional water will be forced to remain on the surface. This saturation may be due to the local 'water table' rising to the surface (Dunne and Black, 1970a; Carson and Sutton, 1971) or to vertical drainage in the soil being limited by a horizon of lower permeability (Weyman, 1971; Wilson and Ligon, 1973; O'Loughlin, 1981, 1986). Saturation may be maintained both by downslope flow of water through the soil and by rainfall or ponded water at the ground surface. It has been shown that the zone of saturation grows in both vertical and upslope extent during a storm (Weyman, 1971; Bernier, 1982). The incidence of surface saturation will be increased by convergent flow conditions in the soil produced by contour cavities and decreasing soil depth in the direction of flow (Dunne and Black, 1970a; Dunne, 1978). Areas of overland flow produced in this way may be limited in extent and need not be directly connected to the stream channel network (Amerman, 1965; Kirkby and Weyman, 1974; Mosley, 1979). However, it appears that this process occurs commonly in the concavities associated with channel heads, such that the effective length of channel may vary considerably during a storm (Weyman, 1971). Saturation excess overland flow may occur at much lower rainfall intensities than might be expected under the Horton model and has been observed after rainfall has ceased.

Usually two forms of throughflow are considered: movement through structural voids or macropores in the soil (Coles and Trudgill, 1985; Germann, 1986) and laminar capillary flow which may be approximated by Darcy's law (Eagleson, 1970). Flow through macropores may be turbulent with velocities of the same order of magnitude as overland flow may consequently be an important mechanism in storm runoff prediction (Beven and Germann, 1982). Ragan (1967) has demonstrated that significant amounts of hillslope storm discharge may derive from flow through the litter layer, while others have raised the possibility of major contributions from water-conducting natural pipes in the soil (Jones, 1971; Gilman and Newson, 1980; Jones, 1981; Bonell et al., 1984)). Flow in macropores will, however, depend on the maintenance of an immediately surrounding saturated layer and may require the initial satisfaction of local storage deficits before continuous flow commences. Hydraulic conductivity discontinuities in the soil profile may again be very important in the creation of saturated conditions.

Soil water flows under the influence of a gradient in both saturated and unsaturated states of the soil. However, velocities of soil water flow may fall markedly with decreasing moisture content and are always much lower than those for either overland flow or pipe flows. Increases in the area of saturation, however, has been found to result in rapidly increasing flow (Carson and Sutton, 1971; Bernier and Hewlett, 1982). This in part is due to the fact that the movement of water through a fully saturated zone, including seepage, responds almost instantaneously to changes at the boundaries of the zone. Effectively, water entering the saturated area causes an immediate displacement of water at the seepage face (Anderson and Burt, 1982). Peak seepage flow will, however, be delayed from the time of peak rainfall (Freeze, 1972b) as a result of the time delay before infiltrated rainfall reaches the saturated zone. It follows that the amount and timing of peak seepage flows will be heavily dependent on initial conditions of soil moisture (Weyman, 1971). In layered soils, saturated conditions may build up above conductivity discontinuities, and seepage from different layers in the soil may exhibit different flow rates and time rates and time delays (van't Woudt, 1954).

Where the response of the soil mass is slow compared with storm duration, and surface flows are not significant, initial storm discharge may be almost entirely generated by rainfall directly into the channel and immediately adjacent areas. Then seepage flow will contribute largely to the recession limb of the hydrograph and ultimately will be indistinguishable from groundwater flow (Sklash and Farvolden, 1979; Nash, 1983).

It should be noted that once the spatial variability of catchment response, even to a uniform rainfall, is recognized, all the components of storm discharge generation specified above be included in a general model. Infiltration excess overland flow should not be viewed as mutually exclusive concepts, but both may occur and depend on the instantaneous conditions of the soil and rainfall intensity. Instead, all the processes of channel precipitation, surface flow and saturated/unsaturated flows in the soil may occur concurrently so that the total basin response will be continually variable in both space and time. This tendency will be reinforced by spatial variation in system inputs and characteristics (Sharon, 1970; Sugawara, 1970). There is rarely sufficient evidence to determine the relative importance of individual processes in the operation of the catchment system and thus separation of flow components from the discharge hydrograph, commonly used in hydrologic analysis, does not make sense.

1.3 Modeling Approaches

A plethora of approaches for modeling hydrologic systems has evolved over the years. These approaches are so diverse and hybrid that it is hardly possible to group them into distinct groups (Singh, 1989). In the following sections, several general approaches to the problem of modeling catchment responses are examined with reference to conceptual knowledge of the system. Categories of models are distinguished on the basis of assumptions made about the system.

1.3.1 Lumped catchment models

The use of a lumped hydrological model is justified in theory only if the response of the system is instantaneously similar throughout the watershed area (Eagleson, 1967). Mathematical procedure for the identification and solution of lumped parameter models are much simpler than for those in which response is allowed to vary spatially, and 'the fact that a basin is not a random assembly of different parts, but a geomorphological system whose parts are related to each other by long common history encourages the hope that simplified concepts may be found adequate to describe the operation of this basin in converting rainfall to runoff' (Nash and Sutcliffe, 1970).

Lumped models may be separated by systems analysis and systems synthesis methods. The former are essentially black-box impulse-response methods relating input to output without reference to the internal structure or processes of the system. The latter incorporate some assumptions, generally empirically derived, about the physical nature of the system.

System analysis

The earliest model that took into account the instantaneous distribution of storm runoff over time as well as its total volume was based on the unit hydrograph concept (Sherman, 1932). This is closely related to the Hortonian surface flow model of catchment storm responses (Horton, 1933), with the assumption that, for a given basin, similar rainfall excess characteristics would yield similar hydrograph shapes. The discharge hydrograph for any arbitrary amount of effective rainfall can be obtained by superposition of the unit hydrograph (Chow, 1964). Calculation of the unit hydrograph requires that the river discharge hydrograph be separated into 'base flow' and 'surface runoff' components and that the rainfall hydrograph be separated into 'effective rainfall' and 'infiltration loss' components (Linsley et al., 1958).

A later development of unit hydrograph theory was the introduction of the concept of instantaneous unit hydrograph (IUH). The IUH is the hydrograph due to an infinitely small duration of effective rainfall (Nash, 1957; Nash, 1983), and has the advantage of being independent of the limiting assumption of a uniform distribution of rainfall excess over time. The IUH, as an impulse response function can be calculated from known rainfall excess and storm runoff by one of the several systems theory techniques (Nash, 1983).

The unit hydrograph method may be applied to a catchment with limited data available since a predictive model can be derived from estimates of effective rainfall and storm runoff for a single storm. Attempts have also been made to correlate the parameters of the functional models of the unit hydrograph and IUH with physical parameters of catchments with known storm response characteristic, so that estimated parameters can be derived for ungauged catchments (Linsley et al., 1958; Nash, 1959b; Nash, 1960; Hudlow and Clark, 1969; Nash; 1983). This approach has had but limited success.

The primary criticism of unit hydrograph methods rest in the assumption of linearity. Several studies have shown that catchment response exhibits non-linearity (Nash, 1960; Amorocho, 1963, 1967; Dooge, 1977).

The necessity of hydrograph separation has also been a criticism of the unit hydrograph method (Nash and Sutcliffe, 1970). In this subjective procedure, and in the calculation of an estimate of effective rainfall, persists the belief that the storm response of a catchment is partially uniform, dominated by overland flow, and that there is a sharp threshold between the processes of storm runoff and those of base flow, with a difference in velocity of an order of magnitude or more. Undoubtedly there are many catchments for which the Hortonian model is a good approximation, but where overland flow is relatively less important in catchment response the use of separation techniques can not be justified physically and will lead to error.

Some attempt has been made to deal with the general problem of non-linear response through the use of models that consist of fundamental series of increasing order (Amorocho, 1967b; Diskin and Boneh, 1973). Linear systems are included as a special case. All these studies have treated the catchment system as spatially lumped although in theory distributed inputs may be included in the analyses. This approach also removes the necessity of hydrograph and hyetograph separation.

"Despite the mathematical sophistication which in the last twenty years has been applied to it, the unit hydrograph concept is nothing but a crude tool and we must always remember that the defects in its origin (i.e. the lack of adequate definition and identification of the quantities which it relates) can not be overcome by any algebraic manipulation no matter how clever" (Nash, 1983).

System synthesis

Linear systems synthesis models evolved as an extension of the unit hydrograph methods. An instantaneous unit hydrograph can be derived by routing an instantaneous input of effective rainfall through a conceptual model of the operation of the catchment response system. These models recognize that the catchment performs both storage and transfer functions and have been essentially composed of linear reservoir and channels (Nash, 1957; Dooge, 1959). The output from a particular model can be defined by mathematical functions, the parameters of which are derived by matching of predicted response with observed storm runoff records. Application of these models remain subject to criticism of the assumption of linearity, spatial uniformity of the input function, and the subjective definition of 'effective rainfall' and direct storm runoff. Other conceptual elements may, however, be included in these models. Mandeville and O'Donnell (1973) review and extend the theory of time variant linear elements, while Prasad (1967) developed relationships for nonlinear storage elements. One of the most widely used models has been the Standford Watershed Model and its derivatives (Crawford and Linsley, 1966; Crawford, 1969a).

The simulated hydrographs which appear in the literature show that many different models reproduce the behavior of the catchment systems with reasonable accuracy. However, the degree of mathematical equivalence with the prototype achieved by these models must not be taken as physical equivalence, particularly in the analysis of watershed changes. Several characteristic features of this approach serve to reinforce this view. These models are subject to the criticisms pertaining to all lumped models in that spatial variability demonstrated in many catchments may be such that physical reality may not be adequately represented by a spatially averaged model. It would appear that the success of this approach depends markedly on the optimization processes by which the model is calibrated for a particular catchment. Most models are sufficiently complex to preclude trial and error optimization and Dawdy and O'Donnell (1965) advocated the use of more objective automatic methods. Such methods still involve, however, the use of a subjectively chosen loss function (also commonly referred to as an error function); usually a measure of agreement between simulated and observed discharges.

Increasing study has shown that hydrological simulation models are not suited to existing automatic optimization methods. In particular, problems are caused by the inclusion of 'a priori' constraints on parameter values, interactions among parameters, threshold parameters, which may operate only occasionally, and a finite, and often short calibration period resulting in a limited range of conditions over which the model may be optimized. These characteristics are manifest as multiple optima of the loss function and insensitive parameters (Ibbitt, 1972). In addition different loss functions may yield different optimum parameter values

(Dawdy and Thompson, 1967). These problems are a suitable reflection of the complex interaction in the prototype but it does seem unlikely that the effects of individual processes or changes in catchment characteristics can be satisfactorily isolated by this type of model.

It seems necessary to reduce the emphasis on the physical significance of this type of model when identification of model parameter values is dependent upon optimization. Certainly optimized parameter values have been shown to exhibit significant sampling variance (Ibbitt, 1972). A better approach would be to view these models as a structure of linear/nonlinear storage/routing elements, the form of which may be suggested by past studies of hydrologic processes (Onstad and Jamieson, 1970). The possibility of mathematical equivalence is retained but parameter values should not be taken as having significance outside the model structure (Nash and Sutcliffe, 1971).

Most non-linear system synthesis models are not suited for application to a catchment directly, since a considerable and continuous length of record is required for satisfactory calibration (Haan, 1972b). However, attempts have been made to simulate the response of ungauged catchments with some limited success. One approach has been to calibrate the model on a neighbouring catchment and use the derived parameter values as estimates of those for the ungauged catchments. The other approach is to calibrate model for a number of catchments, then correlated the derived parameters with physical characteristics of the basins (Jarboe and Haan, 1974; Nash, 1983). These relationships could the be used to predict the parameter values for a wider range of ungauged locations.

1.3.2 Distributed catchment models

Distributed models attempt to take into account at least some of the demonstrated areal variability in the catchment hydrological system. There are practical limits to the degree of distribution that can be included in the model, if only as a result of data and computational limitations, and some spatial averaging of catchment characteristics will be necessary. It is difficult to determine 'a priori' what degree of lumping will prove acceptable but it will depend on the scale of the phenomena modeled.

The simplest models are the extensions of the lumped non-linear synthesis approach. The catchment is broken down into a system of several sub-areas, such as 'unit-source' areas of Amerman (1965) or 'hydrological response zones' of England and Stephenson (1970). These sub-areas are defined on the basis of soils, topography and land use to be relatively homogeneous. Total storm discharge may be estimated by the summation of contributions from the individual elements (Amerman, 1965) but fails to allow the interactions between the sub-areas. Increasing subdivisions, however, leads to a rapidly increasing number of parameters and difficulties in model calibration. Ultimately identification by automatic optimization will be limited by computational requirements and either resort must be made to trail and error methods based on experience, or the distributed parameters must be derived from physical characteristics of the catchment (Ibbitt, 1972b). It is true that with relatively homogeneous sub-areas, measurement or 'a priori' estimation of some parameters, such as the coefficients of infiltration functions, may prove satisfactory. However, the practice of deriving some distributed parameter values, such as storage/flow coefficients for all sub-areas from the catchment discharge records still persists (Holtan, 1970).

Distributed models may also be based on the physical laws governing the individual flow processes in the catchment hydrological system. The following section deals with the physically based distributed models.

Physically-based distributed models

The development and application of physically-based distributed models in hydrology has been very fragmented. There have been numerous papers on the theoretical aspects of modeling various hydrologic processes independently using both analytical methods for simple cases and approximate numerical methods of increasing sophistication. There is a much smaller body of literature on models involving more than one process and on the application of distributed models to real world problems. In this section attention will be given on some general features of distributed modeling with appropriate illustrations from a small number of specific studies.

A catchment is a fully distributed system continuously variable over time and three dimensional space. It is possible to write down general partial differential equations for the processes of mass and energy transfer within the catchment continuum, together with boundary conditions for those equations, based on physically realistic assumptions compatible with current knowledge of hydrological processes. These equations comprise the general distributed model of catchment hydrology (Freeze and Harlan, 1969). The complete system of non-linear equations is impossible to solve analytically for any case of practical interest and resort must then be made to approximate numerical solutions (Freeze, 1978). A considerable amount of research, mostly concentrated on studies of single process, has been aimed at developing solution methods that are sufficiently accurate but remain efficient in terms of computing requirements and the discretization of catchment into nodes.

The earliest solution technique, and still the most commonly used, is the finite difference method pioneered by Richardson (1910). Finite difference techniques were first applied to groundwater flows by Shaw and Southwell (1941), unsaturated flow by Klute (1952) and channel flow by Stoker (1957). Finite difference methods are now applied quite routinely to steady state and transient problem in groundwater and channel routing studies. More recently, however, several other methods have been used in hydrology including finite element methods (Pinder and Grey, 1977), integrated finite difference methods (Norasimhan and Witherspoon, 1976), the method of characteristics (Amein, 1966; Wiggert and Wylie, 1976), and the boundary element method (Brebbia, 1978).

Application of a three dimensional complete catchment model solved by finite difference methods has been demonstrated on limited hypothetical problems by Freeze (1971, 1972a, 1972b). Beven and Kirkby (1979) adopted a physically-based approach (in the sense that the parameters are measurable in the field) which takes into account the distributed effects of channel network topology and dynamic contributing areas. Recently SHE (Systeme Hydrologique Europeen) model appeared in the literature of physically-based distributed type of modeling approaches (Jonch-Clausen, 1979; Abbott et al., 1986).

From the short literature (Beven, 1985) on physically-based models and from the inability of traditional models to serve the purpose, it is evident that further attempts in modeling hydrologic systems should cover the physical aspects of the system. There are four (related) areas for which physically-based spatially distributed hydrological models can fulfil the need of practical applications: catchment changes, spatially variable inputs and outputs, the movements of pollutants and sediments through a catchment, and forecasting the hydrological response of ungauged catchments (Bresler, 1973; Surkan, 1974; Jarboe and Haan, 1974; Selim, 1978).

1.4 On the Present Approach

The process of linking rainfall and runoff is a deterministic one, in that it is governed by definite physical laws which by and large are known. It might, therefore, seem that solution of the problem in any specific case involves only the applications of these laws to the measured rainfall and boundary conditions - the physical description of the catchment and the initial distribution within it. However, many hydrologists consider this impractical. The deterrent is the complexity of the boundary conditions rather than any essential difficulty in the physical laws. As there is little point in applying exact laws with approximate boundary conditions, it is acceptable to use simplified empirical relations.

The fact that a basin is not a random assembly of different parts, but a geomorphological system whose parts are related to each other by a common history. Some empiricism is unavoidable; few would quarrel with the use of Manning's equation for channel resistance, instead of more exact treatment through the Navier-Stokes equations. The traditional hydrological methods have, however, tended to be very empirical. Little use has been made of the established physical laws; instead an empirical, analytical, or a current jargon 'parametric' approach has been adopted (Nash, 1983).

For the present study, a physically-based distributed approach has been chosen for modeling watershed hydrology. It is recognized that such models are computationally expensive and data requirements are great. But it is felt that this approach potentially offers advantages over the other techniques that justify further evaluation and with the availability of low cost computing machines this disadvantage will fade away.

The advantages that a physically-based model can offer are: (1) it allows direct inclusion of a great deal of readily available physical information, such as topography, soil and channel characteristics for catchment under study; (2) it is dependent on the parameters that can be measured or estimated directly, and does not require identification by optimization or extrapolation of parameters from other basins, although it can be done so; (3) this type of model is capable of handling spatial variability of system inputs, catchment characteristics, directly.

It is intended to use this model to evaluate the applicability of a physically-based model in real time simulation problems, using only measured or a priori estimates of parameter values. Also it is hoped that this simulation may help find the relative importance of different processes and the effect of watershed relief in streamflow generation.

1.4.1 Outline of the model

The hydrologic cycle is continuous. However, the expressions describing the components have been developed independently by workers in many different fields. To asses the level of sophistication that is possible with present methodology, it is still convenient to break down the hydrologic regime, using the nomenclature of Fig. 1-1, into the following components.

Unsaturated flow

The unsaturated flow process includes infiltration, redistribution of infiltrated water, deep percolation or groundwater recharge and evaporation. These are modeled using the soil water flow equation. The form of this equation in the vertical direction reads

$$C(\psi)\,\frac{\partial\psi}{\partial t} = \frac{\partial}{\partial z}\left(K(\psi)\,\frac{\partial\psi}{\partial z}\right) - \frac{\partial K}{\partial z} \qquad [1\text{-}1]$$

where

ψ - capillary pressure head

t - time

z - vertical coordinate, positive downwards

K - hydraulic conductivity as a function of ψ

C - specific moisture capacity (defined in section 2.2.2) as a function of ψ

When computing evaporation an estimate of potential evaporation is required. To obtain this estimate the Penman-Monteith equation is used as given by

$$PE = f\,\frac{\Delta R_{nc} + \rho C_p \frac{\delta e}{r_a}}{\lambda\,(\Delta+\gamma)} \qquad [1\text{-}2]$$

where

PE - potential evaporation rate

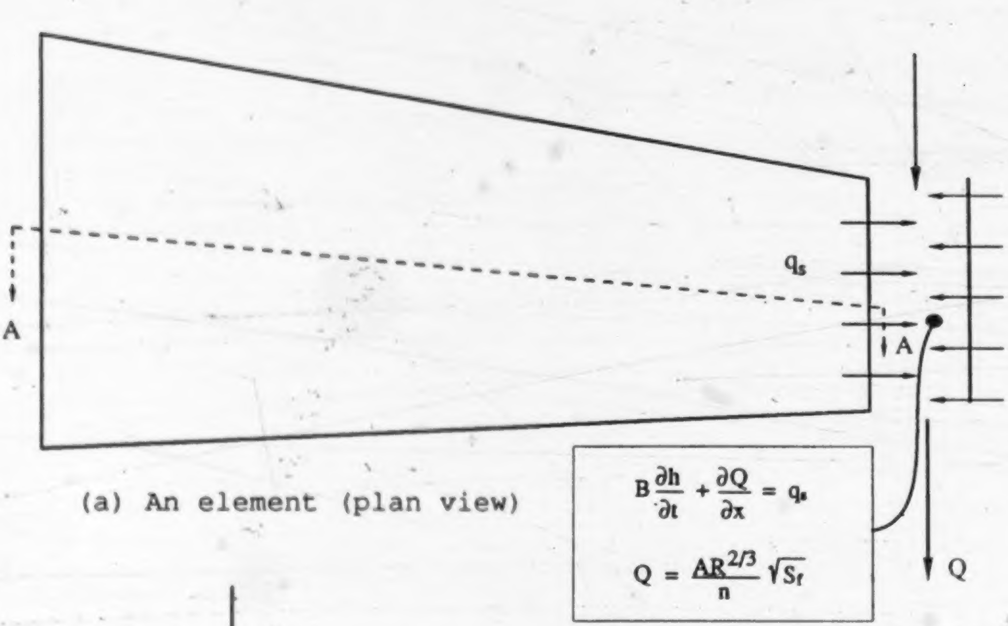
q_s
A
A
$B\frac{\partial h}{\partial t} + \frac{\partial Q}{\partial x} = q_s$
$Q = \frac{AR^{2/3}}{n}\sqrt{S_f}$
Q

(a) An element (plan view)

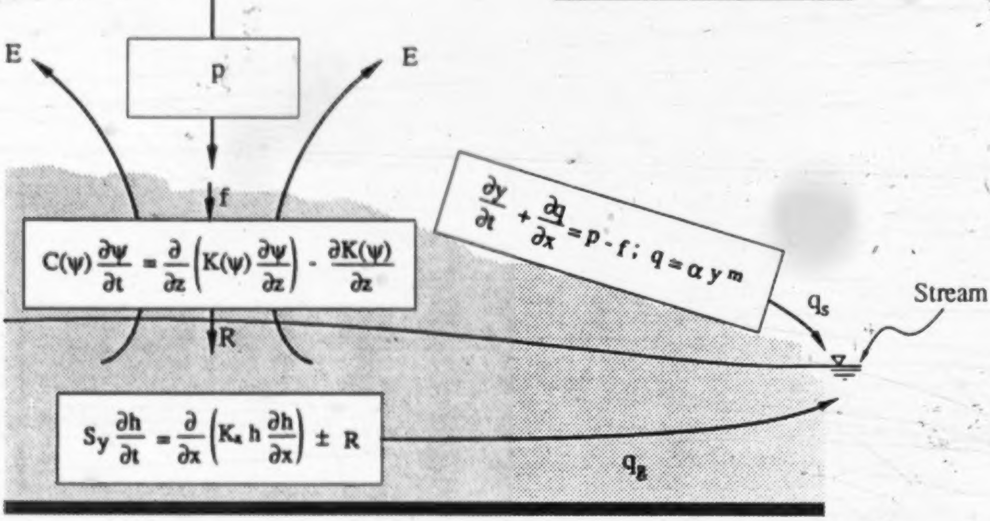
E
p
E
f
$C(\psi)\frac{\partial \psi}{\partial t} = \frac{\partial}{\partial z}\left(K(\psi)\frac{\partial \psi}{\partial z}\right) - \frac{\partial K(\psi)}{\partial z}$
$\frac{\partial y}{\partial t} + \frac{\partial q}{\partial x} = p - f;\ q = \alpha y m$
q_s
Stream
R
$S_y\frac{\partial h}{\partial t} = \frac{\partial}{\partial x}\left(K_s h\frac{\partial h}{\partial x}\right) \pm R$
q_g

(b) Section through A-A

Fig. 1-1. Hydrological processes modeled in this study; p - precipitation; E - evaporation; f - infiltration; q_s - surface runoff; q_g - groundwater flow; R - groundwater recharge; Q - channel flow; the terms in the equations are defined in the text.

f - unit conversion factor

R_{nc} - net radiation absorbed by the plant

Δ - slope of the saturation vapour pressure curve

ρ - air density

C_p - specific heat capacity of dry air

δe - vapour pressure deficit

λ - latent heat of vaporization

γ - psychrometric constant

r_a - aerodynamic resistance

Saturated flow

The saturated flow flow component of the hydrological cycle is modeled by the Dupuit-Forchheimer equation (1-D) which is

$$S_y \frac{\partial h}{\partial t} = \frac{\partial}{\partial x}\left(K_x h \frac{\partial h}{\partial x}\right) \pm R \qquad [1\text{-}3]$$

where

S_y - specific yield or drainable porosity

h - phreatic surface elevation

x - horizontal coordinate

K_x - saturated hydraulic conductivity in x-direction

R - groundwater recharge or evaporation rate

Overland flow

Kinematic wave approximations are used to route runoff over the land surface to the channel system. Following Lighthill et al. (1955) the equations are

$$\frac{\partial y}{\partial t}+\frac{\partial q}{\partial x}=p-f \quad \text{and} \quad q=\alpha y^m \qquad [1\text{-}4]$$

where

y - depth of flow

q - overland flow

p - rainfall rate

f - infiltration rate

m - exponent

α - coefficient, function of surface roughness and slope

Channel flow

Flow in the channel network is modeled by the diffusion wave approximations. These are expressed as

$$\begin{gathered} B\frac{\partial h}{\partial t}+\frac{\partial Q}{\partial x}=q_l \\ Q=\frac{AR^{2/3}}{n}\sqrt{S_f} \end{gathered} \qquad [1\text{-}5]$$

where

Q - discharge in the channel

A - cross-sectional area of the channel

R - hydraulic radius

n - Manning roughness

S_f - friction slope

B - top width of the channel

h - water surface elevation

q_l - lateral inflow into the channel

Additional information regarding all these equations are provided in the respective sections.

To allow for spatial and temporal variations of the different components, they can be specified, computed or assumed at different points in the watershed. These points are referred to as 'nodes' in this treatise. Some assumptions in representing the complex physical system are required. These are with regard to the boundary conditions and assumptions made in the derivation of these differential equations and are discussed later.

Chapter 2 deals with the soil-water realm, Chapter 3 concerns modeling of the groundwater component, Chapter 4 and Chapter 5 deal with the overland and channel flow processes. Chapter 6 contains an analysis of the numerical method used in this study and Chapter 7 contains application of the model to Spring Creek watershed and the simulation results. Finally the conclusions are provided in Chapter 8.

It will be seen that the flow processes dealt with in Chapter 2 through Chapter 5 pose quite similar problems and are solved using the same core technique. Therefore, a general description of the solution method and its accessories are given in the section that follows.

1.5 On the Solution Methods

A mathematical model represents the prototype system by a set of algebraic formulas. A physically-based approach (as the one of this study) to modeling results in differential equations. The solution requires that the geometry of the one, two or three-dimensional region, in which flow is considered, be specified as well as the conditions that apply at the boundary of the flow domain. If at the boundary the value of the dependent variable is given, the boundary condition is known as the Dirichlet condition and flux or Neuman conditions refer to the situation for which the flux normal to the boundary is specified (Richtmyer and Morton, 1967). In cases where different parts of the boundary have different types of boundary conditions, the system is known as the mixed boundary value problem. The use of vanishing derivative boundary conditions for solution of steady state flow problem requires that the net flow out of the flow domain is zero. To arrive at a unique solution for a Neuman problem an additional parameter is required. Well-defined boundary conditions are sufficient to obtain a particular solution of a steady state flow problem. But for the solution of a transient flow problem, initial conditions as well as changes in boundary value with time need to be specified. When these conditions are properly defined, the solutions of the differential equations may be obtained using either **analytical** or **numerical** methods.

Analytical methods

The relationships that describe the flow of water in a watershed are nonlinear equations. Since the coefficients in these equations are functions of dependent variables, exact analytical solutions, for specific boundary conditions, are extremely difficult to obtain. Analytical methods to solve the nonlinear governing equations search for the exact solution in terms of analytical functions. Such an exact solution, if it exists, requires transformation, separation of variables, and usually a series of functions. The commonly used Boltzman transformation reduces the partial differential equations to ordinary differential equations. The Laplace transformation results in removing the time variable. The solution of an equation modified in this way yields a dependent variable as a function of the space variable (Gardner, 1958). The nonlinear mass conservation equation can be solved using various relaxation techniques such as linearisation, quasi-linearisation and transformation of the steady state. Analytical solutions which are found completely by mathematical analysis cannot be obtained for a transient flow in practical situations, unless some nonrealistic assumptions are made (Polubarinova-Kochina, 1962; Philip, 1969). For solving problems, as encountered here, resort must then be made to approximate numerical methods. In fact, the evaluation of some complex analytical solutions may take more computer time than approximate methods of same accuracy (Javandel and Witherspoon, 1969).

Numerical methods

At present, numerical approximations are possible for any complex flow regions having various boundary conditions. Numerical methods are based on subdividing the flow region into finite segments bounded and represented by a series of nodal points at which a solution is obtained. This solution depends on the solutions of the surrounding segments and on an appropriate set of auxiliary conditions.

In recent years, a number of numerical methods have been introduced. The most commonly used numerical methods for the solution of flow problems are finite difference (F-D) methods (Remson et al., 1971). However, lately finite element (F-E) and boundary element (B-E) methods are being used in some instances as well.

In F-D methods the finite differences are derived by expanding the derivatives, usually, in Taylor series over a small interval of space and time, and truncating the series after a small number of terms (Remson et al., 1971). A grid has to be defined with dimensions depending on the number of independent variables that appear in the practical differential equation. If the one-dimensional diffusion eqn.[1-1] is used as an example, the grid will have two coordinates: distance x and time t, as shown in Fig. 1-2 (page 36). Every point in this finite difference grid corresponds to a specific point in space at a specific instant in time. It is convenient to choose a regular grid with constant Δt and Δx but this is by no means a requirement. If the coordinates in the x-t plane are indicated by j,n respectively, the solution at any given grid point or node (j,n) is ψ_j^n. For n=0, initial values for ψ have to be given and if the flow domain is divided into m equal intervals, boundary condition for j = 0 and j = m have to be specified for each time level n. The F-D approach replaces the derivatives of differential equation by their finite difference analogue. This may lead to an explicit or implicit F-D scheme. An explicit scheme is obtained if the time derivative is replaced by a forward difference approximation between n and n+1 time level and the space derivatives are replaced by their F-D analogues at the n time level. Applied to eqn.[1-1] this yields

$$C_j^n \frac{\psi_j^{n+1} - \psi_j^n}{\Delta t} = \frac{K^n_{j-1/2}\left(\psi^n_{j-1} - \psi^n_j\right) - K^n_{j+1/2}\left(\psi^n_j - \psi^n_{j+1}\right)}{\Delta z} - \frac{K^n_{j-1/2} - K^n_{j+1/2}}{\Delta z} \qquad [1\text{-}6]$$

which can be written as

$$\psi_j^{n+1} = \psi_j^n + \frac{\Delta t}{\Delta z C_j^n}\left[K^n_{j-1/2}\left(\psi^n_{j-1}-\psi^n_j\right) - K^n_{j+1/2}\left(\psi^n_j-\psi^n_{j+1}\right) - K^n_{j-1/2} - K^n_{j+1/2}\right] \qquad [1\text{-}7]$$

In eqn.[1-7] the unknown value of the dependent variable at time level n+1 is explicitly expressed in terms of known values at the time level n. To solve eqn.[1-7] Dirichlet conditions have to be specified. Flux conditions involve an extra equation. For instance, if at the boundary x_m the flux q_m^n is specified an imaginary node is induced as follows

$$q^n_m = \frac{K^n_m\left(\psi^n_{m+1} - \psi^n_{m-1}\right)}{2\Delta z} \qquad [1\text{-}8]$$

to be written as

$$\psi^n_{m+1} = \psi^n_{m-1} + \frac{2\Delta z}{K^n_m} q^n_m \qquad [1\text{-}9]$$

With the introduction of imaginary nodes when the flux conditions are specified at the boundary, ψ can be solved at the end of the first time increment through a repeated application of eqn.[1-7]. Once these values are computed, eqn.[1-7] is used again to move the solution forward by another time step. As in this example, explicit schemes are simple straightforward techniques, easy to formulate and easy to program. However, these schemes are often subject to a certain condition that is expressed as a 'mesh ratio' (ratio of time step to distance step) to produce stable F-D schemes (Richtmyer and Morton, 1967). Stability refers to the ability of the scheme to prevent numerical errors from growing in an unbounded or uncontrolled manner. In practical applications, this requirement limits the size of the time step and consequently these schemes are computationally inefficient.

Because stability and convergence criteria imposed on an explicit F-D scheme often lead to unacceptable restrictions on the choice of Δx and Δt, an implicit scheme is usually preferred. According to this scheme, the difference equations are written such that the new values of the dependent variable are not given directly in terms of 'known' values, but as a function of 'unknown' values at the adjacent positions as well. If this scheme is applied to eqn.[1-1] the resulting equation

$$C_j^n \frac{\psi_j^{n+1} - \psi_j^n}{\Delta t} = \frac{K_{j-.5}^n\left(\psi_{j-1}^{n+1} - \psi_j^{n+1}\right) - K_{j+.5}^n\left(\psi_j^{n+1} - \psi_{j+1}^{n+1}\right)}{\Delta z} - \frac{K_{j-.5}^n - K_{j+.5}^n}{\Delta z} \qquad [1\text{-}10]$$

contains three unknowns. If for the first time level eqn.[1-10] is written for each node, this results in (m-1) equations with (m-1) unknowns. Through a simultaneous solution of this set of equations, values for ψ at the first time step are obtained. There are a number of methods to solve the set of equations, such as linearisation, predictor corrector or iteration methods. A complete review of these methods can be found in Remson et al. (1971). One of the advantages of implicit schemes is that they are generally not subject to the restrictive mesh ratio condition for stability. Of course, stability of the scheme does not always ensure correct solutions.

In addition to the above two types of schemes, there are some special methods. The method of characteristics is one of them. It is quite often used in channel flow problems. The method of characteristics is less limited in respect of computational stability than explicit schemes, since the solution is designed to follow the characteristic directions of the equations, along which they can be transformed to ordinary differential equations. Hyperbolic equations of second order have two characteristic equations at every point in the flow domain, and for eqns.[5-1] and [5-3], the slope of the characteristics is given by

$$\frac{dx}{dt} = v \pm \sqrt{gy} \qquad [1\text{-}11]$$

and the equations of the characteristic lines by

$$\frac{d}{dt}(v \pm 2\sqrt{gy}) = g\,(S_0 - S_f) \qquad [1\text{-}12]$$

Four of these characteristics are shown in Fig. 1-3. One of the forward characteristics, as shown in the figure, is emanating from x = 0, t = 0, and one of the backward characteristics is shown to emanate from x = L, t = 0. A disturbance introduced at point Q will travel through

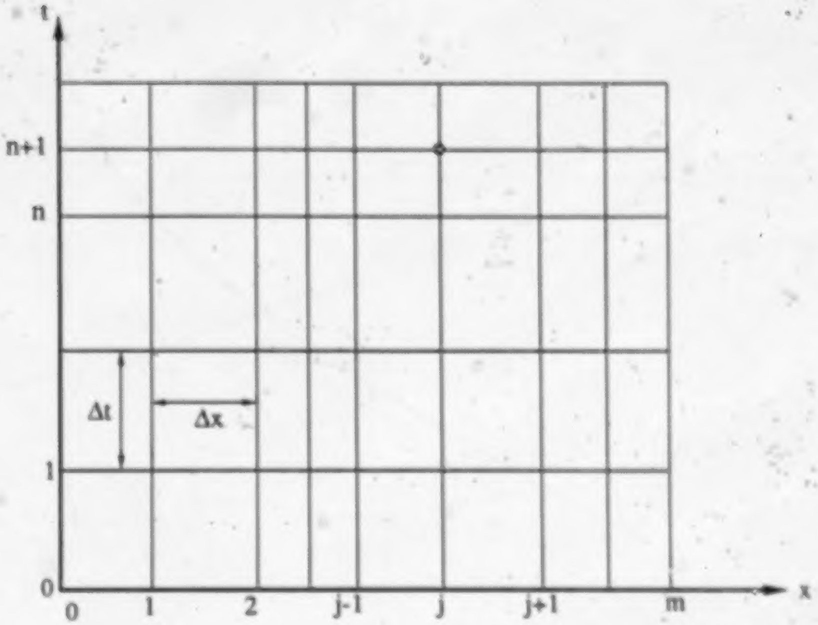

Fig. 1-2. F-D grid for eqn.[1-1] with distance x and time t.

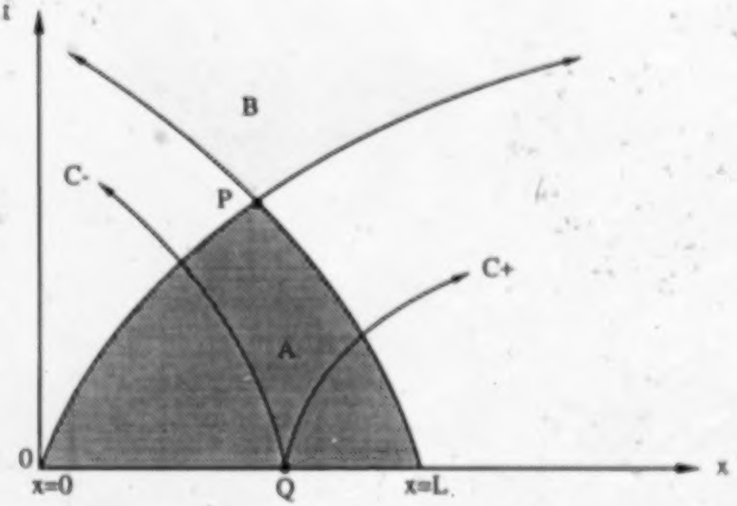

Fig. 1-3. Forward and backward characteristic directions of channel flow equations in the solution domain x,t. The shaded area A represents that part of the domain on which the solution at point P is dependent; the shaded area B represents that part of the domain in which the solution is influenced by the condition at point P.

characteristics C_+ and C_-, with velocity given by eqn.[1-11]. Thus the values of the dependent variable, y, at point P, in the solution domain (x,t) are only dependent on their known initial values at a given time, say t=0, in the shaded area 'A' of Fig. 1-3. A diffusion wave has only one forward characteristic i.e. the wave front or any perturbation propagates only in downstream direction. And the speed of the diffusion wave is given by the kinematic wave speed as provided in Chapter 4. The method of characteristics makes use of the fact that along the characteristic directions, integration of the equations is much simplified. The characteristic equations are usually solved numerically. They may be expressed in explicit or implicit forms using rectangular space-time grids or characteristic grids.

The characteristic grids scheme is theoretically and physically more appealing and perhaps more direct and accurate in many cases. It is useful in determining physical characteristics as the characteristic grids are more dense in the areas in which more rapid change in the flow is taking place. This scheme was used by Amein (1966) and Fletcher and Hamilton (1967) to demonstrate flood routing and by Liggett (1968) to simulate the unsteady flow hydrographs matching with experimental runs in laboratory flumes. With this scheme, however, not only the dependent variables but also x and t have to be determined at each grid point of the characteristic network. In order to arrange the outputs in an orderly and useful format a good 2-D (or bivariate) interpolation scheme is necessary. In the case of multiple-reach, or network flow computations, in which many internal boundary equations have to be solved simultaneously at junctions, or at prescribed times and locations, the characteristic grid scheme is a very unsuitable, inconvenient scheme to use.

With the space-time grid schemes, x and t are predetermined and the dependent variables are to be computed at each unknown point. This scheme has been applied to rivers and estuaries by Lai (1969), Baltzer and Lai (1968); to dam-break problems by Chen and Armbruster (1980); and to flood routing through storm drains by Yevjevich and Barnes (1970). As in characteristic grid schemes, this scheme also requires interpolation, but it is a simple and straightforward 1-D interpolation. The interpolation, however, is performed during the computation (i.e. interpolation is a part of the numerical solution) instead of being done separately in order to extract more meaningful output data. Hence, the accuracy of computation may sometimes suffer numerical dissipation (Lai, 1986).

In contrast to the finite difference procedure which involves a number of local approximations, the finite element method relies on looking at a problem from a global point of view. Firstly, it is recognized that any analytical solution might be expressed as an infinite sum involving a complete set of basis functions. Analytical solutions typically involve series of orthogonal functions. However, in finite element analysis, functions are selected that are intended to be used, typically polynomials of some sort, and require that the solution be expressed as a sum involving these polynomials. Each polynomial in the sum has a coefficient and the solution of the problem thus reduces to solving for these coefficients. Since the solution has been approximated, the differential equation is not necessarily satisfied exactly but may contain an error. Thus solutions are obtained for the coefficient in the summation by requiring the error in the approximation to have certain properties. For instance, it may be desired that error at certain points be zero, or some weighted integral over the entire domain be zero. Sufficient constraints are imposed such that the solution can be obtained for all the coefficients in the series approximation.

To apply a F-E method, the flow region is sub-divided into small parts, called the elements. The size or shape of the element may vary from one another. The independent variable in the interior of the element is expressed in terms of its value at the end (or corner) points (called nodes). Application of this method results in a set of simultaneous equations. Various techniques are available, as mentioned previously, to solve sets of simultaneous equations.

The F-E method is a recent development in the field of hydrology (used especially in subsurface flow problems). Its relative merits or demerits have yet to be established. As evident from Gray (1982):

"... finite element and finite difference methods are numerical procedures which arise from different starting positions but which have similarities in final applications.... In fact, discussions which argue that one method is better than the other often reflect that the author has merely utilized and programmed one method better than he has the other ..."

The most recent approximate method applied to solve unsaturated flow problems is the boundary element method (e.g. Brebbia and Walker, 1980) which is also known as the Boundary Integral Equations. The integral of the domain is eliminated by a set of basic functions and therefore reduces the problem to a so-called boundary problem. The reduction of the order of differentiation results in considerably less computer storage of matrix coefficients. Taigbenu and Liggett (1985) used this method to solve a problem characterised by time dependent governing equations and boundary conditions. For the present studies, F-D (weighted implicit) schemes are used to solve all the flow problems involved. It should be noted that selection of the F-D method has been made arbitrarily without any formal analyses of its relative merits or demerits over the other existing methods. Detailed F-D formulations of the flow equations are described in the respective chapters.

Chapter 2

Unsaturated Flow Model

2.1 Soil and Moisture

Traditionally the science of hydrology has consisted of two main branches: surface water hydrology - dealing with water flowing or stored above the soil surface or in streams and lakes; and groundwater hydrology - concerned with the flow and storage below the water table. In between the two realms lies the unsaturated zone of the soil, a realm too-often neglected by hydrologists probably because it is too complex to deal with. A succinct description regarding the phases of this zone can be found in Chanasyk (1980). One of the phases is the soil moisture regime (only liquid water is considered here). Usually this regime is partitioned into three segments such as hygroscopic water, available water, and gravity water. Hygroscopic water is the moisture held on the soil particle by very strong electric force of the order of 10^{12} Pascal, (de Marsily, 1986); plants find it very hard to utilize this water and hence it is also called unavailable water. Thus the moisture content below which plants can not extract water is termed, specially in agricultural literature, the wilting point. Available water is the water still subjected to a non-negligible attractive force and stays immobile; plants are able to extract this water at ease and hence it is available. The gravity water which is also called free water can be drained by the force of gravity; since it runs away it is not available to plants either. The moisture content above which water drains away is called field capacity. This is a rather a vague term and it is difficult to assign any numerical value, however, it is a useful concept and widely used in the agronomical aspects of soil water. Fig. 2-1 shows the above definitions schematically (Edlefsen and Anderson, 1943).

The volume of solid material and the total void space will vary from soil to soil, depending upon the soil texture and structure. Hence the water holding capacities of soils can be appreciated from information on soil texture. Commonly the range of values normally experienced for any given texture is rather narrow. Chanasyk (1980) presented the following values for the representative soil moisture storages for various soil textures.

Table 2-1. Water holding capacity of different soils.

Soil texture	Gravity water (cm/m)	Available water (cm/m)
Coarse sandy loam	15.8	8.7
Sand	19.0	13.3
Loamy sand	26.9	10.1
Fine sandy loam	23.5	13.1
Loam	14.4	15.6
Silt loam	11.4	19.9
Sandy clay loam	13.4	11.9
Clay loam	13.0	12.7
Silt clay loam	8.4	7.8
Sandy clay	11.6	7.8
Silty clay	9.1	12.3
Clay	7.3	11.5

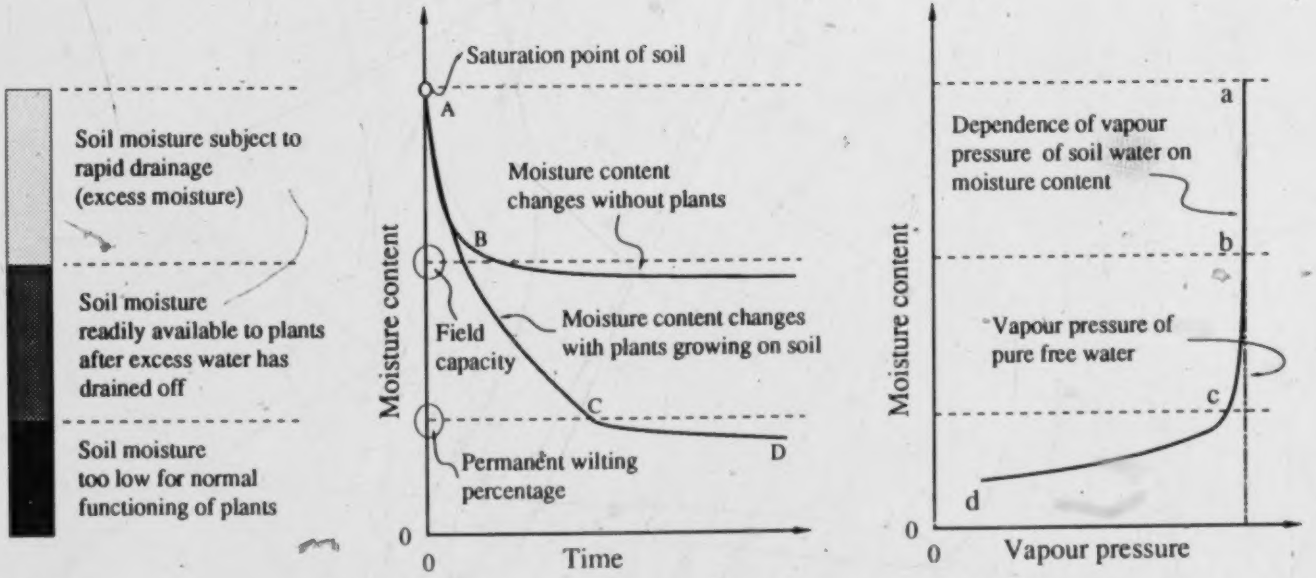

Fig. 2-1. Relation between permanent wilting percentage, field capacity, range of readily available moisture, drainage, vapour pressure, and moisture content (adapted after Edlefsen and Anderson, 1943).

In the continuum of natural hydrological processes, the unsaturated zone occupies a significant position. It forms the lower boundary of a dominantly liquid-gaseous system and is a domain of transition to a dominantly liquid-solid system (van Bavel, 1966). Furthermore, this zone is amenable to manipulations for agriculture, supports forestry, and provides the physical foundation for industrial, commercial and social activities. The environmental associations from part of the soil moisture complex modify the temporal and spatial pattern of the hydrological process. The role of this zone and the influence on the moisture in retention, detention, transmission, or rejections of rainfall or snowmelt provides an important focal point for hydrological synthesis.

This chapter deals with the unsaturated zone in that moisture movements to and from this zone are an integral part of the recharge of groundwater, evaporation, crop moisture demands and runoff formation. Section 2.2 concerns with the process of infiltration and section 2.3 deals with the process of evaporation.

2.2 Infiltration

A large fraction of the water falling as rain on the land surface moves through the unsaturated soil during the subsequent processes of infiltration, drainage, evaporation, and the absorption of soil water by plant roots. Most research on this topic has been done by soil physicists, concerned ultimately with agronomic or ecological aspects of hydrology; but their colleagues in engineering hydrology have exhibited an increasing interest in this field in recent years.

Infiltration, as defined in this context, is the process of entry into the soil of water made available (under appropriately defined conditions) at its surface. The surface may be a natural, more or less horizontal upper surface of the soil; or it may be the bed of natural or artificial furrows or streams, or the walls of a natural or artificial tunnel or cavity (Philip, 1967). Absorption is a particular case of infiltration when the effect of gravity may be neglected, as in horizontal systems, in the early stage of infiltration, and in fine-textured soil in which the influence of moisture gradients dominates that of gravity.

The following sections consider the theory and calculation of infiltration which is vital in the runoff formation process in a watershed.

2.2.1 Mathematical models of infiltration

The first mathematical descriptions of infiltration were empirical formulas developed to describe the results of infiltrometer tests. The earliest infiltrometer was basically a ring driven into the ground, and infiltration rate was measured as the rate of application needed to maintain a constant level of ponded water within the ring. This method has now been largely replaced by a sprinkling application, using a larger bounded area. In either case, the resulting empirical equations describe a rate of infiltration decreasing from an initial maximum rate to a final minimum rate.

The earliest of the infiltration equations was proposed by Green and Ampt (1911). Their equation is

$$f = f_c + \frac{b}{F} \qquad [2\text{-}1]$$

where f_c and b are the characterizing constants (parameters), with f_c being the asymptotic final infiltration flux obtained when t (time) is large in this sense; f_c identifies with the near-saturated hydraulic conductivity. And F is the quantity of water infiltrated in time t per unit cross section of soil surface, such that dF/dt=f (infiltration rate). At t=0, F is also zero, so from eqn.[2-1] f is infinite but decreases asymptotically to its final value f_c.

Later Kostiakov (1932) proposed another equation which is

$$f = B\,t^{-N} \qquad [2\text{-}2]$$

where B and N are constants. This essentially empirical form does provide an infinite initial f, but asserts that it approaches zero as t increases, rather than a constant nonzero f_c. This might have relevance to purely horizontal water absorption, in which gravitational potential does not have any part to play. The absence of a constant f term is a serious weakness of this equation.

The third equation is, a popular one developed by Horton (1940),

$$f = f_c + (f_o - f_c)\, e^{-kt} \qquad [2\text{-}3]$$

where f_c, f, and k are the parameters. Unlike the previous two equations, at t=0 infiltration capacity (infiltrability) is not infinite but takes on the finite value f_o. The constant k determines how quickly f_o is reduced to f_c from f_o, and it is a best fit parameter that has little or no physical significance.

The fourth equation is that of Philip (1957) and is expressed as

$$i = S.t^{1/2} + A.t \qquad [2\text{-}4]$$

where i is the cumulative infiltration, t is time, S is the sorptivity (a parameter), and A a second parameter which is related to the analysis developed by Philip (1957). Once again, the infiltration capacity is infinite at time t equal to zero.

A somewhat more general formula was proposed by Holtan (1961) and Holtan et al. (1967) to describe infiltration and redistribution. This is defined as

$$f = f_c + a\,(S - F)^n \qquad [2\text{-}5]$$

where, f_c, a, S and n are constants S is further specified as the water storage potential of the soil above the first impeding layer (total porosity minus the antecedent soil water, expressed in units of length), but the meaning of S for a soil without an impeding layer is not clear. Furthermore, what is usually not specified explicitly about eqn.[2-5] is that it can only be understood as holding for the range $0<F<S$, since $f=f_c$ can only occur at the single point $F=S$. It is evident that when F exceeds S, the quantity $(S-F)^n$ becomes either positive and increasing, negative and decreasing, or imaginary, depending upon whether n is even, odd or fractional, respectively. It is a nonlinear storage type time dependent formula, fitted empirically to infiltrometer or watershed data.

These few examples should be sufficient to demonstrate the limitations of algebraic-empirical infiltration models. Firstly, many of them consider only infiltration from a ponded surface, which is a poor model for rainfall. Even when sprinklers are used, the data are good for only that rate of application, and assumptions must be made for other rainfall rates. Rainfall seldom falls at a given rate for a long time. Secondly, as pointed out, the parameters developed have little or no physical meaning, in that they can not be determined or estimated from knowledge of the soil, surface cover, etc. Finally, most equations cannot account for changes in initial soil water content and therefore cannot accurately predict the time of beginning of runoff and are not applicable for intermittent rainfall.

To account for the effects of the above mentioned conditions, it seems useful to use transient flow equations of soil moisture flow.

2.2.2 Moisture flow equations

The development and nature of the fundamental transient equations of saturated/unsaturated water flow in porous media are described in detail by, amongst others, Bear et al., (1968), Eagleson (1970), Corey (1986), and Bear (1988). For the purpose of the present study, it is necessary to make simplifying assumptions to facilitate the solution of the equations. The assumptions are as follows: (a) The fluid is assumed to be of constant unit density and viscosity. (b) The flow is assumed to be laminar and of low velocity in an isothermal and non-deformable porous medium. (c) The flow is assumed to be adequately described by Darcy's law, with time-invariant parameters. (d) Only single phase water flow in response to hydraulic pressure gradient are considered, the effects of air and water vapour flows, temperature, osmotic and other forces being neglected.

Within these constraints the governing equations are Darcy's Law and the Continuity Equation.

Darcy's law states that the flux of water (q) is proportional to, and in the direction of, the driving force which is the effect of the potential gradient. Mathematically, it can be stated as

$$q = -K\nabla\phi \qquad [2\text{-}6]$$

where ϕ, the hydraulic potential, is the algebraic sum of the matric potential (ψ) and gravitational potential (z). Expressing in head units (free energy per unit weight), the hydraulic potential can be written as

$$\phi = \psi - z \tag{2-7}$$

where z is the gravitational level expressed as depth below the soil surface. K is the hydraulic conductivity which in an unsaturated soil is a function of the volumetric water content, θ.

The continuity equation, states that the time rate of change of water content in a volume element of soil must equal the divergence of the flux (q)

$$\frac{\partial \theta}{\partial t} = - \nabla . q \tag{2-8}$$

These two relations are combined to give

$$\frac{\partial \theta}{\partial t} = \nabla . \left(K \nabla \phi \right) \tag{2-9}$$

which in three dimensional form can be written as

$$\frac{\partial \theta}{\partial t} = \frac{\partial}{\partial x}\left(K_x \frac{\partial \phi}{\partial x} \right) + \frac{\partial}{\partial y}\left(K_y \frac{\partial \phi}{\partial y} \right) + \frac{\partial}{\partial z}\left(K_z \frac{\partial \phi}{\partial z} \right) \tag{2-10}$$

If a function $d\theta/d\psi$, called the specific moisture capacity (Klute, 1965, 1972), can be defined, it is convenient to develop an equation with ψ as the dependent variable. Thus, substituting $\phi = \psi - z$ into eqn.[2-10] with $C(\psi) = d\theta/d\psi$ and $K = K(\psi)$ or $K = K(\theta)$ the non-linear, parabolic, partial differential equation of moisture flow is obtained as

$$C\frac{\partial\psi}{\partial t} = \frac{\partial}{\partial x}\left(K_x\frac{\partial\psi}{\partial x}\right) + \frac{\partial}{\partial y}\left(K_y\frac{\partial\psi}{\partial y}\right) + \frac{\partial}{\partial z}\left(K_z\frac{\partial\psi}{\partial z}\right) - \frac{\partial K_z}{\partial z} \qquad [2\text{-}11]$$

This is a more general form of the unsaturated flow equation presented by Richard (1931). It should be noted that the relationships $C(\psi)$ and $K(\psi)$ may not be single valued but may exhibit hysteresis so that the values of $K(\psi)$ and $C(\psi)$ at a point will depend on the past history of wetting and drying of the soil (Childs, 1972). For saturated flow $C(\psi) = 0$, the term involving the time derivative disappears, and the hydraulic conductivity will be approximately constant. Then eqn.[2-11] reduces to a quasi-linear elliptic equation.

Perhaps this is the right place to mention that the two and three dimensional soil water flow problems that arise, for example, when water is supplied from a source of finite areal dimensions on the surface, present more difficult problem for solution. However, the flow in the unsaturated soil water zone is predominantly vertical, as the lateral component of the hydraulic gradient (especially when the surface slope is small) is much much less than the vertical one. Hence attention has been focused, in this study, on obtaining solutions to Richard's equation for one dimensional vertical flow. That is the following equation

$$C\frac{\partial\psi}{\partial t}=\frac{\partial}{\partial z}\left(K_z\frac{\partial\psi}{\partial z}\right)-\frac{\partial K_z}{\partial z} \qquad [2\text{-}12]$$

is used in modeling unsaturated flow in the soil matrix.

In view of the analysis to follow, it is convenient to adopt, from this stage onwards, more practical units for some of the quantities appearing in equations of unsaturated flow. Hydraulic potential ϕ ($=z-\psi$) is expressed in cm of water, the unsaturated flow coordinate directions is expressed in cm. As it is intended to use time in hr, K most conveniently has the unit cm hr^{-1}.

2.2.3 Boundary conditions

Very often subsurface flow is treated in two parts separately: the unsaturated and saturated flow. Accordingly an interface between both flow systems is defined. For this purpose the level in the soil where the pressure is atmospheric, known as free water level, water table or phreatic surface is most commonly used. It has the advantage that it is easily measured in the field and constitutes a flow line when there is steady flow without accretion from the overlying unsaturated zone. The actual saturated zone extends to a little above the free water level due to capillary rise. The region of complete saturation above the water table is termed capillary fringe. The height of the capillary fringe depends on air entry value, i.e. the negative pressure at which the soil begins to desaturate. Gradually a less well-defined definition has come into use to include the height above the water table at which desaturation becomes significant or even to include the entire region of unsaturated flow. For solving saturated groundwater problems, the phreatic surface is usually taken as the upper boundary of the flow domain, disregarding water movement in the overlying unsaturated zone. Since the conductivity in the region just above the water table is approximately equal to the saturated hydraulic conductivity, some authors (e.g. Youngs, 1966) include the capillary fringe in the saturated flow domain. However, the height of the capillary fringe is generally small compared to the saturated thickness of the aquifer and for practical purposes the phreatic level is taken as the lower boundary of unsaturated flow and upper boundary of the saturated flow region.

Hence, in this treatise, the unsaturated zone is considered to extend from the ground surface to the water table, and the vertical flow is determined by the boundary conditions at each end of the zone.

The condition at the surface must be specified in order to determine infiltration rate. One of the two possible conditions, when infiltration occurs, is the flux condition (also known as Neuman condition). At the onset of rainfall, depending on the soil moisture status, it is usually considered that infiltration will take place at the rate of rainfall and the subsequent moisture distribution is calculated using

$$P = -K\frac{\partial\psi}{\partial z} + K \qquad [2\text{-}13]$$

If the rainfall continues and if the saturated conductivity times $(1-\delta\psi/\delta z)$ is less than the rain intensity, after some time, soil will attain saturation and ponding of excess rain water will occur. Then the surface boundary condition can be taken as a pressure boundary such that

$$\theta = \theta_s \text{ or } \psi = \psi_s \qquad [2\text{-}14]$$

where θ_s is the saturation moisture content and ψ_s is the corresponding matric potential.

The bottom boundary condition can be taken as a pressure head type as determined by the water table elevation. When groundwater does not affect the flow in the unsaturated zone, the flux condition is applied. In which cases groundwater response is very slow, and for instance over relatively short period, zero flux or no flow boundary may be assumed.

2.2.4 Hydraulic properties of the soil

The solution of eqn.[2-12] depends on a knowledge of two basic hydraulic relationships for the soil involved. These describe the relationships among θ, ψ, and K, expressed as $K(\theta)$ and $\psi(\theta)$, or $K(\psi)$ and $\theta(\psi)$.

It has been known for some time that during moisture uptake each soil exhibits a unique relation between θ and ψ (Green and Ampt, 1911; Moore, 1939; Laliberte et al., 1966) (Fig. 2-2). Unfortunately this curve is not generally determined as a basic soil property. Several investigators have attempted to describe this relation by empirical equations, but the parameters involved generally have no relation to physical, measurable soil properties. This relationship is complicated by the fact that soils exhibit (mentioned earlier) a varying amount of hysteresis between wetting (imbition) and drying (desaturation) processes. If only one or the other process is concerned, this hysteresis can be neglected. Partly due to the experimental difficulties involved in determining imbition curves, many more analyses of desaturation curves for soils are available in literature.

Brooks and Corey (1964) plotted $\ln(\theta_e)$ as a function of $\ln(\psi)$, where $\theta_e = (\theta-\theta_r)/(\theta_s-\theta_r)$. They found that if they omitted data for $\psi<\psi_e$, the data plot on a straight line, provided that a suitable value of θ_r is used to compute θ_e from measured values of θ. In fact, Brooks and Corey (1964) determined θ_r as that value of θ which made the plot a nearly straight line. Accordingly their observation data for all relatively homogeneous isotropic samples provided a linear relationship on a log-log plot. They suggested the following empirical relationship

$$\theta_e = \left(\frac{\psi_e}{\psi}\right)^{\lambda} \qquad [2\text{-}15]$$

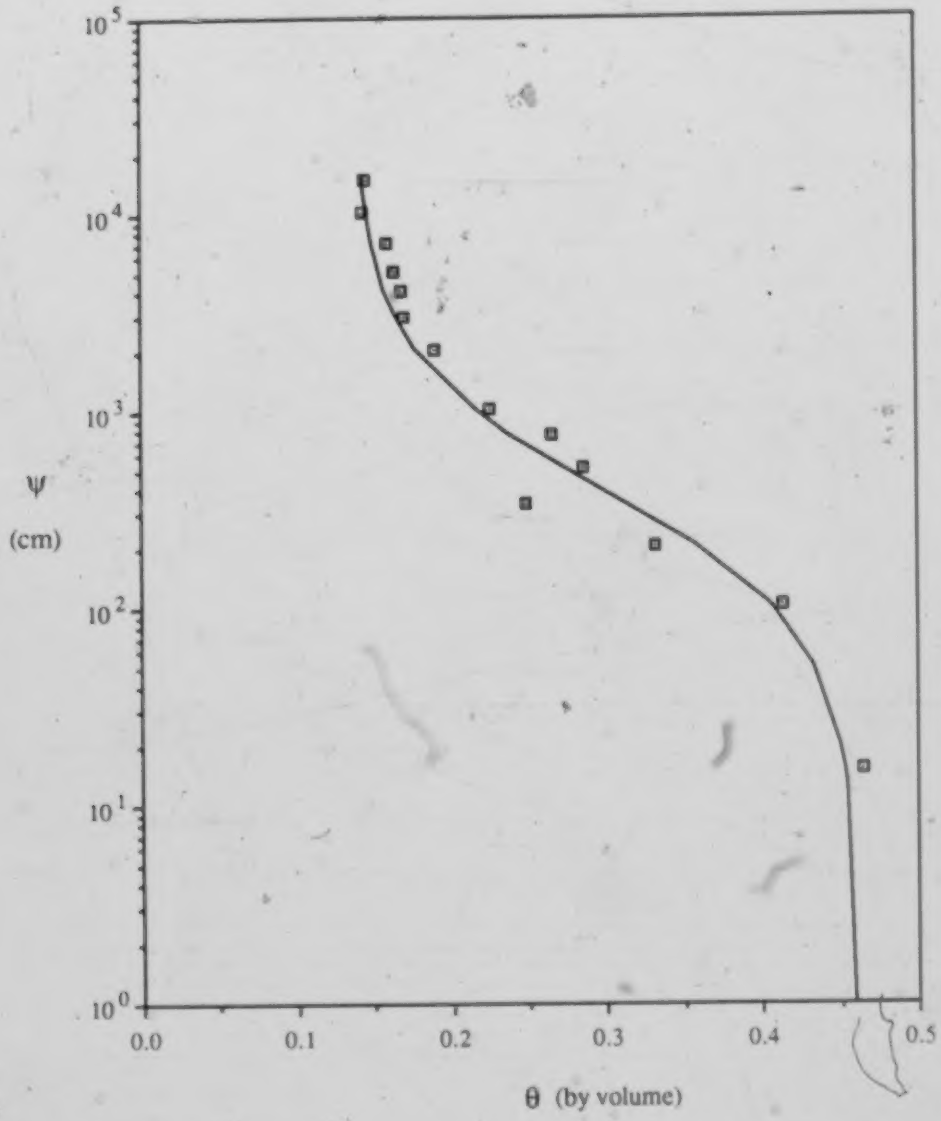

Fig. 2-2. Soil moisture characteristic (experimentally determined) of soil-C (Chapter 7) of Spring Creek watershed.

for $\psi>\psi_e$ and $\theta>\theta_r$. In this relation ψ_e is called the bubbling pressure. Soil scientists define the parameter as the air-entry pressure. Be that as it may, what the term really means is the pressure at which first desaturation in the drainage cycle occurs. According to Bresler (1987) the typical value of λ in eqn.[2-15] is 0.25-0.5.

Another expression, as suggested by Su and Brooks (1975), is

$$\psi = \psi_e \left[\frac{\theta - \theta_r}{a}\right]^{-m} \left[\frac{1 - \theta_s}{b}\right]^{\frac{bm}{a}} \qquad [2\text{-}16]$$

in which a, b, and m are constants. The constant m is roughly equivalent to $1/\lambda$ in the Brooks-Corey relationship. Su and Brooks described the physical interpretation of the constants 'a' and 'b' in their paper. No matter how physically significant these parameters are, this type of function is too expensive (requires evaluation of two exponentiations) to use in computations.

Gardner (1958) proposed a rather simple expression, defined for all ψ, which is

$$\theta(\psi) = \frac{A}{B + \psi^n} \qquad [2\text{-}17]$$

where A, B, and n are parameters and must be evaluated from observations.

From the above review it is apparent that there is no theoretical expression to uniquely describe soil characteristics. Therefore, with the present state of knowledge of soil physics, this θ-ψ relation should be considered a basic soil property to be determined for each soil by experiment.

Determination of soil moisture characteristics (i.e. θ-ψ relationship) by measurement is straightforward. On the other hand unsaturated conductivity, $K(\theta)$ or $K(\psi)$, is very difficult to measure. Even saturated conductivity poses experimental difficulties due to air blockages, leakage between the sample and the container, and the disturbance of the structure in the process of measuring conductivity. It was therefore of interest to infer permeability from a knowledge of pore space geometry by which it would be uniquely determined. As a consequence, there are several formulas expressing permeability in terms of pore size. The best known is perhaps that of Kozeny (1927). Also, similar expressions have been derived by Terzaghi (1925) and Zunker (1933). Kozeny's formula may be written in the form

$$k = \frac{c\,d^2\,p^3}{(1-p)^2} \qquad [2\text{-}18]$$

where k is the permeability (also called specific or intrinsic permeability) which has the dimension of length^2 (K, hydraulic conductivity, has the dimension of velocity), p is the porosity (ratio of pore volume to total apparent volume), c is an empirical constant, and d is a measure of particle size, which is not clearly defined.

Childs and Collis-George (1950) showed that Kozeny's formula (or this type) does not comply with experimental measurements. They developed a relationship connecting unsaturated conductivity and pore-size distribution. Their method was later modified by Marshall (1958). Nielson et al. (1960) compared these two methods with laboratory data and found that the Childs and Collis-George method was in better agreement with experimental data. Millington and Quirk (1961) made further refinements to the pore-size distribution model by considering pore interaction. Jackson et al. (1965) compared the results from all three methods with laboratory-measured conductivity values, and their findings indicate that the Millington-Quirk method fits the experimental data the best if used with a matching factor. The matching factor value may be any measured conductivity value divided by the corresponding calculated conductivity. When known, the saturation conductivity is a convenient value to use for matching purposes. The Millington-Quirk modified equation is written as

$$K(\theta)_i = \frac{K_s}{K_{sc}} \cdot \frac{30\sigma^2}{\rho g \eta} \cdot \frac{\theta}{n^2} \sum_{j=i}^{n} \left[(2j+1-2i) \frac{1}{\psi_j^2} \right] \qquad [2\text{-}19]$$

for i = 1,2,..,n;

where $K(\theta)_i$ = calculated conductivity for a specific moisture content or pressure class (cm/min), K_s/K_{sc} = matching factor {(measured saturated)/(calculated saturated) conductivities}, σ = surface tension of water (dynes/cm), ρ = density of water (g/cm^3), g = gravitational constant (cm/sec^2), η = viscosity of water (g/cm sec), θ = water-filled porosity (cm^3/cm^3), n = total number of pore classes, and ψ = pressure, suction or head (cm).

If the moisture characteristic curve is divided into n equal segments or divisions on the moisture content scale, the average pressure for each division constitutes a pressure or pore class. The ψ_1 and ψ_2 are representative of the first and second pressure classes, respectively, and ψ_n would be the nth pressure class, represented by the largest negative pressure value. As the soil is drained θ is reduced and successive pressure classes are eliminated from the calculations.

Beside this theoretically developed equation, some empirical formulas are also available in the literature, that relate permeability with matric potential (ψ). Gardner (1956) proposed a function, $K(\psi)$, which is expressed as eqn.[2-17] and has three parameters that must be evaluated from experimental data. Later, Gardner (1958) proposed a somewhat simpler expression which is

$$K(\psi) = K_s e^{-a\psi} \qquad [2\text{-}20]$$

where 'a' is a constant. Both the functions are smooth functions that predict finite decrease in $K(\psi)$ with any finite increase in ψ. In this respect, they do not agree with experimental observations, because $K(\psi)$ remains invariant over a significant range of ψ. Arbhabhirama and Kridakorn (1968) gave a similar expression as follows

$$K(\psi) = \frac{K_s}{1 + \left(\frac{\psi}{\psi_e}\right)^n} \qquad [2\text{-}21]$$

in which n is a constant, ψ_e is usually defined as air entry value of ψ.

With a proper choice of constants, however, the functions can be made to approach actual behaviour very closely. Moreover, the use of a smooth function is convenient for computations. Neither eqn.[2-17] nor eqn.[2-20] are dimensionally homogeneous so that the constants used depend upon the units in which the variables are expressed. But eqn.[2-21] is dimensionally consistent.

Another dimensionally homogeneous relationship is that of Brooks and Corey (1964). Their formula is

$$\begin{aligned} K(\psi) &= K_s\left(\frac{\psi_e}{\psi}\right)^{\eta} && \text{for } \psi < \psi_e \\ K(\psi) &= K_s && \text{for } \psi \geq \psi_e \end{aligned} \qquad [2\text{-}22]$$

According to Corey (1986) this function is realistic to the extent that it predicts a finite range of ψ over which $K(\psi)$ is invariant and it comes closer than the other relationships in describing $K(\psi)$. Bresler (1987) reported that the value of η is 2.0-3.5. Brooks and Corey (1964) also provided a formula for expressing η in terms of λ, which is

$$\eta = 2 + 3\lambda \qquad [2\text{-}23]$$

Thus, Brooks and Corey describe the soil hydraulic properties by the four constants, θ_s, θ_r, K_s, η or λ.

In this study the Brooks and Corey relationships is used. Other types of relationships could be used as well.

2.2.5 Solution of flow equation

It has been mentioned in section 1.5 that to obtain an analytical solution, if one exists, for Richard's equation, is extremely difficult. Therefore, numerical approximation methods are often considered as the only means for its solution. Klute (1952) solved this equation numerically, using transformation of variables and constant upper boundary saturation. Later, Philip (1957) showed a method for applying similarity solution techniques to the vertical case, using a series of successive approximations. With a hand calculator, this method was quite laborious. Again, a given saturation at the surface for t>0 was used as the upper boundary condition.

With the advent of high speed computers, the method of F-D was applied to this equation, and researchers have developed methods to solve eqn.[2-12] for boundary conditions that better approximate situations for a variety of applications. Several of the important contributors to the solution techniques for the problem of vertical downward flow of moisture from surface input and the major features of their numerical methods are listed in Table 2-2.

Table 2-2. Review of numerical solutions of unsaturated flow problems.

Type of problem	Solved by
1-dimensional infiltration and drainage	Klute, 1952; Nielsen et al., 1961; Hanks and Bowers, 1962; Rubin and Steinhardt, 1963; Green et al., 1964; Remson et al., 1965; Klute et al., 1965; Wang and Lakshminarayana, 1968; Staple, 1969; Freeze, 1969; Watson, 1971; Whisler et al. 1972;; Hillel and van Bavel, 1976; Kirkham, 1976; Havekamp et al., 1977; Hornung, 1977; Hayhoe, 1978; Dane and Mathis, 1981.
1-dimensional drainage with evaporation	Whisler et al., 1968, 1972; Hanks et al., 1969; Nimah and Hanks, 1973; Feddes, 1985.
2-dimensional partially saturated flow	Rubin, 1968; Hornberger et al., 1969; Verma and Brutsaert, 1970; Brutsaert, 1971; Freeze, 1972a, 1972b; Stephenson and Freeze, 1974; Neuman et al., 1975; Vauclin et al., 1975; Cushman et al., 1979; Fayer and Hillel, 1982.
3-dimensional partially saturated flow	Freeze, 1971a, 1971b; Rovey, 1975.
Solution involving hysteresis	Whisler and Klute, 1965, 1967; Rubin, 1967; Ibrahim and Brutsaert, 1968; Dane and Weiringa, 1975, Hillel, 1977.

2.2.6 Finite difference formulation

Generally F-D equations are derived by approximating the derivatives in the differential equations via a truncated Taylor series. For a grid point 2, midway between points 1 and 3, such that $\Delta x = x_2 - x_1 = x_3 - x_2$, some function, ϕ, can be expanded around point 2 using Taylor series. Truncating the series after the 3rd term (which yields second order accuracy), and by addition and subtraction of the two equations, one can obtain the following expressions for evaluating the first and second order derivatives of the function, ϕ, at point 2.

$$\left(\frac{d\phi}{dx} \right)_2 \approx \frac{\phi_3 - \phi_1}{2\Delta x}$$

$$\left(\frac{d^2\phi}{dx^2} \right)_2 \approx \frac{\phi_1 + \phi_3 - 2\phi_2}{(\Delta x)^2}$$

However, it is not necessary that always three points have to be used to evaluate first and second derivatives. The above example, uses the scheme called centered difference scheme, is just one of the many possible cases. The substitution of such expressions into the differential equation leads to the finite difference equation.

The other way to formulate a differential equation is the control volume method (Patankar, 1980). The basic idea of the control-volume formulation is easy to understand and leads itself to direct physical interpretation. The calculation domain is divided into a number of non-overlapping control volumes such that there is one control volume numbering each grid point. The differential equation is integrated over each control-volume. Piecewise profiles expressing the variation of ϕ between the grid points are used to evaluate the required integrals. The discretization equation obtained in this manner expresses the conservation principle for ϕ for the finite control volume, just as the differential equation expresses it for an infinitesimal control-volume. Nevertheless, there is nothing magical in this formulation, and in fact it can be shown that this formulation is equivalent to centered difference F-D equations for certain choice of linear interpolation.

The present problem of solving unsaturated flow equations has been formulated using the control volume method. In this case, it will be easy to follow the steps in F-D formulation if eqn.[2-8] is considered in lieu of eqn.[2-12]. The one dimensional form of eqn.[2-8] in F-D form can be written as

$$\frac{\Delta\theta}{\Delta t} = \frac{\Delta q}{\Delta z} \qquad [2\text{-}24]$$

Referring to Fig. 2-3, for an interior control volume, j, with $\Delta\theta/\Delta t$ substituted by $C(\psi)(\Delta\psi/\Delta t)$ (see paragraph preceded by eqn.[2-11]), eqn.[2-24] takes the form

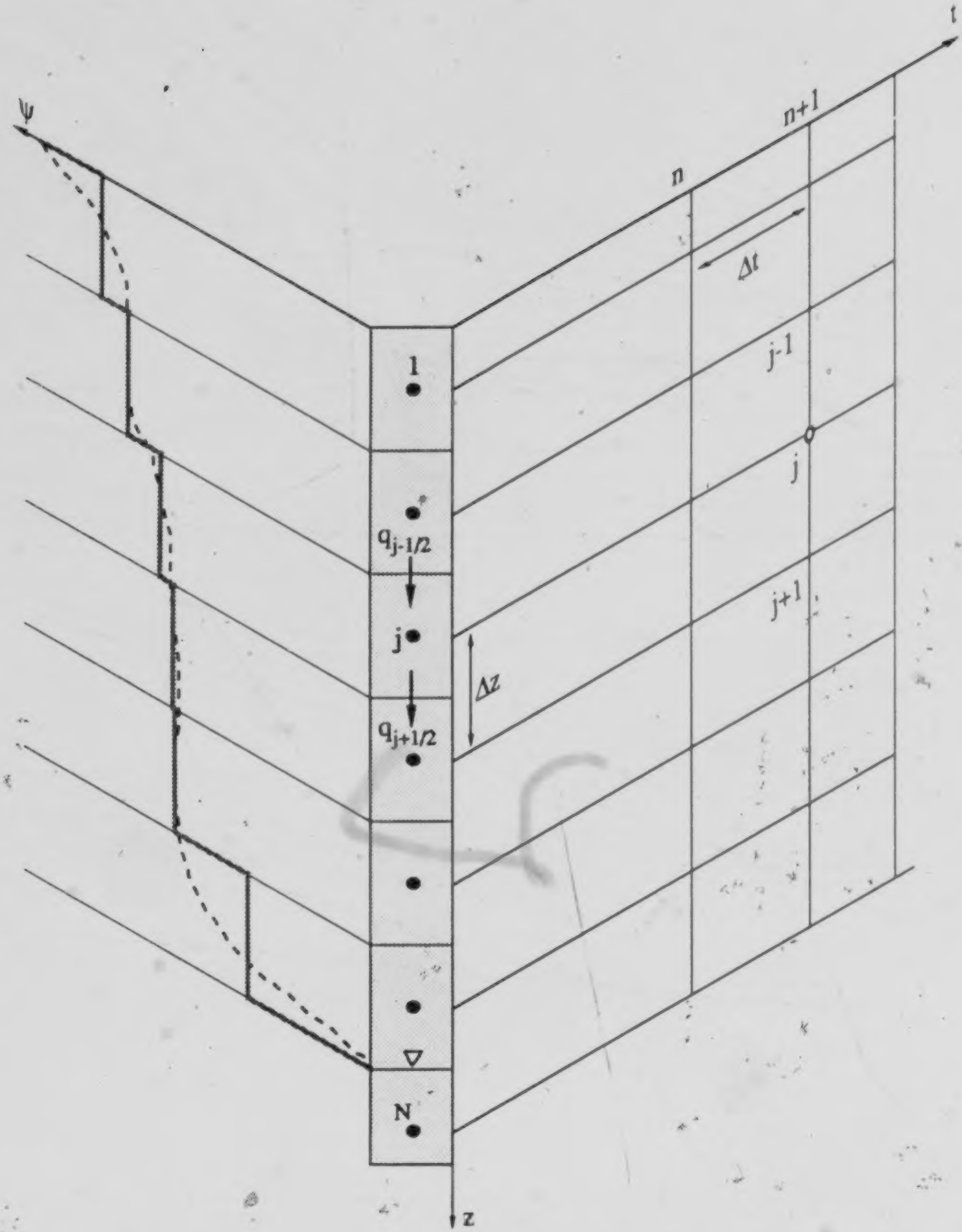
ψ
t
n
n+1
Δt
1
j-1
j
$q_{j-1/2}$
j
j+1
Δz
$q_{j+1/2}$
∇
N
z

Fig. 2-3. F-D grid in the z-t plane showing location of grid points and counter, n, j; actaul (dashed line) and F-D approximate (low intensity line) profiles of matric potential (ψ) at a particular time; q - vertical flow across control volume boundaries; 1, j, N are computational nodes.

$$C_j \frac{\Delta\psi_j}{\Delta t} = \frac{q_{j-1/2} - q_{j+1/2}}{\Delta z} \qquad [2\text{-}25]$$

where $q_{j-1/2}$ and $q_{j+1/2}$ are the inflow to and outflow from the control volume, j (of thickness Δz), and is defined by

$$\begin{aligned} q_{j-1/2} &= -K_{j-1/2}\frac{\phi_{j-1} - \phi_j}{\Delta z} \\ q_{j+1/2} &= -K_{j+1/2}\frac{\phi_j - \phi_{j+1}}{\Delta z} \end{aligned} \qquad [2\text{-}26]$$

Substitution of $\phi=\psi-z$, $q_{j-1/2}$, and $q_{j+1/2}$ in eqn.[2-26] yields

$$C_j \frac{\Delta\psi_j}{\Delta t} = K_{j+1/2}\frac{\psi_j - \psi_{j+1} + \Delta z}{(\Delta z)^2} - K_{j-1/2}\frac{\psi_{j-1} - \psi_j + \Delta z}{(\Delta z)^2} \qquad [2\text{-}27]$$

The weighted implicit F-D form of eqn.[2-27] over one time step is

$$\begin{aligned} &C_j^{n+1/2}\frac{\psi_j^{n+1} - \psi_j^n}{\Delta t}\Delta z = \\ &\omega\left(K_{j+1/2}^{n+1/2}\frac{\psi_j^{n+1} - \psi_{j+1}^{n+1} + \Delta z}{\Delta z} - K_{j-1/2}^{n+1/2}\frac{\psi_{j-1}^{n+1} - \psi_j^{n+1} + \Delta z}{\Delta z}\right) \\ &+ (1-\omega)\left(K_{j+1/2}^{n+1/2}\frac{\psi_j^{n} - \psi_{j+1}^{n} + \Delta z}{\Delta z} - K_{j+1/2}^{n+1/2}\frac{\psi_{j-1}^{n} - \psi_j^{n} + \Delta z}{\Delta z}\right) \end{aligned} \qquad [2\text{-}28]$$

where ω is a weighting factor.

In the above equation the subscript j refers to the spatial increment and the superscript n refers to the time increment. The hydraulic conductivity K is centered in space and time by using the arithmetic mean:

$$\begin{aligned} K_j^{n+1/2} &= K\left(\frac{\psi_j^{n+1} + \psi_j^n}{2}\right) \\ K_{j+1}^{n+1/2} &= K\left(\frac{\psi_{j+1}^{n+1} + \psi_{j+1}^n}{2}\right) \\ K_{j+1/2}^{n+1/2} &= \left(\frac{K_j^{n+1/2} + K_{j+1}^{n+1/2}}{2}\right) \\ C_j^{n+1/2} &= C\left(\frac{\psi_j^{n+1} + \psi_j^n}{2}\right) \end{aligned} \qquad [2\text{-}29]$$

Rearranging eqn.[2-28] the following expression is obtained

$$\begin{aligned} G_j &= \rho C_j^{n+1/2}\left(\psi_j^{n+1} - \psi_j^n\right) \\ &- \omega\left(K_{j+1/2}^{n+1/2}\left[\psi_j^{n+1} - \psi_{j+1}^{n+1} + \Delta z\right] - K_{j-1/2}^{n-1/2}\left[\psi_{j-1}^{n+1} - \psi_j^{n+1} + \Delta z\right]\right) \\ &- (1-\omega)\left(K_{j+1/2}^{n+1/2}\left[\psi_j^n - \psi_{j+1}^n + \Delta z\right] - K_{j+1/2}^{n+1/2}\left[\psi_{j-1}^n - \psi_j^n + \Delta z\right]\right) = 0 \end{aligned} \qquad [2\text{-}30]$$

where $\rho = (\Delta z)^2/\Delta t$, G is just a name given to the equation. Eqn.[2-30] involves 3 unknowns at time n+1 and 3 known values at time n for each node. Writing for all nodes with reference to Fig. 2-3 a system of N-2 equations with N unknowns is obtained. Additional two equations are provided by the top and bottom boundary conditions. The precipitation and constant moisture content conditions at the top and bottom boundaries give

$$\begin{aligned} C_1^{n+1/2}\frac{\psi_1^{n+1} - \psi_1^n}{\Delta t}\Delta z &= \omega\left(R^{n+1} - K_{1+1/2}^{n+1/2}\frac{\psi_1^{n+1} - \psi_2^{n+1} + \Delta z}{\Delta z}\right) \\ &+ (1-\omega)\left(R^n - K_{1+1/2}^{n+1/2}\frac{\psi_1^n - \psi_2^n + \Delta z}{\Delta z}\right) \end{aligned}$$

or

$$G_1 = \rho C_1^{n+1/2} (\psi_1^{n+1} - \psi_1^n) - \omega\left(R^{n+1} - K_{1+1/2}^{n+1/2} [\psi_1^{n+1} - \psi_2^{n+1} + \Delta z]\right) - (1-\omega)\left(R^n - K_{1+1/2}^{n+1/2}\left[\psi_1^n - \psi_2^n + \Delta z\right]\right) = 0 \qquad [2\text{-}31]$$

and

$$G_N = \psi_N^{n+1} - \psi_N^n = 0 \qquad [2\text{-}32]$$

Then the system of N algebraic equations, for the sake of convenience, is written in the form

$$\begin{aligned} &G_1\left(\psi_1^{n+1}, \psi_2^{n+1}\right) && = 0 \\ &G_2\left(\psi_1^{n+1}, \psi_2^{n+1}, \psi_3^{n+1}\right) && = 0 \\ &G_3\left(\psi_2^{n+1}, \psi_3^{n+1}, \psi_4^{n+1}\right) && = 0 \\ &\quad . \;\; . \;\; . && . \\ &G_j\left(\psi_{j-1}^{n+1}, \psi_j^{n+1}, \psi_{j+1}^{n+1}\right) && = 0 \\ &\quad . \;\; . \;\; . && . \\ &G_{N-1}\left(\psi_{N-1}^{n+1}, \psi_N^{n+1}\right) && = 0 \end{aligned} \qquad [2\text{-}33]$$

Since the coefficients ψ's i.e. K's and C's are functions of the dependent variable ψ, the system of equations is nonlinear. The Newton-Raphson (N-R) iterative method is adopted to solve this system of nonlinear equations.

The iterative method

According to the N-R method, computation for the iterative procedure begins by assigning a set of trial values to N unknowns ψ^{n+1}, for j = 1, 2, 3, ..., N. Substitution of the trial values into eqn.[2-33] yields the residuals r(G_j).

New values of ψ^{n+1} are estimated for the next iteration to make the residuals approach to zero. This is accomplished by computing the corrections $\Delta\psi_j$ such that the total differentials of the functions G_j are equal to the negative of the calculated residuals, i.e.

$$\frac{\partial G_j}{\partial \psi_{j-1}^{n+1}} \Delta\psi_{j-1}^{n+1} + \frac{\partial G_j}{\partial \psi_{j}^{n+1}} \Delta\psi_{j}^{n+1} + \frac{\partial G_j}{\partial \psi_{j+1}^{n+1}} \Delta\psi_{j+1}^{n+1} = -r(G_j) \qquad [2\text{-}34]$$

Eqn.[2-34] written for $j = 1, 2, 3, \ldots, N$ forms sets of N linear algebraic equation in N unknowns, $\Delta\psi_j$. In matrix notation, this linear system of equations is

$$\begin{bmatrix} \frac{\partial G_1}{\partial \psi_1^{n+1}} & \frac{\partial G_1}{\partial \psi_2^{n+1}} & 0 & 0 & . & 0 & 0 \\ \frac{\partial G_2}{\partial \psi_1^{n+1}} & \frac{\partial G_2}{\partial \psi_2^{n+1}} & \frac{\partial G_2}{\partial \psi_3^{n+1}} & 0 & . & 0 & 0 \\ 0 & \frac{\partial G_3}{\partial \psi_2^{n+1}} & \frac{\partial G_3}{\partial \psi_3^{n+1}} & \frac{\partial G_3}{\partial \psi_4^{n+1}} & . & 0 & 0 \\ . & . & . & . & . & . & . \\ 0 & 0 & 0 & 0 & . & \frac{\partial G_{N-1}}{\partial \psi_{N-1}^{n+1}} & \frac{\partial G_{N-1}}{\partial \psi_N^{n+1}} \\ 0 & 0 & 0 & 0 & . & 0 & \frac{\partial G_N}{\partial \psi_N^{n+1}} \end{bmatrix} \begin{bmatrix} \Delta\psi_1^{n+1} \\ \Delta\psi_2^{n+1} \\ \Delta\psi_3^{n+1} \\ . \\ \Delta\psi_{N-1}^{n+1} \\ \Delta\psi_N^{n+1} \end{bmatrix} = \begin{bmatrix} -r(G_1) \\ -r(G_2) \\ -r(G_3) \\ . \\ -r(G_{N-1}) \\ -r(G_N) \end{bmatrix} \qquad [2\text{-}35]$$

Numerous techniques exist for the numerical solution of the systems of linear equations such as the ones given above. One of the most widely used methods for solving simultaneous equations is Gaussian elimination. (The term 'elimination' is derived from the process whereby unknowns are successively eliminated by combining equations.) Gaussian elimination is a two-step method. By successive combinations of equations, all of the coefficients in the matrix below the diagonal are eliminated to form an upper triangular matrix. After the upper triangular matrix has been formed, the unknowns such as $\Delta\psi$ are determined by back substitution of the lower equations into those higher in the matrix. The equation used to eliminate the unknowns in the other equations is called the pivot equation.

Matrix solution

It is evident from eqn.[2-35] that the coefficient matrix has a banded structure. Because of the control volume type of formulation (equivalent to centered finite difference scheme) it involves three sequential nodes. As a result this banded matrix turned out to be a tridiagonal one. A similar form will be encountered in cases of saturated flow and overland flow. However, the story is a quite different one, when the flow in the channel network is considered (Chapter 5). Due to the presence of multi-channel junctions in the network the coefficient matrix loses its banded structure. Consequently a different ploy needs to be adopted and is described in the respective sections.

Returning to the present tridiagonal case, which allows solution for the column vector $\Delta\psi_j$ which is an algorithm for Gauss elimination, the computational procedure is discussed now. To conserve storage in the computer, the tridiagonal matrix of coefficients is compressed together with the right hand terms, into an mx4 matrix. Column one holds the coefficients to the left of the diagonal, column two holds the diagonal terms, column three holds the coefficients to the right of the diagonal, and column four holds the right hand side terms. The ith and (i-1)th rows of the compressed matrix correspond to elements in the uncompressed matrix, as shown:

$$\begin{array}{ccccccc}
 & \cdot & \cdot & \cdot & \cdot & & \cdot \\
\cdot & A_{i-1,1} & A_{i-1,2} & A_{i-1,3} & \cdot & \cdot & A_{i-1,4} \\
\cdot & \cdot & A_{i,1} & A_{i,2} & A_{i,3} & \cdot & A_{i,4} \\
\cdot & \cdot & \cdot & \cdot & \cdot & \cdot & \cdot
\end{array}$$

One can eliminate $A_{i,1}$ by substituting $A_{i,1}/A_{i-1,2}$ times the (i-1)st row from the ith row. Since one knows a zero will replace $A_{i,1}$, one does not need actually to perform the arithmetic. Following Thomas algorithm (cf. Gerald, 1980) the values of $A_{i,2}$ and $A_{i,4}$ are changed as given below:

$$A_{i,2} = A_{i,2} - \frac{A_{i,1}}{A_{i-1,2}} * A_{i-1,3}$$

$$A_{i,4} = A_{i,4} - \frac{A_{i,1}}{A_{i-1,2}} * A_{i-1,4}$$

for $i = 2, 3, 4, \ldots, m$.

When the ith row is reduced, $A_{i,3}$ is unaffected because there is a zero above it. Element $A_{1,1}$ and $A_{m,3}$ are never referred to and their values can be anything, or they can be left unaltered.

After reduction, a back-substitution is performed. The elements of the solution vector replace the right hand side vector in the fourth column of the matrix.

The equations for back-substitution are:

$$A_{m,4} = \frac{A_{m,4}}{A_{m,2}}$$

$$A_{i,4} = \frac{A_{i,4} - A_{i,3} * A_{i+1,4}}{A_{i,2}}$$

for i = m-1, m-2, ..., 1.

Solution of equation for a given time-step

It is seen that the coefficients of the matrix consist of partial derivatives and these must be evaluated. This can be accomplished using either analytical or numerical methods. Obtaining derivatives using numerical method was thought to be computationally expensive, hence, an analytical method is used. Accordingly, the derivative coefficients are obtained by differentiating eqn.[2-32] and eqn.[2-31] and these are as follows:

$$\frac{\partial G_1}{\partial \psi_1^{n+1}} = C_1^* + \omega B_1^{n+1} + (1-\omega) B_1^n$$

$$\cdots$$

$$\begin{aligned}
\frac{\partial G_j}{\partial \psi_{j-1}^{n+1}} &= \omega A_{j-1}^{n+1} + (1-\omega) A_{j-1}^n \\
\frac{\partial G_j}{\partial \psi_{j-1}^{n+1}} &= C_j^* + \omega \left(A_j^{n+1} + B_j^{n+1} \right) + (1-\omega) \left(A_j^n + B_j^n \right) \qquad [2\text{-}36] \\
\frac{\partial G_j}{\partial \psi_{j+1}^{n+1}} &= \omega B_{j+1}^{n+1} + (1-\omega) B_{j+1}^n
\end{aligned}$$

$$\cdots$$

where A, B and C^* are given in the page overleaf.

$$
\begin{aligned}
C_1^{*} &= -\rho\, C_1^{n+1/2}\left(\psi_1^{n+1} - \psi_1^{n}\right) - \rho\, C_1^{n+1/2}\\
B_1^{n+1} &= -\frac{\partial K_{1+1/2}^{n+1/2}}{\partial \psi_1^{n+1}}\left(\psi_1^{n+1} - \psi_2^{n+1} + \Delta z\right) - K_{1+1/2}^{n+1/2}\\
B_1^{n} &= -\frac{\partial K_{1+1/2}^{n+1/2}}{\partial \psi_1^{n+1}}\left(\psi_1^{n} - \psi_2^{n} + \Delta z\right)\\
A_{j-1}^{n+1} &= -\frac{\partial K_{j-1/2}^{n+1/2}}{\partial \psi_{j-1}^{n+1}}\left(\psi_{j-1}^{n+1} - \psi_j^{n+1} + \Delta z\right) - K_{j-1/2}^{n+1/2}\\
A_{j-1}^{n} &= -\frac{\partial K_{j-1/2}^{n+1/2}}{\partial \psi_{j-1}^{n+1}}\left(\psi_{j-1}^{n} - \psi_j^{n} + \Delta z\right)\\
C_j^{*} &= -\rho\, C_j^{n+1/2}\left(\psi_j^{n+1} - \psi_j^{n}\right) - \rho\, C_j^{n+1/2}\\
A_j^{n+1} &= -\frac{\partial K_{j-1/2}^{n+1/2}}{\partial \psi_j^{n+1}}\left(\psi_{j-1}^{n+1} - \psi_j^{n+1} + \Delta z\right) - K_{j-1/2}^{n+1/2}\\
A_j^{n} &= -\frac{\partial K_{j-1/2}^{n+1/2}}{\partial \psi_j^{n+1}}\left(\psi_{j-1}^{n} - \psi_j^{n} + \Delta z\right)\\
B_j^{n+1} &= -\frac{\partial K_{j+1/2}^{n+1/2}}{\partial \psi_j^{n+1}}\left(\psi_j^{n+1} - \psi_{j+1}^{n+1} + \Delta z\right) - K_{j+1/2}^{n+1/2}\\
B_j^{n} &= -\frac{\partial K_{j+1/2}^{n+1/2}}{\partial \psi_j^{n+1}}\left(\psi_j^{n} - \psi_{j+1}^{n} + \Delta z\right)\\
B_{j+1}^{n+1} &= -\frac{\partial K_{j+1/2}^{n+1/2}}{\partial \psi_{j+1}^{n+1}}\left(\psi_j^{n+1} - \psi_{j+1}^{n+1} + \Delta z\right) - K_{j+1/2}^{n+1/2}\\
B_{j+1}^{n} &= -\frac{\partial K_{j+1/2}^{n+1/2}}{\partial \psi_{j+1}^{n+1}}\left(\psi_j^{n} - \psi_{j+1}^{n} + \Delta z\right)
\end{aligned}
\tag{2-37}
$$

The following items summarize the main features of the solution process:

1. Soil data input

For calculation of values of $K(\psi)$ and $d\theta/d\psi = C(\psi)$, and all other coefficients in eqn.[2-33], the hydraulic properties of the soil must be known from the experimental measurements of soil properties $K(\psi)$ and $\psi(\theta)$. Before the measurements can be useful in numerical analysis, the input data must be either described with a functional relationship or reduced to tabular form. The empirical equation for soil variables, as described in section 2.2.4, has the ease of handling and programming for a numerical solution. Therefore, some specific functional relationships for the soil property is imposed in this analysis. These functions were fitted to the soil data to evaluate their parameters.

2. Iteration

The iterative procedure applied in the numerical solution within each time-step is as follows:

The coefficients of the equations are evaluated, for node j, using

$$\psi_j^{n+1/2} = \frac{\psi_j^{n+1} + \psi_j^n}{2} \qquad [2\text{-}38]$$

which requires estimates of ψ_j^{n+1}. For the first iteration of the first time-step, these are given by

$$\psi_{j,k=1}^1 = \psi_j^0 \qquad [2\text{-}39]$$

where k is an iterative count and ψ^0_j refers to specified initial values of ψ at node j. For the first iteration of later time-steps a linear interpolation of the solutions over time is used for the initial estimates, of the form

$$\psi_{j,k=1}^{n+1} = \psi_j^n + \frac{\Delta t}{\Delta t'}\left(\psi_j^n - \psi_j^{n-\Delta t'}\right) \qquad [2\text{-}40]$$

where $\Delta t'$ is the previous time step.

Thus a set of simultaneous equations

$$[A]\left\{\Delta\psi\right\}^{n+1} = -\left\{r\right\} \qquad [2\text{-}41]$$

is solved to obtain the corrections $\Delta\psi_j$ and an improved estimate of ψ_j^{n+1} is obtained as

$$\psi_{j,k=2}^{n+1} = \psi_{j,k=1}^{n+1} + \Delta\psi_j^{n+1} \qquad [2\text{-}42]$$

At each time-step the iteration process is continued until the maximum nodal change in ψ i.e. $\Delta\psi$ between iterations (nodal residuals) is less than some convergence criteria, ε, or

$$\left|\Delta\psi_{j,k}^{n+1}\right|_{\max} \leq \varepsilon \qquad [2\text{-}43]$$

At the end of each iteration, the rate of convergence may sometimes be increased by applying an acceleration equation to the calculated values of $\Delta\psi_j$ at each node. This takes the form

$$\psi^{n+1}_{j,k+1} = \psi^{n+1}_{j,k} + w\Delta\psi^{n+1}_{j,k} \qquad [2\text{-}44]$$

where w is an acceleration or over relaxation parameter.

Calculation of infiltration

The cumulative infiltration after the nth time increment, CI^n is just the change in moisture content over that time period and is given as

$$CI^n = \sum_{j=1}^{N} \Delta z_j \left\{\theta_j^{n+1} - \theta_j^0\right\} \qquad [2\text{-}45]$$

where θ^0 is the initial moisture content. The infiltration rate is calculated by

$$I^{n+1/2} = \frac{1}{\Delta t} \sum_{j=1}^{N} \Delta z_j \left\{\theta_j^{n+1} - \theta_j^n\right\} \qquad [2\text{-}46]$$

The infiltration rate can also be found from the finite difference form of Darcy's law as given by

$$I^{n+1/2} = -\left\{\frac{\phi_2^n - \phi_1^n}{2\Delta z} + \frac{\phi_2^{n+1} - \phi_1^{n+1}}{2\Delta z}\right\} K\left(\psi^{n+1/2}_{1/2}\right) \qquad [2\text{-}47]$$

which, on substitution of ψ-z for ϕ and Δz for $z_2 - z_1$ yields

$$I^{n+1/2} = -\left\{\frac{\psi_2^n + \psi_2^{n+1} - \psi_1^n - \psi_1^{n+1} + 2\Delta z}{2\Delta z}\right\} K\left(\psi^{n+1/2}_{1/2}\right) \qquad [2\text{-}48]$$

2.2.7 Some applications of the F-D solutions

According to the preceding description, a computer program has been written in FORTRAN-77 for solving unsaturated flow problems. Using this program a few example problems of different boundary and initial conditions were solved. The first example refers to a one dimensional infiltration problem for which an analytical solution was derived by Philip (1957), solution using 'dynamic simulation language (S/360 CSMP)' was obtained by Bhuiyan et al. (1971), and solution using finite element method was obtained by Hillman (1983). The soil is Yolo Light clay. It is a well reported soil in the literature of infiltration studies (Philip, 1957; Watson, 1965; Rubin, 1968; Parlange, 1971; Bhuiyan et al., 1971; Kirhkam and Powers, 1972; Philip and Knight, 1974; Haverkamp et al., 1977; Hillman, 1983). This soil consists of 23.8% sand, 45% silt, 31.2% clay, with pore space of 50% (Moore, 1939). The soil hydraulic properties, as described by Rubin (1968), are expressed empirically as follows:

$$K = \frac{0.00463}{400 + \psi^2}$$

$$\theta = 0.6009 - 0.05708 \ln (10 - \psi) \qquad [2\text{-}49]$$

$$+ \frac{0.0594}{\cosh (0.747 + 0.0415\psi)} - 0.0133\, e^{(0.4055 + 0.2\,\psi)}$$

Later Haverkamp et al. (1977) fitted another set of empirical curves which are

$$K = K_s \frac{A}{A + |\psi|^B}$$

$$[2\text{-}50]$$

$$\theta = \frac{\alpha\, (\theta_s - \theta_r)}{\alpha + (\ln|\psi|)^\beta} + \theta_r$$

where $K_s = 4.428\times10^{-2}$ cm/hr, A = 124.6, B = 1.77, $\theta_s = 0.495$, $\theta_r = 0.124$ and

$$\alpha = 739\,,\ \beta = 4 \quad \text{for } \psi < -1$$

$$\theta = \theta_s \qquad \text{for } \psi \geq -1$$

Hillman (1983) in his calculation used eqn.[2-49]. As these expressions seemed unwieldy, in this treatise the latter relations were used instead. The solution was obtained for no flow boundaries on either side. The surface node was maintained at saturation (ψ=0) throughout the simulation. The initial condition for the rest of the profile was ψ=-660 cm of water.

For this simulation, the time step, Δt, and grid spacing, Δx, were 3 min and 1 cm respectively. For this essentially very simple problem the solution converged in 2 to 3 iterations with a convergence criteria of 0.01 cm. Fig. 2-4 shows soil moisture profiles after 2.77 hr of infiltration as obtained by different methods. The computational information regarding all these solutions are summarized in Table 2-3. The results of the F-D solution seems in agreement with those of Philip's analytical, Bhuiyan's CSMP, Hillman's finite element solutions.

Table 2-3. Computational imformations.

Solved by	Δx (cm)	Δt (min)	ε	Iteration	CPU time (sec)
Bhuiyan	1	-	-	-	-
Hillman	1	0.666	0.01	4-8	-
Current	1	0.5 - 5.0	0.01	2-3	1.387

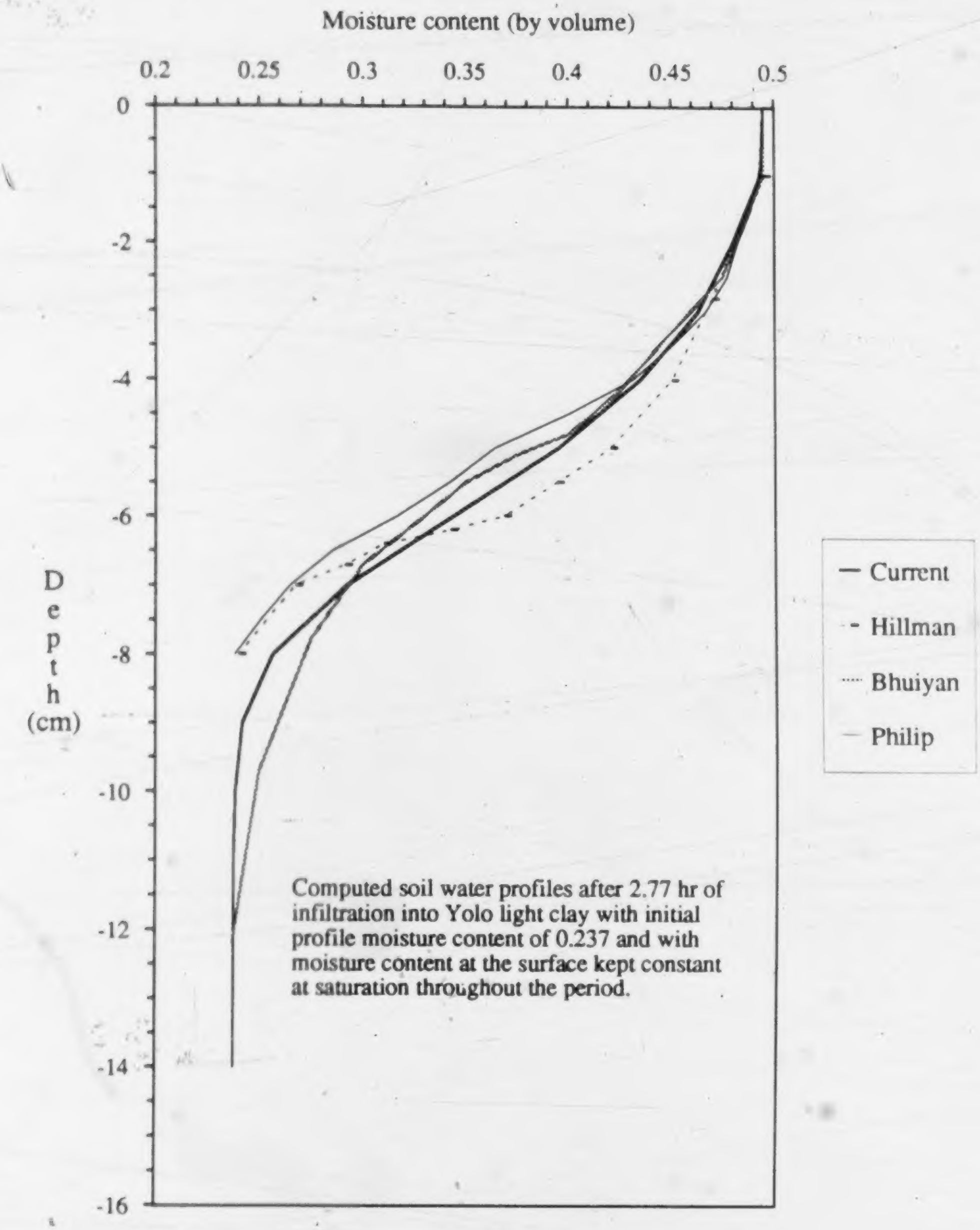

Fig. 2-4. Comparison of current solution with those obtained by Philip (1957), Bhuiyan et al. (1971), and Hillman (1983).

In the previous cases the authors claimed that their solutions are comparable with each other. However, no mention was made regarding agreement with experimental data. Therefore, a second example problem for which experimental data were available (Haverkamp et al., 1977), was solved. Functions characterizing the hydraulic properties are

$$K = K_s \frac{A}{A + \psi^B}$$

$$\theta = \frac{\alpha\,(\theta_s - \theta_r)}{\alpha + \psi^\beta} + \theta_r \qquad [2\text{-}51]$$

where K_s = 34 cm/hr, A = 1.175x10^6, B = 4.74, θ_s = 0.287, θ_r = 0.075 and β = 3.96.

For this problem, the upper (or surface) boundary was a Neuman type with rainfall intensity, P, equal to 13.69 cm per hr and bottom boundary was a Dirichlet type of constant potential (or moisture content = 0.10 cm^3/cm^3) equal to -61.5 cm. Computational parameters such as Δt and Δx were 5 min and 1 cm respectively. Fig. 2-5 presents calculated and experimental moisture profiles at t=0.8 hr after 10.952 cm of water had infiltrated into the soil. From comparison it appears that the calculations and observations are in good agreement. However, another run with Δx=5 cm resulted in a deviated profile (Fig. 2-5). It is discernible that a finer computational mesh produces better solution. It should be noted that refining of the mesh does not necessarily yield a correct solution and even it may introduce instability

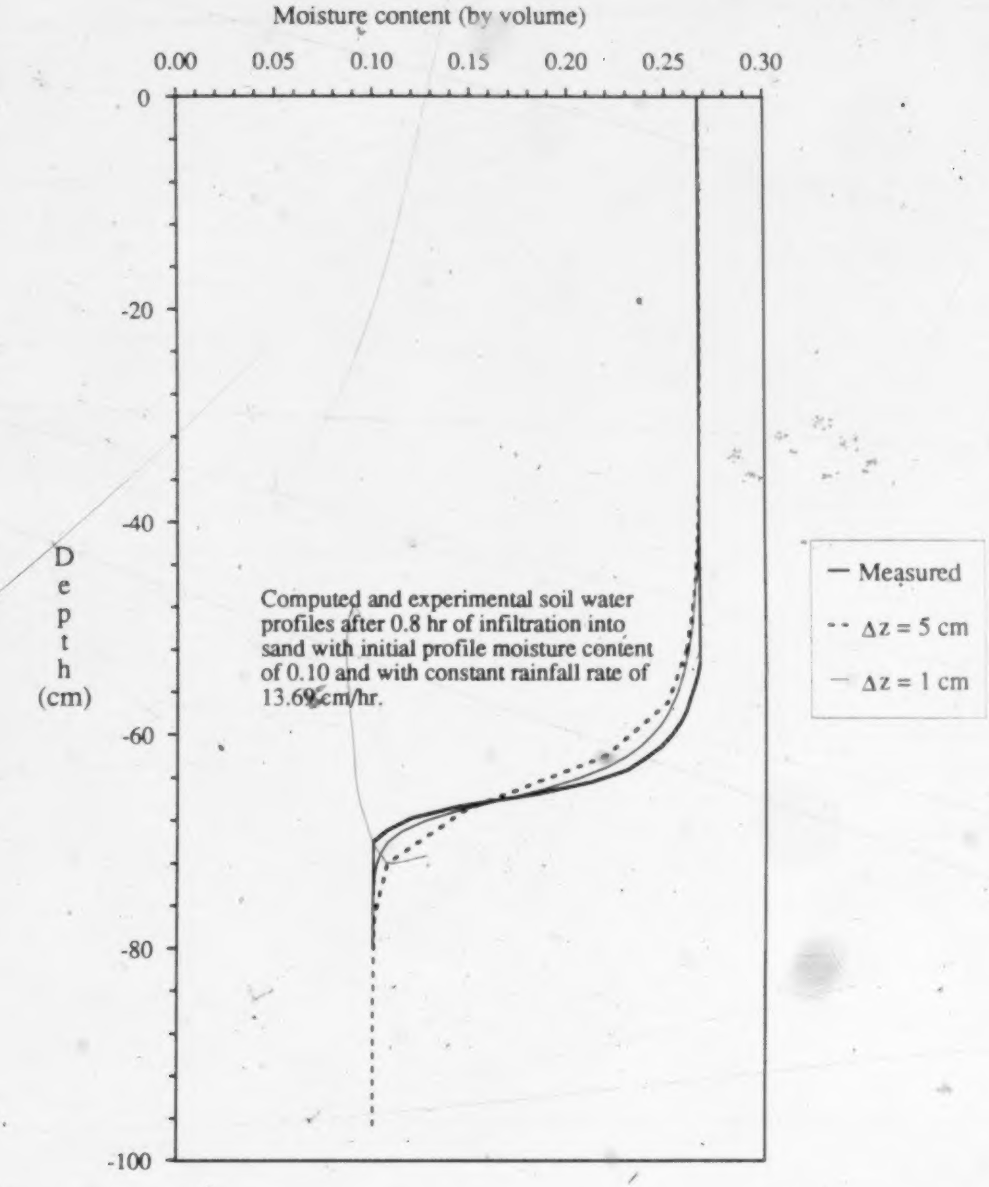

Fig. 2-5. Comparison of current numerical solution with experimental data, obtained from Haeverkamp et al. (1977).

(Abbott, 1979). A detailed analysis of the effect of Δx and Δt is given in Chapter 6 (Analysis of Numerical Techniques). However, to provide an idea about the computational requirements of the present model, Table 2-4 is presented here.

Table 2-4. Computational time requirements.

Simulation time (hrs)	Tolerance (cm)	*Computational nodes (CN)	CPU time (sec)
2.77	0.001	477	1.387
5.00	0.001	852	2.427
25.00	0.001	4500	12.355

* CN = (No. of iteration).(no. of nodes).(simulation time) / Δt.

The third example consists of solving for the infiltration rate, cumulative infiltration and moisture profile for ponded conditions i.e. a certain depth of water (ψ=25 cm) was maintained, throughout the simulation period, on the surface instead of keeping θ_s constant (or ψ=0). Again, the soil is Yolo Light clay. Initial conditions and the lower boundary were as those of the first example. As it was intended to continue the simulation for a prolonged period Δt and Δx values were assigned to be 0.25 hr and 5 cm respectively. Figs. 2-6, 2-7 and 2-8, show the computed infiltration capacity, cumulative infiltration and potential distribution after 34 days. Results seem reasonable. As one would expect the infiltration rate would decrease with time and eventually should reach a constant rate.

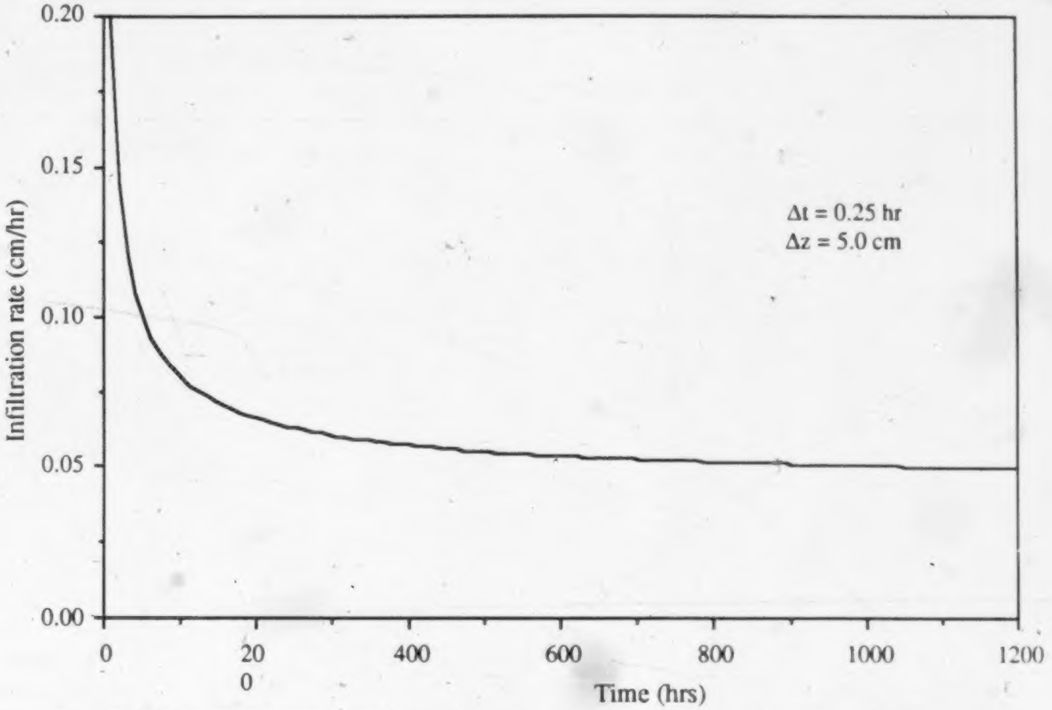

Fig. 2-6. Infiltration rate into Yolo light clay with a constant positive head ψ = 25 cm of water at the soil surface.

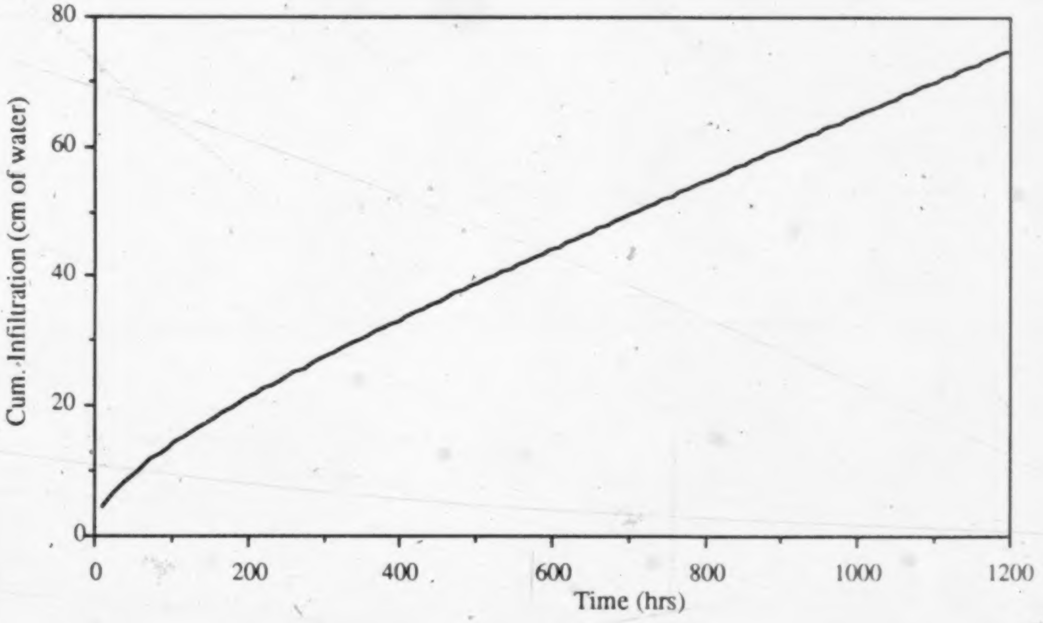

Fig. 2-7. Cumulative infiltration into Yolo light caly corresponding to the above infiltration rate (Fig. 2-6).

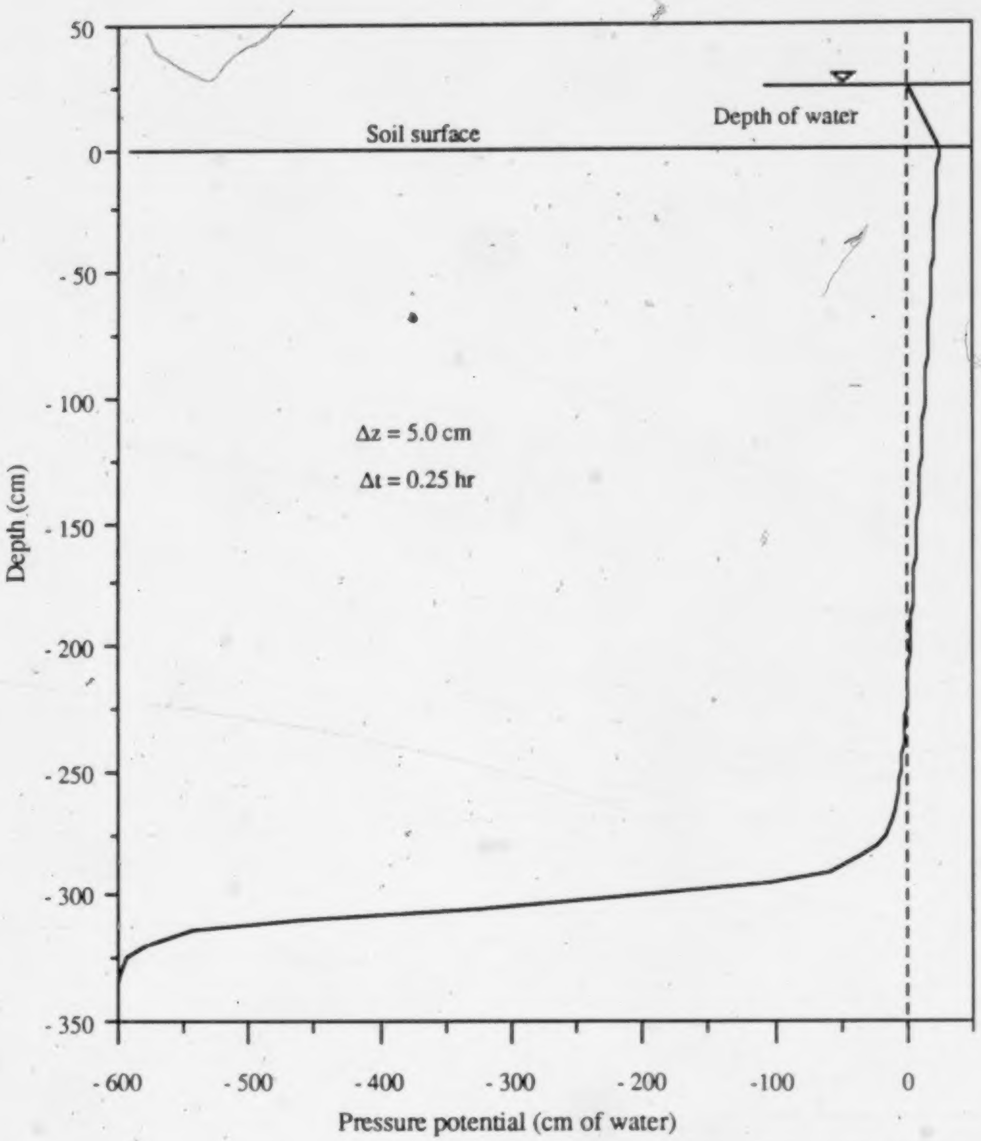

Fig. 2-8. Potential distribution after 34 days of infiltration into Yolo light clay with a constant positive head ψ = 25 cm of water at the soil surface.

The main purpose of the present studies is to apply this model in a real situation, and therefore, no further hypothetical examples were solved. Solution of these few examples were thought to give adequate information about the performances of the model.

2.3 Evaporation

The transfer of water from a surface of the earth into the atmosphere through vaporization is termed as evaporation. Since the evaporated water usually does not come back to the site from where evaporation occurred, this phenomenon is commonly considered as the loss of water. The loss of water by evaporation must be considered from two main aspects. The first, evaporation from an open water surface, is direct transfer of water from lakes and rivers to the atmosphere. The second form of evaporation loss occurs from the transpiring vegetation. This is often termed as evapotranspiration (ET), since loss by direct evaporation of intercepted precipitation, or dew deposition, or overhead irrigation water, on plant surfaces is also included. In general, while intercepted water evaporates, drainage of soil water by plant roots is reduced (Penman, 1967). Thus ET is usually thought of as the total loss by both evaporation and transpiration from a land surface and its vegetation. Whatever the venue, the unavoidable energy requirement for evaporation is the same, at about 2.47×10^6 J/kg of water evaporated.

A major portion of the total precipitation falling on the land surface is returned to the atmosphere by the process of evapotranspiration. As a global average, 57% of the annual precipitation is lost by ET and evapotranspiration amounts to 70% of annual precipitation in Canada, and more than 90% of the precipitation in the semi-arid regions (Brutsaert, 1982). Thus it is a major component of the hydrological cycle.

Quantification of ET is required in the context of many issues, for example, management of water resources, environmental assessment and plant production. Knowledge of ET is basic to the supply and management of surface and groundwater resources, since various land uses affect the partitioning of precipitation input. Through its magnitude and close alliance with plant growth, ET is a highly influential process to be considered and predicted for estimates related to hydrology. The status of soil moisture, which is of special interest in this study, is primarily dependent on time distribution of precipitation and ET. And in turn, soil moisture significantly influences runoff generation.

The complexity of the ET process has long been recognized. Despite this, earlier attempts at estimating ET were based on climatic variables (Penman, 1956; Criddle, 1958; van Bavel, 1966). This was primarily for expediency, since, for a practicing engineer, it is a matter of comfort to be able to predict ET from a number of climatological variates which can be estimated with some degree of regularity, thus bypassing the various soil and plant factors. Now it is well recognized that, for ET to occur, water has to be available at the evaporative surface and sufficient energy must be available to vaporize the water. For the process to continue, the humidified air has to be transported away from the evaporating surface. In broad terms, water is transferred to the atmosphere as a result of atmospheric demand as long as there is a supply of water at the evaporating site. The atmospheric demand is primarily controlled by meteorological factors such as radiation, temperature, humidity and wind speed, while the supply of water to the evaporative surface depends on the water holding and flow properties of the soil and soil-plant systems.

Due to the dynamic nature and the complex interrelations of the processes involved (Cowan, 1965; Stewart, 1983; McIntosh and Thom, 1983), understanding of ET requires expertise from several disciplines e.g. meteorology, physics, hydrology, plant physiology etc. As evidenced in the literature, these disciplines have interests in the processes and have made contributions.

Methods for evaluating evapotranspiration from the earth surface have been outlined in review by Tanner (1968), Webb (1975), Stewart (1984) and Garratt (1984). An account of mechanics of evaporation is given by, among others, Wartena (1974), Balachandra et al. (1975), and Brutsaert (1982). Here, in the following sections the relationships and the topics relevant to the context of this study are reviewed and discussed.

2.3.1 Meteorological conditions

A net input of thermal energy to the body of water increases the free (kinetic) energy of the water molecules to the point where some are able to escape across the liquid gas interface. The amount of heat absorbed by a unit mass of water passing from liquid to the vapour state at constant temperature is called the latent heat of evaporation or latent heat of vaporization. This thermal energy is furnished by radiation. It consists of the short-wave radiation received from the sun and sky, and the long-wave radiation received from the atmosphere. These components are offset by reflected short-wave radiation and long-wave radiation emitted from the surface. On the local scale, the radiation input is independent of the underlying surface, but outgoing short-wave radiation is influenced by the reflective characteristic of the surface, called albedo. The overall balance between the short-wave and long-wave radiation is the net radiation, R_n, and is given by

$$R_n = R_i (1-\alpha) + R_u + R_l \qquad [2\text{-}52]$$

where R_i and R_u are incoming and outgoing short-wave radiation fluxes, R_l is the net downward long-wave flux, and α is the albedo (reflectivity coefficient for short-wave radiation). Typical values of α are about 0.1 for forest, 0.15-0.25 for agricultural crops, and 0.15-0.60 for bare soil (Monteith, 1973). The long-wave emission from rough vegetation such as forests is less than from agricultural crops. Because of this and and lower albedo, R_n is higher for forests than for agricultural crops. The net radiation is partitioned into latent heat flux (λE) used for ET, the sensible heat flux (H) to the air, heat flux (G) into the ground, and into energy (PH) utilized in photosynthesis and heating the plant biomass. This is expressed as

$$R_n = \lambda E + H + G + PH \qquad [2\text{-}53]$$

where λ is the latent heat of vaporization and E is the evaporation. The partition of R_n into latent and sensible heat primarily depends on the availability of water at the evaporative surface and the transferability of the humidified air.

2.3.2 Transport mechanism

The transport of latent and sensible heat from the evaporating surface to the atmosphere is governed primarily by the atmospheric turbulence generated by the wind over the roughness elements of the surface.

Experiments revealed that in an air stream having a steady mean direction and a mean velocity, $\overline{u}$, there are fluctuations in forward velocity, $\pm u'$, there are fluctuating sideway components, $\pm v'$, and there are up-and-down motions, $\pm w'$. By definition, the average values of u', v', and w', over a fraction of an hour are zero, $\bar{v}$ is zero, and, if the surface is horizontal, then $\bar{w}$ is zero, too. Sensitive thermometers and hygrometers will also reveal fluctuations in air temperature T' and in air humidity q' or e'.

When the observations are made at different levels (z_1, z_2, z_3,...) above the ground, two kinds of information can be obtained. First, working at any particular level the fluctuations can be recorded at intervals of very short time. Second, based on mean values over certain periods of time, vertical profiles of wind speed, temperature, and humidity can be derived.

The first kind of information begets the so called fluctuation theory or **eddy correlation method**. If at any point in the atmosphere the air has a density ρ, specific humidity q, and vertical velocity w, the instantaneous rate at which water is being carried upward is ρwq and hence the average rate is ρwq, where the bar represents a time average. This can be split by writing

$$\overline{\rho w q} = \bar{\rho}\,\overline{w}\,\overline{q} + \overline{\rho' w' q'} \qquad [2\text{-}54]$$

where over a site of good horizontal uniformity the value of ρw is zero so the evaporation rate reduces to

$$E = \overline{(\rho w)' q'} \qquad [2\text{-}55]$$

The main limitation to this method is the instrumentation. The slow response of the humidity sensors, and/or the large sensing volume requires high placement and large fetch. The instrumentation developed to date is too complicated (Moore, 1976; Webb et al., 1980).

The second set of observation leads to **profile theory**. The increase of wind speed with height over an extended uniform surface is represented by

$$u = \frac{u_*}{k} \ln \frac{z - d}{z_0} \qquad [2\text{-}56]$$

when the atmosphere is near a state of neutral stability. In conditions of greater or lesser stability more complex expressions are needed and there is a continuing quest for a generalized wind profile (Brutsaert, 1982). In evaporation studies eqn.[2-56] is used even where it is known to be inexact, with corrections for stability applied at the end of computation. In eqn.[2-56], u is the velocity at height z above ground, z_0 is a roughness constant, d is needed to allow for the effect of the crop in effectively displacing ground level upward, k is universal constant (von Karman, k=0.41), and u_* is a constant of the particular profile, and given by

$$u_*^2 = \frac{\tau}{\rho} \qquad [2\text{-}57]$$

where τ is the shearing stress in the moving air, and ρ is, as before, its density. It is assumed that over a period of 10 min or longer the average value of τ is invariant with the height up to 3 m. For greater heights, longer averaging time is required. This implies that the downward flux of momentum is constant in the same layer, and with this condition satisfied, formal analysis is possible. By definition

$$\frac{\tau}{\rho} = K_M \frac{\partial u}{\partial z} \qquad [2\text{-}58]$$

where K_M is the transport constant for momentum and is frequently known as the coefficient of eddy diffusivity. Combining eqn.[2-56] and [2-57], and [2-58] yields

$$K_M = k^2\ (z\text{-}d)^2 \frac{\partial u}{\partial z} \qquad [2\text{-}59]$$

The next assumption is that the mechanism that transports momentum also transport heat and water vapour, and that the eddy diffusivities for heat K_H and for vapour K_V are equal to each other and to K_M. Measurements (Rider, 1954) show that the assumed identity is no more than a good working approximation. One of the formal consequences of the assumption is that the profiles of temperature and vapour pressure should have the same shape as the profile of wind speed, which can be tested by plotting u against T and e at a number of values of z. The result should be straight line, whatever the shape of the profile (Penman and Long, 1960). The formal transport equations are

$$H = -\ \rho\ C_p\ K_H \frac{\partial T}{\partial z} \qquad [2\text{-}60]$$

$$E = -\ K_V \frac{\partial \chi}{\partial z} \qquad [2\text{-}61]$$

where H is the sensible heat transfer, C_p is the specific heat of air, E is the vapour transport rate, and χ is the absolute humidity of air.

As $\chi = \rho q$, where q is the specific humidity (gm of water vapour per gm of air) and is given exactly enough by $q = \varepsilon e/p$, where e and p are total vapour pressure and total pressure, respectively, and ε is the ratio (18/29 ~ 5/8) of the molecular weight of water to the mean molecular weight of dry air, χ in eqn.[2-61] can be replaced by the product $\{\rho C_p/(\gamma\lambda)\}.e$, where

$$\gamma = \frac{\rho C_p}{\lambda \varepsilon} \qquad [2\text{-}62]$$

This is the thermodynamic value of the psychrometric constant, λ being the latent heat of vaporization of liquid water, when p = 1000 mbar, $\gamma = 0.66$ mbar $°C^{-1}$.

As variation in ρC_p and $\gamma\lambda$ with z are usually negligible in comparison with significant vertical gradients in e and T (at least over short vegetation), eqns.[2-60] and [2-61] can often be written in convenient, almost symmetrical, forms

$$H = -\rho C_p K_H \frac{\partial T}{\partial z} \qquad [2\text{-}63]$$

$$\lambda E = \frac{\rho C_p}{\gamma} K_V \frac{\partial e}{\partial z} \qquad [2\text{-}64]$$

which express the respective vertical fluxes of latent heat and sensible heat over a uniform plant community.

When $K_H = K_V = K_M$, and eqn.[2-56] is satisfied, the aerodynamic transport equations reduce to

$$H = -\rho C_p k^2 (z\text{-}d)^2 \frac{\partial u}{\partial z}.\frac{\partial T}{\partial z} \qquad [2\text{-}65]$$

$$\lambda E = -\frac{\rho C_p}{\gamma} k^2 (z\text{-}d)^2 \frac{\partial u}{\partial z}.\frac{\partial e}{\partial z} \qquad [2\text{-}66]$$

Alternatively, in terms of the rates of change of u, e, and T with ln(z-d), rates which have the advantage of being independent of z,

$$H = -\rho C_p k^2 \frac{\partial u}{\partial(\ln(z\text{-}d))}.\frac{\partial T}{\partial(\ln(z\text{-}d))} \qquad [2\text{-}67]$$

$$\lambda E = -\frac{\rho C_p}{\gamma} k^2 \frac{\partial u}{\partial(\ln(z\text{-}d))}.\frac{\partial e}{\partial(\ln(z\text{-}d))} \qquad [2\text{-}68]$$

A pair of equations almost identical to eqns.[2-67] and [2-68] but applicable to measurements at two levels only, can be derived from the relationship defining aerodynamic resistance, as follows:

By definition, it can be written that

$$r_v = -\frac{\rho C_p}{\gamma} \frac{e_1 - e_2}{\lambda E} \qquad [2\text{-}69]$$

$$r_H = -\rho C_p \frac{T_1 - T_2}{H} \qquad [2\text{-}70]$$

[aerodynamic resistance = (concentration difference) / flux]

Invoking similarity with

$$r_M(z_1,z_2) = \frac{1}{k^2}\frac{[\ln\{(z_2-d)/(z_1-d)\}]^2}{u_2-u_1} \qquad [2\text{-}71]$$

it can be written that

$$\lambda E = \frac{\rho C_p k^2}{\gamma}\frac{(u_2-u_1)(e_1-e_2)}{[\ln\{(z_2-d)/(z_1-d)\}]^2} \qquad [2\text{-}72]$$

$$H = \rho C_p k^2 \frac{(u_2-u_1)(T_1-T_2)}{[\ln\{(z_2-d)/(z_1-d)\}]^2} \qquad [2\text{-}73]$$

Eqns.[2-72] and [2-73] apply without modifications only in conditions of full-forced convection. Also there is some debate about their validity in any circumstances within a certain, restricted, number of roughness parameters of vegetation tops (Thom, 1972; McIntosh and Thom, 1983). Furthermore, to use eqn.[2-72] there must be a humidity and wind observation at two levels, and unless an arbitrary value of d is to be used, wind observations are needed at four or more levels to derive a value of d. The precision needed in all these measurements is great. For research, with the resources of a good physics laboratory behind it, these objectives are attainable, but for routine use for climatological surveys there is need for something simpler. There is a requirement for use of single-level observations, such as are made in standard meteorological stations, with an inaccuracy in the final result that is no worse than that in estimating rainfall. Therefore a prediction model was formulated combining both aerodynamics (transport) and energetics (heat) of evaporation (Monteith, 1965, 1981). This equation is widely known as the combination equation.

2.3.3 Combination equation

Considering that sensible heat flux, H, originate on the surface of the vegetation elements where the temperature on average is T(0). The latent heat is driven in the first instance by the evaporation of liquid water, so must originate within the vegetation elements, in the myriads of intercellular spaces, where to a good enough approximation, the vapour is given by the saturation value appropriate to average temperature T(0), i.e. by $e_w\{T(0)\}$, rather than the surface value e(0) (Monteith, 1980).

Inasmuch as the difference {e(0)-e(z)} is proportional to the aerodynamic resistance experienced by a given transpiratory flux, the difference {ew{T(0)}-e(0)] may be treated as similarly proportional to the physiological resistance imposed by the components of the vegetation on that flux. As variations in the size of this resistance are governed almost entirely by changes in the stomatal status of individual leaves, it is referred here as the bulk stomatal resistance r_{st} and is given by

$$r_{st} = \frac{\rho C_p}{\gamma} \frac{[e_w\{T(0)\}-e(0)]}{\lambda E} \qquad [2\text{-}74]$$

From the aerodynamic relationships

$$r_V = \frac{\rho C_p}{\gamma} \frac{[e(0)-e(z)]}{\lambda E} \qquad [2\text{-}75]$$

$$r_H = \rho C_p \frac{[T(0)-T(z)]}{H} \qquad [2\text{-}76]$$

Simply by adding eqns.[2-74] and [2-75] e(0) can be eliminated to give

$$r_{st}+r_V = \frac{\rho C_p}{\gamma} \frac{[e_w\{T(0)\}-e(z)]}{\lambda E} \qquad [2\text{-}77]$$

To eliminate T(0), the following substitution is made

$$e_w\{T(0)\} = e_w\{T(z)\} + \Delta\{T(0)-T(z)\} \qquad [2\text{-}78]$$

where Δ is the slope, in mbar $°C^{-1}$, of the saturation vapour pressure versus temperature curve for water at the mean of T(0) and T(z) (or simply at T(z) when T(0) is unknown).

Assuming that the contribution from the component PH in the energy balance equation (eqn.[2-53]) is negligible, the available energy (R_n - G) can be equated to the sum of the sensible and latent heat fluxes, i.e.

$$R_n - G = \lambda E + H \qquad [2\text{-}79]$$

Eqns.[2-76] and [2-79] are then used to replace {T(0)-T(z)} by the product

$$\{(R_n-G) - \lambda E\} . \frac{r_H}{\rho C_p.}$$

Subsequent substitution of eqn.[2-78] into eqn.[2-77] then permits the latter, with some algebraic manipulation, to be solved for λE, in the form

$$\lambda E = \frac{\Delta (R_n - G) + \rho C_p [e_w\{T(z)\} - e(z)] / r_H}{\Delta + \gamma (r_V + r_{st}) / r_H} \qquad [2\text{-}80]$$

Eqn.[2-80] is the well-known Penman-Monteith equation which belongs to the family of evaporation formulae, called combination methods. These methods make use of a combination of energy balance and aerodynamic transport of water vapour. Eqn.[2-80] differs from the original Penman (1948) equation in the aspect that for unsaturated surfaces, surface (canopy) resistance, r_{st}, which is related to the reduction of humidity, is introduced (Monteith, 1965).

The Penman-Monteith equation is considered physically based and in principle has generality. However, to predict actual, quantitative changes in evaporation from specified changes of r_{st}, r_V, r_H is not at all straightforward because of the existence of complicated feed back processes between vegetation and atmosphere.

An important practical application is the attempt to predict likely rates of evaporation, E_o, from a plant community or vegetated region when its bulk stomatal resistance becomes negligible as a result of rain or irrigation. The upper limit to E_o is given by the so-called potential evaporation rate, PE, obtained by setting $r_{st}=0$. Potential evaporation is discussed in the next section.

Potential Evaporation (PE)

PE is a troublesome term coined by Penman (1948) and Thornthwaite (1948) in an effort to establish a regional index for the maximum possible evaporation under given climatic conditions. The basic definition of PE is 'the rate of evaporation that would take place per unit area if the plot of evaporating vegetation is in the midst of large, unbroken stretch of similar vegetation and the soil moisture so plentiful that uptake by plants would not be inhibited'.

There are several empirical formulas and measurement techniques aimed at quantifying the potential evaporation (PE). One of the early empirical formulas is due to Blaney and Criddle (1950). Their equation is expressed as

$$u = \frac{k\,t\,p}{100} \qquad [2\text{-}81]$$

where u is the monthly consumptive use, t is the mean monthly temperature, p is the mean monthly daytime hours given as percent of the year, and k is consumptive use coefficient available in the literature (Viessman et al., 1977). The other empirical methods are accredited to Makkink and van Heemst (1956), Jensen and Haise (1963). These methods depend on one or more climatic factors and have only limited usefulness in that they do not consider all the factors affecting evaporation.

The first sound expression for PE was developed by Penman (1948), from consideration of the energy balance and aerodynamic transport of water vapour. The well-known expression is

$$\lambda E_p = \frac{\Delta R_n + \gamma f(u_2)[e_s(T_a) - e_a]}{\Delta + \gamma} \qquad [2\text{-}82]$$

where e_s is the surface saturation vapour pressure at air temperature T_a, and e_a is the vapour pressure of air at some reference height. For estimating daily PE (mm/day) Penman expressed e_s and e_a in millimeters of mercury and empirically defined $f(u) = 0.35*(0.5u_2/100)$, where u_2 is mean wind speed 2 m above the ground expressed in miles/day.

The Penman calculation of PE assumes non-advective conditions and a green grass crop of uniform height, completely covering the ground, and well supplied with water. The equation disregards ground heat flux, and doesn't take into account the effects of vegetation roughness and atmospheric stability. This approximate definition has given rise to the generally stated contention that "all well-watered crops have the same PE". However, it is realized that PE of various plant communities can differ considerably, principally because of variations in albedo (affecting R_n), aerodynamic roughness (affecting vapour transfer), and thermal capacity and conductivity (affecting canopy and ground flux).

Accordingly, differing terminologies, and occasional minor variation in the assumption (especially regarding the above factors) made in the derivation, have produced a plethora of relationships. Some of the examples are Slatyer and McIlroy (1961), van Bavel (1966), Priestly and Taylor (1972) and McIlroy (1984). However, the widely accepted definition of PE is the Penman-Monteith combination expression (Monteith, 1965), with negligible surface resistance (r_{st}=0), i.e. eqn.[2-80]. This equation is applicable when the soil or vegetation surface is covered with water, and thus there is no shortage of water supply. Therefore, the PE represents the maximum rate of water loss from a soil or vegetation surface of a particular structure, exposed to a given set of meteorological conditions.

The concept of PE has been useful in conceptual understanding of ET and is widely used in irrigation and other contexts. In many instances (Grindley, 1969; Baier, 1969; Feddes et al., 1974; Stegman, 1983), including this study, the evaluation of PE is the first step towards the evaluation of the actual evaporation (AE). As the second step, Budyko (1956), Thornthwaite and Mather (1955), Penman (1961), and others agreed that AE can be obtained from PE by considering the physiology of plant cover and available soil moisture. This is discussed in the following section.

2.3.4 Actual evaporation (AE)

The climatic conditions impose evaporational potential. The actual rates of evaporation may be the same as PE, or it may deviate from these due to the soil and plant factors or due to restriction in availability of water at the evaporative surfaces.

There are two pathways for evaporation: either through the roots, stems and leaves of plants or directly from the soil surface to the air. In the absence of plants, evaporation from the land constitutes the sole water loss mechanism from the surface. When the capacity of the soil to conduct water to the surface does not equal to the evaporative demand, the surface dries and a parabolic water distribution develops within the soil. The rate at which the bare soil supplies water at the evaporative site is controlled by the water content and the hydraulic conductivity of the soil. These parameters interact to characterize the water diffusivity function which controls liquid flux rates (section 2.2.2).

As in the cases of a vegetative surface (discussed previously) the net radiation absorbed by the soil is used for three ends: to vaporize water, to heat the atmosphere directly and to raise the temperature of the soil mass. The square root of the thermal diffusivity ($D_T^{0.5}$) indicates the depth of penetration of the diurnal temperature wave, and the volumetric heat capacity (C_v) of the soil indicates the amount of heat required to change the temperature of the layer (Philip, 1957). The product of $D_T^{0.5}$ and C_v indicates the rate of heat flux into the soil surface, hence the name thermal coefficient for this quantity. The relative thermal contact coefficients of the air and the underlying ground surface determine the division of the net radiation into sensible heat flow to the soil or into convective transfer to the air.

Density, mineral composition, and the water content are factors that largely control the thermal conductivity of soils. When the soil surface is moist the thermal contact coefficient of the soil is relatively large and more of the net radiation enters the soil. Since water is available, a large part of this heat is used in evaporation rather than in heating the soil. When the soil surface is dry, the thermal contact coefficient of the soil is relatively low and much of the net radiation is used to heat the air. Since evaporation can not occur rapidly from the dry soil, in the absence of evaporational chill, the immediate soil surface become hot. Despite high temperature of the surface, evaporation is restricted since the dry air is an effective thermal insulator.

Surface plant residues generally insulate the surface in addition to reducing energy absorption (Kohnke and Werkhoven, 1963). This reduces heat exchange between the soil and atmosphere and results in a much cooler soil as on forest areas. A vegetative cover intercepts much of the radiant energy before it reaches the soil and the canopy assumes a major role in turbulent transfer (discussed previously) processes as well. Hence the direct evaporation from the soil become very small. The area (Chapter 7) that concerns this treatise is mostly forested (Plate 2-1), therefore, direct evaporation processes from bare soil surfaces will not be considered.

Plate 2-1. Typical vegetation of Spring Creek watershed.

The major part of the evaporation from vegetated surface occurs as transpiration, i.e. the evaporation of water from the internal surfaces of leaves and its diffusion to the exterior mainly through the stomata. Since plants often transpire more water in a day than their own weight, it is clear that transpiration can not be maintained without uptake of water from the soil, and since the water content of plants changes within narrow limits from day to day (Ritchie, 1981), water uptake and transpiration can be regarded as linked processes in which large amount of water is transferred from the soil through plants to the air, with a change from the liquid to the vapour phase in the leaf. This system has been called the soil-plant-atmosphere continuum (Philip, 1966).

The flow of water in this continuum accompanies other forms of matter or energy. However, the movement of water can be thought of as governed by the differences in water potential (Slatyer and Gardner, 1965). A detailed elaboration of the flow mechanisms in different pathways of the soil-plant-atmosphere continuum can be found in Slatyer and Gardner (1965), Cowan (1965) and Newman (1969).

To understand the effect of soil water on transpiration it is necessary to analyse the uptake system. Following Slatyer and Gardner (1965) and Cowan (1965), the uptake rate per unit area may be written as

$$AE = \frac{\Psi_{soil} - \Psi_{leaf}}{R_{soil} + R_{plant}} \qquad [2\text{-}83]$$

where ψ represents potential, R_{soil} the overall hydraulic resistance to movement of liquid water from the bulk soil to the root system and R_{plant} the resistance to movement of water from the plant root surface to the cell of leaf. This is a simple formal representation of a situation which becomes very complex when the variability of both water content and root density with depth is taken into consideration. Acknowledging the fact that, leaf-water potential automatically adjusts to maintain a rate of uptake equal to transpiration, the equation can be arranged in the form

$$\psi_{leaf} = \psi_{soil} - AE\,(R_{soil} + R_{plant}) \qquad [2\text{-}84]$$

and

$$AE = PE \qquad [2\text{-}85]$$

The above equations show that as the soil water potential drops, so also will be that of the leaf. Unless R_{soil} is small relative to R_{plant} the reduction of conductivity in the soil will enhance the effect on the leaf. Leaf-water potential (for concepts and significance see Edlefsen and Anderson, 1943; Weatherley, 1965; Acock and Grange, 1981) fluctuates around a mean value reflecting the diurnal fluctuation in AE (Gardner and Nieman, 1964; reported by Slatyer and Gardner, 1965). As the mean level of ψ_{leaf} decreases progressively from day to day, eventually a stage is reached where stomatal opening is restricted. Thus soil drying leads to a restriction of transpiration, although the consequent restriction of AE somewhat mitigates the fall of ψ_{leaf} with ψ_{soil}.

According to Cowan (1965) the prediction of the effect of soil drying on transpiration rate, therefore, depends on a simultaneous solution of four equations, representing the soil-plant-atmosphere continuum. These are eqns.[2-84], [2-85], and

$$PE = f\left(\text{climatic factor}, \frac{1}{r_l}\right) \qquad [2\text{-}86]$$

and

$$\frac{1}{r_l} = f(\psi_{leaf}) \qquad [2\text{-}87]$$

The experimental investigations of the way in which the transpiration rate responds to the drying of soil have produced diverse conclusions falling roughly into the following categories: (a) transpiration rate is maintained at a maximum potential rate until available water is exhausted, (b) transpiration begins to decline at some intermediate stage of soil water depletion and (c) transpiration declines progressively, though not necessarily linearly, over the whole range of available soil water depletion (Baier, 1969). However, there is increasing experimental and circumstantial evidence that variation of the form of the relation between transpiration and soil water depletion can be explained in terms of varying climate, plant and soil factors which is explained in Fig. 2-9 (Denmead and Shaw, 1962; Slatyer, 1956).

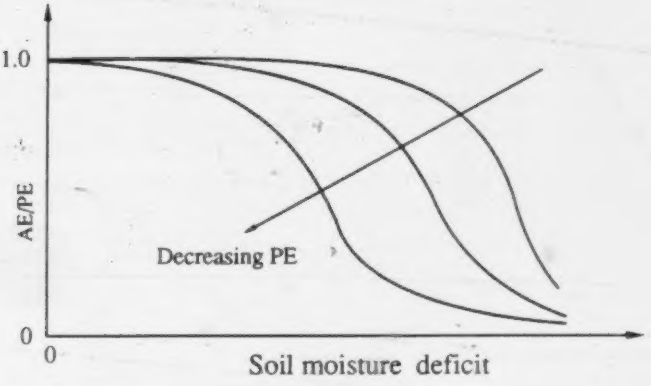

(a)

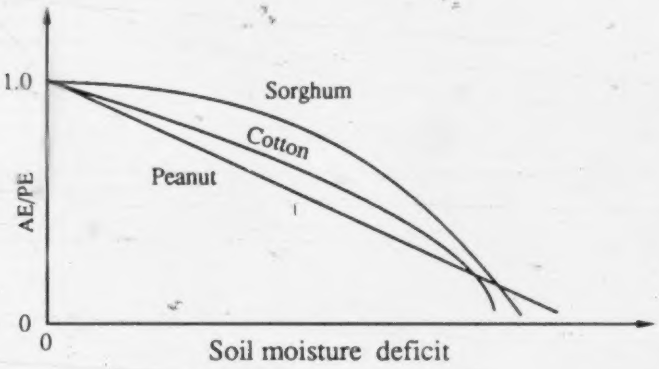

(b)

Fig. 2-9. The relationship (qualitative) of the ratio PE/AE to soil water content as affected by (a) variation of potential transpiration rate (PE) in maize (adapted after Denmead and Shaw, 1962); (b) crops having different root development (adapted after Slatyer, 1956).

2.3.5 Models for AE

There are variations in AE modeling approaches depending on the way they account for the above factors. The first group of models is correlation based. These models require an estimate of potential evapotranspiration and a coefficient, called crop coefficient, K_c. The product of PE and K_c is assumed to give the actual evapotranspiration. The crop coefficient K_c usually includes the effects of the soil as well as the plant, and it is supposed to reflect the effects of the physiology of the crop, and the degree of cover. For irrigated crops, the effects of soil water deficit are not important (Doorenbos and Pruitt, 1977), so the estimates of AE are reasonable. But in dryland conditions or even under irrigated conditions depending on the frequency of irrigation soil water deficit occurs. In some models (Grindley, 1969; Hansen, 1984) this effect is taken into account by expressing AE/PE as a function of soil water content in the root zone. Many empirical relationships between AE/PE and some measures of soil water in the root zone have been in use. Most of them use the concept of available soil water. As defined previously, available soil water is the water stored in the root zone between the upper limit 'field capacity' and the lower limit 'permanent wilting point'.

With the increased understanding of the dynamic aspects of water availability it is now recognized that water availability is not just a function of static, ill-defined soil properties (field capacity and wilting point), but it is dependent on the hydraulic properties of soil and plant characteristics. This suggests that any empirical relationships established between AE/PE and water content can only be applicable within the range of data used.

A further improvement over the above classes of models are those called process-oriented models. The process-oriented combination equation developed for potential evaporation is modified to account for the extra resistance to water flow, when the supply of water is limited. The effects of restricted water availability are reflected through surface resistance or canopy resistance, r_c (Rose, 1984). For dry vegetative surfaces, r_c can be calculated from stomatal resistance r_{st} and the leaf area index (LAI). Thus the problem reduces to estimating stomatal responses to various soil, plant, and environmental variables. Currently, two courses are usually followed to cope with this situation. The first involves empirically relating r_{st} to soil water potential ψ_s (Russell, 1980), and the other relates r_{st} to plant water potential ψ_p or to ψ_p and vapour pressure deficit. Because of large spatial variability of r_{st}, it is a major task to establish a meaningful relationship to predict average r_{st}.

Other process-oriented type of models assume that the rate of water extraction by a root system is equal to the water loss from the plant. Thus stomatal response is modeled indirectly. Potential evaporation calculated by one of the combination equations, is considered as the upper limit of water transfer in the soil-plant-atmosphere system (Jensen, 1981). Evaporation from the soil surface and the wet canopy are neglected or calculated separately. These approaches are based on the idea that water flows in the soil-plant-atmosphere continuum in response to atmospheric demand and determined by potential gradients across the system. These models consider the integrated response of the root system of the plant community on a macroscopic scale. Water uptake by roots is represented by a bulk or sink term. In a number of ways this sink term is expressed as function of root properties (Hillel, 1977; Norman and Campbell, 1983).

In many macroscopic models, the sink term (S_k) is assumed to be directly proportional to hydraulic conductivity of the soil, difference in water potential between the soil and the roots, $\Delta\psi$, and to some empirical root effectiveness function. This function may be represented by surface area of roots per unit soil volume, or by root length and geometry (Feddes et al., 1974; Jarvis et al.,1981). Hence, quantification of root surface area or its measure is essential. The basic problem in the application of the root extraction class of models is the lack of good quality data both on the root surface area, and its distribution with depths.

2.3.6 Present approach

In this study, the processes of the transport of water both as liquid in the soil and as vapour in the atmosphere are described by the soil water flow equation (eqn.[1-1]) and

Penman-Monteith equation (eqn.[2-80]). The two descriptions are coupled through the root zone, where transpired water is extracted through the plant root system. As described in the previous sections, the usual way of modeling this uptake procedure is to add a sink term to the continuity equation of soil water flow.

However, here a different approach is adopted. Since the soil surface under the forest canopy remains blanketed with litter or thick short vegetation (cf. Plate 2-1), direct evaporation from the soil surface can be assumed negligible. Soil moisture depletion caused by evaporation can be considered to occur via root-stem-leaves continuum only. Consequently it can be thought that the water flow resistances of this continuum and of the soil matrix are the determining factors of moisture transfer from soil to the atmosphere. The model is conceptualized as depicted in Fig. 2-10.

Fig. 2-10 shows a schematized soil plant system. The flow path is represented by the zig-zag line. Introduction of the capacitance is to indicate storage and that the flow in this continuum is not constant. Although the moisture can flow from any direction towards the plant root, here it is assumed to be principally vertical. This seems reasonable because in unsaturated condition mainly matric potential drives the flow, while the gravity potential is relatively small.

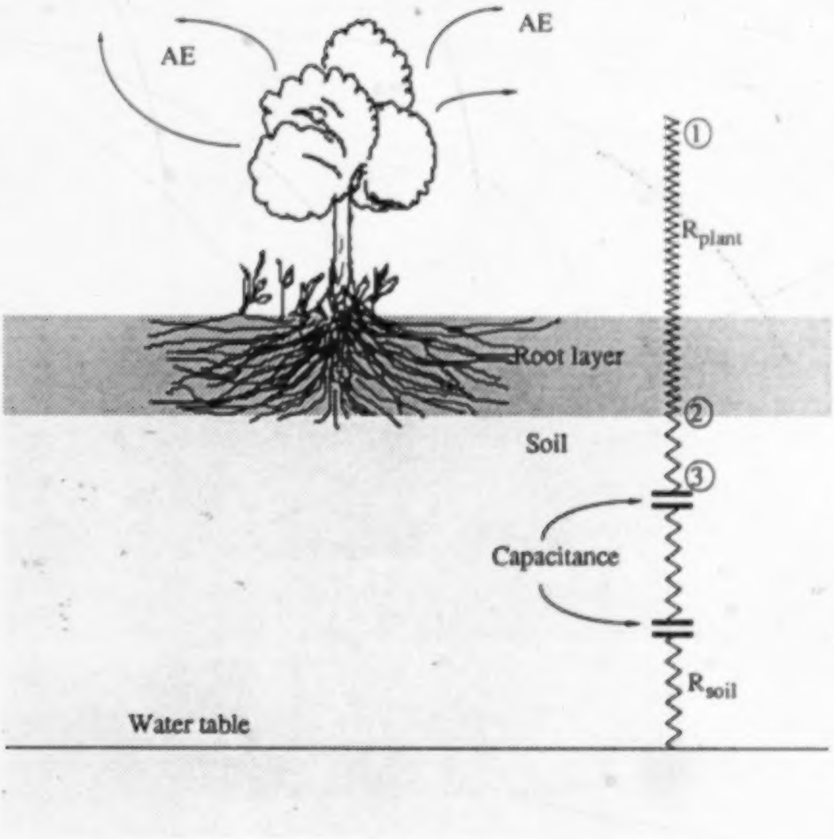
AE
AE
①
R_{plant}
Root layer
②
Soil
③
Capacitance
R_{soil}
Water table

Fig. 2-10. Schematized soil-plant-atmosphere continuum.

In the soil-plant system the soil and the plant impose different resistances in different parts of the continuum. In the solution of eqn.[2-26] this is treated as follows:

Considering the points 1 and 2 (Fig. 2-10) from Darcy's law and Ohm's law it can be written that

$$q = K\frac{\phi_1 - \phi_2}{\Delta z} = \frac{\phi_1 - \phi_2}{\Delta z/K} = \frac{\phi_1 - \phi_2}{R_{plant}}$$

Hence

$$\frac{\Delta z}{K_{soil}} = R_{plant}$$

Defining Δz_e as the virtual length of the flow path between points 1 and 2 it can be written that

$$\Delta z_e = K_{soil}\,(R_{plant})$$

Using this equivalent Δz, the F-D equation for point 2 is expressed as

$$C_2^{n+1/2}\frac{\psi_2^{n+1} - \psi_2^{n}}{\Delta t} = \omega\,\frac{K_{1+1/2}^{n+1}\left(\psi_1^{n+1} - \psi_2^{n+1}\right)/\Delta z_e - K_{2+1/2}^{n+1}\left(\psi_2^{n+1} - \psi_3^{n+1}\right)/\Delta z}{\left(\Delta z_e + \Delta z\right)/2} + (1-\omega)\ \ldots$$

The potential at node 1 is known as a function of time from measurement of humidity.

Boundary conditions

The boundary conditions of this soil-plant-atmosphere continuum are determined both by the atmospheric and soil moisture status. Soil moisture at the bottom of the hypothesized root layer (Fig. 2-10) gives measure of potential at the lower end, leaf surface moisture condition provides the leaf water potential. The major assumption here is that the leaf surface vapour pressure and the leaf water pressure are in equilibrium. The flow, across the plant biomass as governed by the difference of potential at two ends, gives the estimate of actual evaporation. In fact, in the model the root bottom boundary needs not to be specified explicitly as the solution of the moisture flow equation is obtained simultaneously as one continuum.

Upper boundary

From the assumption of equilibrium condition between leaf and air potentials, the leaf water potential can be obtained as (Edlefsen and Anderson, 1943; Nimah and Hanks, 1973; Norman and Campbell, 1983)

$$\psi_{leaf} = \frac{RT}{M_w} \ln \frac{e_a}{e_s} \qquad [2\text{-}88]$$

where R is the universal gas constant and is equal to 8.314 J/mole/°K; M_w is the molar weight of water and is equal to 0.018 kg/mole (for water); T is the surface temperature in Kelvin, e_a is the surface vapour pressure (mbar); and e_s is the surface saturation vapour pressure (mbar) which is calculated from the surface temperature.

Application of the model to the Spring Creek basin and simulation results are given in section 7.4.

Chapter 3

Saturated Flow Model

3.1 Groundwater

Melting snow and ice, and rainfall have supplied over geologic times, percolating waters to build up a body of underground water which exists almost everywhere. Even desert areas receive occasional rains which will contribute deep percolating water to the groundwater body. In the well watered areas of the globe the groundwater mound between stream valleys is never completely drained away but, instead, sustains the flow of the streams so that they continue to flow even though the rains may cease for a considerable period of time.

The discharge from the groundwater reservoir into the channel system responds relatively slowly to an additional supply of infiltration water from rain or snowmelt. In many areas groundwater runoff represents the greatest percentage of the annual runoff volume and is the only source of stream flow. In areas with deep highly permeable soils, overland flow may not occur at all, even after rainstorms of high intensities.

This chapter attempts to model the groundwater flow component of the rainfall-runoff process. A substantial amount of work has been done on groundwater flow with special attention to water wells and regional flows. Toth (1963), Freeze and Witherspoon (1966, 1967), Taylor and Luthin (1969), Frind and Verge (1978), England and Freeze (1988) and Stoertz and Bradbury (1989) are a few of the examples. There is, however, little information on the rigorous treatment of the groundwater component in relation to modeling streamflow except Freeze (1972), Abbott et al. (1986), and Storm (1988). Some of the rainfall-runoff models, indeed, take account of the groundwater flow but in rather empirical manner, for example, the SSAR model (U.S. Army Corps of Engineers, 1972), and the Stanford Watershed Model (Crawford and Linsley, 1966). In the Netherlands, with its flat topography, deep soils, and long lasting rains of relatively low intensity, surface runoff is not a common phenomenon in natural drainage basins. Attention has been given to develop rainfall-runoff models based on groundwater flow (Kraijenhoff van de Leur, 1958) using principles of linear reservoirs.

As cited in Chapter 1, in this study groundwater flow is modeled on the basis of physical laws as is usually done for the calculation of drain discharges and spacing (Fig. 3-1).

3.2 Flow Equations

Combining Darcy's law and the continuity equation one obtains, as shown in Chapter 2, Richard's equation for unsaturated flow. For saturated flow the moisture content, θ, in Richard's equation becomes θ_s, which is called the saturation moisture content, and given by $\theta_s = \rho n$, where ρ is liquid density and n is porosity. In case of an incompressible liquid and a non-deformable porous medium

$$\frac{\partial \theta_s}{\partial t} = \frac{\partial(\rho n)}{\partial t} = 0 \qquad [3\text{-}1]$$

which reduces Richard's equation to the form in 3-dimensions

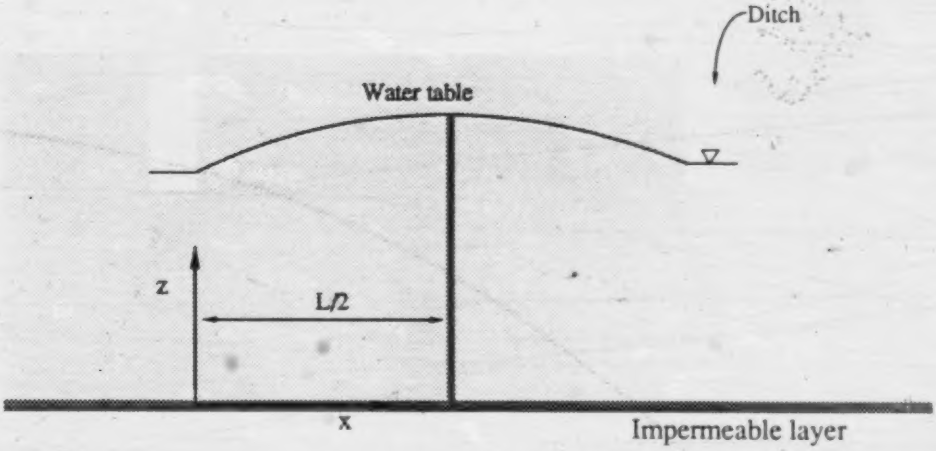
Ditch
Water table
z
L/2
x
Impermeable layer

(a)

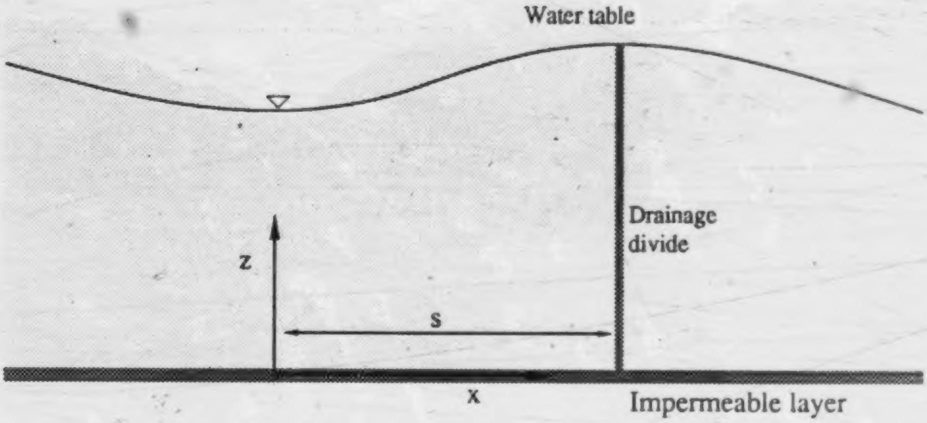
Water table
Drainage divide
z
s
x
Impermeable layer

(b)

Fig. 3-1. Similarity between drainage ditch and stream channel; (a) small scale and (b) regional configuration; L - drain spacing; x and z are horizontal and vertical coordinates.

$$\frac{\partial}{\partial x}\left(K_x\frac{\partial\phi}{\partial x}\right)+\frac{\partial}{\partial y}\left(K_y\frac{\partial\phi}{\partial y}\right)+\frac{\partial}{\partial z}\left(K_z\frac{\partial\phi}{\partial z}\right)=0 \qquad [3\text{-}2]$$

For an isotropic homogeneous medium the above equation takes the form

$$\frac{\partial^2\phi}{\partial x^2}+\frac{\partial^2\phi}{\partial y^2}+\frac{\partial^2\phi}{\partial z^2}=0 \qquad [3\text{-}3]$$

Eqn.[3-3] is called the Laplace equation. Since this equation is time-invariant, its application to unsteady flow problems requires that the time variable be introduced by means of the boundary conditions. Many steady-state solutions have been obtained for it but its use for transient cases has been limited due to the difficulty with a moving boundary. The formulation is basically sound, however, for both transient and steady-state groundwater flows. If the moving boundary difficulties could be overcome it would afford a means for overcoming the difficulties caused by nonlinearities which afflict some other formulations.

A mathematically advantageous formulation is based on the Dupuit-Forchheimer theory (D-F theory). Its origin was traced by De Wiest (1965) to a publication of Dupuit in 1857. The basic assumptions of Dupuit were that (1) all streamlines in a system of gravity flow towards a shallow sink are horizontal and that (2) the velocity along these streamlines is proportional to the slope of the free-water surface but independent of the depth. In addition, it is implied that the free-water surface is a streamline bounding the flow region and, in cases of an open ditch or drain, that the water table terminates at the water level in the ditch. It should be clear that, for the assumptions to be reasonable, their application should be restricted to flow systems that are (3) shallow relative to their areal extent and that (4) exhibit relatively small curvature of the free surface.

Let a prism of base $\Delta x \Delta y$ and height z be considered, from a flow system, bounded above by the free surface and below by an impervious layer. It follows from the D-F assumptions that the hydraulic head, h(x,y), referred to the impervious layer, coincides with the free surface z(x,y). Balancing net outflow and inflow within the prism it can be derived that

$$K_x \frac{\partial}{\partial x}\left(h\frac{\partial h}{\partial x}\right) + K_y \frac{\partial}{\partial y}\left(h\frac{\partial h}{\partial y}\right) \pm R = S_y \frac{\partial h}{\partial t} \qquad [3\text{-}4]$$

where S_y is the drainable porosity, R is the rainfall intensity or evaporation rate.

To derive eqn.[3-4] a constant porosity was assumed without defining the term. The concept implied that the soil is either drained or saturated. The drainable porosity may be defined as the volume of water per unit change in water table height. However, there is evidence that this quantity is not constant, depending at least on the proximity of the water table to the soil surface and on the rate and direction of the water table movement (Dos Santos and Youngs, 1969).

Another complication is associated with the assumption that the water table, or free surface, bounds the saturated flow region. There is normally a region of saturation or near saturation above the water table, frequently referred to imprecisely as the capillary fringe. Since this region clearly is a part of the flow region, one can adjust the flow boundary by some constant distance to account for this capillary fringe. But some workers, for instance, Parlange and Brutsaert (1987) consider this as oversimplification in many situations.

It has long been known (Muskat, 1946) that the D-F theory often results in the correct expression for flux, but does not properly predict the shape of the free surface. In the case of drainage to an open ditch, or seepage through a dam, the D-F theory forces the free surface to exit at the point where the water level stands in the ditch. A surface of seepage is not accounted for. Charnei as reported by Polubarinova-Kochina (1962), avoided the assumption of a horizontal velocity independent of depth and showed that the D-F result for flux through a dam was indeed correct.

By and large, equations that correctly describe the water table motion is difficult to obtain. As Higgins (1980) stated: "The physics and mathematics of the problem are complex. Drainage near the falling water table is not completely understood. Soil masses may show substantial variation in properties from point to point, and the exact mathematical description of the physical problem may not yield a manageable solution or any solution at all. Necessity forces the simplification of the physical and mathematical descriptions of the problem to a point where a solution can be found."

It is generally believed that the D-F equation reflects enough of the physics of the free surface saturated flow and the solution of it yields useful information. The D-F equation has been extensively used, specially in drainage and unconfined saturated flow studies by amongst others Harr (1962), Dagan (1964), Kirkham (1967), Wesseling (1972). Above all as Bear (1988) put it: "the Dupuit assumptions are probably the most powerful tool for treating unconfined flows. In fact, it is the only simple tool available to most engineers and hydrologists for solving such problems". Hence, in the present study, the D-F equation is used for modeling the groundwater contribution to the streamflow.

3.2.1 Boundary conditions

There is evidence that on a regional scale, the predevelopment water table closely follows the form of the topographic surface (Toth, 1963; Hitchon, 1969). The form of the predevelopment water table is normally a subdued replica of the land surface (Hubbert, 1940; Freeze and Cherry, 1979). Therefore, it seems reasonable to assume that the height of the phreatic surface (water table) increases from the valley bottom toward the water divide. Accordingly, the boundary of the groundwater flow region has been taken as shown in Fig. 3-2 (page 128). The pressure p at the water table (phreatic surface) equals the atmospheric pressure p_0; thus

$$\phi = h(\text{water table elevation}) = f(x,y,R,t) \qquad [3\text{-}5]$$

Let 's' be the horizontal distance between the valley bottom and the water divide; then the following boundary conditions can be written for the water table and the impermeable boundary:

$$\begin{aligned} h &= h_0 && \text{for } 0 < x < s && \text{at } t = 0 \\ h &= d && \text{for } x = 0 && \text{at } t > 0 \\ \frac{\partial h}{\partial x} &= 0 && \text{for } x = s && \text{at } t > 0 \end{aligned} \qquad [3\text{-}6]$$

3.2.2 Solution methods

Analytical solution

For two-dimensional problems, such as parallel drains or streams, eqn.[3-4] reduces to

$$K_x \frac{\partial}{\partial x}\left(h \frac{\partial h}{\partial x}\right) \pm R = S_y \frac{\partial h}{\partial t} \qquad [3\text{-}7]$$

Because this nonlinear differential equation is difficult to solve, it is frequently linearised (Polubarinova-Kochina, 1962). One method of linearisation is based on the assumption that the variation in h is small compared to that in dh/dx leading to

$$K \bar{h} \frac{\partial^2 h}{\partial x^2} \pm R = S_y \frac{\partial h}{\partial t} \qquad [3\text{-}8]$$

Here $\bar{h}$ is considered constant. A second type of linearisation is obtained by writing $u = h^2$ and assuming that $\bar{h} = u^{1/2}$ is constant. Accordingly, it can be written that

$$K \sqrt{\bar{u}} \frac{\partial^2 u}{\partial x^2} \pm 2 \sqrt{\bar{u}} R = S_y \frac{\partial u}{\partial t} \qquad [3\text{-}9]$$

or

$$K \bar{h} \frac{\partial^2 u}{\partial x^2} \pm 2 \bar{h} R = S_y \frac{\partial u}{\partial t} \qquad [3\text{-}9]$$

Both methods of linearisation have been applied to drainage problems depending on the assumption that the change in depth of the water-bearing stratum is small compared to the average depth. Thus their application must be restricted to $\Delta h << h$ as well as $h << L$, as required by the D-F assumptions (slope of the phreatic surface should be in the order of 0.001 to 0.01; Bear, 1988). Here Δh refers to the change in h with time as well as with horizontal position.

Boussinesq (reported by Wesseling, 1972) and, subsequently but independently, Glover (reported by Dumm, 1954) showed that eqn.[3-5] could be solved for the water table drawdown from an initial condition characterised by the cessation of the previously constant precipitation rate (R=0) when the drains or streams penetrate to the impervious layer of a shallow aquifer (d=0) by assuming that the variables are separable (Wesseling, 1972). When the drains do not penetrate to the impervious layer (d=0), the Boussinesq type of solution breaks down. To circumvent this difficulty, several investigators - Glover, Kraijenhoff van de Leur (1958), and Maasland (1959) have used eqn.[3-6]. Starting from an initially flat water table (with R = 0) (Fig. 3-3), the boundary conditions may be written as

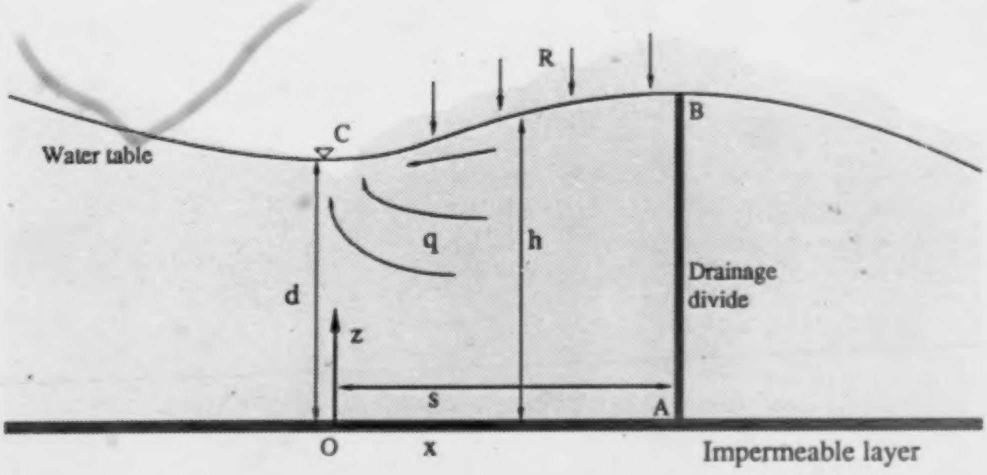
R
B
C
Water table
q
h
Drainage divide
d
z
s
A
O
x
Impermeable layer

Fig. 3-2. Schematized saturated flow domain (OABC).

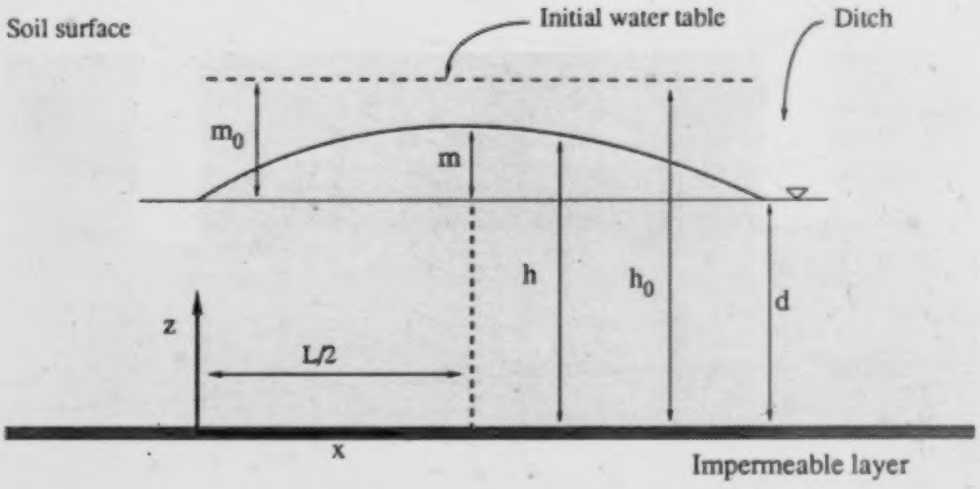
Soil surface
Initial water table
Ditch
m_0
m
h
h_0
d
z
L/2
x
Impermeable layer

Fig. 3-3. Falling water table; L - drain spacing; h - water table elevation at time t.

$$\begin{aligned} &h = h_0 = d + m_0 && \text{for } 0 < x < L && \text{at } t = 0 \\ &h = d && \text{for } x = 0 && \text{at } t > 0 \\ &\frac{\partial h}{\partial x} = 0 && \text{for } x = L/2 && \text{at } t > 0 \end{aligned} \qquad [3\text{-}11]$$

Using Fourier series, the solution becomes

$$h(x,t) = d + \frac{4m_0}{\pi} \sum_{n=1,3,5,\ldots}^{\infty} \frac{1}{n} \sin\left(\frac{n\pi x}{L}\right) e^{-n^2\pi^2 \frac{KDt}{S_y L^2}} \qquad [3\text{-}12]$$

Here, following Glover (reported by Dumm, 1954), the average depth h has been taken to be D = d + m_0/2 or the average initial depth of the water-bearing stratum.

Tapp and Moody (reported by Dumm, 1964) observed that the initial water table shape encountered in the field was more often parabolic than flat. They modified the initial condition accordingly and found a solution that differed from eqn.[3-12] only in that the numerical constant 4 was replaced by 3.4.

The methods discussed so far consider the fall of water table after precipitation ends. However, there are some methods that do not assume R = 0 for obtaining a solution. Werner (1957) presented a solution to this problem that, in principle, was based on superposition of solutions obtained from eqn.[3-9]. Maasland (1959) illustrated a similar application for a regular square-step irrigation or precipitation pattern, based on eqn.[3-9]. The design procedure described by Dumm and Winger (1964) for drainage systems in irrigated areas in effect is a practical application of the approach advocated by Maasland (1959). Krayenhoff van de Leur (1958), who studied the response to an arbitrary precipitation pattern approximated by a bar histogram, recognized a system parameter which he called 'reservoir coefficient' that characterizes the drainage soil system.

Numerical solution

The analytical solution of the D-F equation, as described in the previous sections, have been obtained with certain assumptions on the initial and boundary conditions. A general analytical solution of the equation subject to more general initial and boundary conditions has not yet been found because of its nonlinearity. However, numerical methods may be used for an approximate solution of the mixed boundary.

In this study a finite-difference implicit scheme is used to obtain a solution to the D-F equation.

3.2.3 Numerical formulation

In a similar way as has been done in Chapter 2, with reference to Fig. 3-4 the the D-F equation can be written, for the jth control volume, as

$$S_y W_j \Delta x \frac{\partial h_j}{\partial t} = q_{in} - q_{out} \pm R \qquad [3\text{-}13]$$

where R is the vertical recharge or discharge to or from the water table aquifer, W_j is the width of the control volume and S_y the drainable porosity could be assumed constant.

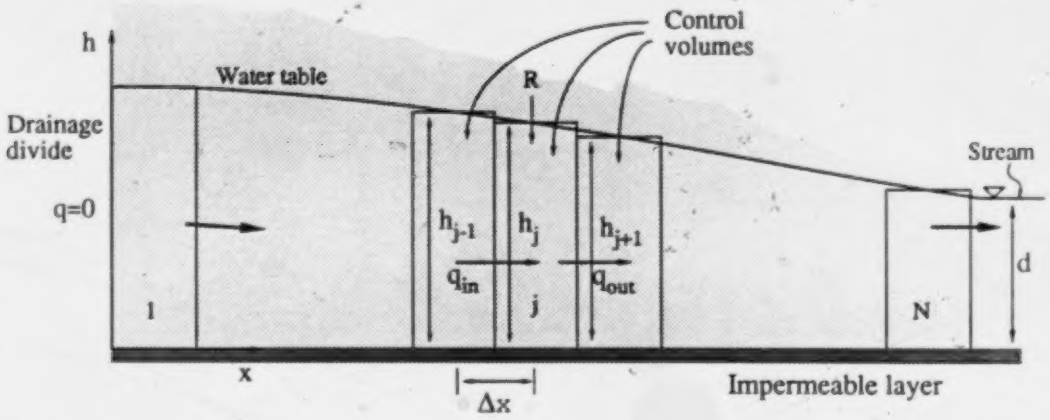
Control
volumes
h
Water table
R
Drainage
divide
Stream
q=0
h_{j-1}
h_j
h_{j+1}
q_in
q_out
d
1
j
N
x
Δx
Impermeable layer

(a) Profile

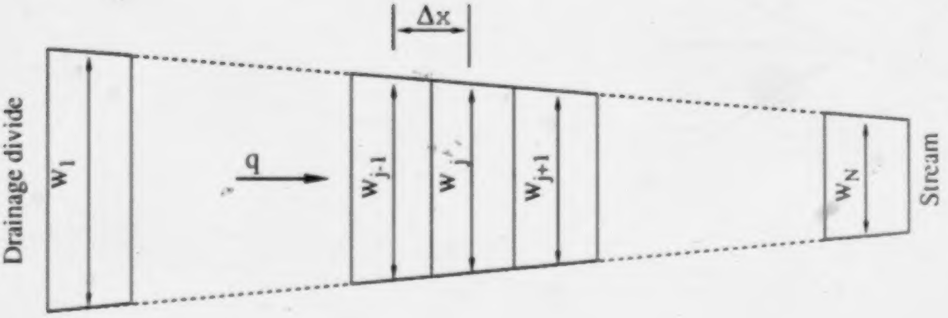
Δx
Drainage divide
w_1
q
w_{j-1}
w_j
w_{j+1}
w_N
Stream

(b) Plan

Fig. 3-4. Discretization of flow domain.

Substituting q_{in} and q_{out}, as obtained using Darcy's law, the finite-difference approximation of the D-F equation is obtained as

$$S_y W_j \Delta x \left(h_j^{n+1} - h_j^n\right) / \Delta t$$

$$= \omega \left[\begin{array}{c} \frac{W_{j-1}+W_j}{2} \frac{h_{j-1}^{n+1} + h_j^{n+1}}{2} K \frac{h_{j-1}^{n+1} - h_j^{n+1}}{\Delta x} \\ - \frac{W_j+W_{j+1}}{2} \frac{h_j^{n+1} + h_{j+1}^{n+1}}{2} K \frac{h_j^{n+1} - h_{j+1}^{n+1}}{\Delta x} \pm R^{n+1} \end{array} \right] \qquad [3\text{-}14]$$

$$+ (1-\omega) \left[\begin{array}{c} \frac{W_{j-1}+W_j}{2} \frac{h_{j-1}^{n} + h_j^{n}}{2} K \frac{h_{j-1}^{n} - h_j^{n}}{\Delta x} \\ - \frac{W_j+W_{j+1}}{2} \frac{h_j^{n} + h_{j+1}^{n}}{2} K \frac{h_j^{n} - h_{j+1}^{n}}{\Delta x} \pm R^{n} \end{array} \right]$$

Defining $\rho=4(\Delta x)S_y/(K\Delta t)$ eqn.[3-14] can be expressed as follows

$$G_j = \rho W_j \left(h_j^{n+1} - h_j^n\right)$$

$$- \omega \left[\begin{array}{c} W_{j-1/2} \left(h_{j-1}^{n+1} + h_j^{n+1}\right)\left(h_{j-1}^{n+1} - h_j^{n+1}\right) \\ - W_{j+1/2} \left(h_j^{n+1} + h_{j+1}^{n+1}\right)\left(h_j^{n+1} - h_{j+1}^{n+1}\right) \pm \frac{4\Delta x}{K} R^{n+1} \end{array} \right] \qquad [3\text{-}15]$$

$$- (1-\omega) \left[\begin{array}{c} W_{j-1/2} \left(h_{j-1}^{n} + h_j^{n}\right)\left(h_{j-1}^{n} - h_j^{n}\right) \\ - W_{j+1/2} \left(h_j^{n} + h_{j+1}^{n}\right)\left(h_j^{n} - h_{j+1}^{n}\right) \pm \frac{4\Delta x}{K} R^{n} \end{array} \right] = 0$$

For the control volume at the drainage divide (no flow condition), the D-F equation can be written as

$$S_y W_1 \Delta x \frac{\partial h_1}{\partial t} = q_{in}(=0) - q_{out} \pm R \qquad [3\text{-}16]$$

The finite difference form of it is

$$\begin{aligned} & S_y W_1 \Delta x \left(h_1^{n+1} - h_1^n\right) / \Delta t \\ & = \omega\left[- \frac{W_1+W_2}{2} \frac{h_1^{n+1} + h_2^{n+1}}{2} K \frac{h_1^{n+1} - h_2^{n+1}}{\Delta x} \pm R^{n+1} \right] \\ & + (1-\omega)\left[- \frac{W_1+W_2}{2} \frac{h_1^{n} + h_2^{n}}{2} K \frac{h_1^{n} - h_2^{n}}{\Delta x} \pm R^{n} \right] \end{aligned} \tag{3-17}$$

or

$$\begin{aligned} & G_1 = \rho W_1 \left(h_1^{n+1} - h_1^n\right) \\ & - \omega\left[- W_{1+1/2}\left(h_1^{n+1} + h_2^{n+1}\right)\left(h_1^{n+1} - h_{21}^{n+1}\right) \pm \frac{4\Delta x}{K} R^{n+1} \right] \\ & + (1-\omega)\left[- W_{1+1/2}\left(h_1^{n} + h_2^{n}\right)\left(h_1^{n} - h_2^{n}\right) \pm \frac{4\Delta x}{K} R^{n} \right] = 0 \end{aligned} \tag{3-18}$$

Similarly for the control volume at the river side (water level condition), the D-F equation is

$$S_y W_N \Delta x \frac{\partial h_N}{\partial t} = q_{in} - q_{out} \pm R \tag{3-19}$$

In difference form

$$\begin{aligned} & S_y W_N \Delta x \left(h_N^{n+1} - h_N^n\right) / \Delta t \\ & = \omega\left[\begin{array}{l} \frac{W_{N-1}+W_N}{2} \frac{h_{N-1}^{n+1} + h_N^{n+1}}{2} K \frac{h_{N-1}^{n+1} - h_N^{n+1}}{\Delta x} \\ - \frac{W_{N+1/2}}{2} \frac{h_N^{n+1} + d^{n+1}}{2} K \frac{h_N^{n+1} - d^{n+1}}{(\Delta x/2)} \pm R^{n+1} \end{array} \right] \\ & + (1-\omega)\left[\begin{array}{l} \frac{W_{N-1}+W_N}{2} \frac{h_{N-1}^{n} + h_N^{n}}{2} K \frac{h_{N-1}^{n} - h_N^{n}}{\Delta x} \\ - \frac{W_{N+1/2}}{2} \frac{h_N^{n} + d^{n}}{2} K \frac{h_N^{n} - d^{n}}{(\Delta x/2)} \pm R^{n} \end{array} \right] \end{aligned} \tag{3-20}$$

or

$$\begin{aligned} G_N &= \rho W_N \left(h_N^{n+1} - h_N^{n}\right) \\ &- \omega \left[\begin{array}{c} W_{N-1/2}\left(h_{N-1}^{n+1} + h_N^{n+1}\right)\left(h_{N-1}^{n+1} - h_N^{n+1}\right) \\ - W_{N+1/2}\left(h_N^{n+1} + d^{n+1}\right)\left(h_N^{n+1} - d^{n+1}\right) \pm \frac{4\Delta x}{K} R \end{array} \right]^{n+1} \\ &+ (1-\omega) \left[\begin{array}{c} W_{N-1/2}\left(h_{N-1}^{n} + h_N^{n}\right)\left(h_{N-1}^{n} - h_N^{n}\right) \\ - W_{N+1/2}\left(h_N^{n} + d^{n}\right)\left(h_N^{n} - d^{n}\right) \pm \frac{4\Delta x}{K} R^{n} \end{array} \right] = 0 \end{aligned} \qquad [3\text{-}21]$$

As has been done in Chapter 2, writing equations for all the computational nodes including boundary nodes a set of N nonlinear equations is obtained and solved using the N-R iterative method. The derivative coefficients in matrix form are

$$\begin{bmatrix} \frac{\partial G_1}{\partial h_1^{n+1}} & \frac{\partial G_1}{\partial h_2^{n+1}} & 0 & 0 & \cdots 0 & 0 \\ \frac{\partial G_2}{\partial h_1^{n+1}} & \frac{\partial G_2}{\partial h_2^{n+1}} & \frac{\partial G_2}{\partial h_3^{n+1}} & 0 & \cdots 0 & 0 \\ 0 & \frac{\partial G_3}{\partial h_2^{n+1}} & \frac{\partial G_3}{\partial h_3^{n+1}} & \frac{\partial G_3}{\partial h_4^{n+1}} & \cdots 0 & 0 \\ \vdots & \vdots & \vdots & \vdots & \cdots \vdots & \vdots \\ 0 & 0 & 0 & 0 & \cdots \frac{\partial G_{N-1}}{\partial h_{N-1}^{n+1}} & \frac{\partial G_{N-1}}{\partial h_N^{n+1}} \\ 0 & 0 & 0 & 0 & \cdots 0 & \frac{\partial G_N}{\partial h_N^{n+1}} \end{bmatrix} \begin{bmatrix} \Delta h_1^{n+1} \\ \Delta h_2^{n+1} \\ \Delta h_3^{n+1} \\ \vdots \\ \Delta h_{N-1}^{n+1} \\ \Delta h_N^{n+1} \end{bmatrix} = \begin{bmatrix} -r(G_1) \\ -r(G_2) \\ -r(G_3) \\ \vdots \\ -r(G_{N-1}) \\ -r(G_N) \end{bmatrix} \qquad [3\text{-}22]$$

The derivative coefficients of the above matrix are evaluated using an analytical method and these are as follows:

$$\begin{gathered}
\frac{\partial G_1}{\partial h_1^{n+1}} = \rho W_1 + 2\omega h_1^{n+1} \\
\frac{\partial G_1}{\partial h_2^{n+1}} = -2\omega h_2^{n+1} \\
\dots \quad \dots \quad \dots \\
\frac{\partial G_j}{\partial h_{j-1}^{n+1}} = -2\omega h_{j-1}^{n+1} \\
\frac{\partial G_j}{\partial h_j^{n+1}} = \rho W_j + 2\omega h_j^{n+1} \\
\frac{\partial G_j}{\partial h_{j+1}^{n+1}} = -2\omega h_{j+1}^{n+1} \\
\dots \quad \dots \quad \dots \\
\frac{\partial G_N}{\partial h_{N-1}^{n+1}} = \rho W_N + 2\omega h_{N-1}^{n+1} \\
\frac{\partial G_N}{\partial h_N^{n+1}} = -2\omega h_N^{n+1}
\end{gathered} \tag{3-23}$$

3.3 Solution of Example Problem

According to the above numerical formulation, a computer program in FORTRAN-77 has been written. Following the general trend of computing and comparing results obtained by different methods, this program is used to solve an example problem.

The example is a hypothetical drainage problem as shown in Fig. 3-3. In fact this example was given by Wesseling (1972) to demonstrate the application of the Glover-Dumm solution of the D-F equation in order to calculate drain spacing for agricultural lands. The problem consists of calculating drawdown due to gravity drainage from a plot into ditches of constant water level. The initial position of the horizontal water table was 0.8 m above the ditch water level of 7.7 m from the impervious layer. This gives: at t = 0, m_0 = 0.8 m, d = 7.7 m and, therefore, for all x from 0 to L (= 90 m), h = h_0 = 7.7 + 0.8 = 8.5 m (Fig. 3-3). Since the system is symmetrical about the vertical plane at x = L/2 i.e. x = 45 m, the solution domain was considered to be x = 45 to x = 90 m. The material properties such as drainable porosity, S_y, and saturated hydraulic conductivity, K_s, were respectively 0.05 and 1 m/day (0.0694 cm/min). It was intended to compare the present numerical solution with that of the Glover-Dumm equation (in which recharge rate must be zero, therefore, R was taken zero).

Solutions for both water table location and discharge were obtained, as mentioned, using numerical and the Glover-Dumm analytical method. In case of the numerical method, discharge or outflow was computed from Darcy's equation such as

$$q = \frac{h_N(t)+d}{2} K \frac{h_N(t)-d}{\Delta x} \text{ m}^2\text{/day/m} \qquad [3\text{-}24]$$

where h_N is the water level at node-N (Fig. 3-4).

And in case of the analytical (Glover-Dumm) method, discharge is given by

$$q = \frac{KD}{L}\left[\frac{\partial h}{\partial x}\right]_{x=L} \text{ m}^2\text{/day/m}$$

Differentiating eqn.[3-12] with respect to x and substituting x = L in the above expression it can be written that

$$q = \frac{2KDm_0}{L^2} \sum_{n=1,3,5,\ldots}^{\infty} e^{-n^2\pi^2\frac{KDt}{S_y L^2}} \ m^2/day/m \qquad [3\text{-}25]$$

Using n=50, the transient phreatic surface and outflow, q, from the piece of landmass were obtained from eqns.[3-12] and [3-25] respectively.

The calculated water table position and discharge are presented graphically in Figs. 3-5a and 3-5b.

Once again, the same story as of the previous chapter; the numerical solution seems in agreement with that of analytical method in both cases (phreatic surface and outflow hydrograph). However, this seems to be of very little significance except to prove that the FORTRAN coding was correct. Inasmuch as there were not any readily available experimental data no attempt was made to test the simulation accuracy.

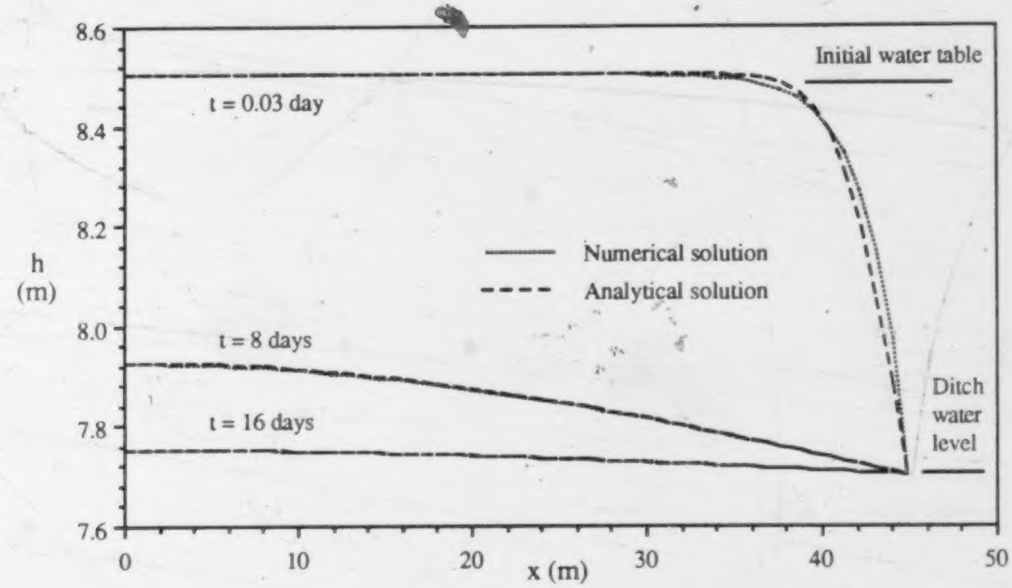

(a) Water table

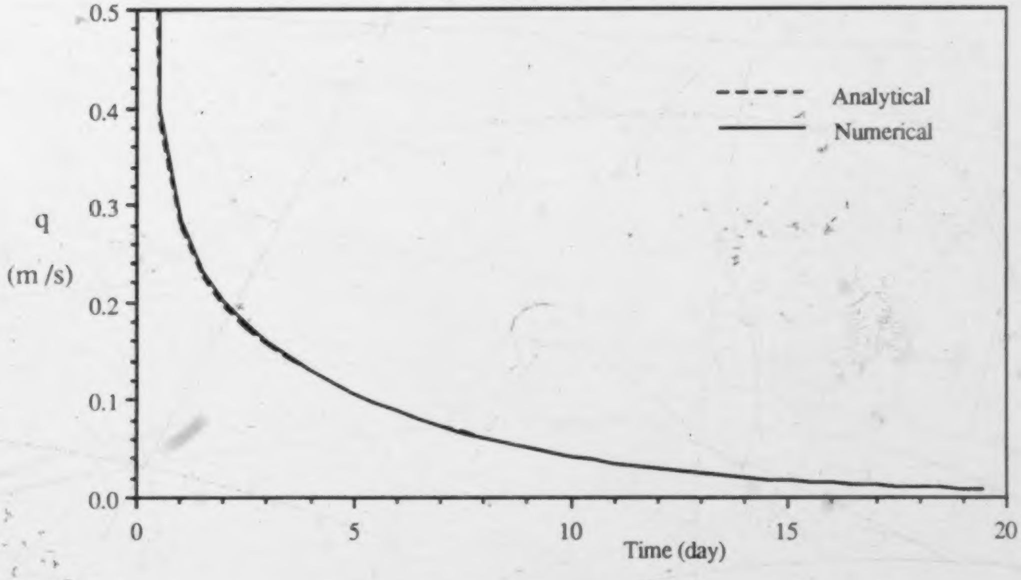

(b) Discharge hydrograph

Fig. 3-5. Computed water table location and discharge using numerical and anlytical methods.

Chapter 4

Overland Flow Model

4.1 Overland Flow

Overland flow is the surface runoff that occurs in the form of sheet (as usually conceptualized) flow on the land surface without concentrating in a clearly defined channels. This type of flow is the first manifestation of surface runoff, since the latter occurs first as overland flow before it has a chance to flow into channels and become streamflow.

As in channel flow, overland flow theory is also based on the established principles of fluid mechanics such as laminar and turbulent flow, mass and momentum conservation.

It will be seen in Chapter 5 that the kinematic-wave (K-W) model is one of the approximations of the dynamic-wave model. K-W theory describes a distinctive type of wave motion that can occur in many one-dimensional flow problems (Lighthill and Whitham, 1955).

Application of K-W theory to channel routing has been described by Weinmann and Laurenson (1979), Henderson (1963), and Brakensiek (1967). Cunge (1969) showed that the Muskingum routing method can be considered a finite-difference approximation of the K-W model. Thus, K-W theory has been widely used for the problems of water routing in irrigation systems (Cunge and Woolhiser, 1975) and storm water runoff (Dawdy et al., 1978).

Overland flow is viewed as a wide, shallow-channel flow and is often analyzed on unit width basis with lateral inflow originating from rainfall excess (Henderson, 1966). A large amount of work has been done on overland flow problem. Selected examples are Henderson and Wooding (1964), Woolhiser and Liggett (1967), Schaake (1970), and Borah et al. (1980). Very often K-W theory produce inaccurate results when applied in channel routing, however, it is recommended for application in overland flow problems.

The K-W model is used in the present study. Derivation of the equations can be found in Chow (1959), Liggett (1975), and Viessman et al. (1988). The following section states the K-W model and the justification of the assumptions made.

4.2 Flow Equation

For overland flow, some of the terms in the dynamic equation i.e. eqn.[5-3], are insignificant. Neglecting the q component, the equation can be written as

$$\underset{(1)}{S_f} = \underset{(2)}{S_o} - \underset{(3)}{\frac{\partial y}{\partial x}} - \underset{(4)}{\frac{v}{g}\frac{\partial v}{\partial x}} - \underset{(5)}{\frac{1}{g}\frac{\partial v}{\partial t}} \qquad [4\text{-}1]$$

where S_f and S_0 are the friction and bed slopes respectively, y is the depth of flow, v is the mean cross-sectional flow velocity, g is the acceleration due to gravity, x and t are the space and time coordinates.

The order of magnitude of each of the five terms is evaluated below for shallow flow. If the bed slope (2) is 0.01, the longitudinal rate of the change in water depth (3) is unlikely to exceed 0.1m/100m = 0.001. The longitudinal velocity gradient term (4) will also be less than

$(1m/s/10m/s^2)(1m/s/100m) = 0.001$, and the time rate of change in velocity term (5) will in all probability be less than $(1/10)(1/100) = 0.001$.

Terms (3), (4), and (5) are therefore at least an order of magnitude less than (2) for depth up to 1 m, and for flow depth less than 0.1 m they will be two orders of magnitude less. Those terms can therefore be neglected in overland flow problems. The inaccuracy in solutions omitting these terms for runoff hydrographs was evaluated by various researchers (Woolhiser and Liggett, 1967; Morris and Woolhiser, 1980).

The resulting simplified dynamic equation omitting terms (3), (4), and (5) simply states that the friction gradient is equal to the bed gradient. The friction gradient can be evaluated using any suitable friction equation. The two equations referred to as the kinematic equations, are the continuity equation

$$\frac{\partial y}{\partial t} + \frac{1}{B}\frac{\partial q}{\partial x} = p - f \qquad [4\text{-}2]$$

and a friction equation of the form (Emmett, 1978)

$$q = B\alpha y^m \qquad [4\text{-}3]$$

where B is the width of the strip, m is an exponent and α is a function of the water properties, surface roughness, bed slope and gravity. Since it is taken that $S_f \equiv S_0$ and $A/P \equiv y$, α and m can be evaluated for turbulent flow from Manning's formula as $\alpha = S_0/n$ and $m = 2/3$ and for laminar flow from

Poiseuille's formula as $\alpha = gS_0/3\nu$ and $m = 2$, where ν is the kinematic viscosity of the fluid. Emmett (1978) provides some experimental justification for the values of the exponent in each case, on both natural and artificial surfaces.

4.2.1 Boundary conditions

The above quasi-steady flow approximation was originally termed the kinematic wave approximation (Lighthill and Whitham, 1955) since waves can only travel downstream and are represented entirely by the continuity equation. Since the dynamic forces are omitted, the wave speed is not given by $c=(gy)^{1/2}$ but may be derived by finding dx/dt for which dy/dt = p-f, that is

$$\frac{dx}{dt} = c = m\alpha y^{m-1} \qquad [4\text{-}4]$$

Eqn.[4-3] has only a single characteristic that is described by the kinematic wave theory as above. Any disturbances of the flow will be propagated forwards through the system with that speed. Thus, only one boundary condition is necessary to effect a solution, and this is provided at the upstream edge of the flow region where

$$q_{x=0} = 0 \qquad [4\text{-}5]$$

which under kinematic assumption gives

$$y_{x=0} = 0 \qquad [4\text{-}6]$$

Hydrologically more realistic conditions are zero discharge with positive depth at the upstream boundary and critical depth at the base of the slope. For small depths this difference would hardly matter.

4.2.2 Solution techniques

The K-W equations are partial differential equations for which there are no analytical solutions except in a few idealized situations. Thus recourse is found in numerical methods. Many numerical solution techniques have been developed to solve K-W equations. Usually these techniques involve finite-difference (F-D) methods (Kibler and Woolhiser, 1970) or the method of characteristics (Borah et al., 1980) or the finite-element method (F-E). In this study the F-D method is used for the approximate solution of the K-W equations.

4.3 Numerical Formulation of K-W Equation

Unlike the unsaturated and saturated cases, the overland flow equation is formulated according to the box method instead of the control volume method. Because of the absence of downstream boundary conditions a complication crops up when the control volume formulation is used. In the box method, difference equations are written using four points as shown in Fig. 4-1.

Thus the F-D approximation of eqn.[4-2] for box T is written as

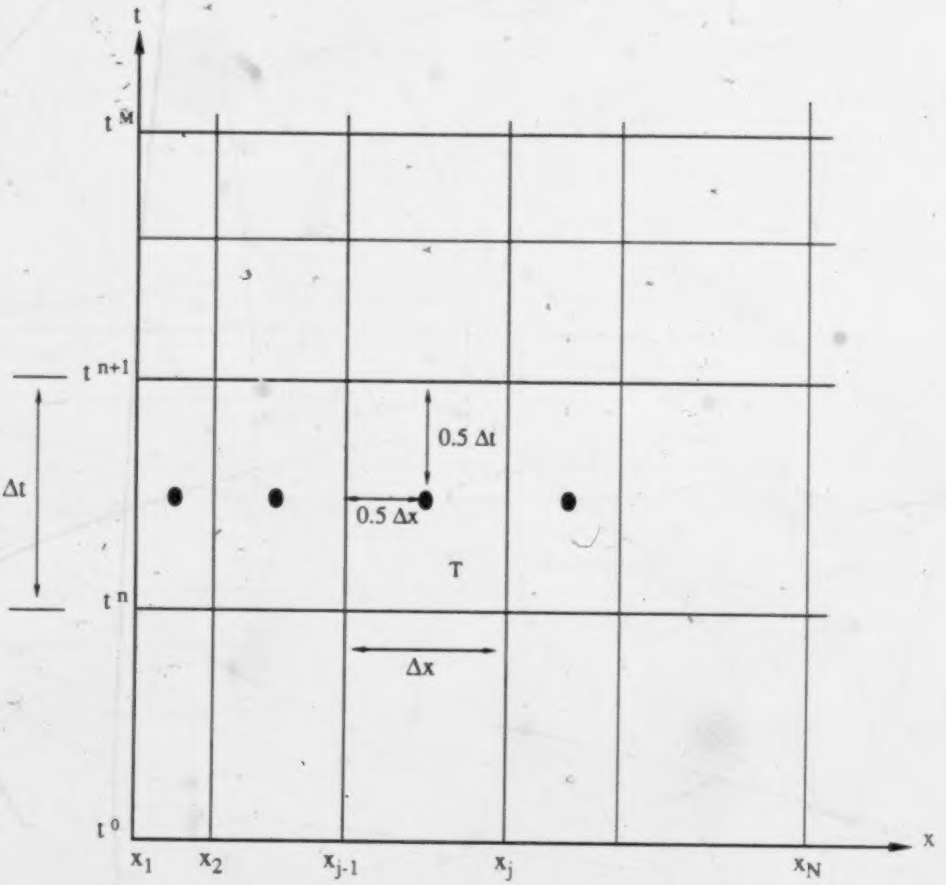
t
t^M
t^{n+1}
Δt
$0.5\ \Delta t$
$0.5\ \Delta x$
T
t^n
Δx
t^0
x_1
x_2
x_{j-1}
x_j
x_N
x

Fig. 4-1. Space-time-grid system for F-D approximations using the box method.

$$\frac{y_j^{n+1} - y_j^n + y_{j-1}^{n+1} - y_{j-1}^n}{2\Delta t} + \frac{1}{2}\,\frac{1}{B_{j-1/2}\Delta x}\left(A_j H_j^{n+1} - A_{j-1}H_{j-1}^{n+1}\right)$$
$$+ \frac{1}{2}\,\frac{1}{B_{j-1/2}\Delta x}\left(A_j H_j^n - A_{j-1}H_{j-1}^n\right) - \frac{1}{4}\left(r_j^{n+1} + r_j^n + r_{j-1}^{n+1} + r_{j-1}^n\right) = 0 \qquad [4\text{-}7]$$

where $A = B\alpha$, $H = y^{m+1}$ and $r = p-f$ or rainfall excess. Rearranging the above equation it can be written that

$$G_j = \frac{B_{j-1/2}\Delta x}{\Delta t}\left(y_j^{n+1} - y_j^n + y_{j-1}^{n+1} - y_{j-1}^n\right) + \left(A_j H_j^{n+1} - A_{j-1}H_{j-1}^{n+1}\right)$$
$$+ \left(A_j H_j^n - A_{j-1}H_{j-1}^n\right) - \frac{B_{j-1/2}\Delta x}{2}\left(r_j^{n+1} + r_j^n + r_{j-1}^{n+1} + r_{j-1}^n\right) = 0 \qquad [4\text{-}8]$$

Writing equations for all the boxes from 1 to N, a set of nonlinear simultaneous equations is obtained. These equations are also solved using the N-R iteration method. The derivative coefficient matrix is as follows:

$$\begin{bmatrix} \frac{\partial G_1}{\partial y_1^{n+1}} & \frac{\partial G_1}{\partial y_2^{n+1}} & 0 & 0 & \cdots & 0 & 0 \\ 0 & \frac{\partial G_2}{\partial y_2^{n+1}} & \frac{\partial G_2}{\partial y_3^{n+1}} & 0 & \cdots & 0 & 0 \\ 0 & 0 & \frac{\partial G_3}{\partial y_3^{n+1}} & \frac{\partial G_3}{\partial y_4^{n+1}} & \cdots & 0 & 0 \\ \vdots & \vdots & \vdots & \vdots & & \vdots & \vdots \\ 0 & 0 & 0 & 0 & \cdots & \frac{\partial G_{N-1}}{\partial y_{N-1}^{n+1}} & \frac{\partial G_{N-1}}{\partial y_N^{n+1}} \\ 0 & 0 & 0 & 0 & \cdots & 0 & \frac{\partial G_N}{\partial y_N^{n+1}} \end{bmatrix} \begin{bmatrix} \Delta y_1^{n+1} \\ \Delta y_2^{n+1} \\ \Delta y_3^{n+1} \\ \vdots \\ \Delta y_{N-1}^{n+1} \\ \Delta y_N^{n+1} \end{bmatrix} = \begin{bmatrix} -r(G_1) \\ -r(G_2) \\ -r(G_3) \\ \vdots \\ -r(G_{N-1}) \\ -r(G_N) \end{bmatrix} \qquad [4\text{-}9]$$

The derivative coefficients are evaluated analytically as

$$
\begin{aligned}
&\frac{\partial G_1}{\partial y_1^{n+1}} = 0 \\
&\frac{\partial G_1}{\partial y_2^{n+1}} = 0 \\
&\frac{\partial G_2}{\partial y_2^{n+1}} = \frac{B_{2\text{-}1/2}\Delta x}{\Delta t} - A_2(m+1)[y_2^m]^{n+1} \\
&\frac{\partial G_2}{\partial y_3^{n+1}} = \frac{B_{2\text{-}1/2}\Delta x}{\Delta t} + A_3(m+1)[y_3^m]^{n+1} \\
&\vdots \\
&\frac{\partial G_j}{\partial y_j^{n+1}} = \frac{B_{2\text{-}1/2}\Delta x}{\Delta t} - A_j(m+1)[y_j^m]^{n+1} \\
&\frac{\partial G_2}{\partial y_{j+1}^{n+1}} = \frac{B_{2\text{-}1/2}\Delta x}{\Delta t} + A_{j+1}(m+1)[y_{j+1}^m]^{n+1} \\
&\vdots \\
&\frac{\partial G_N}{\partial y_{N-1}^{n+1}} = \frac{B_{2\text{-}1/2}\Delta x}{\Delta t} - A_{N-1}(m+1)[y_{N-1}^m]^{n+1} \\
&\frac{\partial G_2}{\partial y_N^{n+1}} = \frac{B_{2\text{-}1/2}\Delta x}{\Delta t} + A_N(m+1)[y_N^m]^{n+1}
\end{aligned}
\qquad [4\text{-}10]
$$

The matrix obtained, as result of the box scheme formulation, is a bidiagonal type. Since the upstream boundary condition is assumed invariant, the correction Δy_1 is zero at all time steps and in every iteration. This leads to the following recurrence relation to obtain Δy:

$$
\begin{aligned}
&\Delta y_2 = r\,(G_1) / \frac{\partial G_1}{\partial y_2} \\
&\Delta y_3 = \left[r\,(G_2) - \frac{\partial G_2}{\partial y_2}\Delta y_2 \right] / \frac{\partial G_3}{\partial y_3}
\end{aligned}
\qquad [2\text{-}11]
$$

This algorithm is very simple and computationally efficient.

4.4 Solution of Example Problem

The iterative solution steps, again, are the same as those of section 2.2. A computer program in FORTRAN 77 has been written. This program was tested against experimental data given by Abdel-Razaq et al. (1967). Observed and predicted hydrographs are given in Fig. 4-2 showing that the model provides a reasonably satisfactory simulation. It should be noted that the observed hydrograph was established under carefully controlled laboratory conditions and refers to flow over a much smoother surface than would be encountered on most natural slopes.

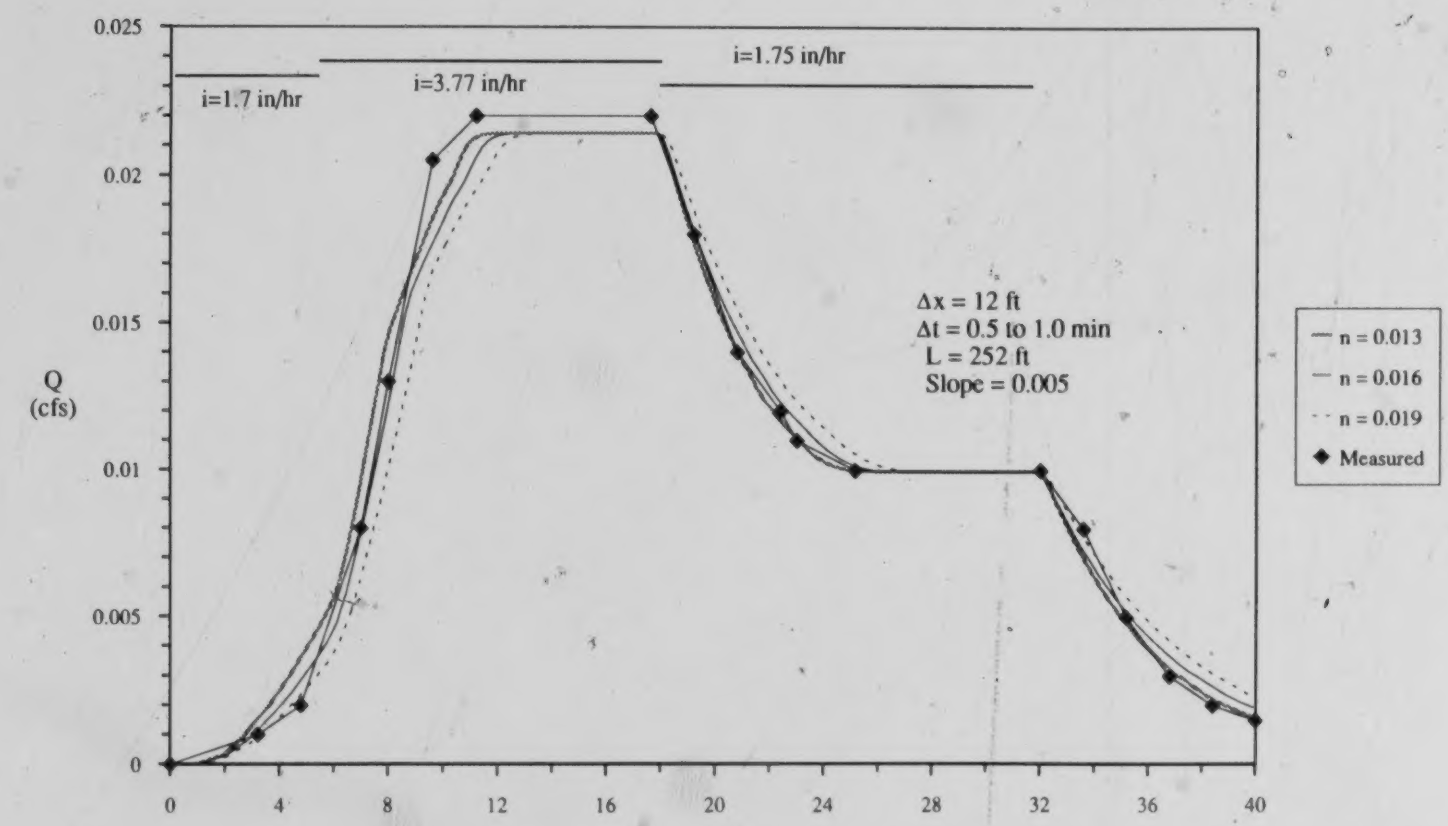

Fig. 4-2. Comparison of simulated and observed overland flow (experimental data obtained from Abdel Razaq et al., 1967).

Chapter 5

Channel Network Flow Model

5.1 Channel Routing

The channel network flow model is based upon one-dimensional, nonlinear partial differential equations governing unsteady flow in a channel with lateral inflow from adjacent land surfaces. The dependent variables are the flow rate, Q, and water surface elevation, h. The application of the model is subject to the basic assumptions and limitations (which could be found in Abbott (1979) and Lai (1986)) inherent in the equation's formulation.

Mechanics of open channel flow is a familiar subject. Derivation and analyses of the flow equations are available in any open channel texts including the aforementioned references. Hence, no attempt is made here to derive them. Instead, with a brief statement of the equations, the network modeling procedure is described in the sections to follow.

5.2 Flow Equations

The one dimensional partial-differential equations governing transient flow in open channels have been reported previously in the literature (Baltzer and Lai, 1968; Strelkoff, 1969; Yen, 1973b). The system of differential equations presented by Baltzer and Lai constitute the basis of the open channel network flow equations. Using the water surface elevation, h, and the channel discharge, Q, as the dependent variables, the equation of continuity can be written as

$$B\frac{\partial h}{\partial t} + \frac{\partial Q}{\partial x} = q_l \qquad [5\text{-}1]$$

in which B is the channel top width, shown in Fig. 5-1, and q_l is lateral inflow. The distance, x, in the longitudinal direction and the elapsed time, t, are the independent variables. The equation of motion for one-dimensional open channel flow can be obtained as

$$\frac{\partial Q}{\partial t} + \frac{Q}{A}\frac{\partial Q}{\partial x} + Q\frac{\partial (Q/A)}{\partial x} + gA\frac{\partial h}{\partial x} + \frac{gk}{AR^{4/3}}|Q|Q = 0 \qquad [5\text{-}2]$$

where g is the acceleration of gravity, A is the cross sectional area, R is the hydraulic radius, and k is function of the flow resistance coefficient, n, which can be expressed as $k = n^2$ [in the British System $k = (n/1.49)^2$]. Eqn.[5-2] can also be expressed as

$$\frac{\partial v}{\partial t} + v\frac{\partial v}{\partial x} + g\frac{\partial y}{\partial x} - g(S_o - S_f) = 0 \qquad [5\text{-}3]$$

where v is the cross-sectional average velocity, y is flow depth, S_0 and S_f are bed and friction slopes respectively.

Eqns.[5-1] and [5-2] or [5-3] represent the conservation of mass and momentum of flow of the fluid in the channel. These equations are nonlinear, hyperbolic, partial differential equations and represent a nonlinear, deterministic, distributed, time variant system. They are sometimes referred to as the St. Venant equations. The fundamental assumptions that are made in the derivation of the St. Venant equations are: (i) the flow is one-

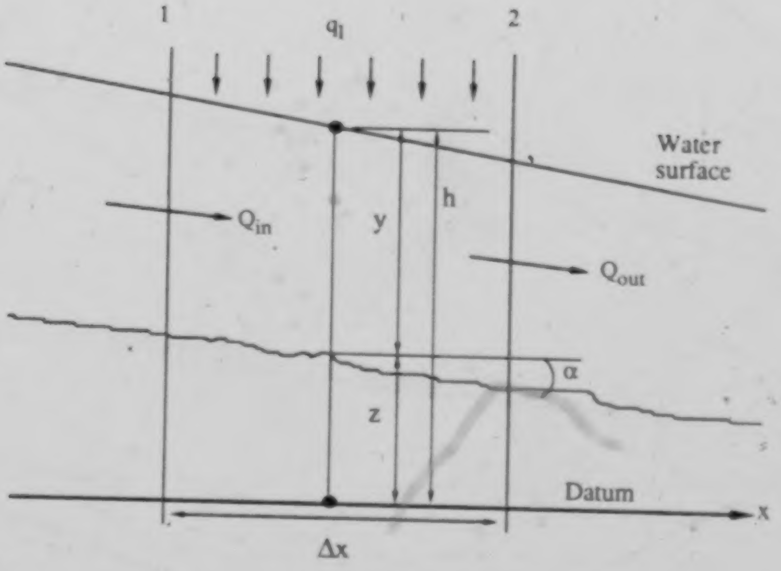
1
q_l
2
Water surface
Q_{in}
y
h
Q_{out}
α
z
Datum
x
Δx

(a) Profile

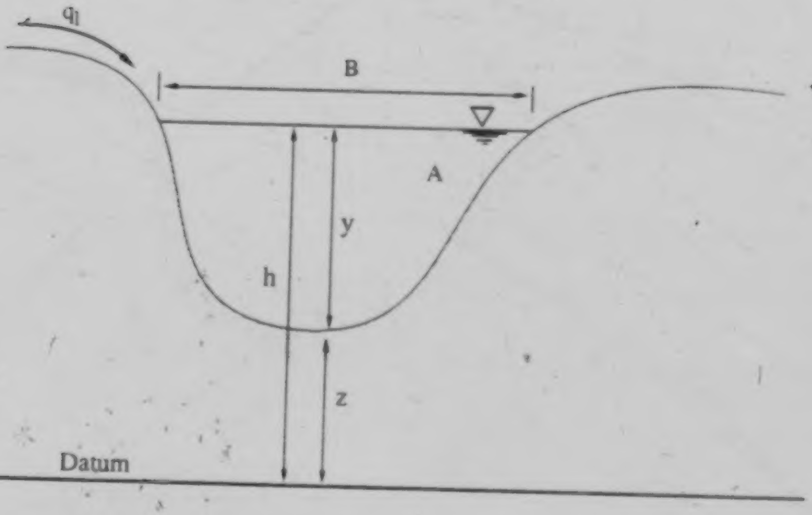
q_l
B
A
y
h
z
Datum

(b) Cross Section

Fig. 5-1. Definition sketch of a channel element (adapted after Baltzer and Lai, 1968).

dimensional, i.e. the flow in the channel can be well approximated with uniform velocity over each cross-section and the free surface is taken to be a horizontal line across the section; (ii) the pressure is hydrostatic, i.e. the vertical acceleration is neglected; (iii) the effect of boundary friction and turbulence can be accounted for through the introduction of a resistance force which is described by the empirical 'Manning', or 'Darcy Weisbach' friction factor equation.

5.2.1 Diffusion wave equation

Eqns.[5-1] and [5-2] or [5-3] are acceptable for fully one dimensional overland and open channel flow routing. These equations describe both the forward or downstream wave propagation characteristics as well as the backward or upstream characteristics. It is assumed that flood waves in streams move downstream as the runoff always runs down slope, the backward characteristics are simply backwater effects, and in some flow routing instances, they can have substantial impact and control on the flow. As such, these equations are known generally as the dynamic wave equations. As a runoff hydrograph passes through channel irregularities, slough and riffle patterns, natural, beaver and man made roughness and gravity forces act to reduce the hydrograph peak while lengthening the time base. That is, the peak of the hydrograph is attenuated while the shape is dispersed in time (also in space). The dynamic wave equations account well for hydrograph attenuation. However, two drawbacks to the wholesale general use of these equations are the large data requirements and the necessity for numerical integration. Very often, based on the nature of flow domain and flood wave characteristics, it is possible to make valid simplifying assumptions that allow utilization of approximations to the dynamic wave equations (Table 5-1). When this is possible, advantages in terms of ease of solution and data requirements are often realized.

Table 5-1. Order of magnitude of terms in St.Venant equation (adapted after Schaake, 1965).

Type of Flow	Accln. $\frac{1}{g}\frac{\partial v}{\partial t}$	C.Accl. $\frac{v}{g}\frac{\partial v}{\partial x}$	Pressure $\frac{\partial h}{\partial x}$	Gravity S_0	Friction $\frac{v\lvert v\rvert}{C^2R}$	Units
River	0.05	0.12-0.25	0.50	26.00	25.50	ft/ml
Gutter Flow	4.90	4.90	9.80	182.00	180.00	ft/ml
Overland Flow	1.64	1.64	16.40	212.00	212.00	ft/ml

One of the two approximations is the diffusion wave model and the other is the kinematic wave model (Henderson, 1966; Yen, 1973b). The Kinematic wave model has been discussed in Chapter 4 in the context of modeling overland flow. The diffusion wave model assumes that the inertia terms in the equation of motion, eqn.[5-2], are negligible compared with the pressure, friction and gravity terms. Thus, the diffusion model equations are continuity, eqn.[5-1], and the following simplified form of the conservation of momentum equation.

$$Q = \frac{1}{n} A R^{2/3} \left(- \frac{\partial h}{\partial x} \right) / \sqrt{\frac{\partial h}{\partial x}} \qquad [5\text{-}4]$$

Eqn.[5-4] accounts for flows in both positive and negative x directions. This diffusion wave model has been used for flood routing in the channel network of the present study. The assumptions made are very reasonable as will be seen in section 5.6 where computed results of diffusion and dynamic wave models are compared. Akan and Yen (1977) and Katopodes (1982) demonstrated the ability of the diffusion wave approximation in accounting for the downstream backwater effect.

5.3 Boundary Conditions

Solution of the flow equations requires specification of boundary conditions throughout the duration of simulation at the physical extremities (external junctions) of the network, as well as at branch junctions (or internal junctions) within the network (Fig. 5-2).

5.3.1 Compatibility at internal junctions

The most common boundary conditions encountered in networks of interconnected channels occurs at junctions where two or more branches join. This situation typically occurs where a channel is joined by a tributary or where a channel is divided by the presence of an island.

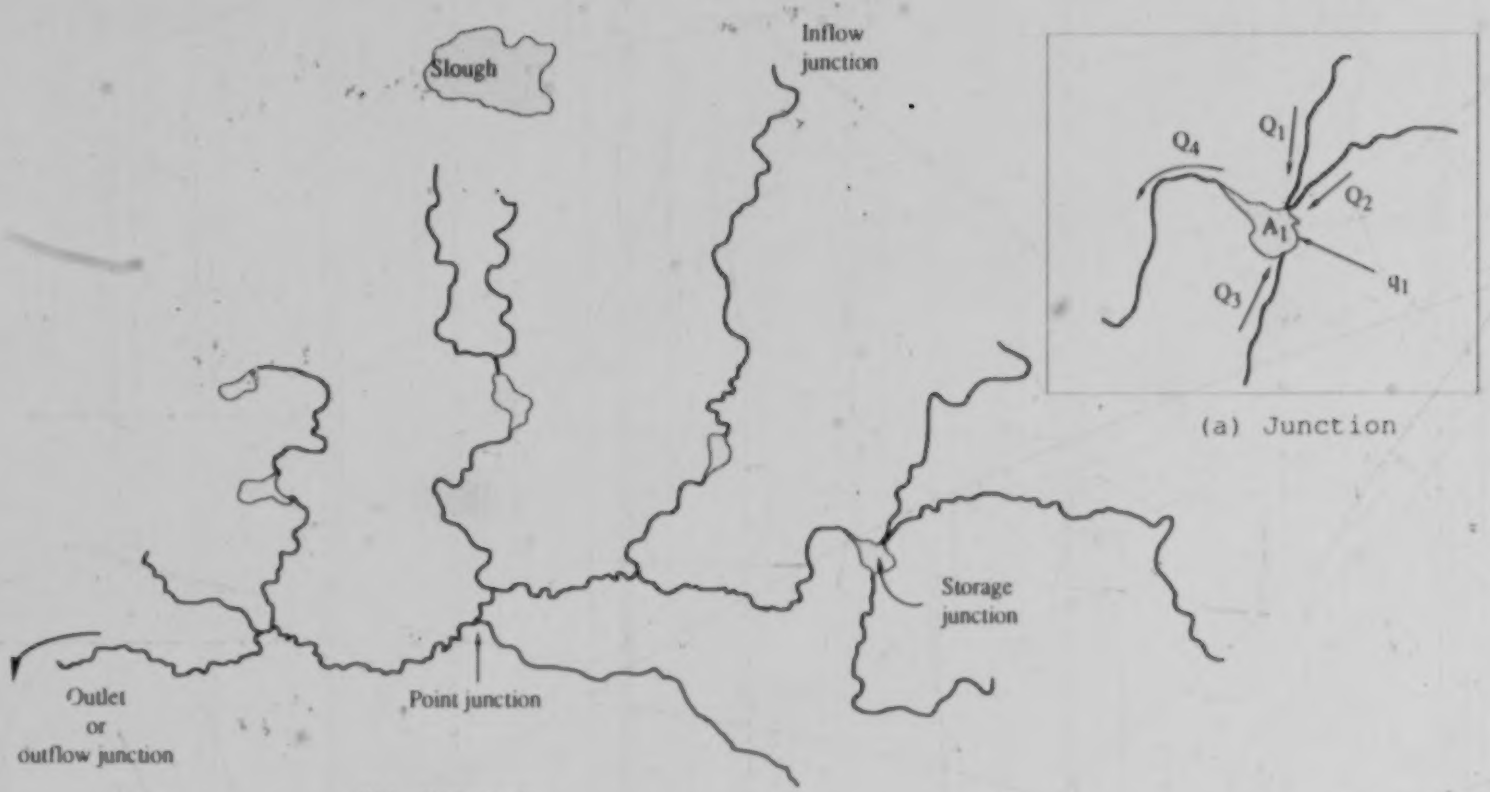
Slough
Inflow junction
Storage junction
Point junction
Outlet or outflow junction
Q_1
Q_2
Q_3
Q_4
A_1
q_1

(a) Junction

(b) Network

Fig. 5-2. Channel network of Spring Creek watershed.

The most important feature of a junction is that it imposes backwater effects to the channel connected to it. A junction provides, in addition to a volume of temporal storage, redistribution and dissipation of energy and mixing and transfer of momentum of flow and of the sediment and pollutant it carries. The precise, detailed hydraulic description of the flow in a junction is rather complicated. However, a reasonably correct representation of the junction is possible in realistic simulation and reliable computation of the flow in a stream network.

The continuity equation of the water in a junction is

$$\sum_{i=1}^{NC} Q_j^i + q_j = \frac{dS}{dt} \qquad [5\text{-}5]$$

in which S is the storage, Q_j^i is the flow into or out from the junction j, by NC joining channels (Fig. 5-2a; NC = 4), being positive for inflow and negative for outflow; q_j represents the direct, temporarily variable water inflow into (positive), or the overflow or leakage out from (negative) the junction j; the index j equals 1 to NJ, where NJ is the number of junctions in the network (Fig. 5-2b).

Two types of internal junctions are encountered in the real stream network of this study; the storage junction and the point junction (Fig. 5-2b). For a storage junction, the storage capacity of the junction is relatively large in comparison with the flow and hydraulically it behaves like a reservoir. A water surface and hence the depth in the junction can be defined without great difficulty. The kinetic energy carried by the upstream channels are dissipated in the junction. If the horizontal area of the junction A_j remains constant, and therefore, independent of the junction depth y, the storage is $S = A_j y$. Hence,

$$\frac{dS}{dt} = A_j \frac{dy}{dt} = A_j \frac{dh}{dt} \qquad [5\text{-}6]$$

where h=y+z is the water surface elevation above the reference datum and where z is the elevation of the junction bottom. Therefore, from eqns.[5-5] and [5-6], the continuity equation for a constant surface area storage junction is

$$\sum_{i=1}^{NC} Q_j^i + q_j = A_j \frac{dh}{dt} \qquad [5\text{-}7]$$

In case of a point junction, the storage capacity is negligible and the junction is treated as a single confluence point. Hence, eqn.[5-7] is reduced to

$$\sum_{i=1}^{NC} Q_j^i + q_j = 0 \qquad [5\text{-}8]$$

The subcritical flow in the channel is subject to the backwater effect from the junction. Since the junction is treated as a point, the dynamic condition of the junction is usually represented by a kinematic compatibility condition of a common water surface at the junctions for all the joining channels.

$$h_i = h_j \qquad [5\text{-}9]$$

Therefore, at an internal junction there are discharge continuity and stage compatibility conditions that must be satisfied.

5.3.2 At the external junctions

In addition to the required boundary conditions at internal junctions, boundary conditions must be specified at all external junctions, that is, junctions with singular connecting branches identified as inflow or outflow junction in Fig. 5-2b. Various combinations of boundary conditions can be specified at the external junctions of a channel network. External boundary conditions can consist of a zero discharge (as for example, at a dead-end branch), known discharge as a function of time, known stage as a function of time, or a known unique stage-discharge relationship.

5.4 Initial Conditions

In order to initiate a solution of the system of equations with the specified boundary conditions, initial values of the unknown quantities are required. These values may be obtained from measurements, computed from some other source, such as stage-state approximations, or computed from previous simulations. Successive use of newly computed values as initial values permits the computation to proceed step-by-step until the boundary-value data are exhausted or the simulation is otherwise terminated. Successful convergence of the computation to the correct solution requires that the initial values be reasonably accurate; the less accurate the initial values, the longer the computation takes to dissipate the initialization error and converge to the true solution.

5.5 Solution of the Channel Flow Equations

No analytical solutions are available for the solution of the nonlinear diffusion wave equation with generalized initial and boundary conditions. Therefore, these equations are solved numerically.

A number of numerical methods are reported in the literature for the numerical solution of hyperbolic partial differential equations, and are described in detail in a number of texts on the numerical analysis of partial differential equations. Ames (1969) gives a clear and simple account, while various approaches to the particular problem of one dimensional overland and channel flows are critically reviewed by Liggett and Woolhiser (1967, 1969), Strelkoff (1970), Price (1974), Joliffe (1982) and Lai (1986). In the channel flow problems the common numerical methods (or numerical schemes) can be classified in three groups such as explicit, implicit, and the method of characteristics (from these a number of hybrid methods have been developed).

The above numerical schemes have been described in Chapter 1. Here, the F-D formulation of the flow equation using a weighted implicit scheme is described. Again, this is based on the method proposed by Patankar (1980) i.e. the control volume method. Solution is obtained using the N-R iteration.

5.5.1 Numerical formulation

For the sake of above mentioned formulation method, the diffusion wave equations i.e. the continuity and simplified momentum equations are written in the following guise

$$\Delta x \, B \frac{\Delta h}{\Delta t} = Q_{in} - Q_{out} + q_l \qquad [5\text{-}10]$$

and

$$Q = C\left(-\frac{\Delta h}{\Delta x}\right) / \left|\frac{\Delta h}{\Delta x}\right|^{0.5} = \mathrm{sign}\left(\frac{\Delta h}{\Delta x}\right) C \left|\frac{\Delta h}{\Delta x}\right|^{0.5} \qquad [5\text{-}11]$$

considering a tiny control volume (shaded area) as shown in Fig. 5-3. These two equations are not different from eqns.[5-1] and [5-4] except that they are written in difference form. In eqn.[5-11], C (conveyance) is equal to $(AR^{2/3})/n$ and the term 'sign' means that the sign of the argument is preserved while computing the square root of the absolute value of $\Delta h/\Delta x$.

To describe the F-D formulation of eqns.[5-10] and [5-11] the channel network shown in Fig. 5-4 is considered. The total channel reach of the system is divided into N control volumes. Numerical solutions are sought for h at the center and for Q at the edges of each control volume and the junctions are treated as a control volume of a special type. The reach segments, Δx, are allowed to vary in the model, however, they are treated here as constant for simplicity's sake.

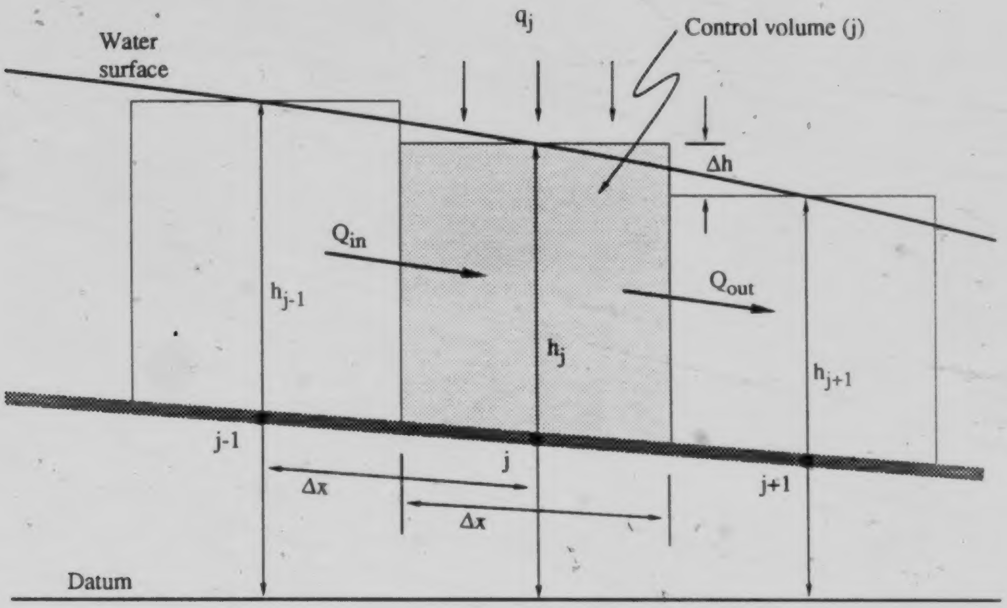
Water surface
q_j
Control volume (j)
Δh
Q_{in}
Q_{out}
h_{j-1}
h_j
h_{j+1}
j-1
j
j+1
Δx
Δx
Datum

(a) Profile

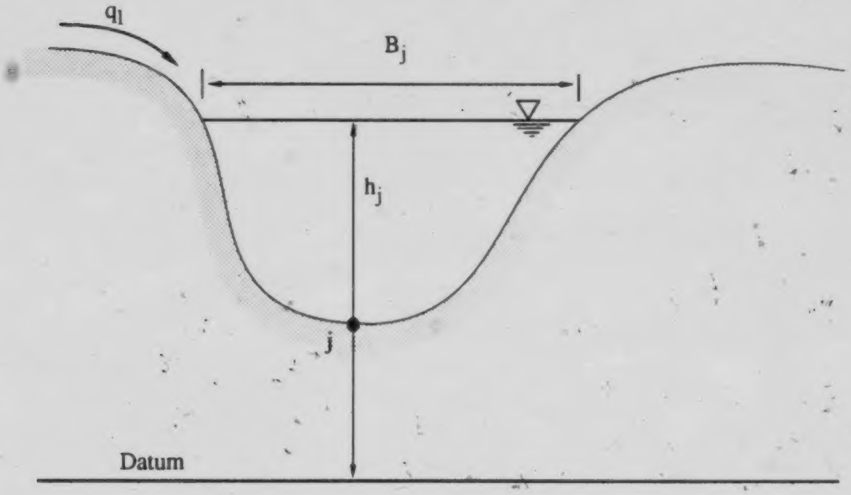
q_l
B_j
h_j
j
Datum

(b) Cross section

Fig. 5-3. Definition sketch of control volume.

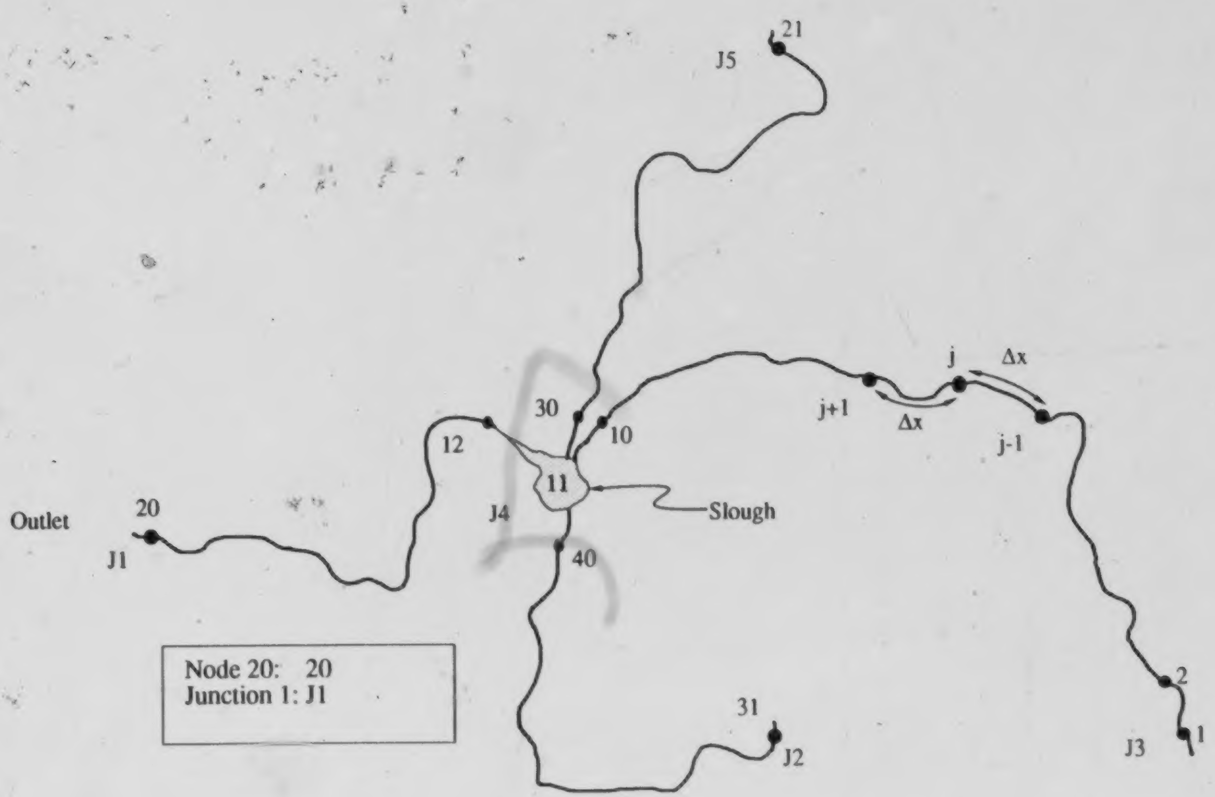
21
J5
j
Δx
30
10
j+1
Δx
j-1
12
11
Slough
Outlet
20
J1
J4
40
Node 20: 20
Junction 1: J1
31
J2
2
1
J3

Fig. 5-4. Discretization of channel network.

With reference to Fig. 5-5, eqn.[5-10] is written in weighted implicit finite difference quotients for the jth control volume as

$$\Delta x\, B_j^{n+1/2}\left(h_j^{n+1} - h_j^n\right)/\Delta t = \omega\left[Q_{j-1/2}^{n+1} - Q_{j+1/2}^{n+1} + q_j^{n+1}\right] + (1-\omega)\left[Q_{j-1/2}^{n} - Q_{j+1/2}^{n} + q_j^{n}\right] \qquad [5\text{-}12]$$

and

$$Q_{j-1/2} = C_{j-1/2}\sqrt{\frac{h_{j-1} - h_j}{\Delta x}} \qquad [5\text{-}13]$$

[Sign of $(h_{j-1} - h_j)$ is preserved in the model]

Substituting eqn.[5-13] into eqn.[5-12] and writing $K = C/(\Delta x)^{0.5}$, the following expression is obtained

$$\begin{aligned} &B_j^{n+1/2}\left(h_j^{n+1}-h_j^n\right)/\Delta t \\ &= \frac{\omega}{\Delta x}\left[K_{j-1/2}^{n+1}\sqrt{h_{j-1}^{n+1}-h_j^{n+1}} - K_{j+1/2}^{n+1}\sqrt{h_j^{n+1}-h_{j+1}^{n+1}} + q_j^{n+1}\right] \\ &+ \frac{1-\omega}{\Delta x}\left[K_{j-1/2}^{n}\sqrt{h_{j-1}^{n}-h_j^{n}} - K_{j+1/2}^{n}\sqrt{h_j^{n}-h_{j+1}^{n}} + q_j^{n}\right] \end{aligned} \qquad [5\text{-}14]$$

After rearrangement eqn.[5-14] takes the form

$$\begin{aligned} G_j = {} & \rho B_j^{n+1/2}\left(h_j^{n+1} - h_j^n\right) \\ & - \omega\left[K_{j-1/2}^{n+1}\sqrt{h_{j-1}^{n+1}-h_j^{n+1}} - K_{j+1/2}^{n+1}\sqrt{h_j^{n+1}-h_{j+1}^{n+1}} + q_j^{n+1}\right] \\ & -(1-\omega)\left[K_{j-1/2}^{n}\sqrt{h_{j-1}^{n}-h_j^{n}} - K_{j+1/2}^{n}\sqrt{h_j^{n}-h_{j+1}^{n}} + q_j^{n}\right] = 0 \end{aligned} \qquad [5\text{-}15]$$

where $\rho = \Delta x/\Delta t$.

In this expression, ω is a weighting factor, specifying the time at which these quantities are evaluated between the t^n

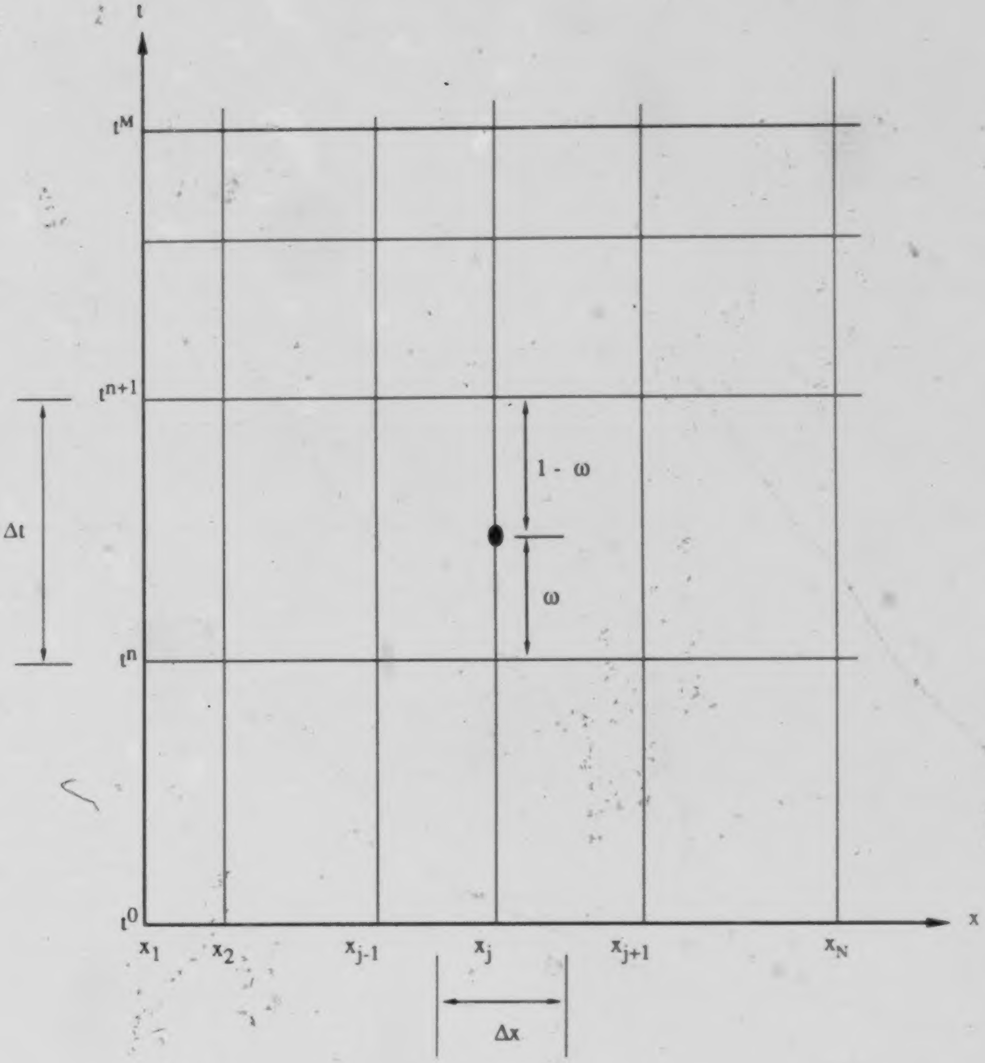
t
t^M
t^{n+1}
Δt
1 - ω
ω
t^n
t^0
x
x_1
x_2
x_{j-1}
x_j
x_{j+1}
x_N
Δx

Fig. 5-5. Space-time-grid system for F-D approximation (control volume method); ω - weighting factor.

and t^{n+1} adjacent time levels at the midpoint of the jth cell. In the finite difference scheme, ω is a real constant, generally thought of as lying in the interval 0<ω<1.

Writing eqn.[5-15] for each computational cell of Fig. 5-4 results in 35 equations containing 40 unknowns. The additional 5 equations are supplied by the boundary conditions to the problem. The conditions are as follows:

Inflow hydrograph conditions at nodes 1, 21, 31 generate

$$\begin{aligned}
G_1 &= \rho B_1^{n+1/2}\left(h_1^{n+1}-h_1^n\right)-\omega\left[q_1^{n+1}-K_{1+1/2}^{n+1}\sqrt{h_1^{n+1}-h_2^{n+1}}\right] \\
&\qquad -(1-\omega)\left[q_1^n-K_{1+1/2}^n\sqrt{h_1^n-h_2^n}\right]=0 \\
G_{21} &= \rho B_{21}^{n+1/2}\left(h_{21}^{n+1}-h_{21}^n\right)-\omega\left[q_{21}^{n+1}-K_{21+1/2}^{n+1}\sqrt{h_{21}^{n+1}-h_{21+1}^{n+1}}\right] \\
&\qquad -(1-\omega)\left[q_{21}^n-K_{21+1/2}^{n+1}\sqrt{h_{21}^n-h_{21+1}^n}\right]=0 \\
G_{31} &= \rho B_{31}^{n+1/2}\left(h_{31}^{n+1}-h_{31}^n\right)-\omega\left[q_{31}^{n+1}-K_{31+1/2}^{n+1}\sqrt{h_{31}^{n+1}-h_{31+1}^{n+1}}\right] \\
&\qquad -(1-\omega)\left[q_{31}^n-K_{31+1/2}^{n+1}\sqrt{h_{31}^n-h_{31+1}^n}\right]=0
\end{aligned} \qquad [5\text{-}16]$$

The rating curve at node 20 yields

$$\begin{aligned}
G_{20} = {} & \rho B_{20}^{n+1/2}\left(h_{20}^{n+1}-h_{20}^n\right) \\
& -\omega\left[K_{20-1/2}^{n+1}\sqrt{h_{20-1}^{n+1}-h_{20}^{n+1}}-C_1\left(h_{20}^{n+1}\right)^{C_2}\right] \\
& -(1-\omega)\left[K_{20-1/2}^n\sqrt{h_{20-1}^n-h_{20}^n}-C_1\left(h_{20}^n\right)^{C_2}\right]=0
\end{aligned} \qquad [5\text{-}17]$$

Junction of several channels at node 11 (slough with surface area A) provides the following equation (Fig. 5-6)

$$\begin{aligned}
& A_{11}^{n+1/2}\left(h_{11}^{n+1}-h_{11}^n\right)/\Delta t \\
& =\omega\left[Q_{30,11}^{n+1}+Q_{10,11}^{n+1}+Q_{40,11}^{n+1}-Q_{11,12}^{n+1}+q_{11}^{n+1}\right] \\
& +(1-\omega)\left[Q_{30,11}^n+Q_{10,11}^n+Q_{40,11}^n-Q_{11,12}^n+q_{11}^n\right]
\end{aligned} \qquad [5\text{-}18]$$

or substituting the expression for Q it can be written as

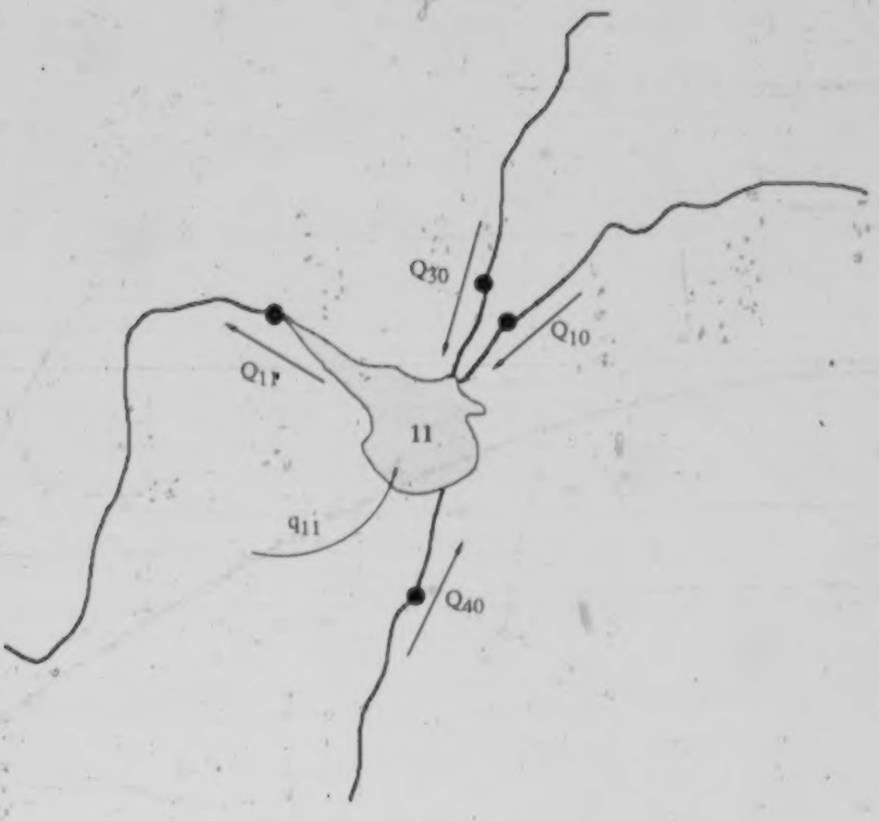
Q30
Q10
Q11
11
q11
Q40

Fig. 5-6. Storage junction-11.

$$\begin{aligned} G_{11} &= A_{11}^{n+1/2}\left(h_{11}^{n+1}-h_{11}^{n}\right)/\Delta t \\ &- \omega\left[\begin{aligned} &K_{30,11}^{n+1}\sqrt{h_{30}^{n+1}-h_{11}^{n+1}}+K_{10,11}^{n+1}\sqrt{h_{10}^{n+1}-h_{11}^{n+1}} \\ &+K_{40,11}^{n+1}\sqrt{h_{40}^{n+1}-h_{11}^{n+1}}-K_{11,12}^{n+1}\sqrt{h_{11}^{n+1}-h_{12}^{n+1}}+q_{11}^{n+1}\end{aligned}\right] \\ &-(1-\omega)\left[\begin{aligned} &K_{30,11}^{n}\sqrt{h_{30}^{n}-h_{11}^{n}}+K_{10,11}^{n}\sqrt{h_{10}^{n}-h_{11}^{n}} \\ &+K_{40,11}^{n}\sqrt{h_{40}^{n}-h_{11}^{n}}-K_{11,12}^{n}\sqrt{h_{11}^{n}-h_{12}^{n}}+q_{11}^{n}\end{aligned}\right] \approx 0 \end{aligned} \qquad [5\text{-}19]$$

Eqn.[5-15] for each cell, together with the 5 boundary conditions are succinctly written as

$$\begin{array}{lcl} G_1\left(h_1^{n+1},\ h_2^{n+1}\right) & \approx & 0 \\ G_2\left(h_1^{n+1},\ h_2^{n+1},\ h_3^{n+1}\right) & \approx & 0 \\ G_3\left(h_2^{1+1},\ h_3^{n+1},\ h_4^{n+1}\right) & \approx & 0 \\ \dots\ \dots\ \dots & & \dots \\ G_{11}\left(h_{10}^{n+1},\ h_{11}^{n+1},\ h_{12}^{n+1},\ h_{30}^{n+1},\ h_{40}^{n+1}\right) & \approx & 0 \\ \dots\ \dots\ \dots\ \dots\ \dots & & \dots \\ G_{20}\left(h_{19}^{n+1},\ h_{20}^{n+1}\right) & \approx & 0 \\ \dots\ \dots\ \dots & & \dots \\ G_{30}\left(h_{11}^{n+1},\ h_{29}^{n+1},\ h_{30}^{n+1}\right) & \approx & 0 \\ \dots\ \dots\ \dots & & \dots \\ G_{40}\left(h_{11}^{n+1},\ h_{39}^{n+1},\ h_{40}^{n+1}\right) & \approx & 0 \end{array} \qquad [5\text{-}20]$$

The resulting 40 equations in 40 unknowns are nonlinear, as the A's, B's and K's are functions of h and all h values contain exponents other than unity. These may be solved using any iterative method; in this case, the generalized N-R method has been chosen.

The solution steps for this problem is the same as outlined in Chapter 2. The dependant variable, h, is first estimated from the known values and is then substituted in the governing equation (eqn.[5-20]) to calculate residuals R_1^{n+1}, through R_{40}^{n+1} at the (n+1)th time step. The set of flow correction equations is obtained as

$$\begin{bmatrix} \frac{\partial G_1}{\partial h_1^{n+1}}\Delta h_1^{n+1}+\frac{\partial G_1}{\partial h_2^{n+1}}\Delta h_2^{n+1} \\ \frac{\partial G_2}{\partial h_1^{n+1}}\Delta h_1^{n+1}+\frac{\partial G_2}{\partial h_2^{n+1}}\Delta h_2^{n+1}+\frac{\partial G_2}{\partial h_3^{n+1}}\Delta h_3^{n+1} \\ \frac{\partial G_3}{\partial h_2^{n+1}}\Delta h_2^{n+1}+\frac{\partial G_3}{\partial h_3^{n+1}}\Delta h_3^{n+1}+\frac{\partial G_3}{\partial h_4^{n+1}}\Delta h_4^{n+1} \\ \vdots \\ \frac{\partial G_{11}}{\partial h_{10}^{n+1}}\Delta h_{10}^{n+1}+\frac{\partial G_{11}}{\partial h_{11}^{n+1}}\Delta h_{11}^{n+1}+\frac{\partial G_{11}}{\partial h_{12}^{n+1}}\Delta h_{12}^{n+1}+\frac{\partial G_{11}}{\partial h_{30}^{n+1}}\Delta h_{30}^{n+1}+\frac{\partial G_{11}}{\partial h_{40}^{n+1}}\Delta h_{40}^{n+1} \\ \vdots \\ \frac{\partial G_{20}}{\partial h_{19}^{n+1}}\Delta h_{19}^{n+1}+\frac{\partial G_{20}}{\partial h_{20}^{n+1}}\Delta h_{20}^{n+1} \\ \vdots \\ \frac{\partial G_{30}}{\partial h_{11}^{n+1}}\Delta h_{11}^{n+1}+\frac{\partial G_{30}}{\partial h_{29}^{n+1}}\Delta h_{29}^{n+1}+\frac{\partial G_{30}}{\partial h_{30}^{n+1}}\Delta h_{30}^{n+1} \\ \vdots \\ \frac{\partial G_{40}}{\partial h_{11}^{n+1}}\Delta h_{11}^{n+1}+\frac{\partial G_{40}}{\partial h_{39}^{n+1}}\Delta h_{39}^{n+1}+\frac{\partial G_{40}}{\partial h_{40}^{n+1}}\Delta h_{40}^{n+1} \end{bmatrix} = \begin{bmatrix} -R_1^{n+1} \\ -R_2^{n+1} \\ -R_3^{n+1} \\ \vdots \\ -R_{11}^{n+1} \\ \vdots \\ -R_{20}^{n+1} \\ \vdots \\ -R_{30}^{n+1} \\ \vdots \\ -R_{40}^{n+1} \end{bmatrix} \qquad [5\text{-}21]$$

Eqn.[5-21] is solved for flow corrections Δh_i. All the residuals are zero or approximately zero when the correct solution has been found.

5.5.2 Coefficient matrix

Examination of eqn.[5-20], which has be solved to evaluate each flow correction, reveals that it loses its banded structure for channel networks. For a single channel problem the maximum number of unknowns in any eqn.[5-20] is three and an efficient solution procedure can be used by solving the banded set of simultaneous equations.

For channel networks the matrix is no longer banded. The maximum number of unknowns in any equation depends upon the number of channels connecting at a junction and the number of unknowns is independent of the computational nodes immediately adjacent to the junctions. To solve this matrix, the special Gauss-Jordan elimination technique of Gupta and Tanji (1977) can be used. In this technique, three arrays are required to store the coefficient matrix of eqn.[5-21]. One array stores the actual partial derivative coefficients while the integer arrays are used to store the actual locations of the coefficients in the matrix and the number of unknowns in each constituent equation. For the example of Fig. 5-4 the three arrays would be those given in Fig. 5-7.

The computational algorithm can be found in Gupta and Tanji (1977). The authors (Gupta and Tanji, 1977) compared their technique with several other techniques and found that theirs is computationally more efficient while retaining the same accuracy of the solution. Joliffe (1984) used this solver to solve St. Venant equation for routing floods in hypothetical channel networks.

However, for the sake of curiosity, this sparse matrix solver was used for solving a 150x150 matrix having a banded structure of bandwidth 13, resulting from an implicit F-D formulation of the two dimensional convection diffusion equation. The matrix was also solved using another band-

$$
\begin{bmatrix}
\frac{\partial G_1}{\partial h_1^{n+1}} & \frac{\partial G_1}{\partial h_2^{n+1}} & & & \\
\frac{\partial G_2}{\partial h_1^{n+1}} & \frac{\partial G_2}{\partial h_2^{n+1}} & \frac{\partial G_2}{\partial h_3^{n+1}} & & \\
\frac{\partial G_3}{\partial h_2^{n+1}} & \frac{\partial G_3}{\partial h_3^{n+1}} & \frac{\partial G_3}{\partial h_4^{n+1}} & & \\
 & & \vdots & & \\
\frac{\partial G_{11}}{\partial h_{10}^{n+1}} & \frac{\partial G_{11}}{\partial h_{11}^{n+1}} & \frac{\partial G_{11}}{\partial h_{12}^{n+1}} & \frac{\partial G_{11}}{\partial h_{30}^{n+1}} & \frac{\partial G_{11}}{\partial h_{40}^{n+1}} \\
 & & \vdots & & \\
\frac{\partial G_{20}}{\partial h_{19}^{n+1}} & \frac{\partial G_{20}}{\partial h_{20}^{n+1}} & & & \\
 & & \vdots & & \\
\frac{\partial G_{30}}{\partial h_{11}^{n+1}} & \frac{\partial G_{30}}{\partial h_{29}^{n+1}} & \frac{\partial G_{30}}{\partial h_{30}^{n+1}} & & \\
 & & \vdots & & \\
\frac{\partial G_{40}}{\partial h_{11}^{n+1}} & \frac{\partial G_{40}}{\partial h_{39}^{n+1}} & \frac{\partial G_{40}}{\partial h_{40}^{n+1}} & &
\end{bmatrix}
\begin{bmatrix}
1 & 2 & & & \\
1 & 2 & 3 & & \\
2 & 3 & 4 & & \\
 & \vdots & & & \\
10 & 11 & 12 & 30 & 40 \\
 & \vdots & & & \\
19 & 20 & & & \\
 & \vdots & & & \\
11 & 29 & 30 & & \\
 & \vdots & & & \\
11 & 39 & 40 & &
\end{bmatrix}
\begin{bmatrix}
2 \\ 3 \\ 3 \\ \vdots \\ 5 \\ \vdots \\ 2 \\ \vdots \\ 3 \\ \vdots \\ 3
\end{bmatrix}
$$

Fig. 5-7. The arrays of the coefficient matrix.

matrix solver available in the IMSLmath library. It was found that computational time and storage requirement was almost twice in the case of the sparse matrix solver than those of the other solver, whereas the numerical values of the solution vector were almost the same in both the cases. In any case, this is not beyond expectation. It can be realized that for the same number of elements in a banded matrix, the sparse matrix solver requires two arrays whereas the band-matrix solver requires one array of the same size. In addition, the sparse matrix solver inverts the coefficient matrix at every iteration hence requires evaluation of the coefficients as well, thus increasing the number of computations.

Despite the above perceived drawbacks, the sparse matrix solver is the only recourse. For instance, in the present example network, the storage requirement for this solver is 40x5+40x5+40x1 = 440 whereas that of the band-matrix solver is 40x30=1200 (30 is the band width, see eqn.[5-21]). Besides, due to the fact that matrix coefficients are functions of the dependent variable (e.g. h), they have to be evaluated at each iteration anyway. Hence, for the complex channel network as the one encountered in this study, the sparse matrix technique is the right choice. Therefore, Gupta and Tanji's (1977) sparse matrix solver has been used.

5.5.3 Evaluation of partial derivatives

To be able to develop a model for complex networks it is necessary to obtain an efficient method for evaluating the partial derivatives in eqn.[5-21]. Joliffe (1984) used both numerical and analytical methods to evaluate the derivatives and found that the analytical method is more handy to use. In this present study, therefore, analytical method has been used for the evaluation of the required derivatives.

Differentials of eqn.[5-15] through [5-18] give the expressions as presented in pages 175 and 176.

5.6 Solution of Example Problems

Two hypothetical examples are presented here to demonstrate the validity of applying the proposed model to routing floods in river networks. The hypothetical networks adopted in the examples consist of (a) the network of Yen and Akan (1976) and (b) the network presented by Joliffe (1984) as shown in Figs. 5-8 and 5-9.

The network of Yen and Akan (1976) consist of six branches of rectangular cross section and their length and width are listed in Table 5-2. The channel slope is equal to 0.001 and Manning's roughness factor n equal to 0.028 for all the branches. The floods that enter each of the upstream branches of the network are identical, consisting of a symmetrical triangular hydrograph rising from the base flow of 10 cfs to the peak rate of 135 cfs in 25 minutes and the receding in 25 minutes back to the base flow rate of 10 cfs. However, there is a time lag of the flood input for different branches as shown in Fig. 5-10a. Branches 1 and 2 receive their floods at the same time. Branch 3 lags behind by 25 minutes and branch 4 lags by another 10 minutes. This is

Eqns.[5-17] through [5-19] i.e. the equations resulted from inflow hydrograph conditions at nodes 1, 21, 31 yield:

$$\frac{\partial G_1}{\partial h_1^{n+1}} = \rho\,\frac{\partial B_1^{n+1/2}}{\partial h_1^{n+1}}\left(h_1^{n+1}-h_1^{n}\right) + \rho\, B_1^{n+1/2}$$

$$-\,\omega\left[-\,\frac{\partial K_{1+1/2}^{n+1}}{\partial h_1^{n+1}}\sqrt{h_1^{n+1}-h_2^{n+1}} - \frac{1}{2}\,K_{1+1/2}^{n+1}\,\frac{1}{\sqrt{h_1^{n+1}-h_2^{n+1}}}\right]$$

$$\frac{\partial G_1}{\partial h_2^{n+1}} = -\,\omega\left[\frac{\partial K_{1+1/2}^{n+1}}{\partial h_2^{n+1}}\sqrt{h_1^{n+1}-h_2^{n+1}} + \frac{1}{2}\,K_{1+1/2}^{n+1}\,\frac{1}{\sqrt{h_1^{n+1}-h_2^{n+1}}}\right]$$

$$\frac{\partial G_{31}}{\partial h_{31}^{n+1}} = \rho\,\frac{\partial B_{31}^{n+1/2}}{\partial h_{31}^{n+1}}\left(h_{31}^{n+1}-h_{31}^{n}\right) + \rho\, B_{31}^{n+1/2}$$

$$-\,\omega\left[-\,\frac{\partial K_{31+1/2}^{n+1}}{\partial h_{31}^{n+1}}\sqrt{h_{31}^{n+1}-h_{32}^{n+1}} - \frac{1}{2}\,K_{31+1/2}^{n+1}\,\frac{1}{\sqrt{h_{31}^{n+1}-h_{32}^{n+1}}}\right]$$

$$\frac{\partial G_{31}}{\partial h_{32}^{n+1}} = -\,\omega\left[\frac{\partial K_{31+1/2}^{n+1}}{\partial h_{32}^{n+1}}\sqrt{h_{31}^{n+1}-h_{32}^{n+1}} + \frac{1}{2}\,K_{31+1/2}^{n+1}\,\frac{1}{\sqrt{h_{31}^{n+1}-h_{32}^{n+1}}}\right]$$

Equations for the intermediate nodes (j) of the channels yield:

$$\frac{\partial G_j}{\partial h_{j-1}^{n+1}} = -\,\omega\left[\frac{\partial K_{j-1/2}^{n+1}}{\partial h_{j-1}^{n+1}}\sqrt{h_{j-1}^{n+1}-h_j^{n+1}} + \frac{1}{2}\,K_{j-1/2}^{n+1}\,\frac{1}{\sqrt{h_{j-1}^{n+1}-h_j^{n+1}}}\right]$$

$$\frac{\partial G_j}{\partial h_j^{n+1}} = \rho\,\frac{\partial B_j^{n+1/2}}{\partial h_j^{n+1}}\left(h_j^{n+1}-h_j^{n}\right) + r\, B_j^{n+1/2}$$

$$-\,\omega\left[\begin{array}{l}\dfrac{\partial K_{j-1/2}^{n+1}}{\partial h_j^{n+1}}\sqrt{h_{j-1}^{n+1}-h_j^{n+1}} - \dfrac{1}{2}\,K_{j-1/2}^{n+1}\,\dfrac{1}{\sqrt{h_{j-1}^{n+1}-h_j^{n+1}}}\\[2ex] -\,\dfrac{\partial K_{j+1/2}^{n+1}}{\partial h_j^{n+1}}\sqrt{h_j^{n+1}-h_{j+1}^{n+1}} - \dfrac{1}{2}\,K_{j+1/2}^{n+1}\,\dfrac{1}{\sqrt{h_{j1}^{n+1}-h_{j+1}^{n+1}}}\end{array}\right]$$

$$\frac{\partial G_j}{\partial h_{j+1}^{n+1}} = -\,\omega\left[\frac{\partial K_{j+1/2}^{n+1}}{\partial h_{j+1}^{n+1}}\sqrt{h_j^{n+1}-h_{j+1}^{n+1}} + \frac{1}{2}\,K_{j+1/2}^{n+1}\,\frac{1}{\sqrt{h_j^{n+1}-h_{j+1}^{n+1}}}\right]$$

The equation resulting from rating curve boundary condition at node 20 is

$$\frac{\partial G_{20}}{\partial h_{19}^{n+1}} \approx -\omega\left[\frac{\partial K_{20\text{-}1/2}^{n+1}}{\partial h_{19}^{n+1}}\sqrt{h_{19}^{n+1}-h_{20}^{n+1}}+\frac{1}{2}K_{20\text{-}1/2}^{n+1}\frac{1}{\sqrt{h_{19}^{n+1}-h_{20}^{n+1}}}\right]$$

$$\frac{\partial G_{20}}{\partial h_{20}^{n+1}} = \rho\,\frac{\partial B_{20}^{n+1/2}}{\partial h_{20}^{n+1}}\left(h_{20}^{n+1}-h_{20}^{n}\right)+\rho\,B_{20}^{n+1/2}$$
$$-\omega\left[\frac{\partial K_{20\text{-}1/2}^{n+1}}{\partial h_{20}^{n+1}}\sqrt{h_{19}^{n+1}-h_{20}^{n+1}}-\frac{1}{2}K_{20\text{-}1/2}^{n+1}\frac{1}{\sqrt{h_{19}^{n+1}-h_{20}^{n+1}}}-\sqrt{\Delta x}\,C_1C_2\left(h_{20}^{n+1}\right)^{C_2-1}\right]$$

The equation resulting from junction condition at node 11 is

$$\frac{\partial G_{11}}{\partial h_{11}^{n+1}} \approx \rho\,\frac{\partial A_{11}^{n+1/2}}{\partial h_{11}^{n+1}}\left(h_{11}^{n+1}-h_{11}^{n}\right)+\rho\,A_{11}^{n+1/2}$$
$$-\omega\left[\begin{array}{l}\dfrac{\partial K_{30,11}^{n+1}}{\partial h_{11}^{n+1}}\sqrt{h_{30}^{n+1}-h_{11}^{n+1}}-\dfrac{1}{2}K_{30,11}^{n+1}\dfrac{1}{\sqrt{h_{30}^{n+1}-h_{11}^{n+1}}}\\[2ex]+\dfrac{\partial K_{10,11}^{n+1}}{\partial h_{11}^{n+1}}\sqrt{h_{10}^{n+1}-h_{11}^{n+1}}-\dfrac{1}{2}K_{10,11}^{n+1}\dfrac{1}{\sqrt{h_{10}^{n+1}-h_{11}^{n+1}}}\\[2ex]+\dfrac{\partial K_{40,11}^{n+1}}{\partial h_{11}^{n+1}}\sqrt{h_{40}^{n+1}-h_{11}^{n+1}}-\dfrac{1}{2}K_{40,11}^{n+1}\dfrac{1}{\sqrt{h_{40}^{n+1}-h_{11}^{n+1}}}\\[2ex]-\dfrac{\partial K_{11,12}^{n+1}}{\partial h_{11}^{n+1}}\sqrt{h_{11}^{n+1}-h_{12}^{n+1}}-\dfrac{1}{2}K_{11,12}^{n+1}\dfrac{1}{\sqrt{h_{11}^{n+1}-h_{12}^{n+1}}}\end{array}\right]$$

$$\frac{\partial G_{11}}{\partial h_{30}^{n+1}} \approx -\omega\left[\frac{\partial K_{30,11}^{n+1}}{\partial h_{30}^{n+1}}\sqrt{h_{30}^{n+1}-h_{11}^{n+1}}+\frac{1}{2}K_{30,11}^{n+1}\frac{1}{\sqrt{h_{30}^{n+1}-h_{11}^{n+1}}}\right]$$

$$\frac{\partial G_{11}}{\partial h_{10}^{n+1}} \approx -\omega\left[\frac{\partial K_{10,11}^{n+1}}{\partial h_{10}^{n+1}}\sqrt{h_{10}^{n+1}-h_{j11}^{n+1}}+\frac{1}{2}K_{10,11}^{n+1}\frac{1}{\sqrt{h_{10}^{n+1}-h_{11}^{n+1}}}\right]$$

$$\frac{\partial G_{11}}{\partial h_{40}^{n+1}} \approx -\omega\left[\frac{\partial K_{40,11}^{n+1}}{\partial h_{40}^{n+1}}\sqrt{h_{40}^{n+1}-h_{11}^{n+1}}+\frac{1}{2}K_{40,11}^{n+1}\frac{1}{\sqrt{h_{40}^{n+1}-h_{11}^{n+1}}}\right]$$

$$\frac{\partial G_{11}}{\partial h_{12}^{n+1}} \approx -\omega\left[-\frac{\partial K_{11,12}^{n+1}}{\partial h_{12}^{n+1}}\sqrt{h_{11}^{n+1}-h_{12}^{n+1}}+\frac{1}{2}K_{11,12}^{n+1}\frac{1}{\sqrt{h_{11}^{n+1}-h_{12}^{n+1}}}\right]$$

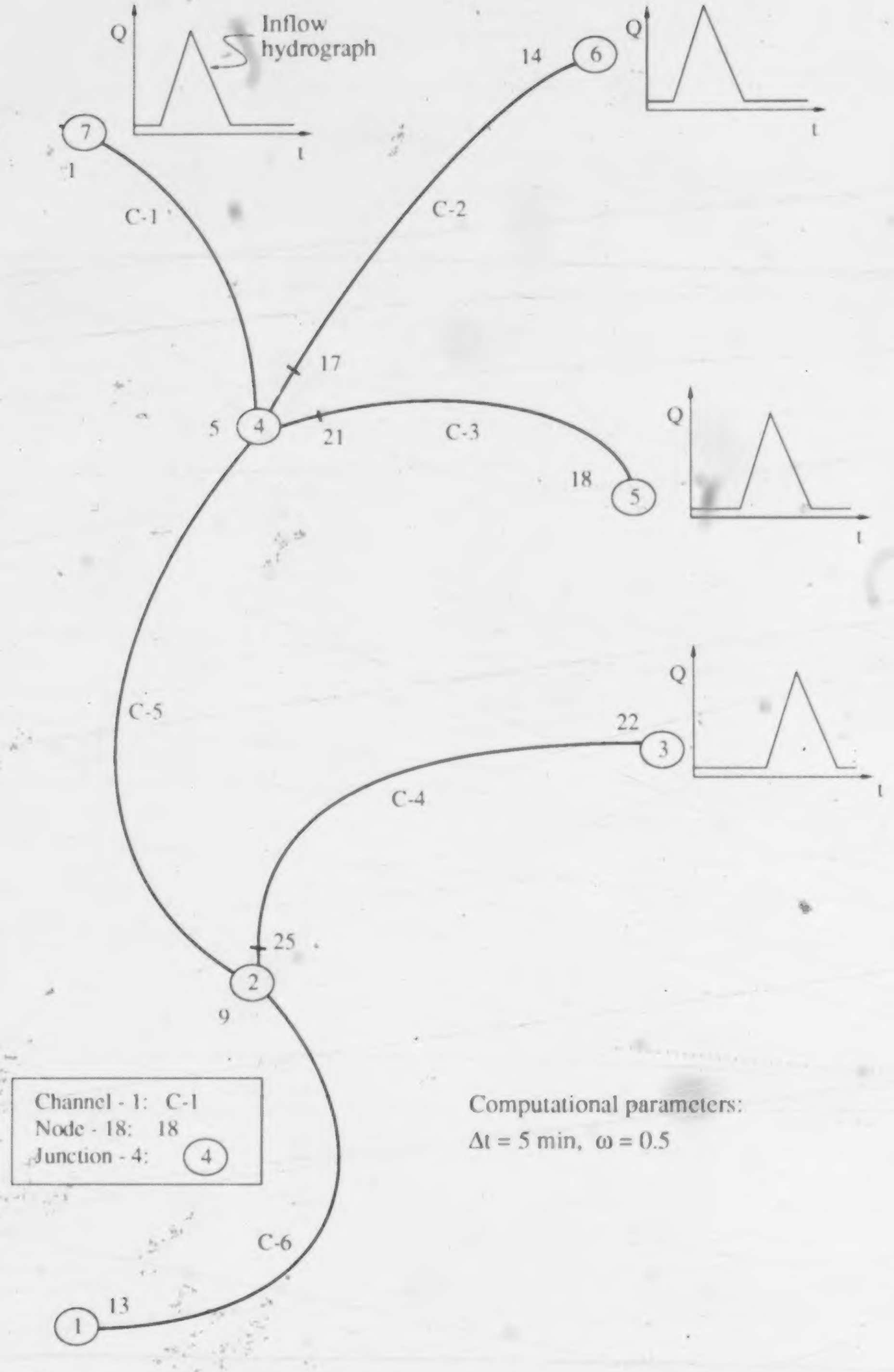
Q
Inflow
hydrograph
t
Q
t
14
6
7
1
C-1
C-2
17
5
4
21
C-3
Q
t
18
5
Q
t
C-5
22
3
C-4
25
2
9
Channel - 1: C-1
Node - 18: 18
Junction - 4: 4
Computational parameters:
Δt = 5 min, ω = 0.5
C-6
13
1

Fig. 5-8. Example network-1 (adapted after Yen and Akan, 1976).

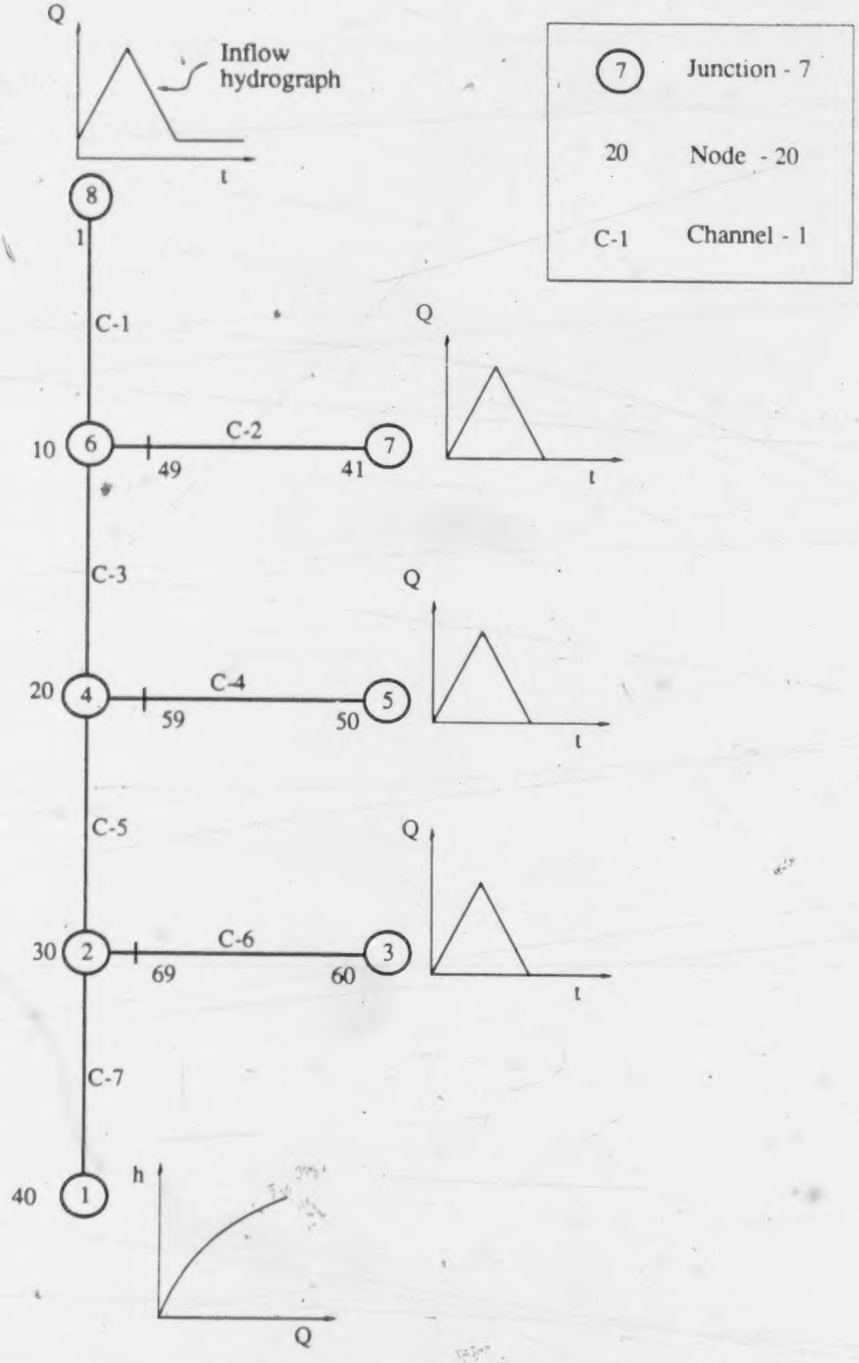
Q
Inflow hydrograph
t
7
Junction - 7
20
Node - 20
C-1
Channel - 1
8
1
C-1
10
6
49
C-2
41
7
Q
t
C-3
20
4
59
C-4
50
5
Q
t
C-5
30
2
69
C-6
60
3
Q
t
C-7
40
1
h
Q

Fig. 5-9. Example network-2 (adapted after Joliffe, 1984)

similar to the situation when a rainstorm is moving from the upstream end towards the downstream end producing a flash flood. The inflow hydrographs that enter the respective branches and the computed hydrographs are shown in Fig. 5-10.

The second network (Joliffe, 1984) consists of 7 branches of prismatic channels of trapezoidal cross sections and their lengths and widths are listed in Table 5-3. All the branches have identical Manning's roughness factors of 0.02, and side slopes of 1:1. Branches 1, 3, 5, and 7 have a bed slope of 0.0001 and branches 2, 4, and 6 have zero bed slope. Initial depths in all the branches are 0.2 m, while initial discharges in branches 1, 3, 5, and 7 are 0.169 m^3/s and those in branches 2, 4, and 6 are zero i.e. still water. The inflow hydrographs and the computed hydrographs for this case are shown in Fig. 5-11.

In all the cases, agreement of the simulated outputs using the present diffusion model and the dynamic models is good. The better side of the diffusion model is that it is simple and computationally less expensive.

Table 5-2. Channel characteristics of example network-1.

Features	Channels 1, 2, & 3, 4	Channel 5	Channel 6
Shape	Rectangular	Rectangular	Rectangular
Length	2000 ft	2938 ft	3906 ft
Width	20.0 ft	58.756 ft	78.032
Manning's n	0.028	0.028	0.028
Channel slope	0.001	0.001	0.001
Initial Q	10.0 ft^3/s	10.0 ft^3/s	10.0 ft^3/s

Table 5-3. Channel characteristics of example network-2.

Features	Channels 1, 3, 5, 7	Channels 2, 4, 6
Shape	Trapezoidal	Trapezoidal
Length	1000 m	1000 m
Side slope	1:1	1:1
Base width	5.0 m	5.0 m
Manning's n	0.02	0.02
Channel slope	0.0001	0.0000001
Initial depth	0.20 m	0.20 m
Initial Q	0.17 m^3/s	0.0

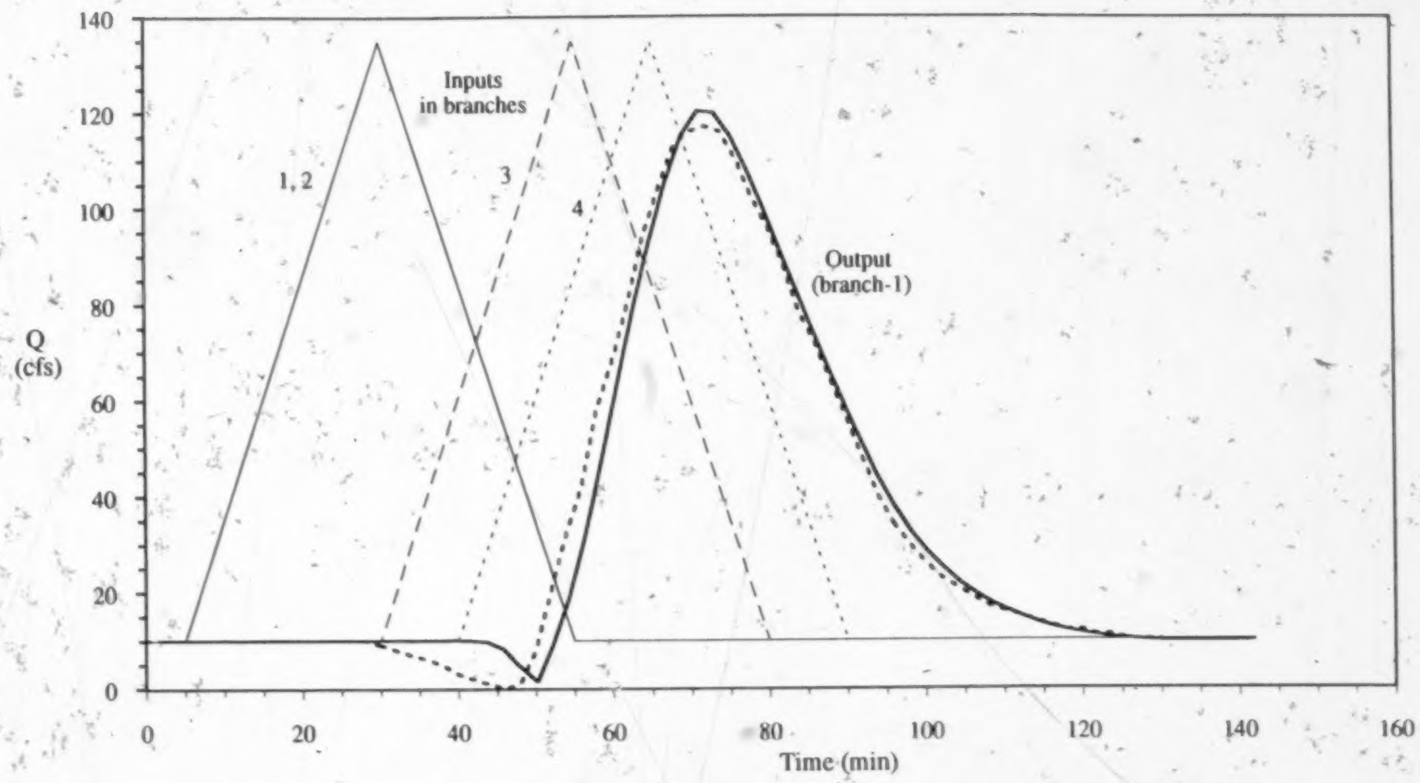

Fig. 5-10a. Computed discharge at the end of branch-1: present solution using diffusion model (solid line) and the solution obtained by Yen and Akan (1976) using dynamic wave model (dotted line).

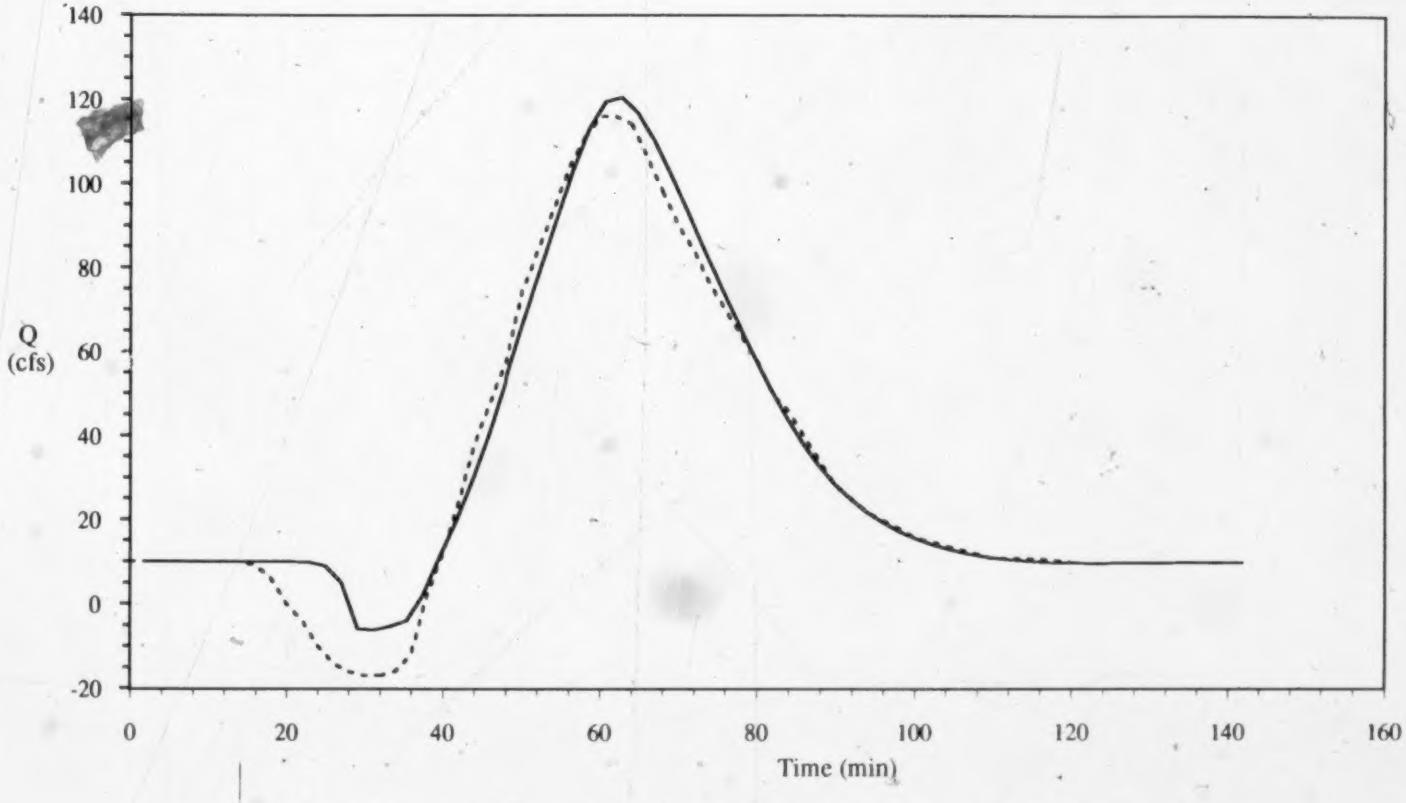

Fig. 5-10b. Computed discgharge at the end of branch-3: solution obtained using diffusion model (solid line) and solution obtained by Yen and Akan (1976) using dynamic wave model (dotted line).

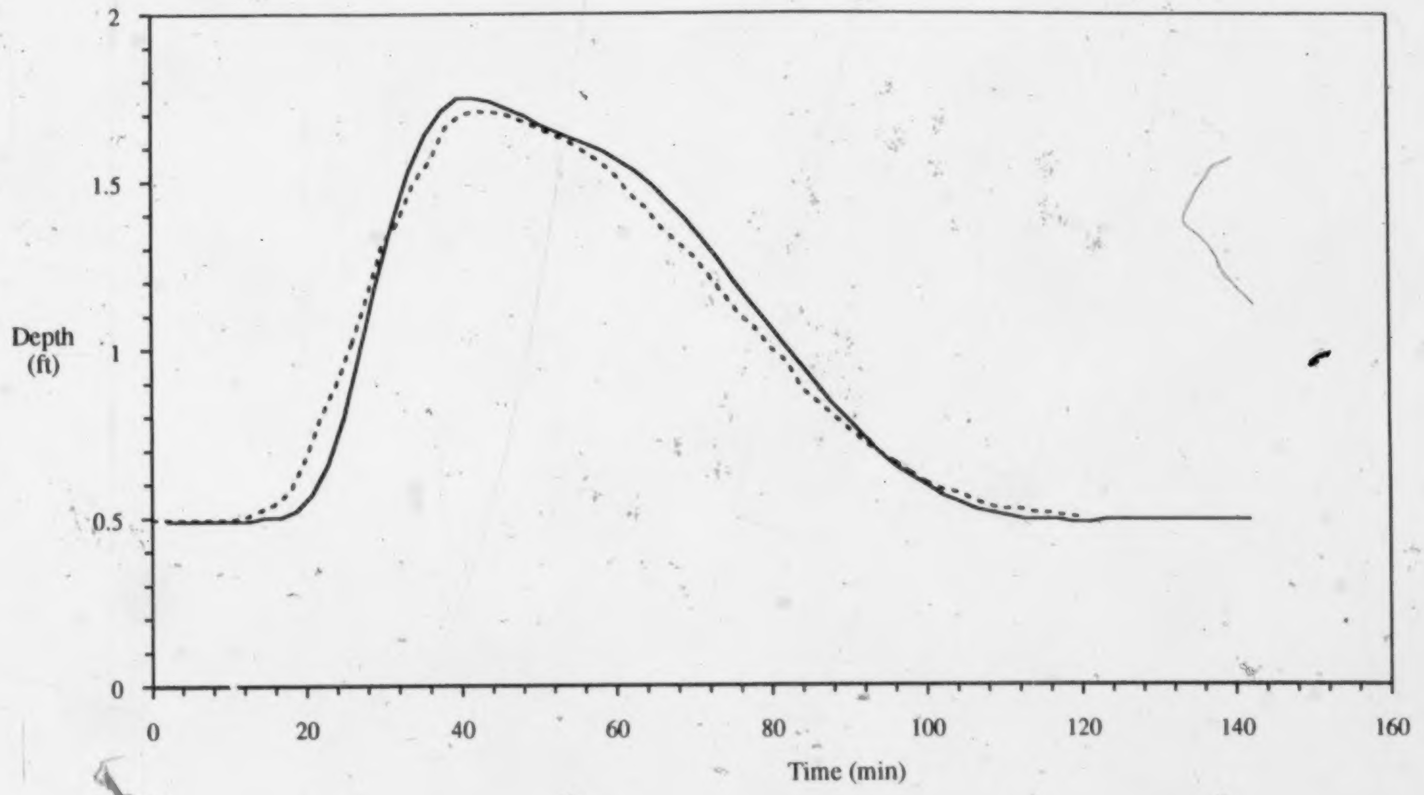

Fig. 5-10c. Computed depth at junction-3: using present diffusion model (solid line) and using dynamic wave model of Yen and Akan (1976) (dotted line).

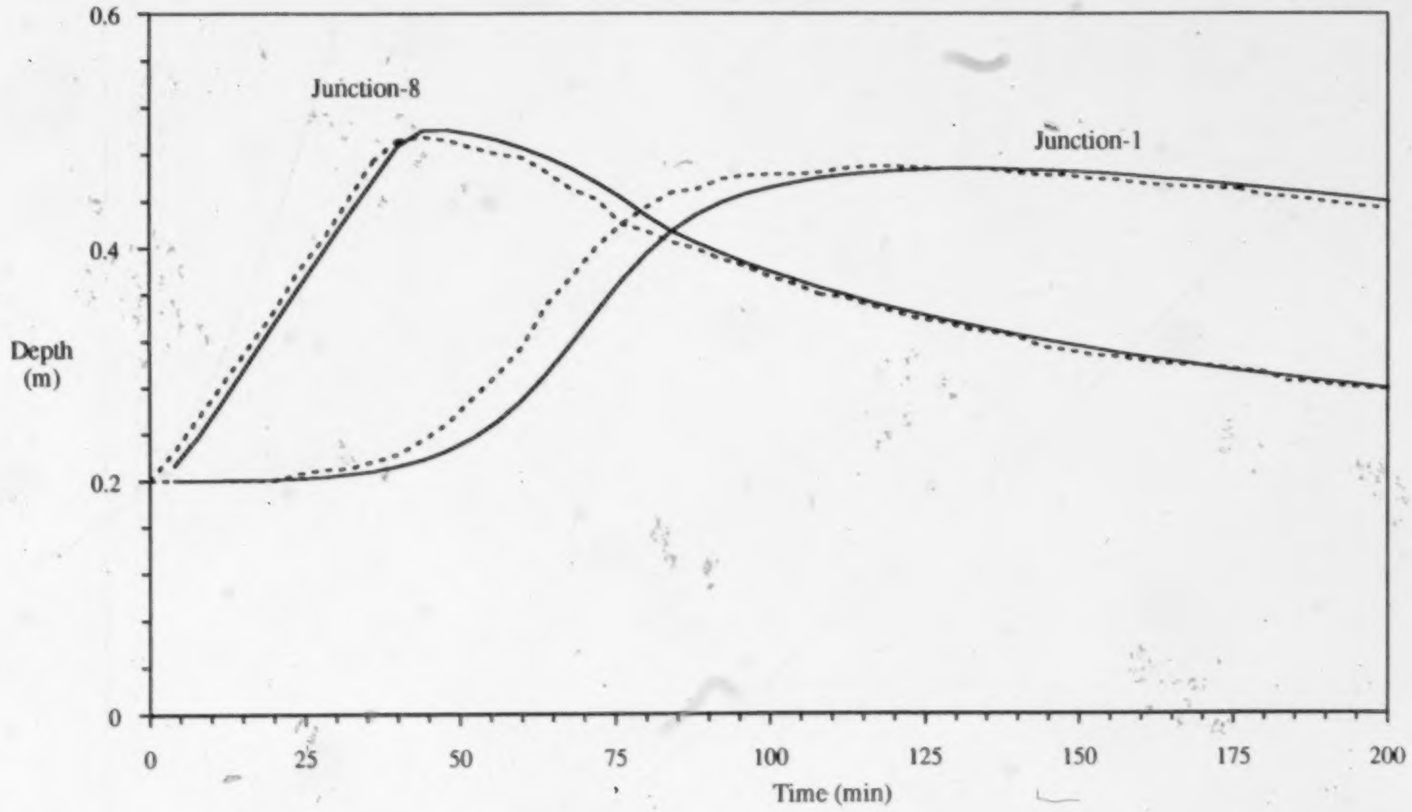

Fig. 5-11a. Computed depth at junctions 1 and 8 (network-2): solution obtained using diffusion model (solid line) and solution obtained by Joliffe (1984) using dynamic wave model (dotted line).

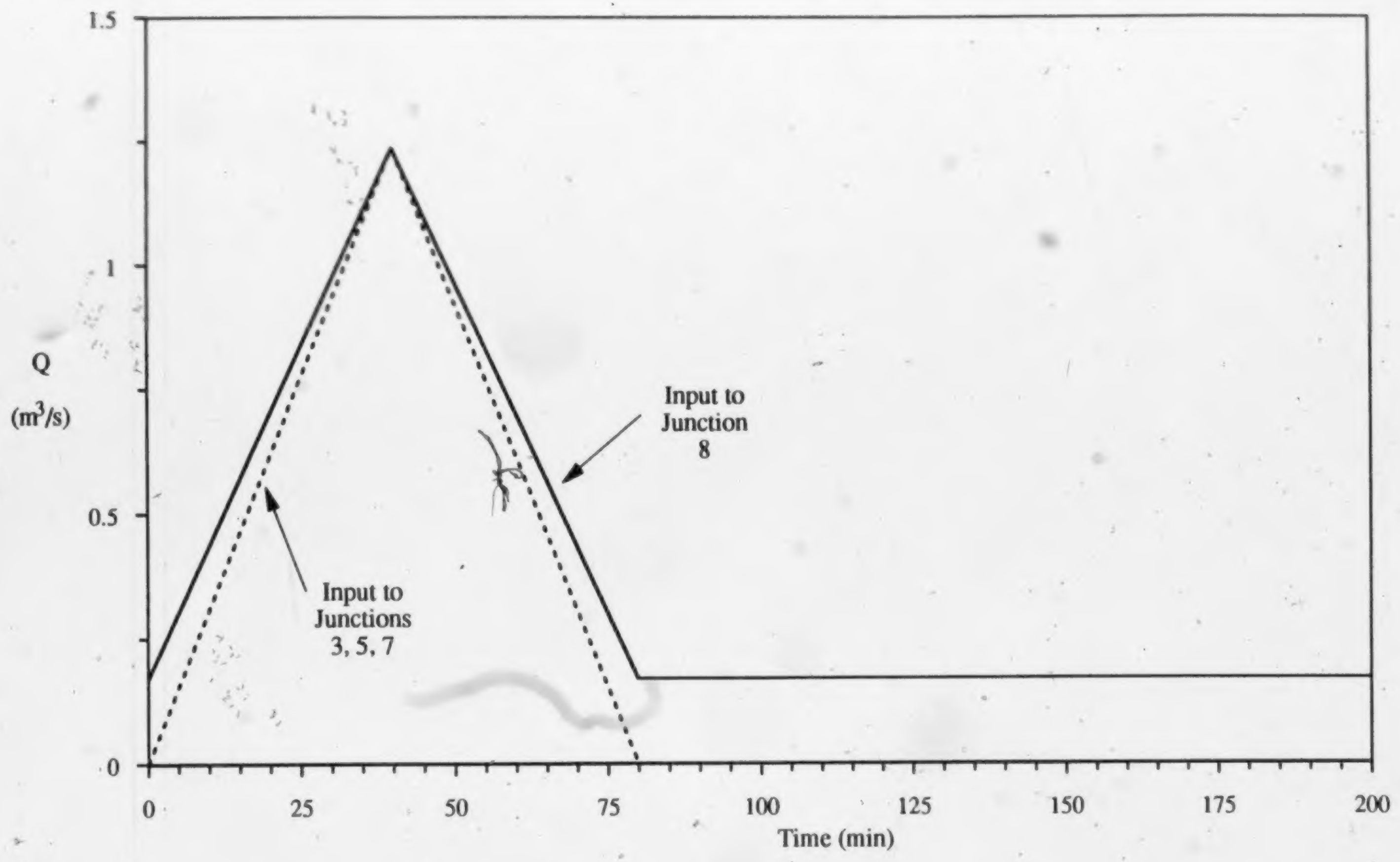

Fig. 5-11b. Input to the network-2.

Chapter 6

Analysis of the Numerical Techniques

6.1 On the Accuracy of the Solution

The numerical solution of a differential equation is obtained by integrating it in discrete steps of time and space using a discrete representation (i.e. the finite difference approximations) of the continuous equation. To obtain a meaningful solution it is necessary that the discrete representation of the continuous system be consistent which means that it (the discrete form) truly represents the continuous system. And it is also necessary that the discrete steps in the integration have a solution which is bounded i.e. the solution is stable. Finally it is essential that the solution obtained using the discrete representation converges to the solutions represented by the continuous equation.

In this chapter it is intended to examine the conditions necessary to consistency, stability and convergence of the finite difference representations of the flow equations used in the study. In addition, application of the derived relationships in the context of the present study, such as specification of Δx and Δt, are also described.

6.2 Consistency

A finite difference representation of a partial differential equation is said to be consistent when the finite difference approximation approaches the partial differential equation in the limit when the mesh size approaches zero. The consistency of a numerical scheme may be evaluated by determining the functional form of the truncation error or discretization error. This is found by expanding each term of the difference equation in Taylor series about the point at which the differential equation is computed. In fact consistency is easy to establish and is practically gauranteed by any reasonable choice of difference schemes (Steffler, 1989).

On the other hand, convergence is harder to gaurantee and it's being a crucial point in a numerical solution, derivation and analysis of convergence criteria has been made. No attempt has been made to derive the expression of the truncation errors which require a great amount of algebra.

6.3 Stability

The stability of a numerical scheme with respect to a differential equation can be estimated by numerical experiments (Amein and Fang, 1970; Fread, 1973a) or by detailed analysis of the numerical properties of the schemes (Fread, 1974; Katopodes, 1984). For the schemes which are used in this study, an attempt has been made to investigate the stability through a detailed analysis of the numerical properties.

For analyzing the stability of the schemes the von Neuman and Goldstein (1947) analytical technique (subsequently elaborated by O'Brien et al., 1950) is used. According to the von Neuman method a Fourier expansion of a line of errors is followed as time progresses. However, it is only applicable to linear differential equations. Whereas the equations used here are nonlinear. Hence, it is necessary to linearise these equations. In addition, the linearised equations are then simplified by omitting certain terms on the basis of their relatively small magnitude in order to facilitate the stability analysis. Thus the equations analyzed are models of the original nonlinear equations. Nevertheless, a substantial amount of information regarding the numerical properties of the nonlinear equations can be obtained from this kind of analysis (Fread, 1974; Abbott, 1979; Katopodes, 1984). The stability and hence the convergence conditions are determined for all the flow problems involved in this study.

It is evident that the unsaturated flow equation is of convection-diffusion type. And so is the channel flow equation. The nonlinear saturated flow equation does not contain a convection term, however, when it is linearised a pseudo-convection term appears. The overland flow (i.e. the K-W equation) equation is purely convective, no diffusion term is involved. Whatever the nature of the equations the linearisation method followed here is the same in all the cases. A brief description of the lnearisation process is given here using the unsaturated flow equation as an example.

For the sake of convenience the nonlinear unsaturated flow equation is rewritten here which is

$$C\frac{\partial\psi}{\partial t} = \frac{\partial}{\partial z}\left(K\frac{\partial\psi}{\partial z} - K\right) \qquad [6\text{-}1]$$

Since matric potential, ψ, is the dependent variable, to linearise this equation a small perturbation in ψ, $\delta\psi$ above mean potential, ψ_0, is substituted. As the other dependent variables (or coefficients, whatever they may be called) C and K are functions of ψ, δC and δK can be expressed as function of $\delta\psi$ also. These are as follows:

$$\begin{aligned} \psi &= \psi_0 + \delta\psi \\ C &= C_0 + a\delta\psi \\ K &= K_0 + b\delta\psi \end{aligned} \qquad [6\text{-}2]$$

where

$$a = \frac{\partial C}{\partial\psi}$$

$$b = \frac{\partial K}{\partial\psi}$$

and C_0 and K_0 are the values of C and K corresponding to ψ_0. Substituting eqn.[6-2] into eqn.[6-1] it can be written that

$$(C_0+a\delta\psi)\frac{\partial}{\partial t}(\psi_0+\delta\psi) = \frac{\partial}{\partial z}\left[(K_0+b\delta\psi)\frac{\partial}{\partial z}(\psi_0+\delta\psi) - K_0 - b\delta\psi\right] \qquad [6\text{-}3]$$

After multiplication and neglecting the terms of relatively small magnitude, such as $\delta\psi.\delta\psi$ and so on, the following model equation is obtained:

$$\frac{\partial(\delta\psi)}{\partial t} + A\delta\psi + U_{un}\frac{\partial(\delta\psi)}{\partial z} = D_{un}\frac{\partial^2(\delta\psi)}{\partial z^2} \qquad [6\text{-}4]$$

where (subscript 'un' to indicate unsaturated flow)

$$A = -\frac{1}{C_0}\left(b\frac{\partial^2\psi_0}{\partial z^2}\right)$$

$$U_{un} = -\frac{1}{C_0}\left(\frac{\partial K_0}{\partial z} + b\frac{\partial \psi_0}{\partial z} - b\right)$$

$$D_{un} = \frac{K_0}{C_0}$$

With an additional assumption that the contribution of the term 'A' is relatively small, one can further trim eqn.[6-4] to give

$$\frac{\partial(\delta\psi)}{\partial t} + U_{un}\frac{\partial(\delta\psi)}{\partial z} = D_{un}\frac{\partial^2(\delta\psi)}{\partial z^2} \qquad [6\text{-}5]$$

Similarly the linearised form of the saturated, channel and overland flow equations can be obtained as

$$\frac{\partial(\delta h)}{\partial t} + U_{sat}\frac{\partial(\delta h)}{\partial x} = D_{sat}\frac{\partial^2(\delta h)}{\partial x^2} \qquad [6\text{-}6]$$

$$\frac{\partial(\delta y)}{\partial t} + U_{ch}\frac{\partial(\delta y)}{\partial x} = D_{ch}\frac{\partial^2(\delta y)}{\partial x^2} \qquad [6\text{-}7]$$

and

$$\frac{\partial(\delta y)}{\partial t} + U_{ol}\frac{\partial(\delta y)}{\partial x} = 0 \qquad [6\text{-}8]$$

respectively. Where the coefficients are defined as

$$U_{sat} = 2\frac{K_{sat}}{S_y}\frac{\partial h_0}{\partial x}$$

$$D_{sat} = \frac{K_{sat}}{S_y}h_0$$

$$U_{ch} = \sqrt{S_0}\ \frac{\partial C_\bullet}{\partial y}$$

$$D_{ch} = \frac{C_\bullet}{2\sqrt{S_0}}$$

$$U_{ol} = Bm\alpha y_0^{m-1}$$

In the above expressions the subscripts of U and D indicate the flow processes (e.g. ch for channel flow and so forth). The zero subscript is to indicate the value about which the nonlinear equation has been linearised.

It has been alluded that the centered finite difference scheme is used in this study (except the overland flow case). Again taking the unsaturated flow equation as an example, the centered finite difference approximations to the model equation (eqn.[6-5]) can be written as

$$\frac{\delta\psi_j^{n+1} - \delta\psi_j^n}{\Delta t} + U_{un}\left[\omega\frac{\delta\psi_{j-1}^{n+1} - \delta\psi_{j+1}^{n+1}}{2\Delta z} + (1-\omega)\frac{\delta\psi_{j-1}^{n} - \delta\psi_{j+1}^{n}}{2\Delta z}\right]$$

$$= D_{un}\left[\omega\frac{\delta\psi_{j-1}^{n+1} - 2\delta\psi_j^{n+1} + \delta\psi_{j+1}^{n+1}}{(\Delta z)^2} + (1-\omega)\frac{\delta\psi_{j-1}^{n} - 2\delta\psi_j^{n} + \delta\psi_{j+1}^{n}}{(\Delta z)^2}\right]$$

Defining $C_r = U_{un}\Delta t/(2\Delta z)$ (a parameter describing translation) and $r = D_{un}\Delta t/(\Delta z^2)$ (another discretization parameter describing diffusion) and simplifying further, the above expression can be written as

$$-\omega\,(C_r + r)\,\delta\psi_{j-1}^{n+1} + (1 + 2r\omega)\,\delta\psi_j^{n+1} + \omega\,(C_r - r)\,\delta\psi_{j+1}^{n+1} \qquad [6\text{-}9]$$
$$= (1-\omega)\,(C_r + r)\,\delta\psi_{j-1}^{n} + [1 - 2r(1-\omega)]\,\delta\psi_j^{n} - (1-\omega)\,(C_r - r)\,\delta\psi_{j+1}^{n}$$

Mention has already been made that Fourier series expansion is used for error analysis. To further ease the analysis, only one term of the Fourier series need to be considered since eqn.[6-5] now is a linear equation.

Now let us assume that $\delta\psi$'s at time level n and n+1 are given by

$$\delta\psi_j^n = H\,e^{i\frac{2\pi}{L}j\Delta z}$$
$$\delta\psi_j^{n+1} = \gamma H\,e^{i\frac{2\pi}{L}j\Delta z}$$

where i is the complex imaginary unit equal to $(-1)^{1/2}$; L is the wave length and is defined as the product of the wave period and the propagation speed of the wave; H is amplitude; γ is the complex amplification over the time step, Δt, and $j\Delta z = z$.

Substituting the above two expressions into eqn.[6-9], solving for γ and writing γ as γ_n (n to indicate numerical) it can be shown that

$$\gamma_n = \frac{(1-\omega)\,(C_r + r)\,e^{-i\frac{2\pi}{L}\Delta z} + [1 - 2r(1-\omega)] - (1-\omega)\,(C_r - r)\,e^{i\frac{2\pi}{L}\Delta z}}{-\omega\,(C_r + r)\,e^{-i\frac{2\pi}{L}\Delta z} + (1 + 2r\omega) + \omega\,(C_r - r)\,e^{i\frac{2\pi}{L}\Delta z}}$$

Expressing the complex exponential in terms of sine and cosine functions and separating the real and imaginary parts the following is obtained

$$\gamma_n = \frac{[1 - 2(1-\omega)\, r] + 2(1-\omega)\, r \cos\left(\frac{2\pi}{L}\Delta z\right) - i\, 2\,(1-\omega)\, C_r \sin\left(\frac{2\pi}{L}\Delta z\right)}{(1 + 2\omega\, r) - 2\omega\, r \cos\left(\frac{2\pi}{L}\Delta z\right) + i\, 2\,\omega\, C_r \sin\left(\frac{2\pi}{L}\Delta z\right)}$$

To carry these clumsy terms forward with ease, they are abbreviated as follows

$$R_1 = [1 - 2(1-\omega)\, r] + 2(1-\omega)\, r \cos\left(\frac{2\pi}{L}\Delta z\right)$$

$$I_1 = -\, 2(1-\omega)\, C_r \sin\left(\frac{2\pi}{L}\Delta z\right)$$

$$R_2 = [1 + 2\,\omega\, r] - 2\,\omega\, r \cos\left(\frac{2\pi}{L}\Delta z\right)$$

$$I_2 = 2\omega\, C_r\, \mathrm{sins}\left(\frac{2\pi}{L}\Delta z\right)$$

Hence

$$\gamma_n = \frac{R_1 + i\, I_1}{R_2 + i\, I_2}$$

Multiplying both numerator and denominator by $R_2 - iI_2$, γ_n is expressed as

$$\gamma_n = \frac{R_1R_2 + I_1I_2}{R_2^2 + I_2^2} + i\,\frac{R_2I_1 - R_1I_2}{R_2^2 + I_2^2} \qquad [6\text{-}10]$$

From which

$$|\gamma_n| = \left[\left(\frac{R_1R_2 + I_1I_2}{R_2^2 + I_2^2}\right)^2 + \left(\frac{R_2I_1 - R_1I_2}{R_2^2 + I_2^2}\right)^2\right]^{1/2}$$

and

$$\theta_n = \tan^{-1}\left(\frac{R_2I_1 - R_1I_2}{R_1R_2 + I_1I_2}\right) \qquad [6\text{-}11]$$

In order for a difference equation to be stable, it is necessary that the error at time level n+1 be smaller than that at level n. Hence, γ_n derived above must be smaller than or equal to unity. It is possible to relate γ_n, $2\pi/L$, and the coefficients of the difference equation containing Δz and Δt, for example, C_r and r. The von Neuman stability criterion is required to be satisfied for all possible $2\pi/L$, and determines the final relation between γ_n and the coefficients.

Stability in the sense of von Neuman is based on the conjecture that linear operators with variable coefficients are stable if and only if their localized operators in which the coefficients are taken as constants are stable. Thus in this technique when it is found that $\gamma_n < 1$ is independent of the values of Δt and Δz, the difference equations are unconditionally linearly stable; however, if $\gamma_n <$ for only certain intervals of $\Delta t/\Delta z$, the equations are conditionally stable. When $\gamma_n = 1$, the difference equations are neutrally or weakly stable; and when $\gamma_n > 1$, the equations are unconditionally linearly unstable (Richtmyer and Morton, 1967).

It should be noted that stability does not always ensure a solution of the differential equation (Abbott, 1979). In order to obtain a meaningful solution the convergence criterion should be satisfied. This is discussed in the following section.

6.4 Convergence

If a scheme is neither consistent nor stable it will not be convergent. A convergent scheme implies consistency and stability. Therefore, it is important to establish conditions of convergence.

Unfortunately, it is very difficult to work out the conditions of convergence for more complicated equations such as those encountered in this study. However, as it has been done in case of stability, it is possible to predict the conditions of convergence from a simplified form of the equations.

6.4.1 Amplification ratio

Amplification ratio is defined as the ratio of the solution of the differential equation to that of the difference equation. This ratio helps obtain information about the convergence of a difference scheme.

As the model equation (eqn.[6-5]) is linear an analytical solution to such a linear differential equation can be obtained. Eqn.[6-5] is solved analytically as described here: Let $\delta\psi$ = H(t).F(z), where F(z) is $e^{i(2\pi/L)z}$. Substitution of $\delta\psi$ in eqn.[6-5] yields

$$\frac{dH}{dt} = -U_{un} H\, i \frac{2\pi}{L} + D_{un} H\, i^2 \left(\frac{2\pi}{L}\right)^2$$

Hence

$$H = e^{-t\left(U_{un}\, i \frac{2\pi}{L} + D_{un}\left(\frac{2\pi}{L}\right)^2\right)}$$

Therefore, the solution for $\delta\psi$ is obtained as

$$\delta\psi = e^{-t\left(U_{un}\frac{2\pi}{L} + D_{un}\left(\frac{2\pi}{L}\right)^2\right)}\, e^{i\frac{2\pi}{L}z}$$

Solution at time $t = t_n$ and $t = t_n + \Delta t$ can be written as

$$\delta\psi_j^n = e^{-t_n\left(i\,U_{un}\frac{2\pi}{L} + D_{un}\left(\frac{2\pi}{L}\right)^2\right)} e^{i\frac{2\pi}{L} j\Delta z}$$

and

$$\delta\psi_j^{n+1} = e^{-(t_n + \Delta t)\left(i\,U_{un}\frac{2\pi}{L} + D_{un}\left(\frac{2\pi}{L}\right)^2\right)} e^{i\frac{2\pi}{L} j\Delta z}$$

Therefore, the amplification over one time step, Δt, can be obtained as

$$\frac{\delta\psi_j^{n+1}}{\delta\psi_j^n} = \gamma_a = e^{-2i\,C_r\frac{2\pi}{L}\Delta z - r\left(\frac{2\pi}{L}\right)^2(\Delta z)^2} \qquad [6\text{-}12]$$

where C_r and r has been defined previously. The celerity of the wave is given by

$$\theta_a = -2C_r\frac{2\pi}{L}\Delta z \qquad [6\text{-}13]$$

The amplification (γ_n) and celerity (θ_n) for the centered difference scheme used for the unsaturated flow equation has been determined already. The amplification and wave celerity ratios for the unsaturated flow problem are

$$C_d = \frac{|\gamma_n|}{|\gamma_a|} = \frac{\left[\left(\frac{R_1R_2 + I_1I_2}{R_2^2 + I_2^2}\right)^2 + \left(\frac{R_2I_1 - R_1I_2}{R_2^2 + I_2^2}\right)^2\right]^{1/2}}{e^{-r\left(\frac{2\pi}{L/\Delta z}\right)^2}} \qquad [6\text{-}14]$$

and

$$C_\theta = \frac{\theta_n}{\theta_a} = \tan^{-1}\left(\frac{R_2I_1 - R_1I_2}{R_1R_2 + I_1I_2}\right)\Big/\left(-2C_r\frac{2\pi}{L}\Delta z\right) \qquad [6\text{-}15]$$

From the expressions it is seen that C_d and C_θ are functions of ω, C_r and r. In turn C_r and r are functions of Δt, Δz, L, U_{un} and D_{un}. Thus C_d, $C_\theta = f(\Delta t, \Delta z, L, U_{un}, D_{un})$. The interrelations of these quantities are dealt with in the section that follows.

Computation of amplification ratio

Before beginning the calculations, perhaps it will be convenient if the term $(2\pi/L).\Delta z$ is written as $2\pi/(L/\Delta z)$. Since L is the wave length and Δz is a length segment, the quantity $L/\Delta z$ indicates the number of nodes per wave length.

Computations for C_d and C_θ with variations in $L/\Delta z$ were performed for different C_r, r and ω values. The computed results are presented in the figures that follow. Figs. 6-1a and 6-6b are the plot of C_d and C_θ against $L/\Delta z$ for several values of C_r, r and ω.

The values of $L/\Delta z$ are examined from 2 to 100. The trends are such that for all conditions the amplification ratio tends towards 1.0 at high values of $L/\Delta z$. It is not hard to visualize that when one wants to approximate a curve by a number of straight line segments, the smaller the segment length the better the approximation. For a specific ω, lower C_r and r, yield amplification ratios closer to 1.0 for all $L/\Delta z$ and a wave speed ratio closer to 1.0 for most $L/\Delta z$.

From the above figures, it is clear that one should be able to decide on the size of the discretization necessary for a scheme to be convergent (when the amplification and celerity ratios are unity). However, to size the mesh it is essential to determine the significant wave length, L. Before stepping into the business of wave length, the fate of the remaining three equations such as saturated flow, channel

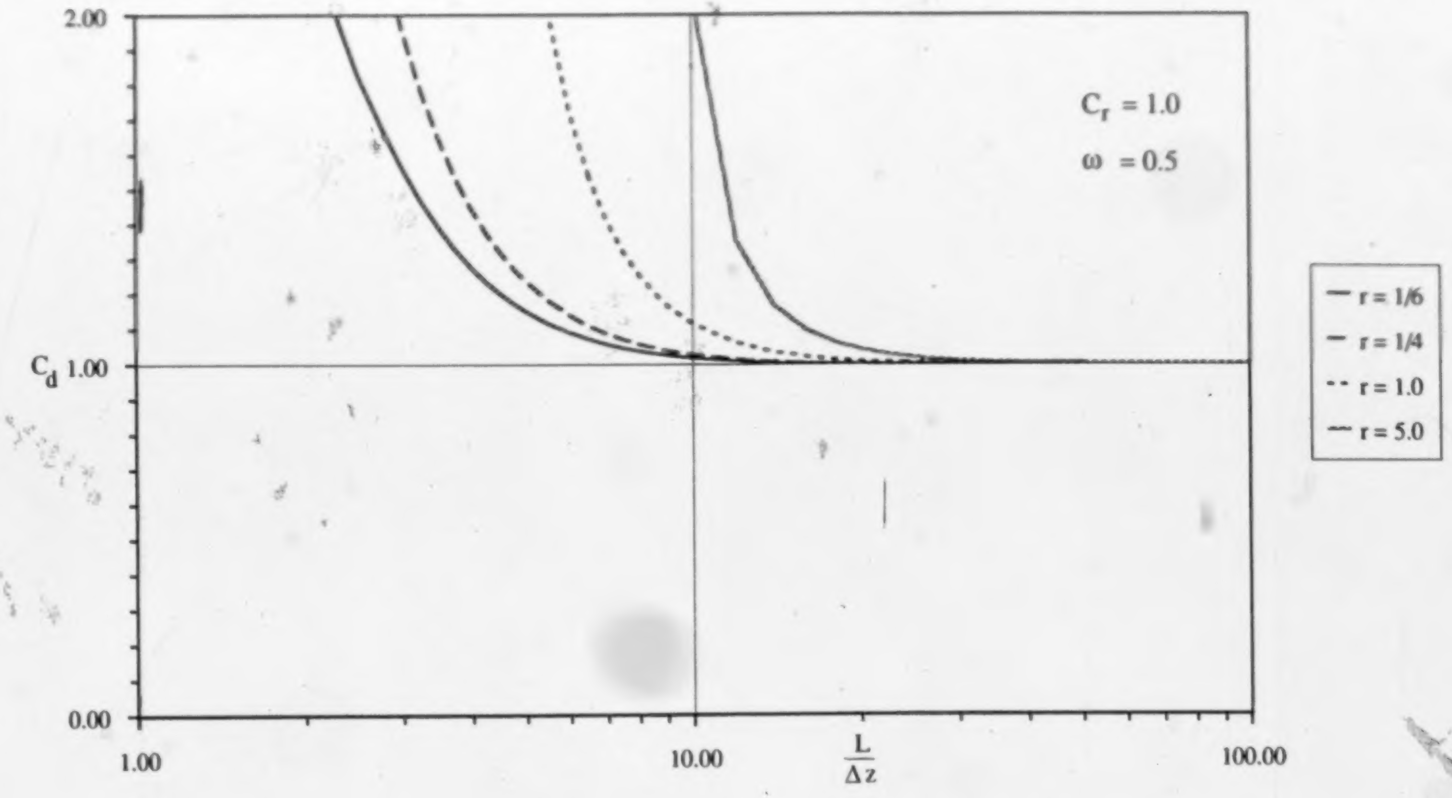

Fig. 6-1a. Amplification ratio against space-time discretization.

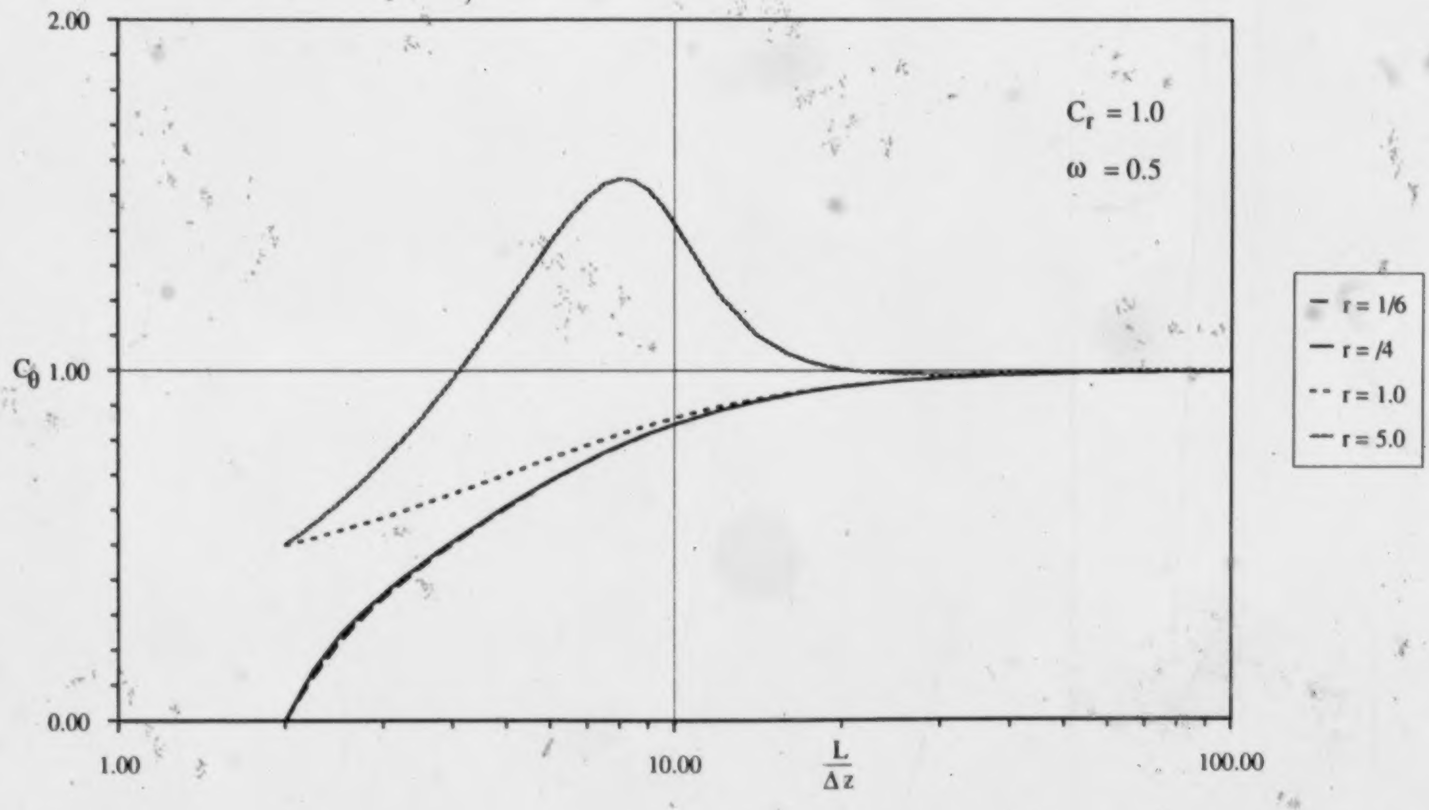

Fig. 6-1b. Celerity ratio against space-time discretization.

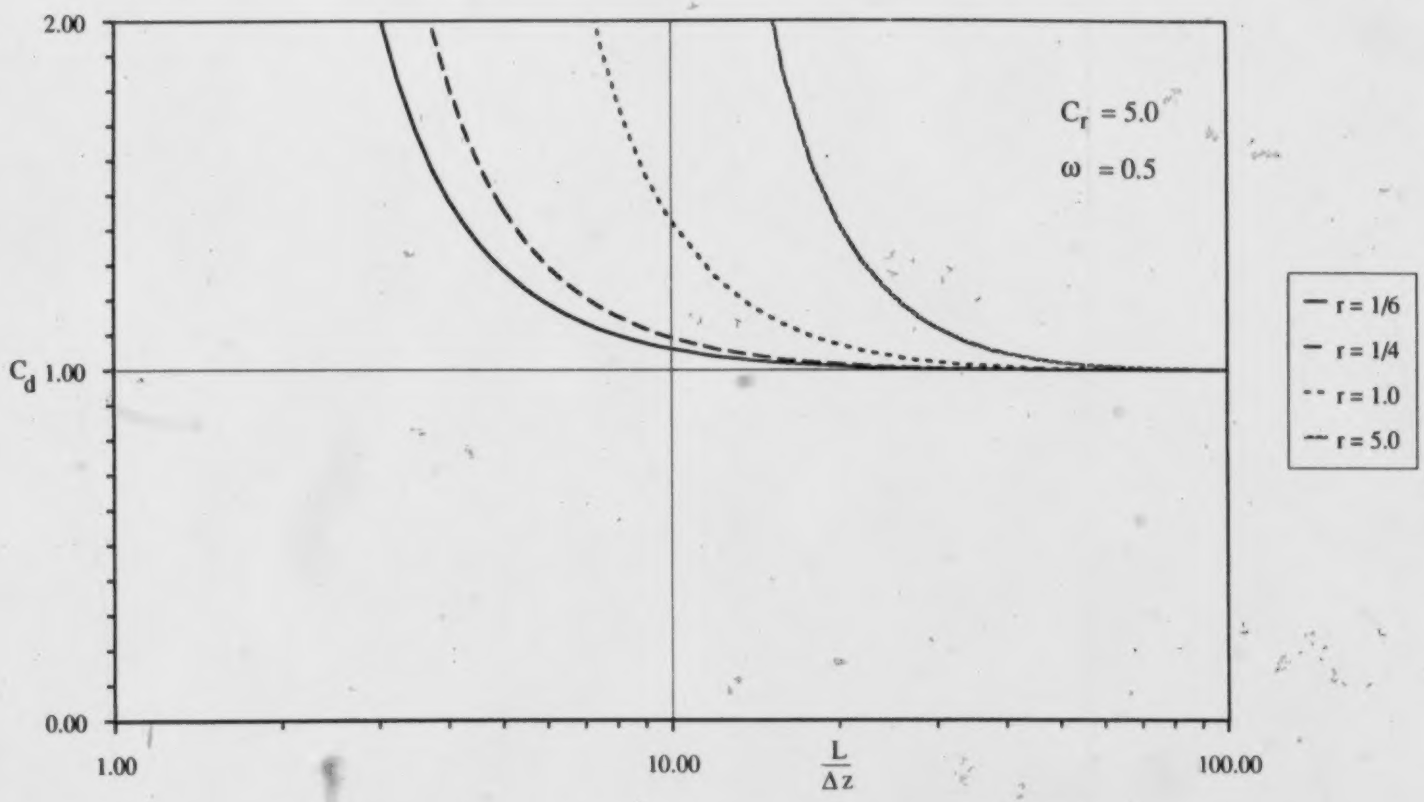

Fig. 6-2a. Amplification ratio against space-time discretization.

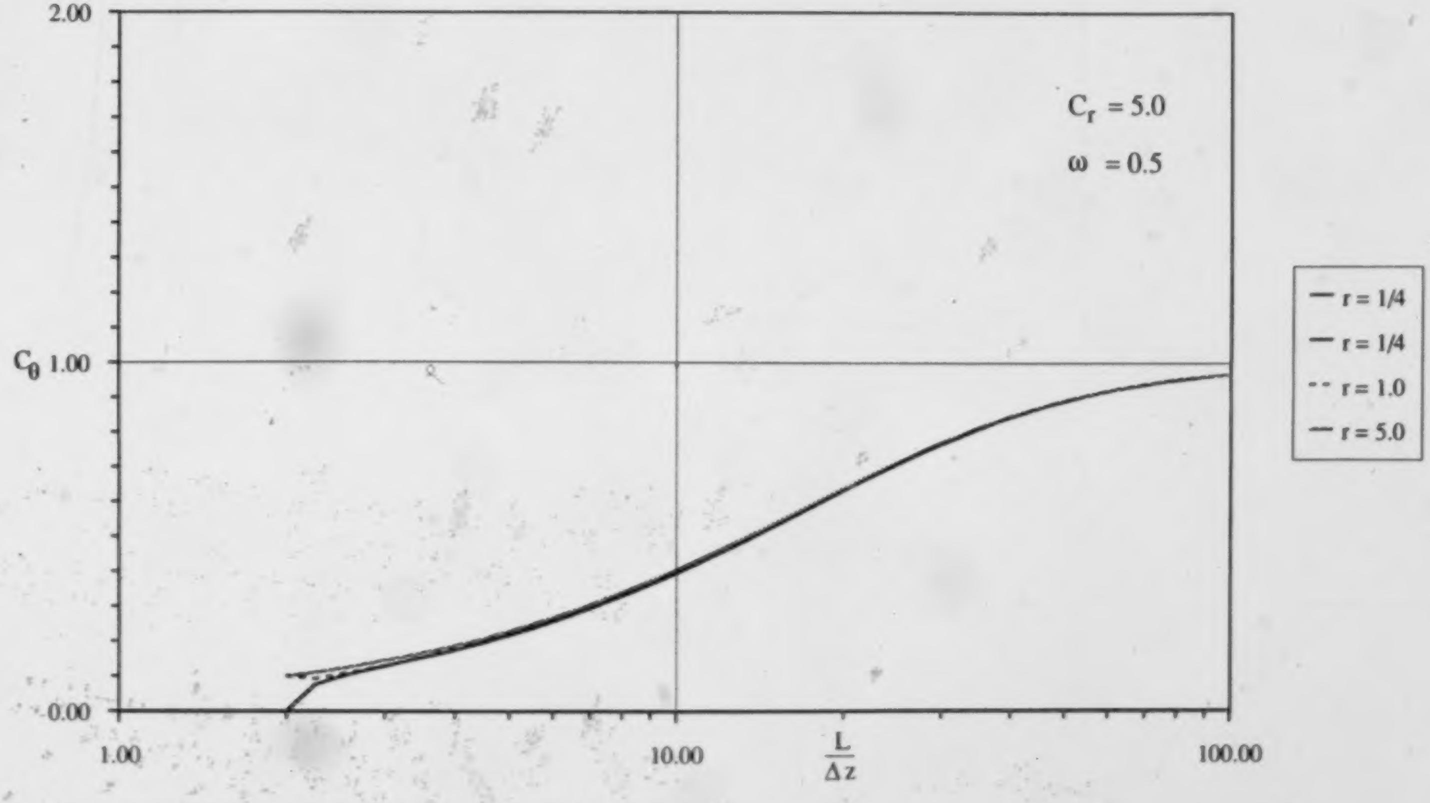

Fig. 6-2b. Celerity ratio against space-time discretization.

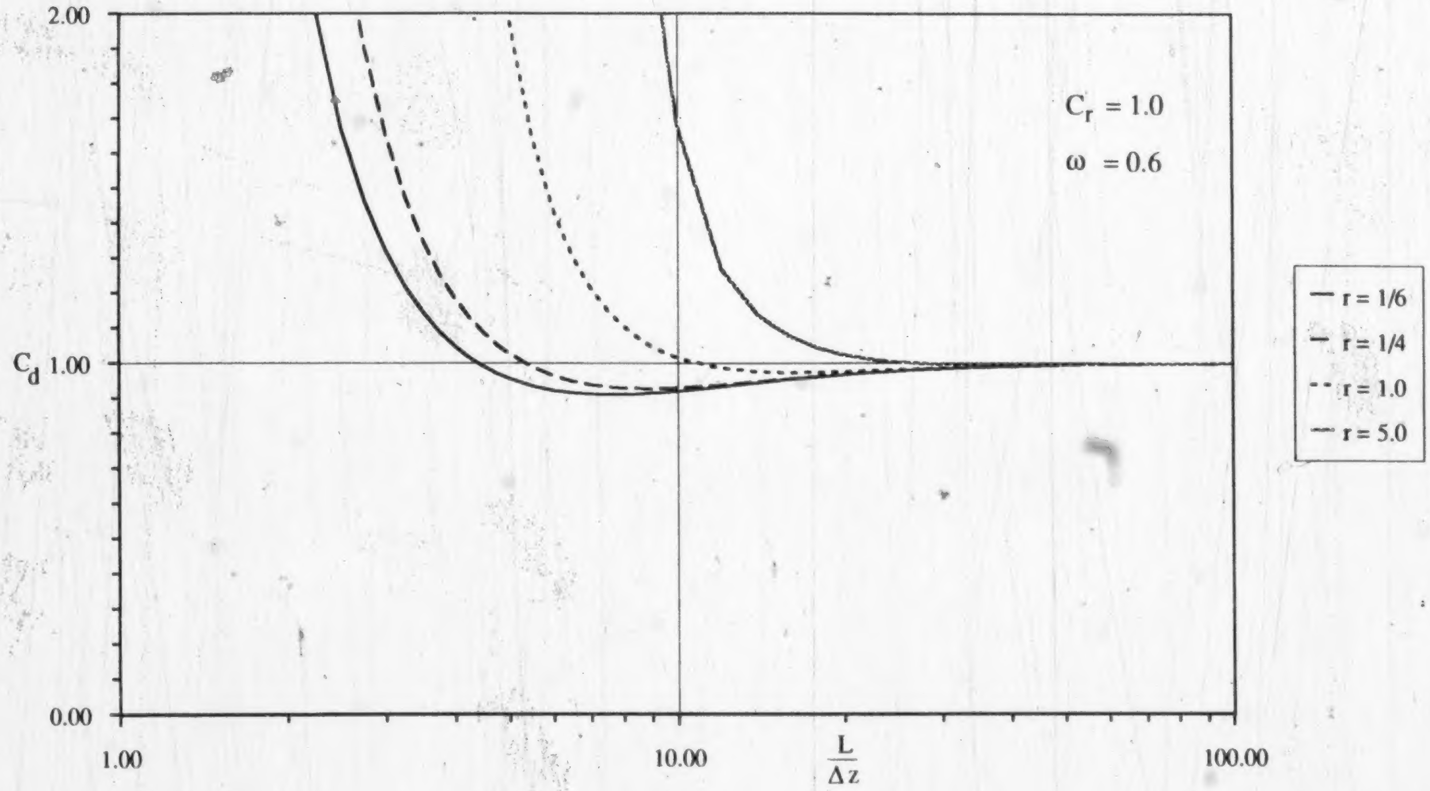

Fig. 6-3a. Amplification ratio against space-time discretization.

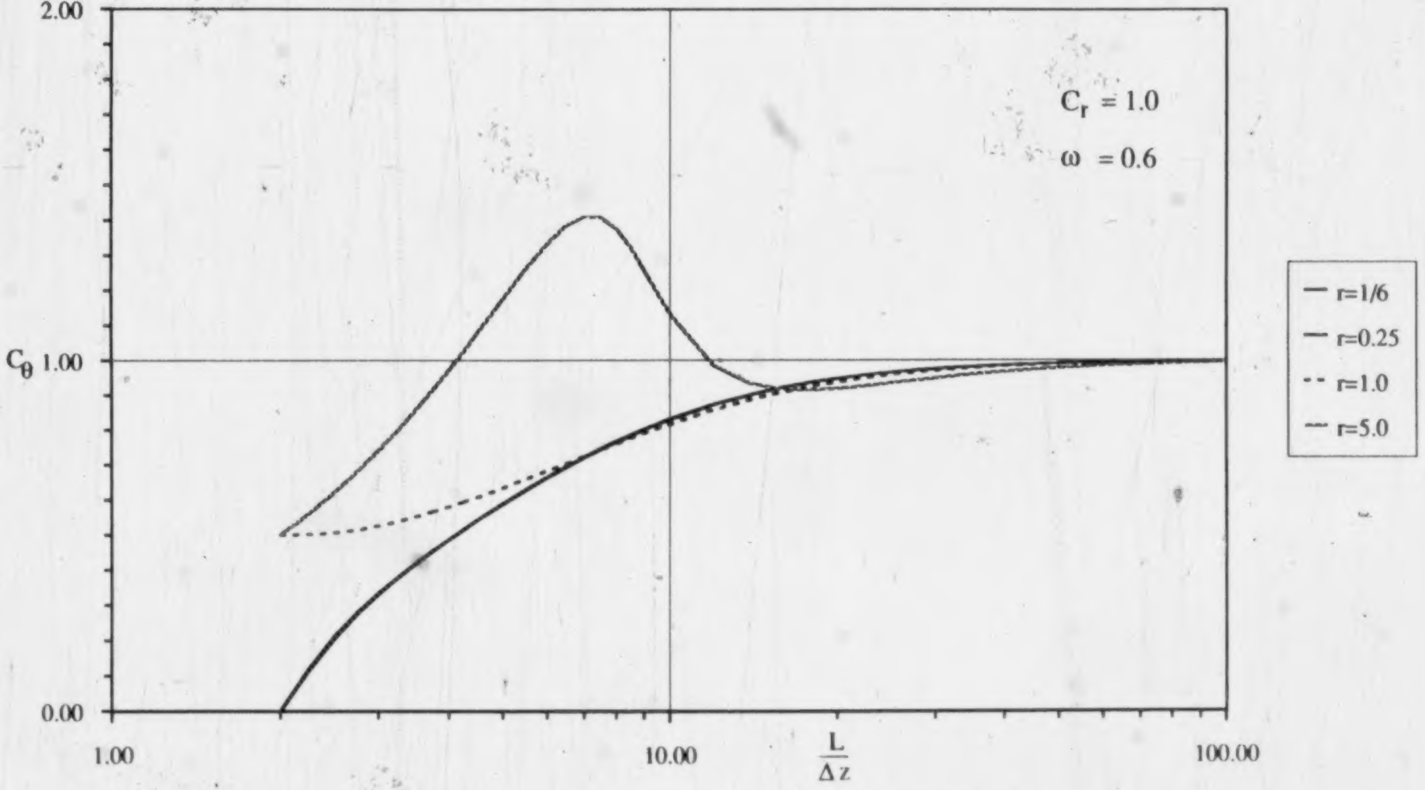

Fig. 6-3b. Celerity ratio against space-time discretization.

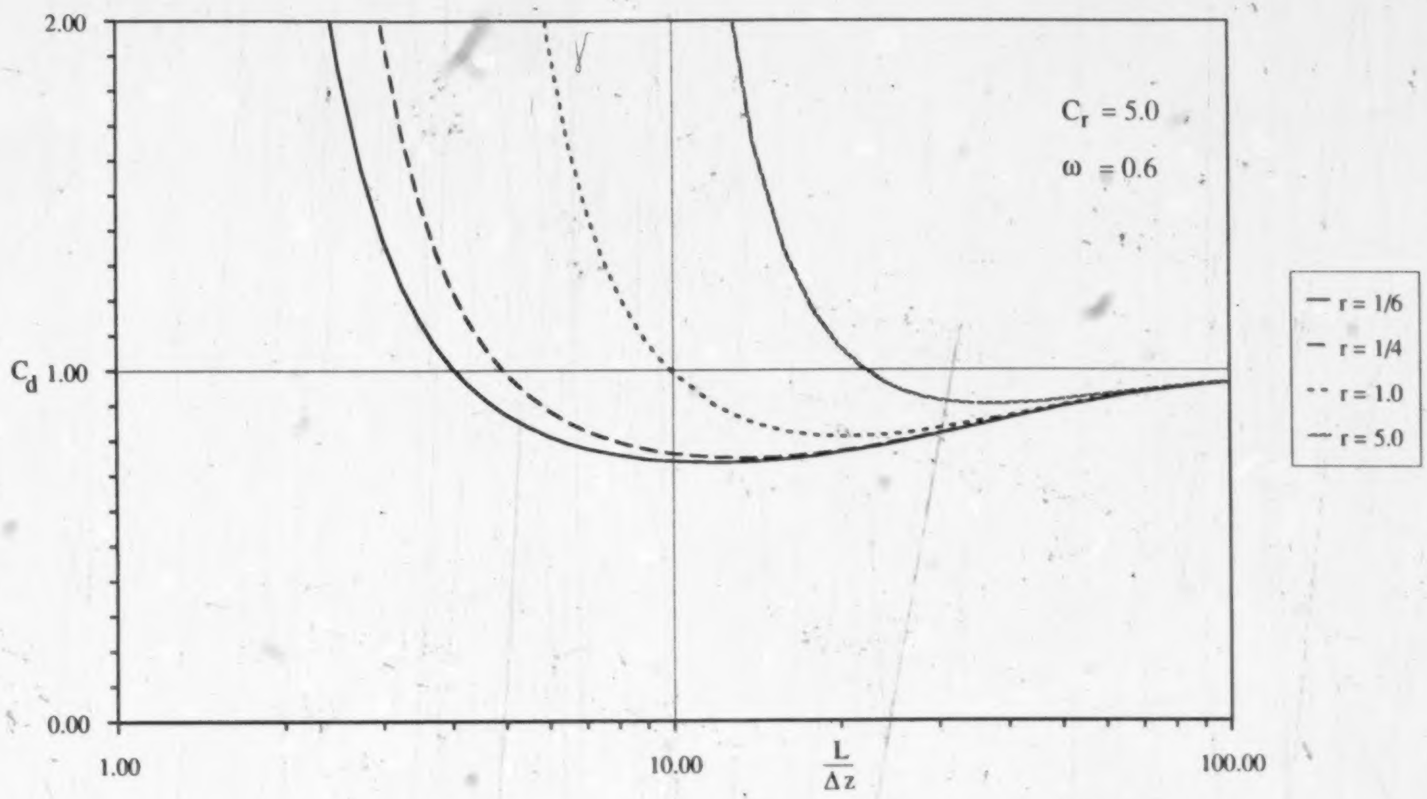

Fig. 6-4a. Amplification ratio against space-time discretization.

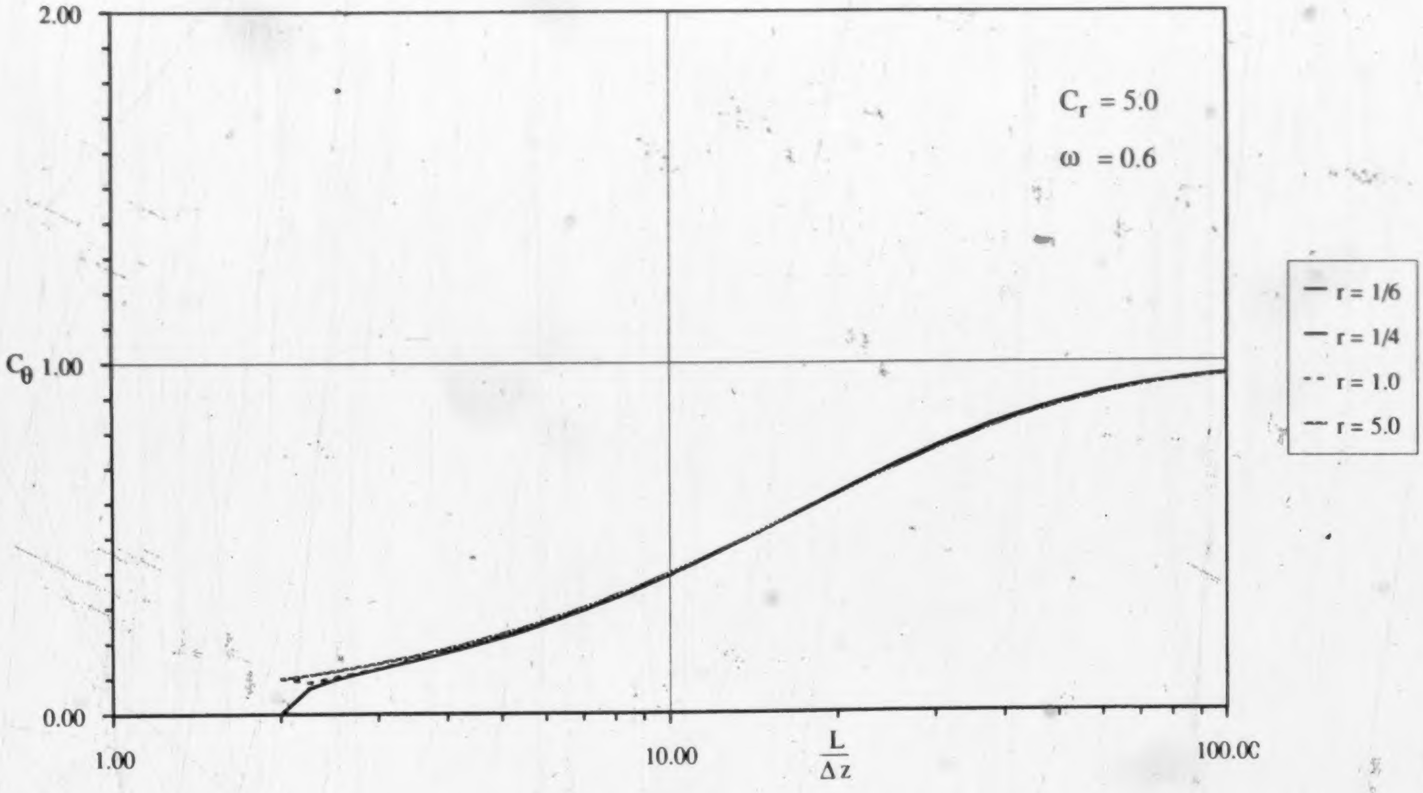

Fig. 6-4b. Celerity ratio against space-time discretization.

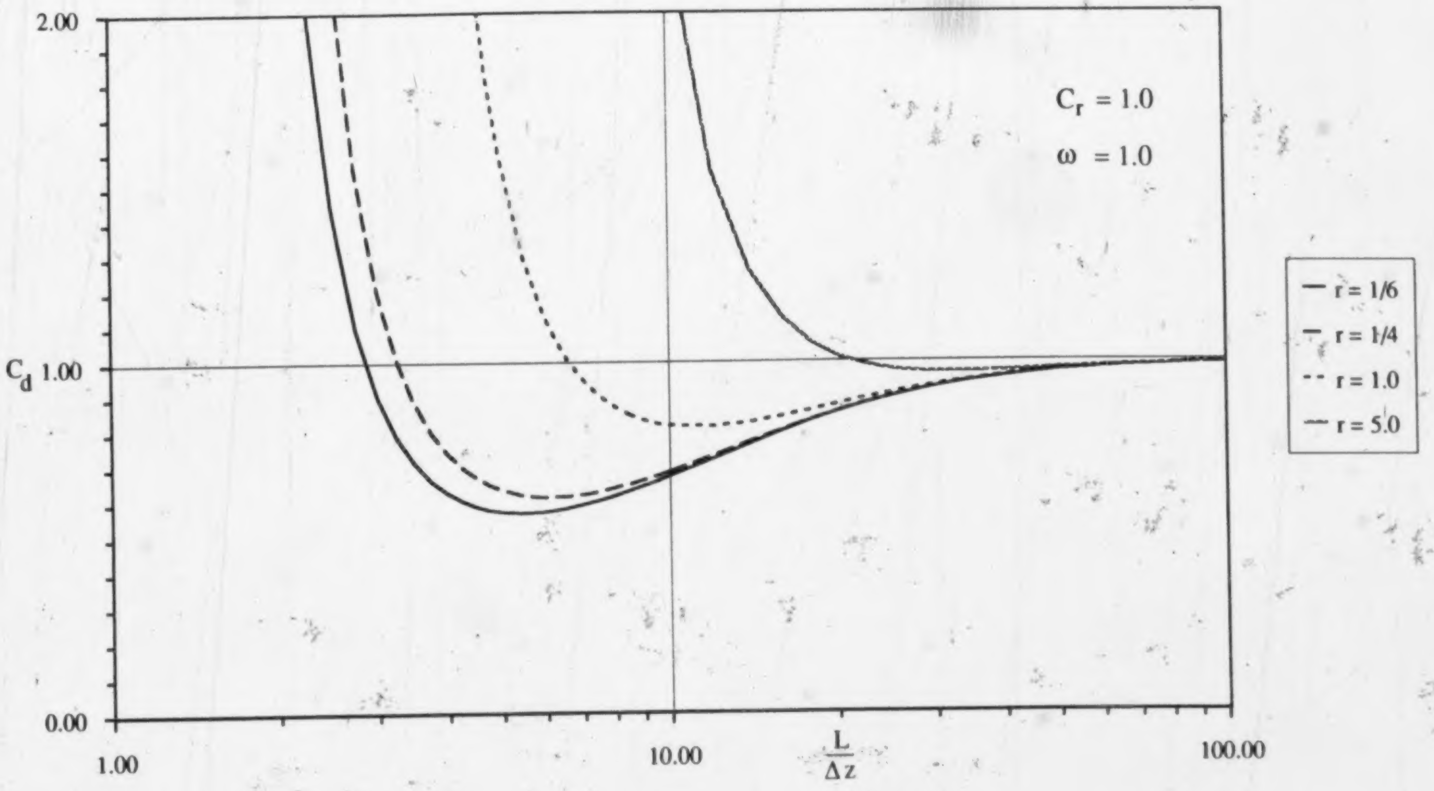

Fig. 6-5a. Amplification ratio against space-time discretization.

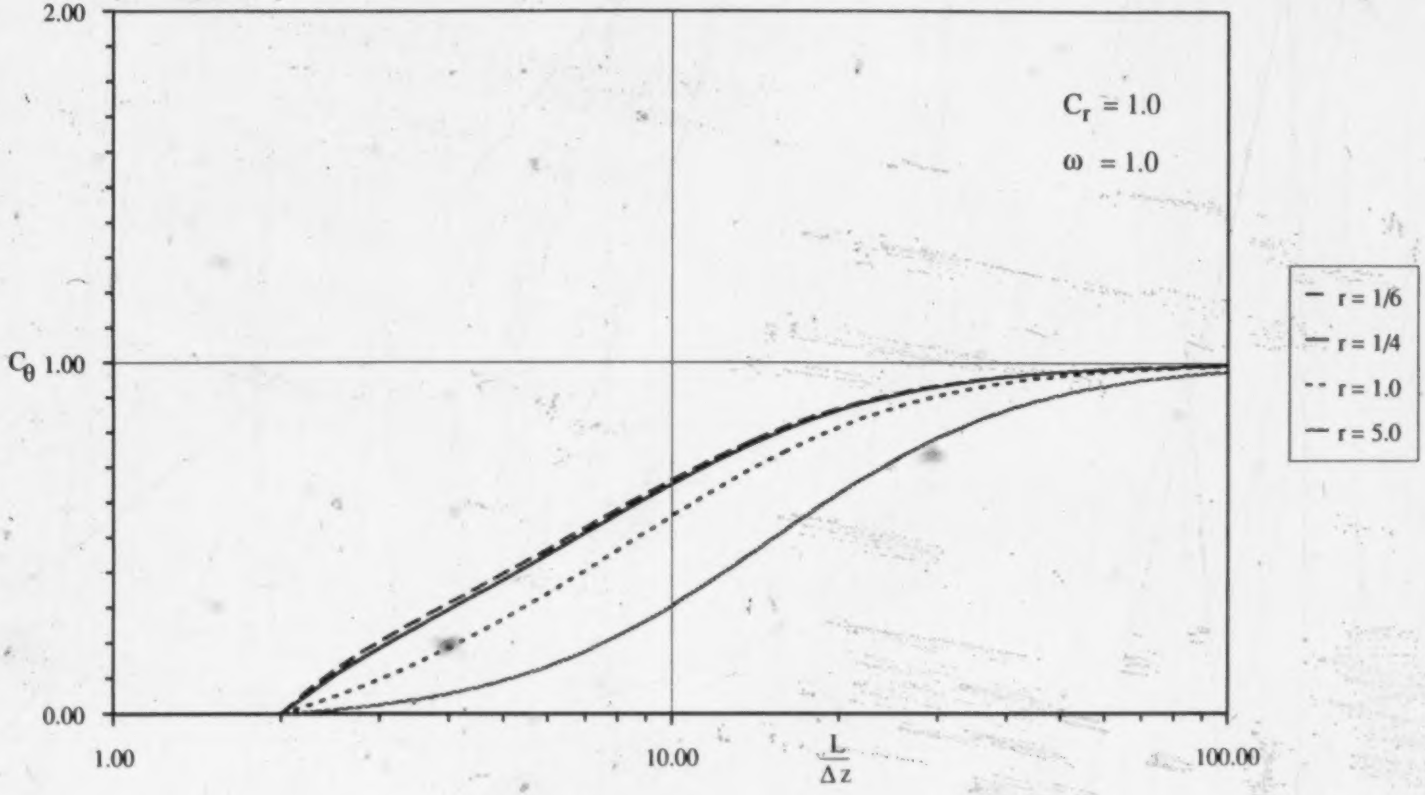

Fig. 6-5b. Celerity ratio-against space-time discretization.

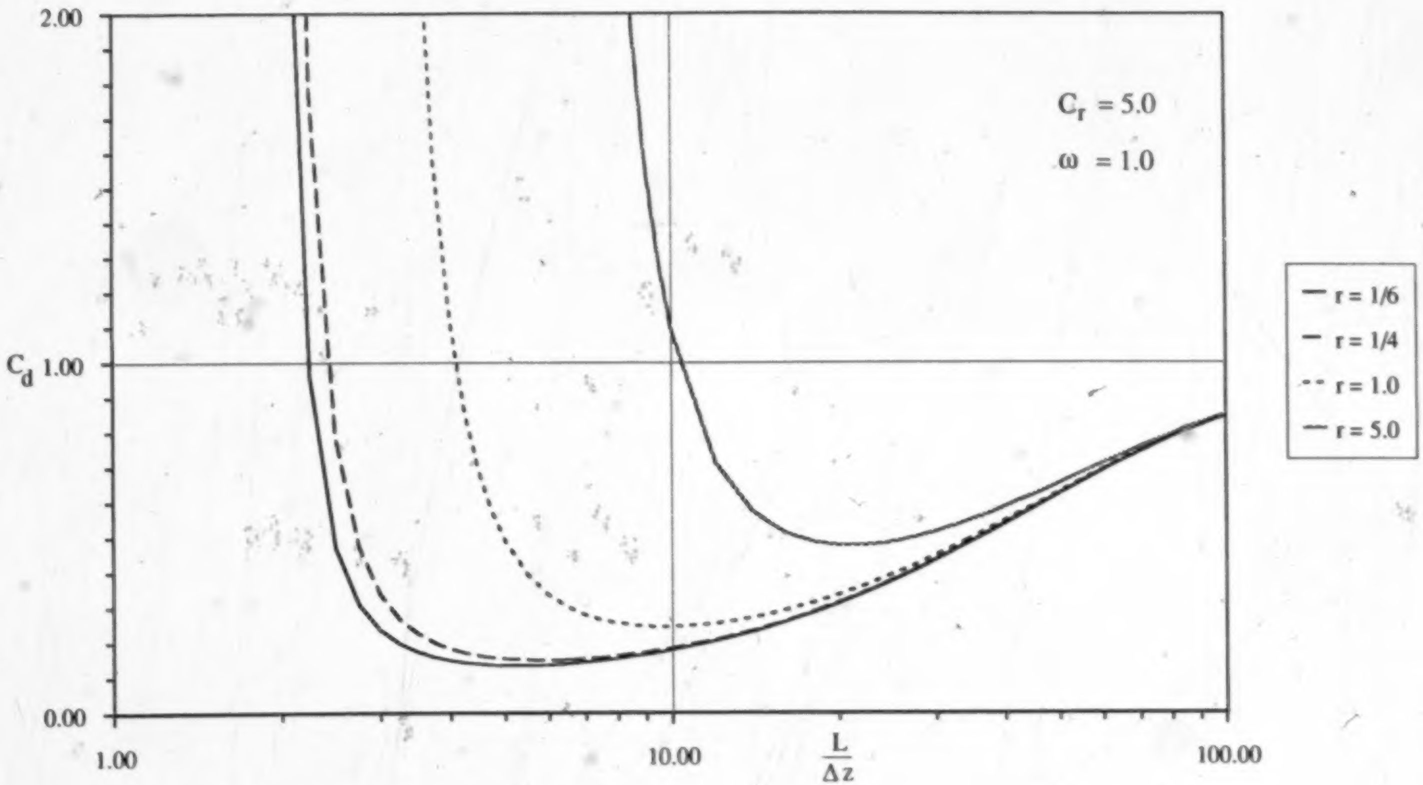

Fig. 6-6a. Amplification ratio against space-time discretization.

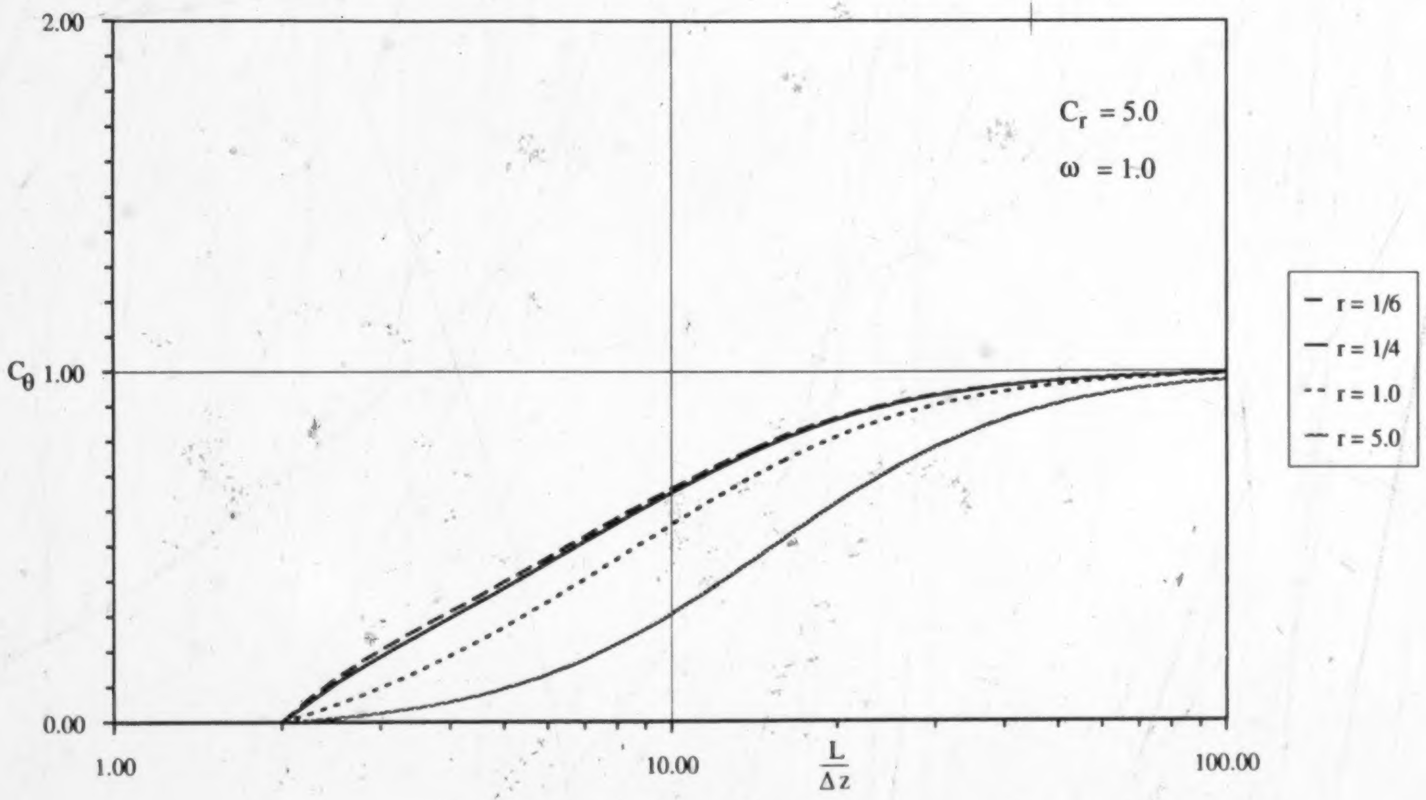

Fig. 6-6b. Celerity ratio against space-time discretization.

flow and overland flow equations are discussed briefly in the following paragraphs.

As previously noted, the linearised saturated and channel flow equations have the same form as the unsaturated flow equation (cf. eqns.[6-5], [6-6] and [6-7]). In addition the solution schemes used are also the same (centered finite difference). Hence, the expressions describing amplification and celerity ratios for these two equations are exactly the same as those given in eqns.[6-14] and [6-15].

The overland flow equation is somewhat different (i.e. the diffusion term is missing). Beside, the nature of the required boundary conditions necessitated the use of a different numerical scheme to solve it. Instead of the traditional centered finite difference scheme the box method is used. Following the same procedure as before, the amplification and celerity for the analytical solution are obtained as

$$\gamma_a = e^{-i C_r (2\pi/L/\Delta x)} \qquad [6\text{-}16]$$

$$\theta_a = -C_r \frac{2\pi}{L/\Delta x} \qquad [6\text{-}17]$$

while those for the numerical solution are

$$\gamma_n = \frac{(1+C_r)+(1-C_r)\left[\cos\left(\frac{2\pi}{L}\Delta x\right)+i\sin\left(\frac{2\pi}{L}\Delta x\right)\right]}{(1-C_r)+(1+C_r)\left[\cos\left(\frac{2\pi}{L}\Delta x\right)+i\sin\left(\frac{2\pi}{L}\Delta x\right)\right]} \qquad [6\text{-}18]$$

$$\theta_n = \tan^{-1}\left(\frac{RQ-PS}{PR+QS}\right) \qquad [6\text{-}19]$$

where

$$P = (1+C_r) + (1-C_r)\cos\left(\frac{2\pi}{L}\Delta x\right)$$

$$Q = (1-C_r)\sin\left(\frac{2\pi}{L}\Delta x\right)$$

$$R = (1-C_r) + (1+C_r)\cos\left(\frac{2\pi}{L}\Delta x\right)$$

$$S = (1+C_r)\ \sin\left(\frac{2\pi}{L}\Delta x\right)$$

and C_r is defined as

$$C_r = \frac{U_{ol}\Delta t}{\Delta x}$$

Therefore, the following expressions give the amplification and celerity ratios, for the kinematic wave equation when solved using the box method.

$$C_d = \left[\left(\frac{PR+QS}{R^2+S^2}\right) + \left(\frac{RQ-PS}{R^2+S^2}\right)\right]^{1/2} \qquad [6\text{-}20]$$

$$C_\theta = \tan^{-1}\left(\frac{RQ-PS}{PR+QS}\right) / \left(-\frac{2\pi}{L}\Delta x\ C_r\right) \qquad [6\text{-}21]$$

Unlike the previous situations, C_d and C_θ are the functions of C_r and L/Δx only. For different values of C_r, C_d and C_θ are computed and plotted as function of L/Δx as shown in Figs. 6-7a and 6-7b.

6.4.2 Space time discretization

So far the derivation and discussion included mainly the theoretical aspects of stability and convergence, coded in some terms such as waves, celerity etc. Perhaps one would wonder if the amplification ratio, expressed as a function of wave length, can possibly be used especially in the context of unsaturated flow problems. But it is not very difficult to

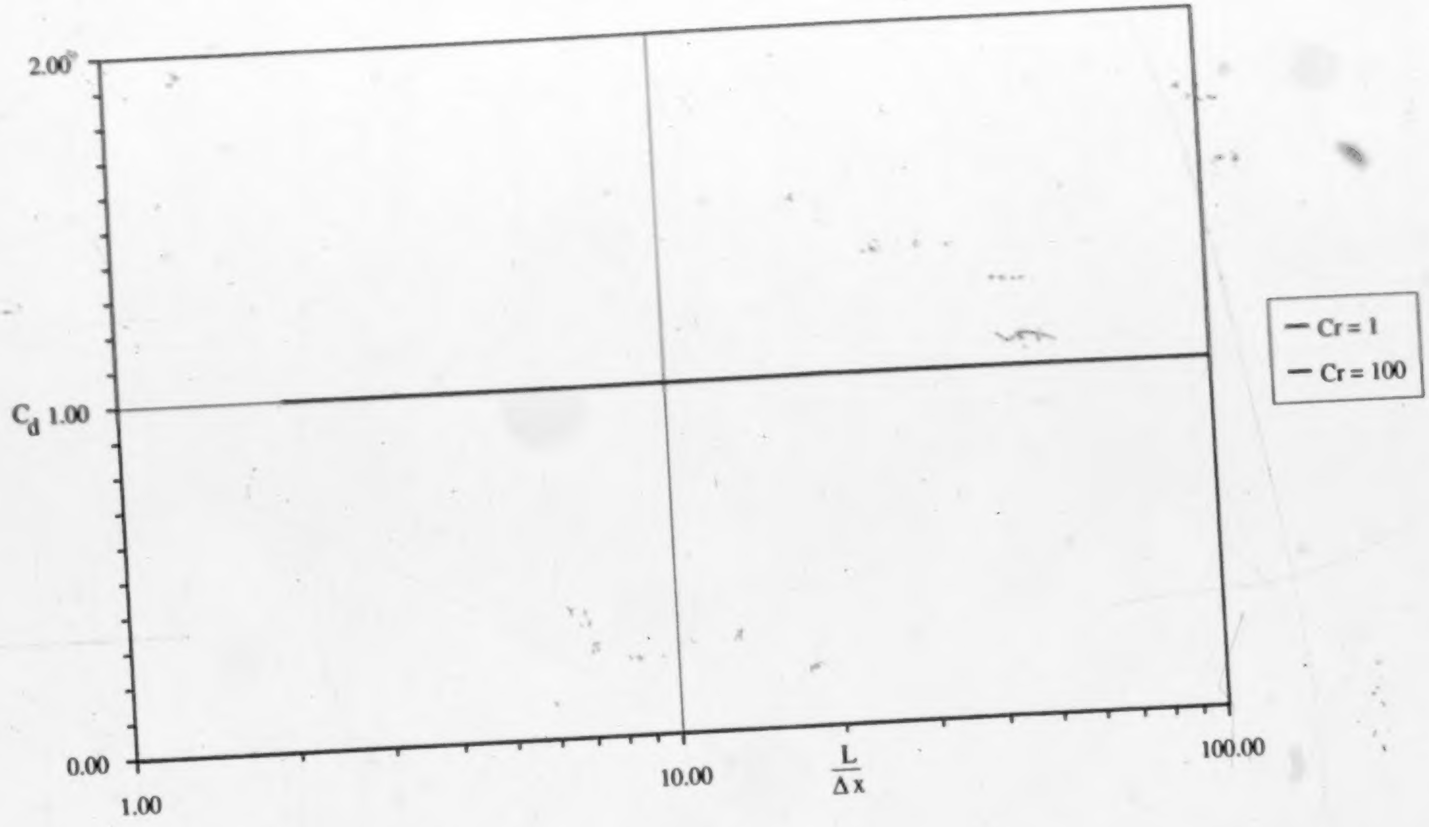

Fig. 6-7a. Amplification ratio against space-time discretization for box method.

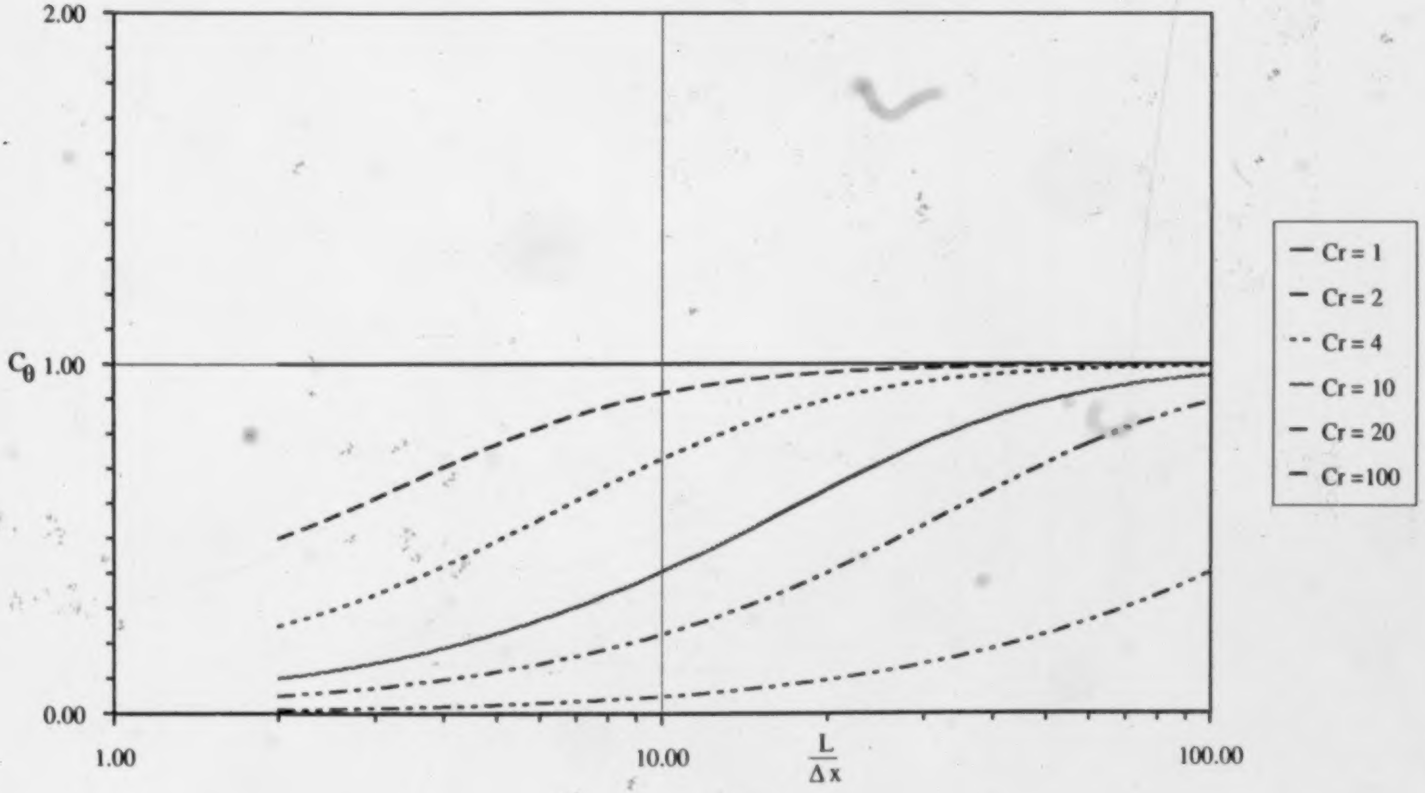

Fig. 6-7b. Celerity ratio against space-time discretization for box method.

visualize the existence of the wave form in the soil moisture profile. For instance, Figs. 6-8a and 6-8b can be considered. The moisture profile presented in Fig. 6-8a can be thought of as a monoclinic wave (solid line) often assumed in open channel flow situation or as sine or cosine wave (dotted line). Whereas the profile shown in Fig. 6-8b can be considered a diffusive wave with stationary peak (at point A).

However, these are the output waves. The frequency spectrum of these waves are the damped out form of the spectrum of the input function (such as rainfall). It is necessary to maintain the degree of discretization in space and time for the highest frequency i.e. the shortest significant wave length that could exist in the transient moisture flow. Hence to obtain an accurate prediction for the discretization, the input frequency spectrum should be considered. But here it is thought that the use of the input spectrum would simply provide a conservative form of the discretization criteria without any added advantage. Furthermore, the unsaturated flow system does not seem to respond to all the frequencies of the input function. Some of the rainfall may run off before entering into the system. The wave form (hence the wave length) resulting after the first few minutes of infiltration into very dry soil can be used for determining the discretization criteria. To this profile a sine wave can be fitted from which the discretization wave length is determined.

Unlike the unsaturated flow problem, in the saturated, overland and channel flow cases the significant wave frequency and hence the wave length is determined from the system response function. The logic here is that the frequencies of the obtained output are limited by the dominating frequencies of the system response function. Hydrologic systems, generally, possess a significant energy within the lower frequencies. This is also the case of the linear model (here the linearised differential equations) used to represent the system response, most of the energy within the system may be retained without the consideration of the very high frequencies of the input functions.

Knowing the system input and output, it is not very difficult to determine the response function and its frequency spectrum, with, of course, some simplified assumptions regarding the system's nature. For the flow systems, as encountered in this study, the response function can be derived following the linear system theory (Fig. 6-9). According to the theory a linear system is characterised by the following equation

$$f(t) = \int_{-\infty}^{\infty} i(\tau)\, h(t-\tau)\, d\tau \qquad [6\text{-}16]$$

where i(t) is an input function; h(t) is the system response function, characterised as the response to a unit impulse; and f(t) is the response of the system to the input i(t).

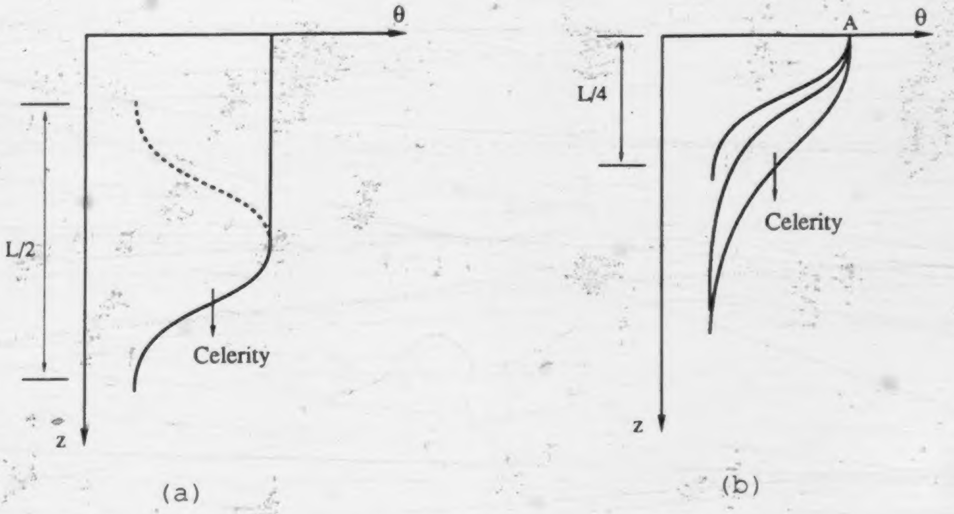
θ
L/2
Celerity
z
A
θ
L/4
Celerity
z

(a) (b)

Fig. 6-8. Waves forms in soil moisture profiles; (a) monoclinic wave; (b) diffusive wave; L - wave length; θ - moisture content; z - depth.

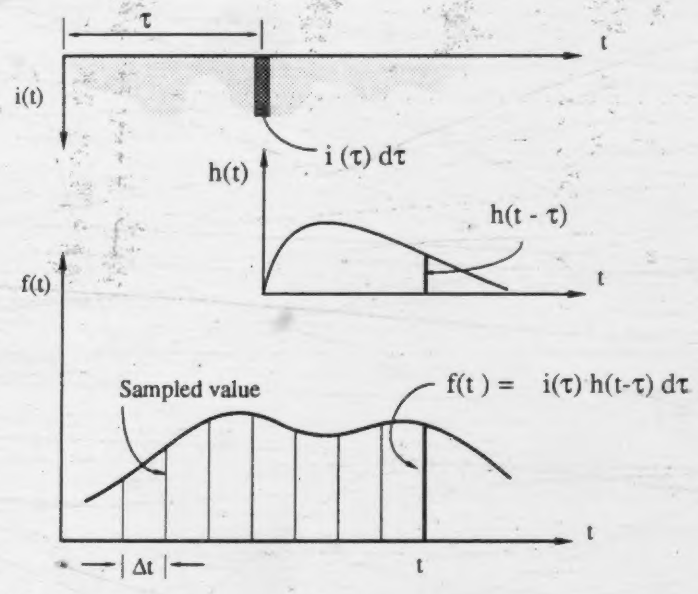
τ
t
i(t)
i (τ) dτ
h(t)
h(t - τ)
t
f(t)
Sampled value
f(t) = i(τ) h(t-τ) dτ
t
Δt
t

Fig. 6-9. A linear system; i(t) - input function; h(t) - transfer function; f(t) - output function.

Application of the Fourier Transform (FT) to eqn.[6-16] yields

$$F(\omega) = \frac{1}{2\pi} \int_{-\infty}^{\infty} f(t)\, e^{-j\omega t}\, dt \qquad [6\text{-}17]$$

Letting s=t-τ and changing the order of integration, the above equation reduces to

$$F(\omega) = \frac{1}{2\pi} \int_{-\infty}^{\infty} i(\tau)\, e^{-j\omega\tau}\, d\tau \,.\, \int_{-\infty}^{\infty} h(s)\, e^{-j\omega s}\, ds \qquad [6\text{-}18]$$

which can be written as

$$F(\omega) = H(\omega)\,.\,I(\omega) \qquad [6\text{-}19]$$

where $F(\omega)$, $H(\omega)$ and $I(\omega)$ are the FT of the output, system response and input functions. From this expression it appears that the convolution integral can be reduced to simple multiplication of transformed values. Therefore, the unknown system response function $H(\omega)$ can be obtained from

$$H(\omega) = \frac{F(\omega)}{I(\omega)} \qquad [6\text{-}20]$$

To describe the procedure leading to discretization, the overland flow process is considered as an example. A pulse of constant intensity rainfall of 1 m/hr (never occurred on earth; for the sake of example only) is applied as an input for a duration of 1 hour over a 1700x500 m^2 plot with n = 0.1 and S_0 = 0.01. The response function due to this input is computed using a finer computational mesh. The errors in the mass balance (discussed later) is taken as an indication of the computational accuracy (Figs. 6-10 and 6-11). Using 'Mathematica' (Wolfram, 1988) the Fourier Transforms of the input and output functions are evaluated. Subsequently, utilizing eqn.[6-20] the system unit impulse response was obtained. Fig. 6-12 shows the normalized energy spectrum of the unit impulse response. From the frequency spectrum of the impulse response function the significant wave frequency, at 10% cutoff level, is obtained.

Similarly response function and significant wave frequencies of the channel flow system are also derived. A channel of length 10864 m of the Spring Creek watershed is considered here (channel characteristics are described in the later paragraphs). Following the example of the overland flow case a pulse input of 35 m^3/s is dumped at the upstream end of the channel. The resulting output hydrograph in the middle section of the channel is used to obtain the impulse response (cf. Figs. 6-13 and 6-14 for channel flow case).

It should be realized that the troubles are not yet over. The determination of the significant frequency in no way enables one to obtain the significant wave length (which is being pursued relentlessly in this section). This requires the wave speed or the celerity.

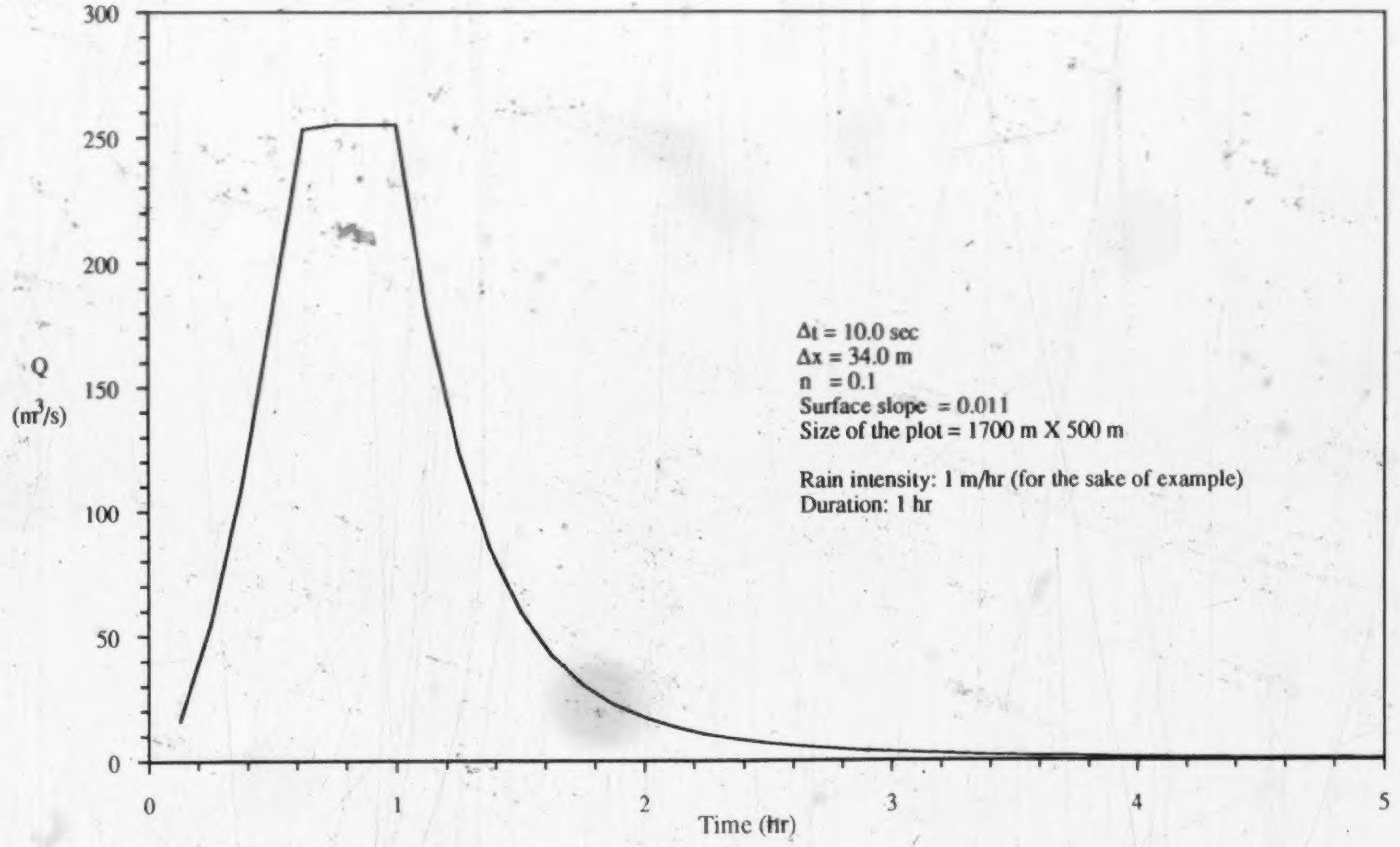

Fig. 6-10. Overland flow response to a unit pulse.

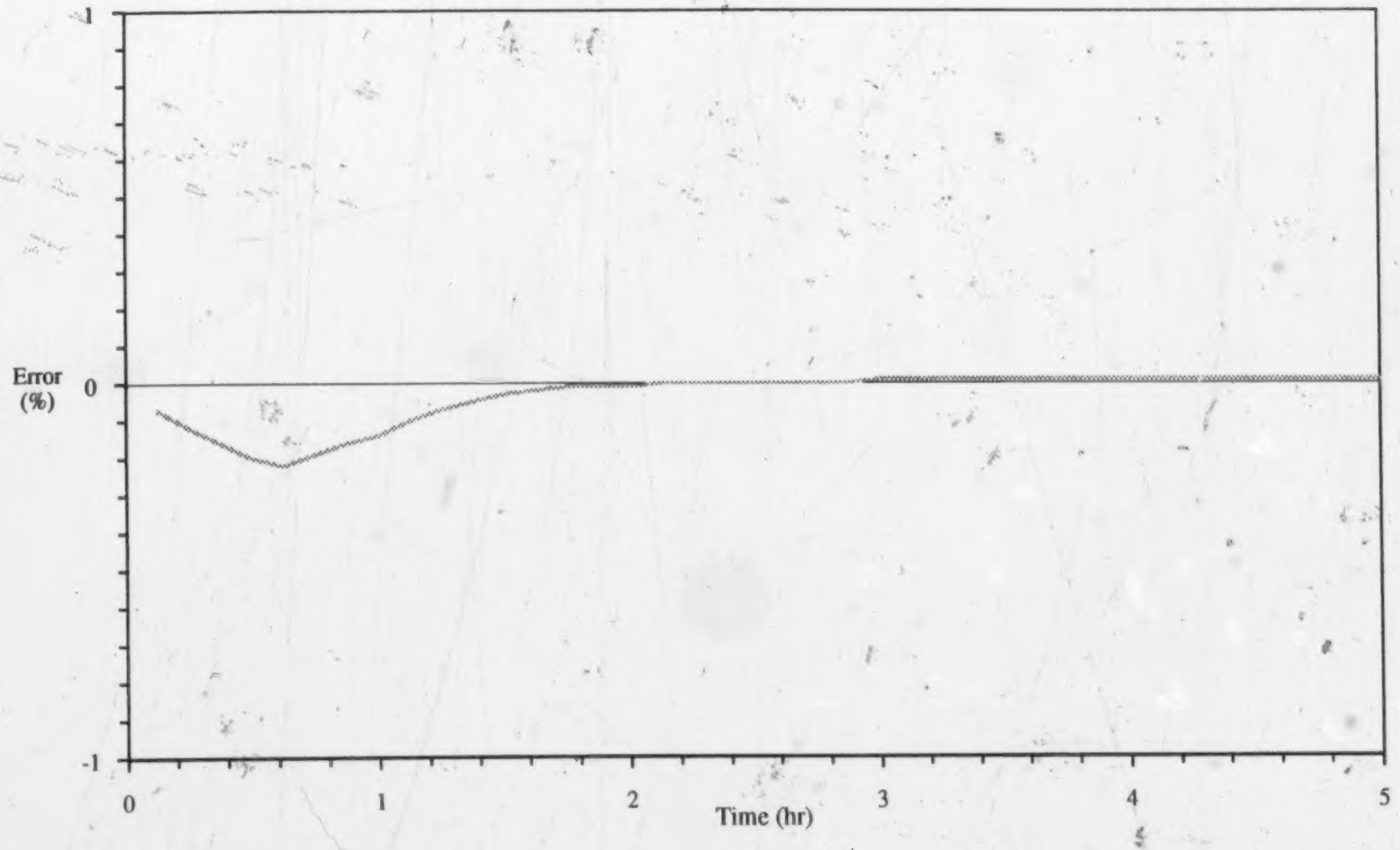

Fig. 6-11. Mass balance error of overland flow computation.

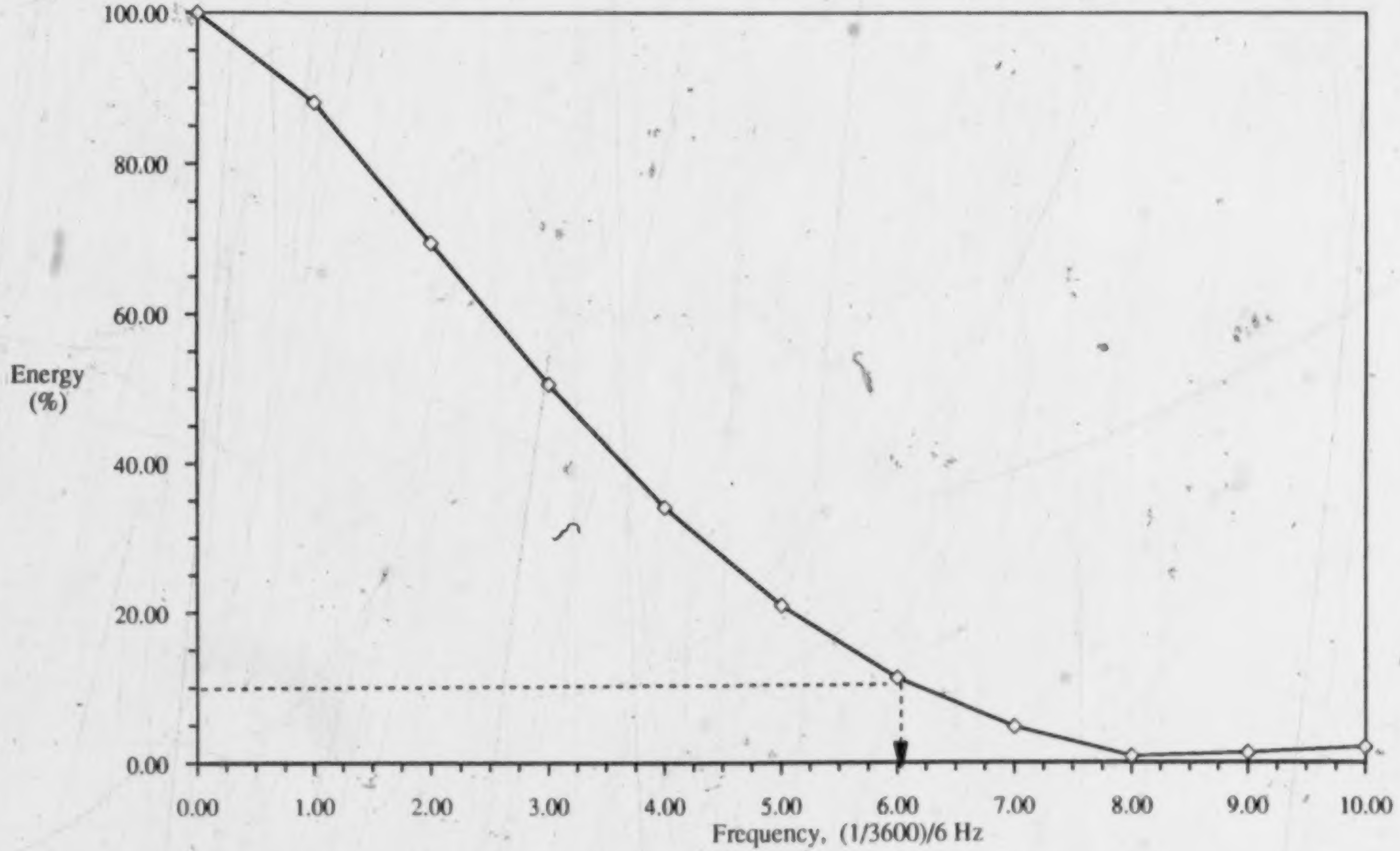

Fig. 6-12. Energy spectrum of the overland flow transfer function.

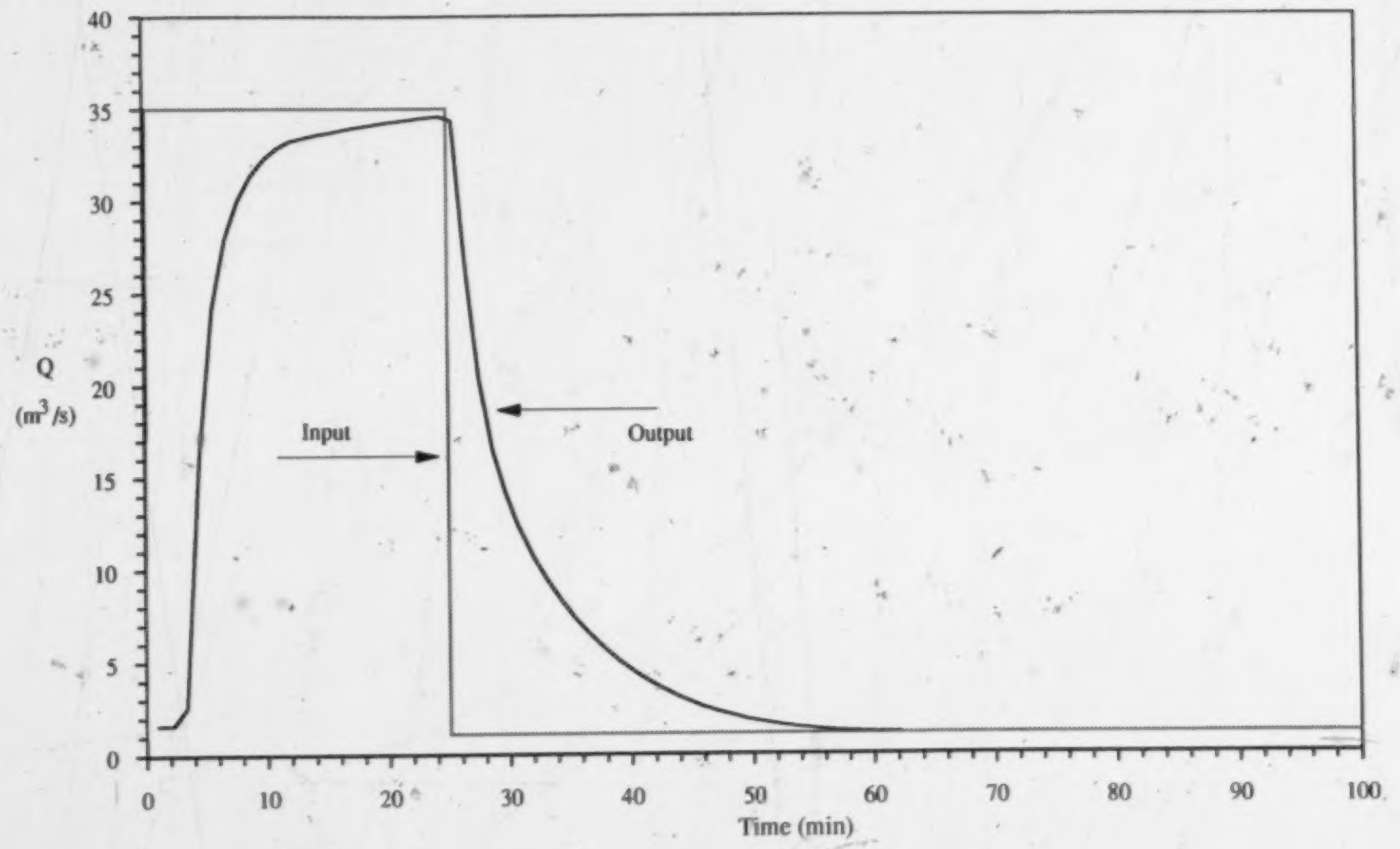

Fig. 6-13. Channel response to a pulse input.

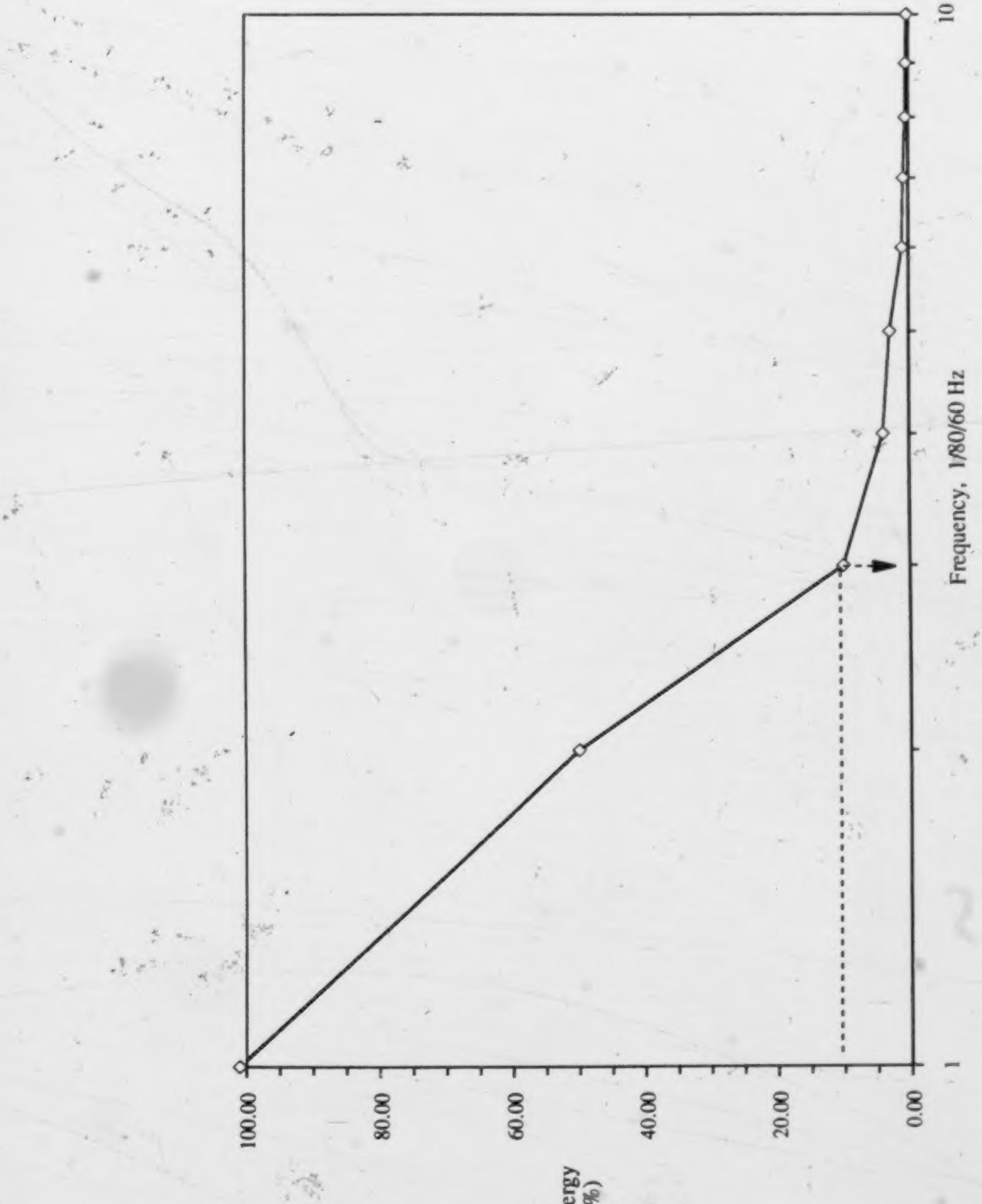

Fig. 6-14. Energy spectrum of channel response.

Again the overland flow case is considered. The kinematic wave speed (mentioned in Chapter 4) is given by $c = (1+m)\alpha y^m$. Since the mean water velocity is given by $v = \alpha y^m$, the kinematic wave celerity is $c = (1+m)v$. For a reference depth y_0 (i.e. linearisation depth) the corresponding water velocity v_0 and hence c_0 or directly c_0 from y_0 can be determined. Using the significant wave frequency, f, (at 10% cutoff level, Fig. 6-12) the significant wave length is calculated as $L = c_0/f$.

In general for a desired accuracy the suitable $L/\Delta x$, and C_r are chosen from Figs. 6-1a through 6-6b. A higher C_r and r level leads to a higher Δt for a constant Δx. If $L/\Delta x = N_\lambda$ then: $\Delta x = L/N_\lambda$. If, for example, C_r is chosen as C_n then $\Delta t = C_n(\Delta x)/c_0$ and the number of nodes in the profile will be $L_x/\Delta x + 1$; where L_x is the profile length.

Test of discretization

For the purpose of verifying these discretization criteria several test problems are solved. This is done separately in the following paragraphs for different flow processes starting with the **unsaturated flow**.

The problem used here consists of solving the unsaturated flow equation for infiltration in the Spring Creek watershed. The hydraulic properties for the soil are as described by eqns.[7-1] and [7-2]. The differential equation is linearised about the mean moisture content of 0.30 (i.e. $\theta_0 = 0.30$) which gives corresponding ψ_0, K_0 and C_0 as 800 cm, 2×10^{-5} cm/min and 7×10^{-5} cm^{-1} (Fig. 6-15). The wave length is

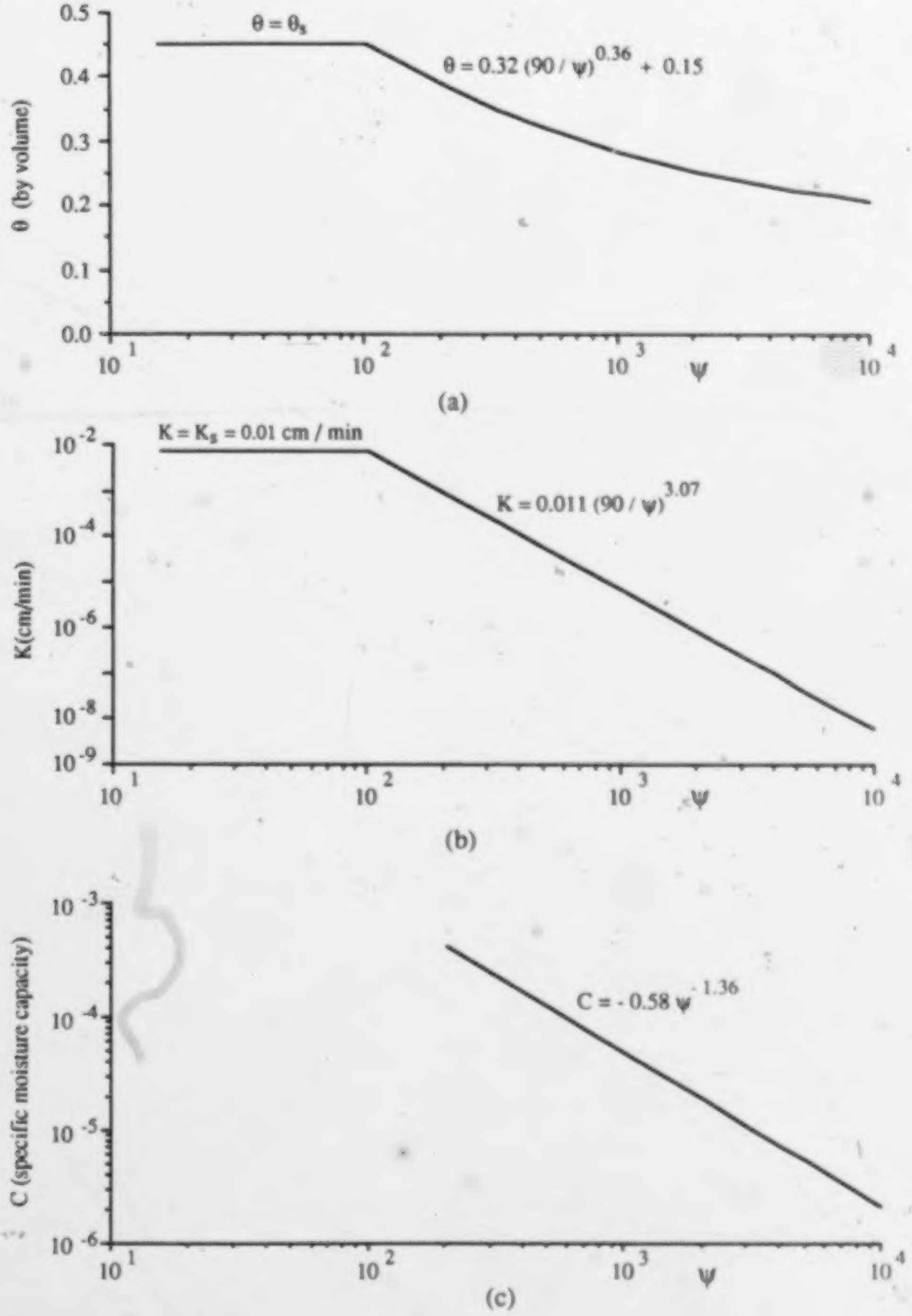

Fig. 6-15. Hydraulic properties of the soil-C of Spring Creek watershed.

read off from the Fig. 6-16 which gives $L/4 = 6$ cm. Hence $L = 24$ cm. For an amplification ratio $C_d = 1.0$, $r = 1.0$, $C_r = 1.0$ and $\omega = 0.5$ it is obtained that $L/\Delta z = 20$ (Fig. 6-1a). Therefore, $\Delta z = 24/20 = 1.2$ cm.

To calculate the time step it is necessary to evaluate the terms U_{un} and D_{un} in eqn.[6-5]. This is accomplished as follows: Take an approximate δz and obtain θ from the moisture profile at depth δz above or below the linearisation point O (Fig. 6-16, point A). From Fig. 6-16 corresponding to point A, θ_A is obtained which is roughly 0.25. Using this θ_A, $\psi_A = 2300$ cm is obtained from Fig. 6-15a and from Fig. 6-15b K_A is read off as 6×10^{-7} cm/min. Thus

$$\frac{\partial K_0}{\partial z} \approx \frac{K_0 - K_A}{\delta z} \approx \frac{2\times10^{-5} - 6\times10^{-7}}{1.0} \approx 1.94\times10^{-5}\left[\frac{1}{\text{min}}\right]$$

$$\frac{\partial \psi_0}{\partial z} \approx \frac{\psi_0 - \psi_A}{\delta z} \approx \frac{-800 + 2300}{1.0} \approx 1500$$

In the definition of U_{un}

$$b = \frac{\partial K}{\partial \psi} = 0.011\,(90)^{3.07}\,(3.07)\,\frac{1}{\psi^{4.07}}$$

Hence evaluating at $\psi_0 = 800$ cm

$$b = 0.011\,(90)^{3.07}\,(3.07)\,\frac{1}{800^{4.07}}$$
$$= 5.158\times10^{-8}\left[\frac{1}{\text{min}}\right]$$

Therefore

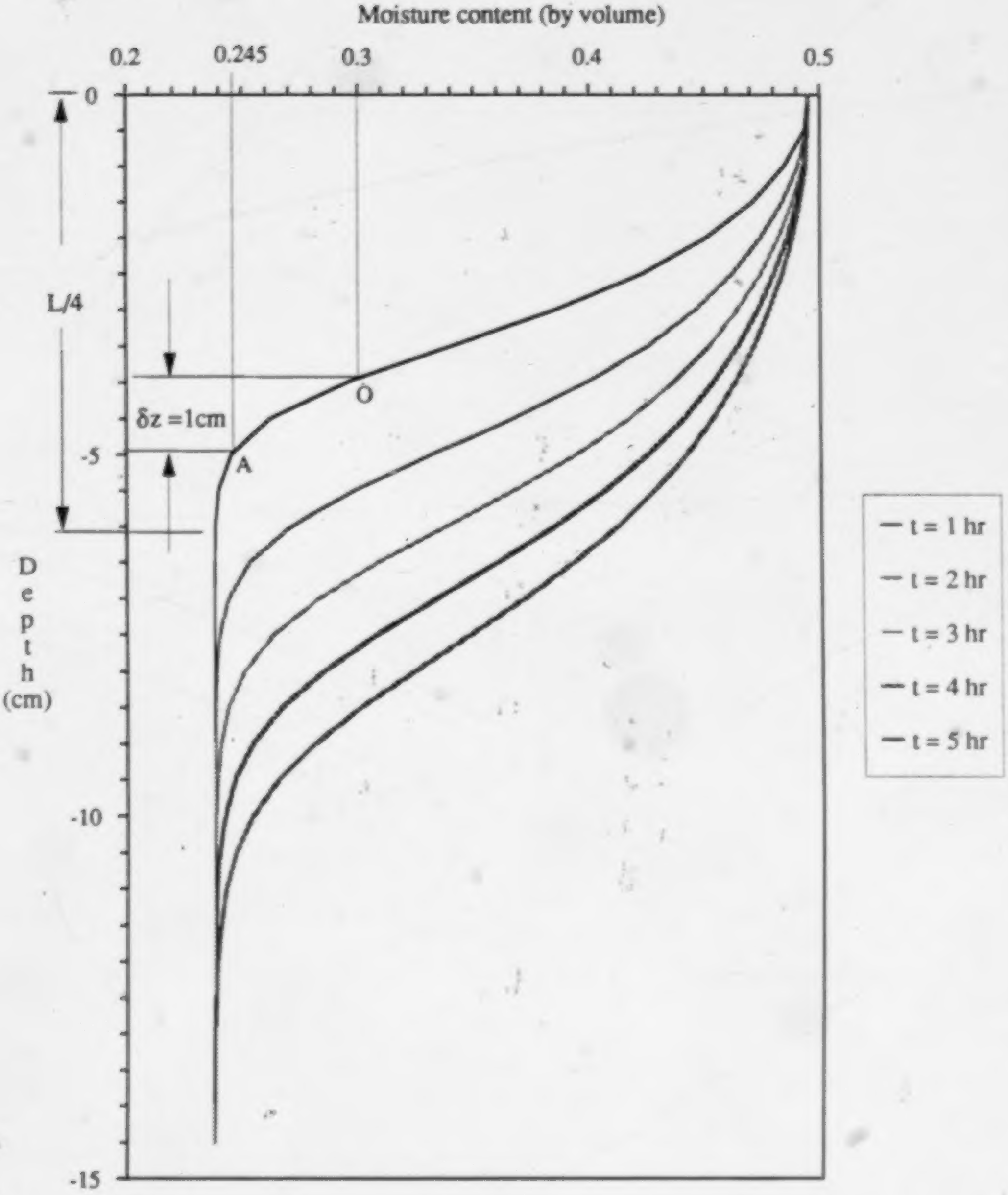

Fig. 6-16. Evaluation of derivatives for unsaturated flow case (infiltration in the soil-C of Spring Creek; initial moisture content: 0.237); L - wave length.

$$U_{un} = \frac{1}{7\mathrm{x}10^{-5}\left[\frac{1}{\mathrm{cm}}\right]}\left\{1.94\mathrm{x}10^{-5}\left[\frac{1}{\mathrm{min}}\right] + 5.158\mathrm{x}10^{-8}\ \mathrm{x}1500\left[\frac{1}{\mathrm{min}}\right] - 5.158\mathrm{x}10^{-8}\left[\frac{1}{\mathrm{min}}\right]\right\}$$

$$\approx 1.4\ \mathrm{cm/min}$$

Similarly D_{un} is evaluated at ψ_0 = 800 cm as

$$D_{un} = \frac{K_0}{C_0} = \frac{2 \times 10^{-5}\mathrm{cm\ min^{-1}}}{7 \times 10^{-5}\mathrm{cm^{-1}}} = 0.286\ \frac{\mathrm{cm^2}}{\mathrm{min}}$$

Therefore from $C_r = U_{un}\Delta t/(2\Delta z)$ it can be obtained that Δt = (2x1.2) / 1.4 = 1.71 min and also from $r = D_{un}\Delta t / (\Delta z^2)$, Δt = 1.2^2/ (0.286) = 5.03 min. Hence a numerical solution using the minimum of the two Δt's (e.g. 1.7 min) should not create a stability problem.

Overland flow: For this example the linearisation depth y_0 is considered to be 0.15 m (for the sake of example only). Considering the area (n = 0.1, S_0 = 0.01) which was used for obtaining the response function, the water velocity corresponding to this depth (i.e. 0.15 m) is calculated as $v_0 = (0.01)^{1/2}/(0.1)\ .(0.15)^{0.67}$ = 0.28 m/s. This gives c_0 = (1+0.67) .(0.28) = 0.46 m/s. From Fig. 6-11 for 10% cutoff frequency f is obtained as 0.0002 cycles/s which yields L = 0.46 /0.0002 = 1650 m. It is evident that the scheme is stable for any C_r. However, Fig. 6-7b indicates that the discretization criteria should be satisfied for the correct celerity of the numerical solution. Therefore if C_r is taken to be 1, the required $L/\Delta x$ is 30 in order to preserve the celerity ratio as unity. Thus, Δx = 1650/30 = 55 m. Using the expression for C_r it can be derived that Δt = (55)(1) /0.46 =

120 sec. A few test runs were done for overland flow computation with this discretization along with some other arbitrarily selected Δx. The results are presented in Figs. 6-17 and 6-18.

Channel flow: In this case the linearisation parameters such as y_0, Q_0, C^* etc. are evaluated considering the main channel of the Spring Creek watershed. The bed width of this channel was assumed to be 10 m. The maximum flood discharge ever recorded is 30 m^3/s. The mean slope of the channel is 0.0075 (obtained from map survey) which gives S_0 and Manning's roughness coefficient n is considered to be 0.03. The base discharge of linearisation is taken as 10 m^3/s. To make the calculations simple, it is further assumed that the channel cross section is rectangular. Therefore conveyance C^* is expressed as $C^* = y^{5/3}/n$ per meter width of the channel. This gives $\delta C^*/\delta y = (5/3)y^{2/3}/n$. From the Manning equation the normal depth y_0 (which is considered as the linearisation depth) for a discharge of 10 m^3/s is obtained as $y_0 = 0.58$ m. Accordingly the value of U_{ch} can be obtained as 3.3 m/s which in fact is the wave celerity.

From Fig. 6-14 at 10% cutoff level the significant frequency, f, is approximated as 0.0006 Hz. Hence wave length, $L = U_{ch}/f = 3.3 / 0.0006 = 5500$ m. For $C_r = 1$, $r = 1$ and $\omega = 0.5$ (weighting factor) and satisfying the stability criteria, from Fig. 6-1a it can be obtained that $L/\Delta x$ is about 20. This gives $\Delta x = 5500/20 = 275$ m.

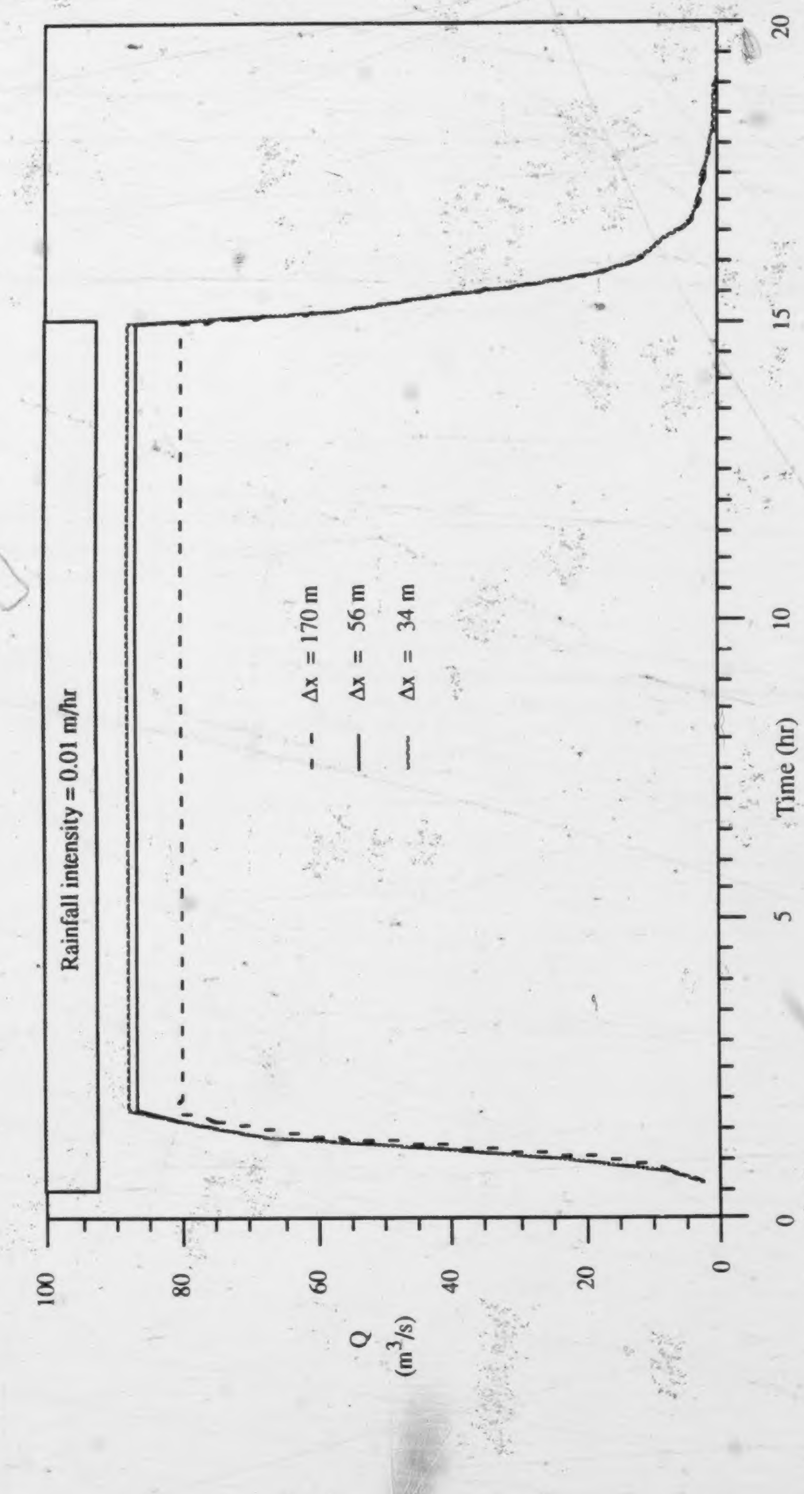

Fig. 6-17. Effect of discretization on hypothetical overland flow hydrograph.

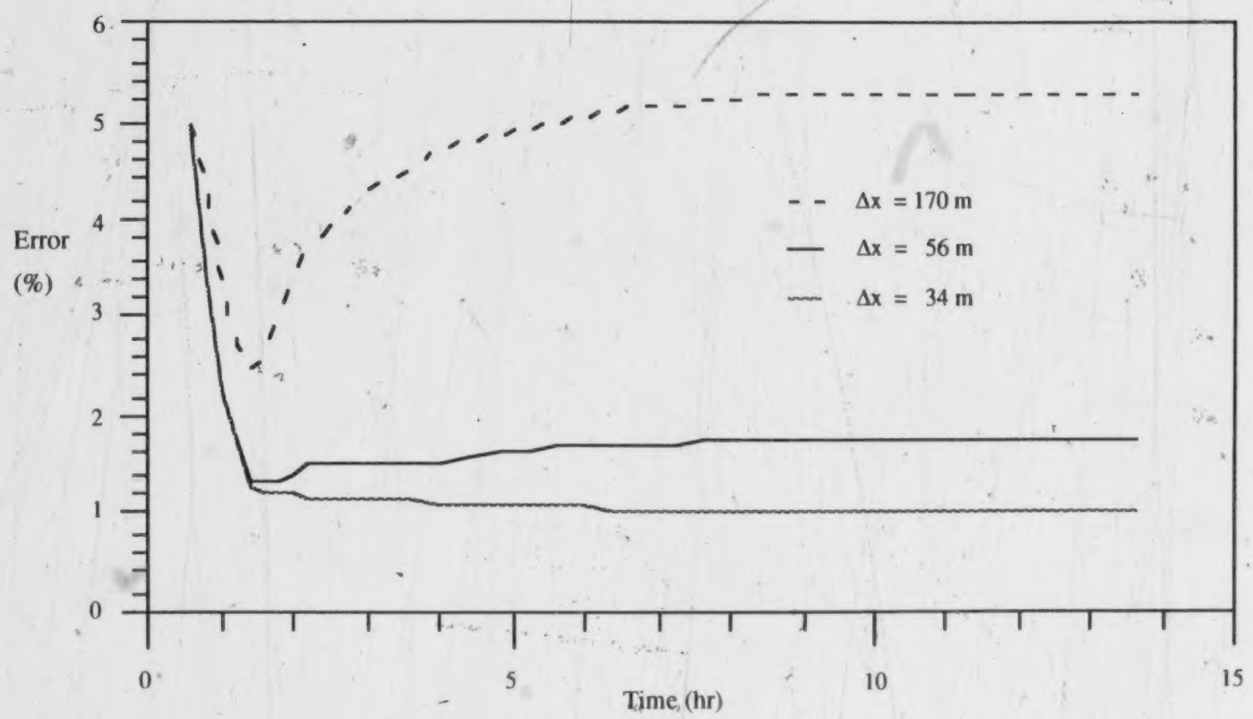

Fig.6-18. Effect of discretization on mass balance of overland flow computation (Fig. 6-17).

The time step Δt should satisfy the stability requirement as indicated by the C_r and r relationships. It has been mentioned that D_{ch} is defined as $C^*/(2S_0^{1/2})$. Hence for linearisation depth of 0.58 m, $D_{ch} = 0.58^{5/3} /n /(2S_0^{1/2}) = 77.6$. From the definition of r, Δt can be calculated as $\Delta t = r.(\Delta x)^2 /D_{ch} = (275)^2 /77.6 = 980$ s. Similarly from the definition of C_r, $\Delta t = 2(\Delta x)/U_{ch} = 2(275)/3.3 = 166$ s which is the limiting size of the time step. This could be increased using higher C_r. But it is evident from Figs. 6-1b through 6-6b that a higher C_r value leads to an out of phase solution in most of the cases.

Saturated flow: Being a very slow process the saturated flow is thought to impose no additional restriction on the size of the time step. Hence the above calculations are not performed for this case.

6.5 Mass Conservation

This has been mentioned several times previously, referring as mass balance. It is an important indicator of the convergence of a numerical scheme. It can be defined as to what extent the scheme conserves mass between the boundaries of the system. Therefore, while performing the aforementioned tests with analytically obtained discretization (i.e. the size of Δt and Δz or Δx), the mass balances were computed not only for predicted sizes of Δz or Δx and Δt but also for some other sizes.

Taking the unsaturated flow case, the mass balance is computed by integrating the continuity equation (eqn.[2-8])

over the flow domain of depth z and an arbitrary time interval t_1 and t_2, thus

$$\int_0^Z \theta d\theta + \int_{t_1}^{t_2} q dt = 0$$

This in finite difference form can be written as

$$\sum_{i=1}^{N} \left(\theta_i^{n+1} - \theta_i^{n}\right)\Delta z + \left(R^{n+1/2} - q^{n+1/2}\right)\Delta t = 0 \qquad [6\text{-}21]$$

where R is the infiltration or evaporation rate, and q is the outflow or inflow through the bottom of the domain. Similar expressions can be obtained for all the other flow processes, however, these are not shown here.

The error in the mass balance is indicated by the fact that the summation of all the storage changes does not equal the net boundary inflow or outflow. This error can be expressed as a percentage of net inflow into the system.

For the test examples of the overland flow problem, cumulative mass balances were performed as the computation progressed. The errors are presented in Figs. 6-17 and 6-18 showing the effect of discretization. It is evident that as the discretization exceeds the requirements of the convergence criteria, the errors are significant.

In application of the model (Chapter 7) to the Spring Creek watershed Δx and consequently the computation time steps, Δt, are decided according to the procedure described in the previous section.

Chapter 7

Application to the Spring Creek Watershed

7.1 Introduction

The model which was outlined and tested (in fragments through solutions of different hypothetical examples) in the previous chapters, is applied to the Spring Creek watershed of Alberta (Fig. 7-1). Since this was an experimental basin, a fair amount of necessary information was available and this availability of data was one of the important incentives for selecting Spring Creek basin to test the model performance. Instrumentation in the watershed included 6 precipitation gauges, 5 discharge measurement sites, one temperature and humidity recording and one casual soil moisture sampling site. However, the most required moisture characteristics of soils typical of the basin were not available. Hence they were obtained through measurements in the laboratory.

The first half of this chapter concerns measurements of soil parameters and simulation of moisture dynamics at a particular site in the basin. The remaining portion presents application and performances of the model on a catchment basis. But first, a brief description of the basin is given below.

7.2 The Spring Creek Basin

The Spring Creek is an east bank tributary of the Simonette river located 32 km southwest of Valleyview, Alberta (Fig. 7-1). It drains a watershed area of 111 km^2 on the southern margin of the Peace river region; an extensive plain which is mantled largely by glacio-lacustrine deposits

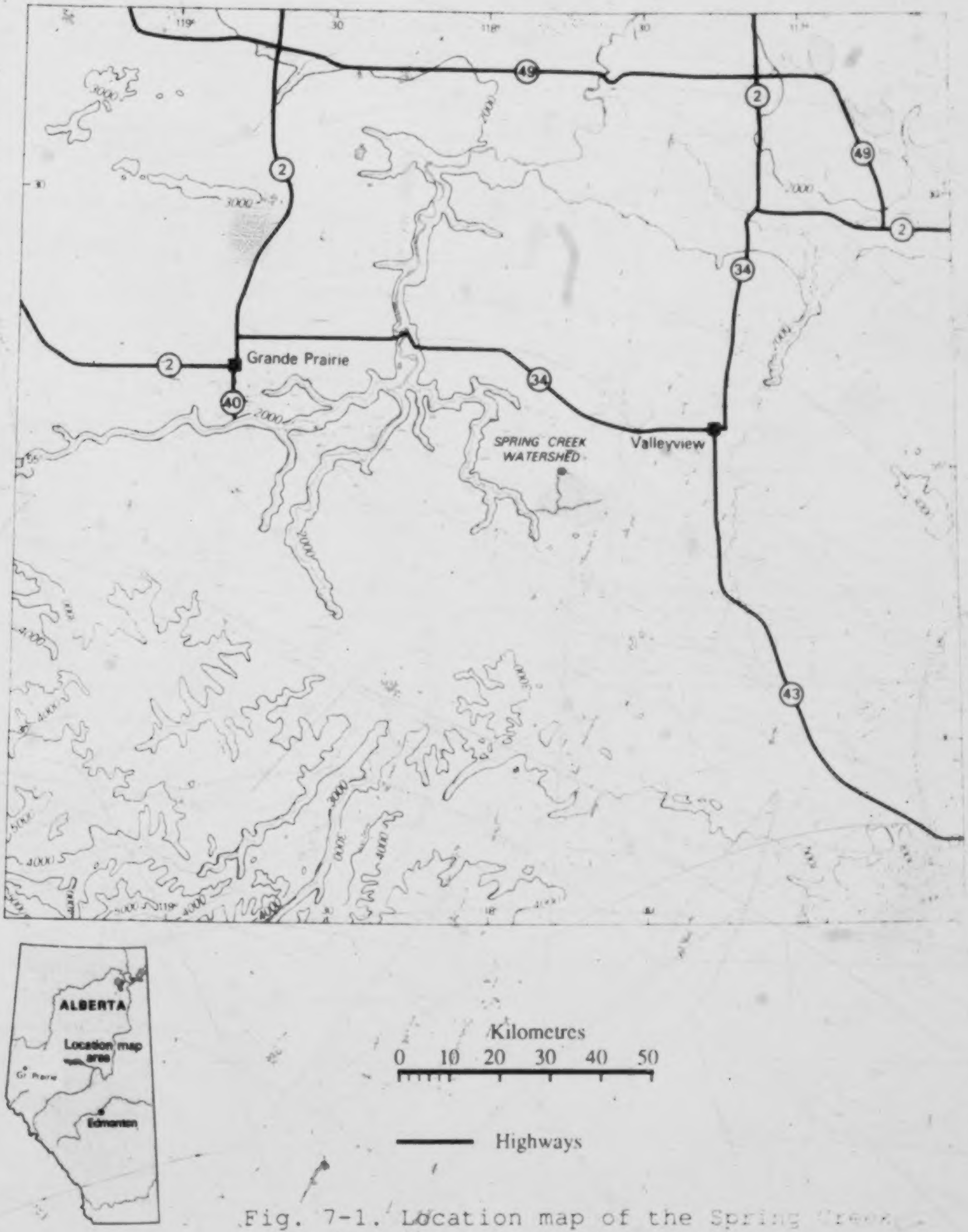
119°
30
118°
117°
49
2
2
49
2
34
2
Grande Prairie
40
34
Valleyview
SPRING CREEK WATERSHED
43
3000
2000
4000
5000
ALBERTA
Location map area
Gr Prairie
Edmonton
Kilometres
0 10 20 30 40 50
Highways

Fig. 7-1. Location map of the Spring Creek watershed (map obtained from Alberta Environment, Edmonton, Canada).

and supports a parkland Boreal mixed wood ecosystem (Martz, 1978). The Peace river region has a sub-humid microclimate and despite its northerly location, successful agricultural development similar to that of the southern prairies has taken place.

The land system is shown in Fig. 7-2 (Martz, 1978). The watershed is underlain by horizontally bedded sandstone, siltstone and shale of the Upper Wapiti formation (Holecek, 1967). Above this is till mantled by a variable thickness of stony glacio-lacustrine deposits. In the central and southern parts of the watershed, this mantle is very thin and patchy and thus these areas are classified as till. Much of the watershed, where the mantle is more nearly continuous, is designated lacustro-till. The dominant soil series in the catchment are Braeburn and Codesa. Soils range from clay loam to sandy loam. Low lying areas are the site of marshes and muskegs which occupy about 25% of the watershed (Martz, 1978). In the areas of moderately poor drainage and high water table, meadows have developed. They support a growth of native grasses and willows and the occasional poplar bluff. The rest of the catchment has a forest cover dominated by aspen poplar.

Six tributary watersheds have been defined within the Spring Creek basin (Fig. 7-2) and are referred by the names of the creeks which drain them.

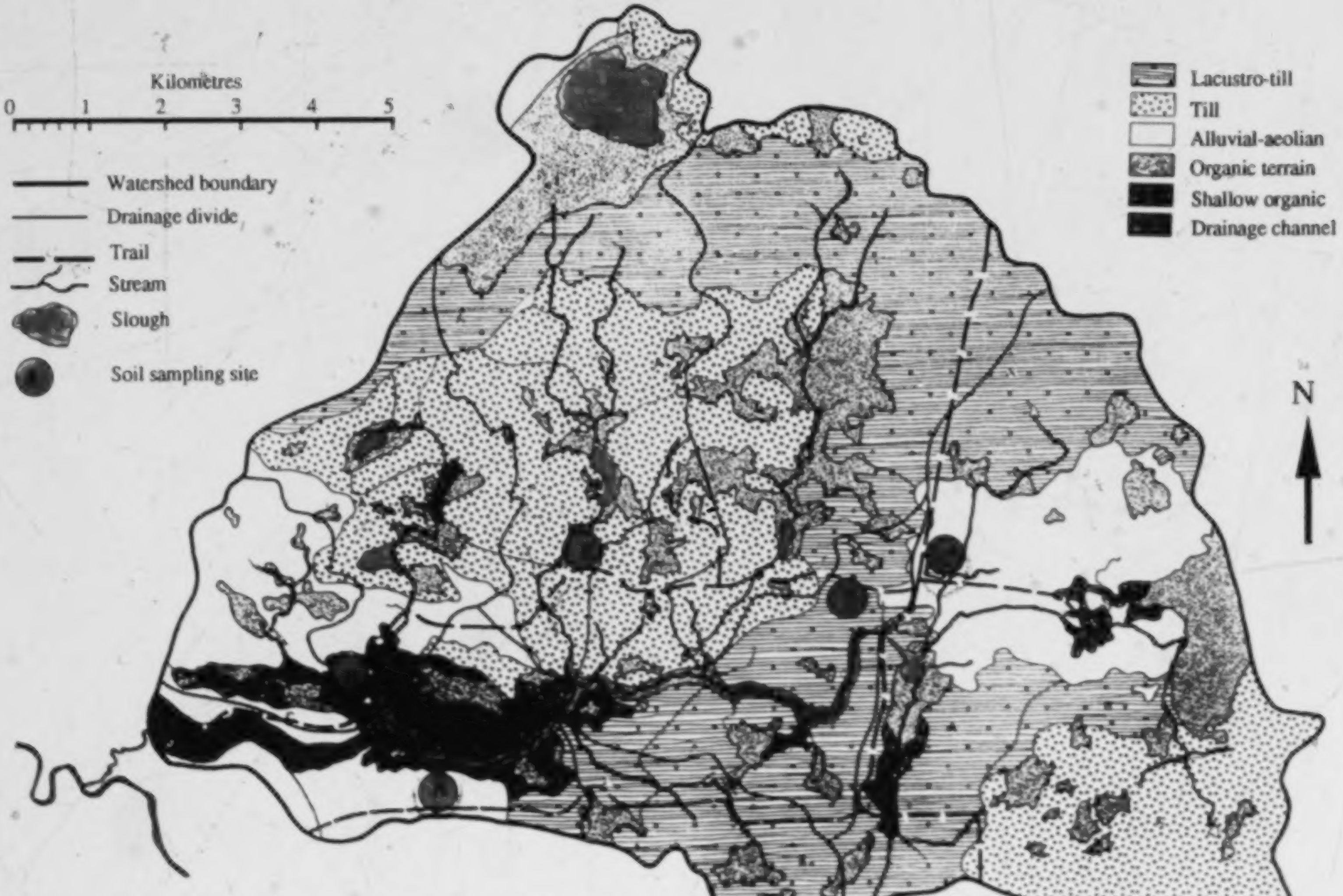
Kilomètres
0
1
2
3
4
5
Watershed boundary
Drainage divide
Trail
Stream
Slough
Soil sampling site
Lacustro-till
Till
Alluvial-aeolian
Organic terrain
Shallow organic
Drainage channel
N

Fig. 7-2. Spring Creek watershed: [illegible] system and other features (map [illegible] from Alberta Environment, Edmonton).

7.3 Measurements of the Model Parameters

The information available, includes the qualitative description of the nature and the distribution of soils within the watershed and a topographic map of the area. This data can be of help when the catchment is discretized (described in section 7.5) into small elements. However, necessary parameters must be obtained by direct measurements or be estimated. The required parameters and informations are summarized in Table 7-1.

7.3.1 Soil properties

The unsaturated and saturated flow model parameters are related to soil properties. Hence, they need to be determined or derived from measurements on soils. In order to do so, soil samples were collected from 5 locations within the watershed. Three samples (at depths 0-0.1 m, 0.4-0.5 m, 0.9-1.0 m) from each location were taken. The sampling sites are shown in Fig. 7-2. Considering the extent of the watershed these few samples may not be representative (Petersen and Calvin, 1964; Nielsen et al., 1973; Russo and Bresler, 1980), but within limited time and resources no more samples could be obtained.

One of the fundamental constitutive relations required in solving the unsaturated flow is the soil moisture characteristic. The moisture characteristic expresses the functional relation between volumetric moisture content θ and matric potential ψ. To establish this expression for each of the samples, moisture contents were measured at desaturation

Table 7-1. Model parameters.

Model Fragments	Comments
Unsaturated flow	
Saturated conductivity, K_s	Derived from experiment
Saturated moisture content, θ_s	Measured
$\theta(\psi)$ expression	Determined by experiment
$K(\psi)$ expression	Inferred from $\theta(\psi)$
Plant resistant, R_{plant}	From literature (Feddes et al., 1978)
Saturated flow	
Saturated conductivity, K_s	Derived from experiment
Drainable porosity, S_y	Inferred from material properties (Jones, 1976)
Depth to impermeable layer, d	Guess from previous report (Ryckborst and Holecek, 1977)
Overland flow	
Manning n	Inferred from report (Neil et al., 1972)
Exponent m in eqn.[4-3]	Assumed turbulent flow, m=2/3 (Emmett, 1978)
Width of the discretized surface, W	From topographic map
Slope, S_0	From topographic map
Channel flow	
Base width of channel, b	Guess
Side slope, s	From visualization
Length, C_l	Obtained from map survey
Bed slope, S_0	From topographic map

pressures of 0.015, 0.1, 0.2, 0.33, 0.5, 0.75, 1.0, 2.0, 3.0, 4.0, 5.0, 7.0, 10.0, 15.0 bars. This type of measurements is straightforward and is routinely done in the laboratory. The procedure uses a pressure chamber. Samples are subjected to pressure which forces water out of the soil until the matric potential is equal to the pressure potential. The samples are then removed and their moisture content is determined. The experimental results are presented in Fig. 7-3.

Fig. 7-4a shows moisture characteristics, ($\theta(\psi)$), of the soils at site-A at depths of 0-0.1 m, 0.4-0.5 m, and 0.9-1.0 m. Fig. 7-4b represents moisture characteristics of all the soils sampled at 4 locations at depths of 0.4-0.5 m. From Fig. 7-3 it is obvious that there are variations among $\theta(\psi)$ values. A comparison of Figs. 7-4a and 7-4b provides an impression that variation in $\theta(\psi)$ over depths at a specific site is greater than that over distances. By and large, this, however, makes sense. Unfortunately, heterogeneity in a soil profile is not incorporated in this complex model. But because of the distributed nature of the model spatial variability is easily handled.

Before proceeding further, perhaps it should be mentioned that the watershed soil systems is assumed homogeneous in vertical extent despite the measurement variations. Therefore, inferences to be made regarding model parameters are based on the mean of the measurements performed on three samples from each profile.

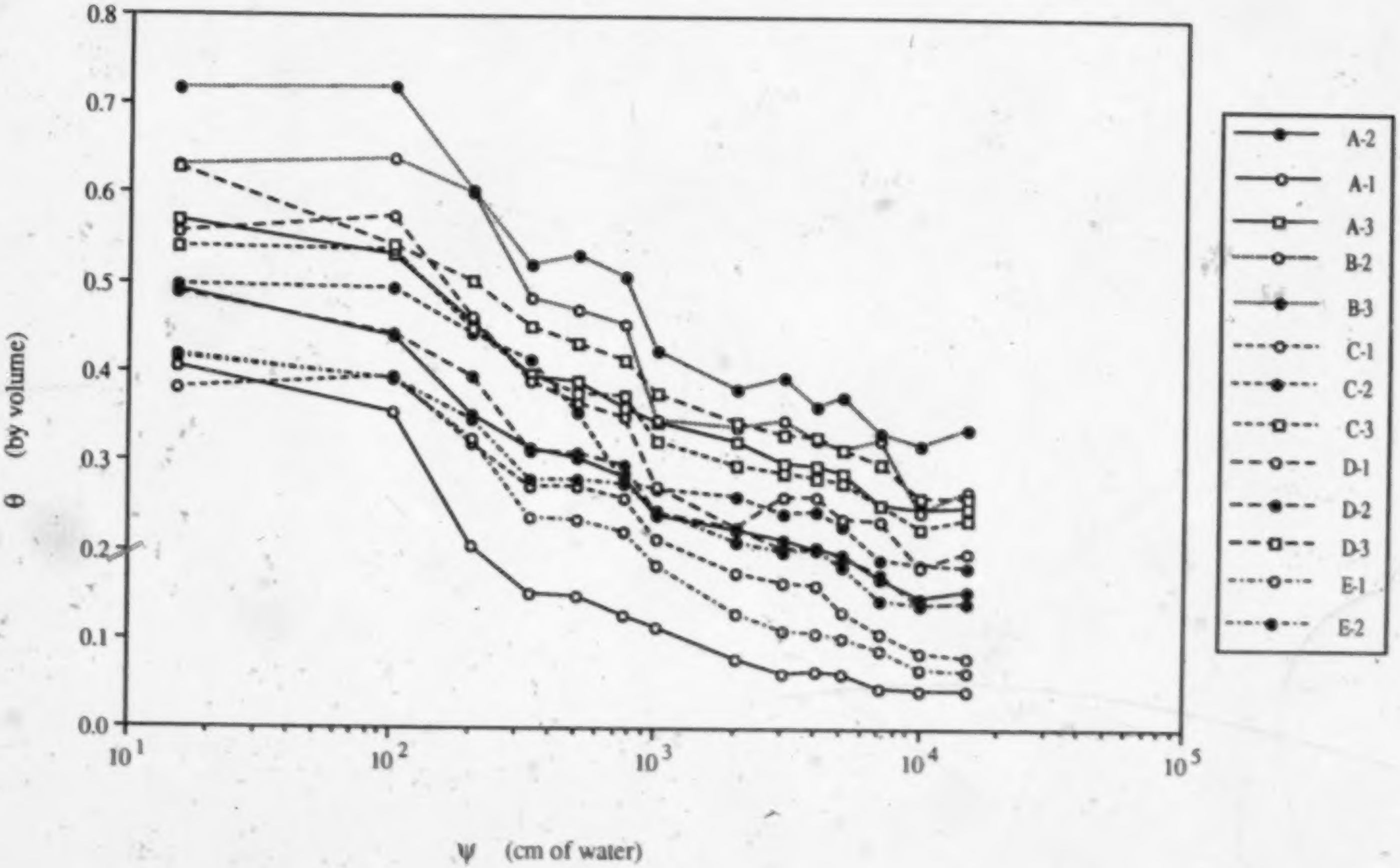

Fig. 7-3. Moisture characteristic curves of the sampled soils; A-1: site-A, depth 0-0.1 m; A-2: site-A, depth 0.4-0.5 m.

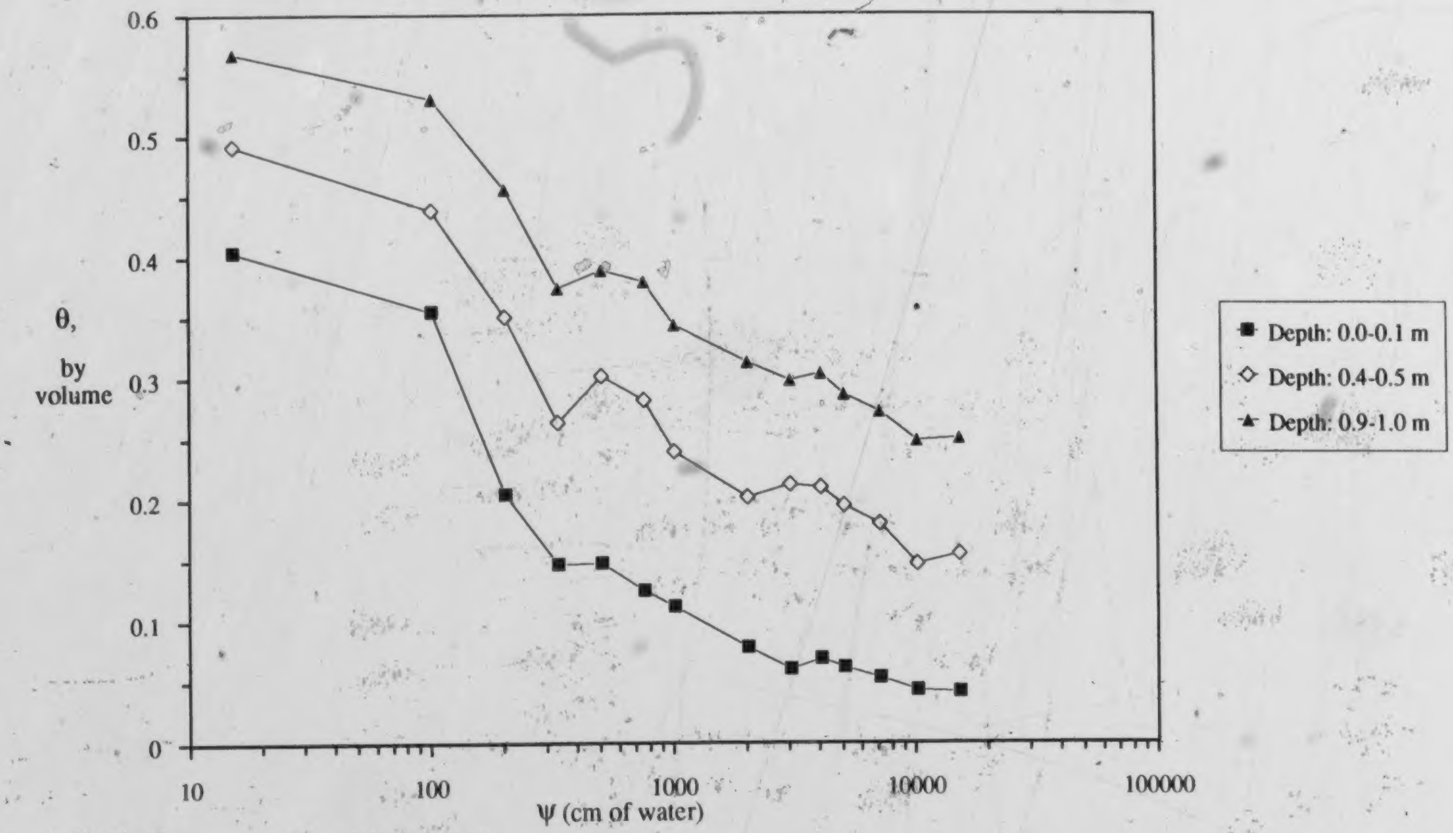

Fig. 7-4a. Variation of soil characteristics with depth at site-A.

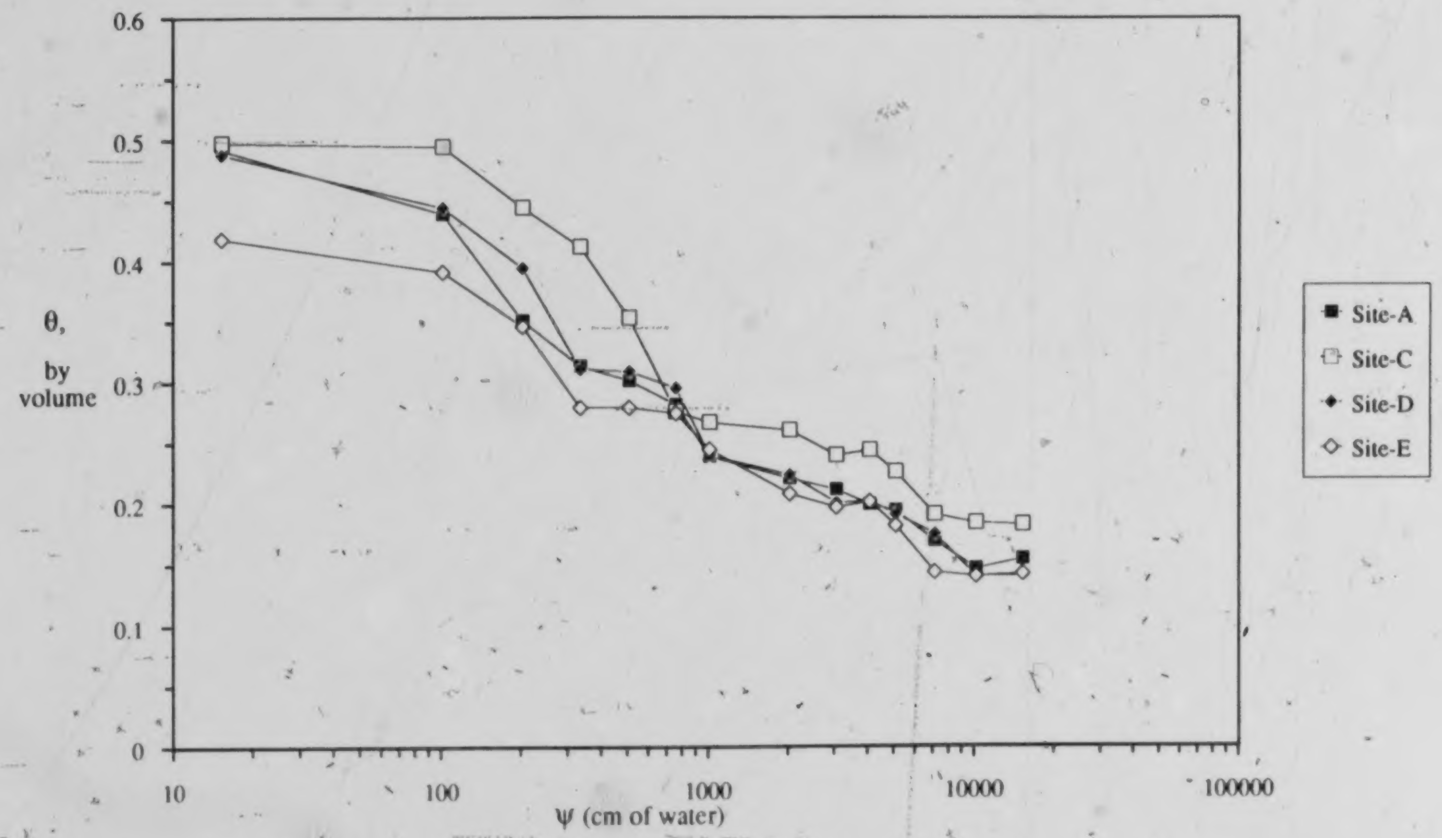

Fig. 7-4b. Spatial variation of soil characetristics at depth 0.4-0.5 m.

It is recognized that, in general, permeability (or intrinsic permeability) will increase with porosity and the size of the pores through which fluid has to pass. One way has been to infer the geometry of the pore space from the size and packing of the particles which form the framework of the pores. The easily recognizable features of texture and structure are commonly used as clues for assessing the permeability of soils (Marshall and Holmes, 1979). Besides permeability, other parameters such as specific yield, field capacity etc. are also sometimes inferred from soil texture (Davis et al, 1964; Salter and Williams, 1965; Jones, 1976).

Hence, to obtain textural information of the Spring Creek soils, another experiment called particle size analysis was done for each of the samples. Since the soils appeared clayey, the hydrometer method of particle size analysis was used. This method depends fundamentally upon Stokes' equation. The depth to which a hydrometer sinks when placed in the suspension is dependent on the suspension density. As the larger particles fall past the depth at which the hydrometer is suspended, the liquid density becomes lower and the hydrometer drops giving lower readings.

The experimental results are presented graphically in Fig. 7-5. It should be noted that the plotted particle size distribution is the mean over each sampled profile. Table 7-2, defining probable soil classes of the Spring Creek basin, was derived from Fig. 7-5.

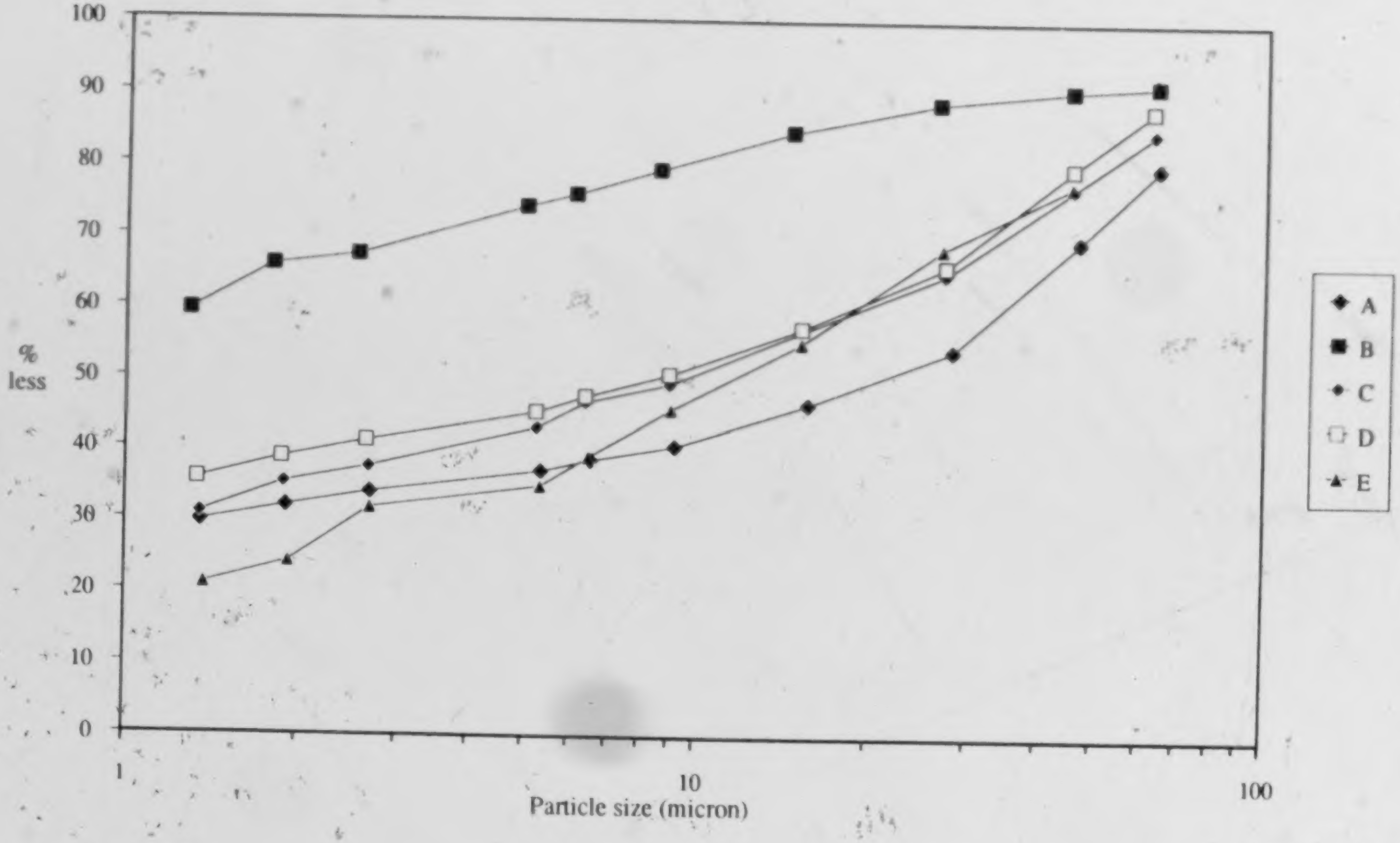

Fig. 7-5: Particle size distribution; A: sampling site-A.

Table 7-2. Classification of the soils of Spring Creek.

Site	% Clay (<.002 mm)	% Silt (.002-.05 mm)	%Sand (>.05 mm)	[1]Soil Type
A	32	40	28	Clay loam
B	64	30	6	Clay
C	35	43	22	Clay loam
D	39	43	18	Silty clay loam
E	24	54	22	Silt loam

Similar to the expression $\theta(\psi)$, another important relation $K(\psi)$ is also required to obtain the unsaturated flow solution. It has been alluded in section 2.2.4 that measurement of $K(\theta)$ or $K(\psi)$ are extremely difficult. This requires delicate instruments and needs prolonged experimentation to establish a meaningful $K(\psi)$ function (Klute, 1965, van Genuchten and Nielsen, 1985). Therefore, in this study, no attempt was made to do so. Instead it was estimated from the $\theta(\psi)$ expression as described in the section that follows.

Derivation of soil parameters

The values of ψ and θ, as obtained by measurements, could be used in the model in tabular form. Then the intermediate values of θ or ψ for given ψ or θ must be obtained by interpolation. This does not seem computationally efficient, in addition raw data are rife with measurement errors. Even if it is assumed that data are error free (which is absurd; Kempthorne and Allmaras, 1965), the apparent scatter in the data would introduce instability in the program. Therefore, it was intended to fit smooth curves to these data.

---

[1] Obtained from textural table given by Hillel (1982)

The first attempt was to fit a function of the kind as shown in eqn.[2-17]. This function is defined over the entire range of data points (i.e. from saturation to air dry condition). As this is not dimensionally consistent, parameters must be evaluated in cases where different units are used. However, this does not seem to pose any problem, since parameter estimation is not difficult and a good fit can be obtained with ease with the advanced computational facilities. Because no measurements for the determination of $K(\psi)$ were made, it must be obtained from $\theta(\psi)$ in some way. As Gardner's expression [eqn.2-17] describes $K(\theta)$ or $K(\psi)$ by a set of parameters independent of those of the $\theta(\psi)$ function, it was not possible to infer $K(\theta)$ from measured $\theta(\psi)$. However, it could be a possibility that eqn.[2-17] be used for $\theta(\psi)$ and the Millington-Quirk formula be used to calculate $K(\theta)$. But when the solution must be obtained by an iterative method this sort of calculation technique does not seem efficient. Moreover, the Millington-Quirk method does not always seem to give good approximations (Fig. 7-6). Furthermore, a decision regarding the matching factor must be made. Without any knowledge of the saturated conductivity, K_s, it is very difficult.

Therefore, it was decided to fit the Brooks-Corey expression to θ and ψ measurements. Since the parameters of

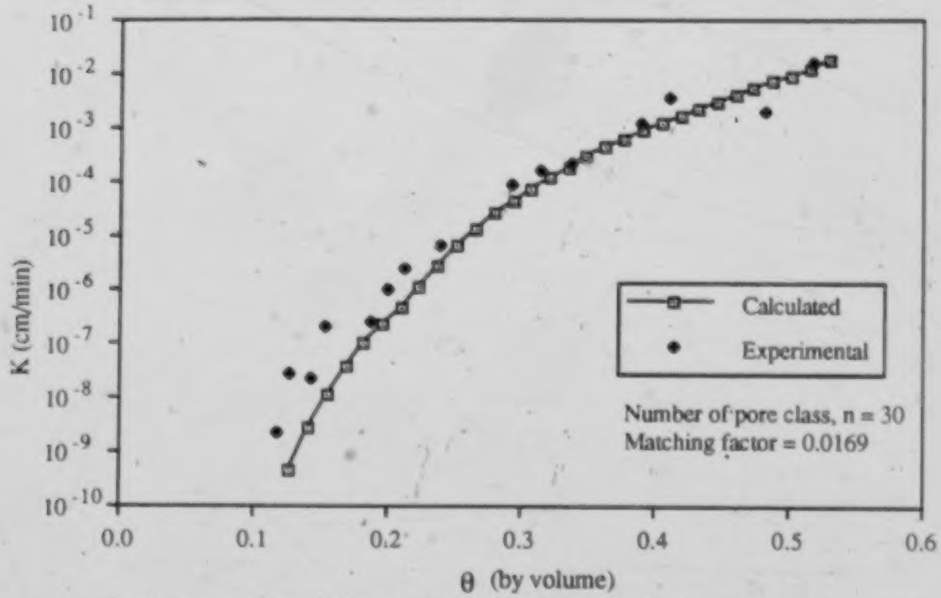

Fig. 7-6a. Hydraulic conductivities: comparison of measured (data obtained from Kunze et al., 1968) and calculated (using Millington-Quirk method) values .

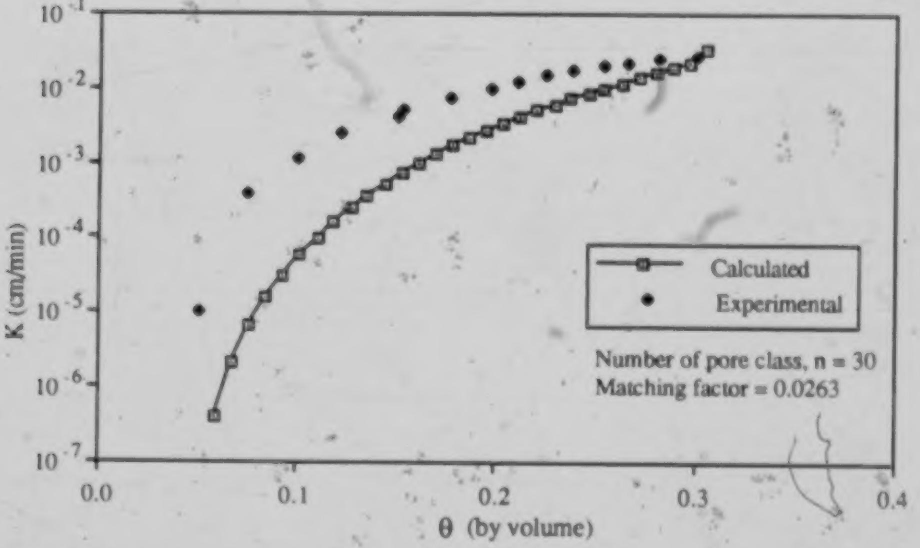

Fig. 7-6b. Hydraulic conductivities: comparison of measured (data obtained from Kunze et al., 1968) and calculated (using Millington-Quirk method) values.

their $K(\psi)$ expression can be derived from those of $\theta(\psi)$. There are several ways to evaluate the Brooks-Corey parameters from water retention data. In cases of a large quantity of data parameters are obtained by least squares (Brakensiek et al., 1981) or by an optimization technique (Milly, 1987). In the present study, however, the straightforward graphical method, as described by Brooks and Corey (1964), was used.

To obtain useful curves from θ and ψ measurements the data points for θ were used to derive λ in eqn.[2-15], by logarithmic plotting of θ_e vs ψ. In most cases a straight line fit could be obtained (see Fig. 7-7 for example). The region near the saturation where the curvature is negative was neglected. Relative saturation, θ_e, is then computed by the relation $\theta_e = (\theta-\theta_r)/(\theta_s-\theta_r)$, where θ_r is the residual moisture content and θ_s is the saturation moisture content. The residual moisture content, θ_r, as used in this context, is merely a value chosen to make the θ_e vs ψ curve linear on a logarithmic plot. This parameter was proposed by Brooks and Corey simply as a fitting parameter. Here θ_s and θ_r are obtained by smoothing θ-ψ measurements as shown in Fig. 7-8 for example. Saturation moisture content, θ_s, and residual moisture content, θ_r, are read off the smooth curve at very small and very high ψ as indicated in the figure. The slope and interception of the fitted straight line (Fig. 7-7) give λ and ψ_e respectively.

Having estimated λ from the $\log(\theta_e)$ vs $\log(\psi)$ curve, the exponent describing the conductivity curve is derived from

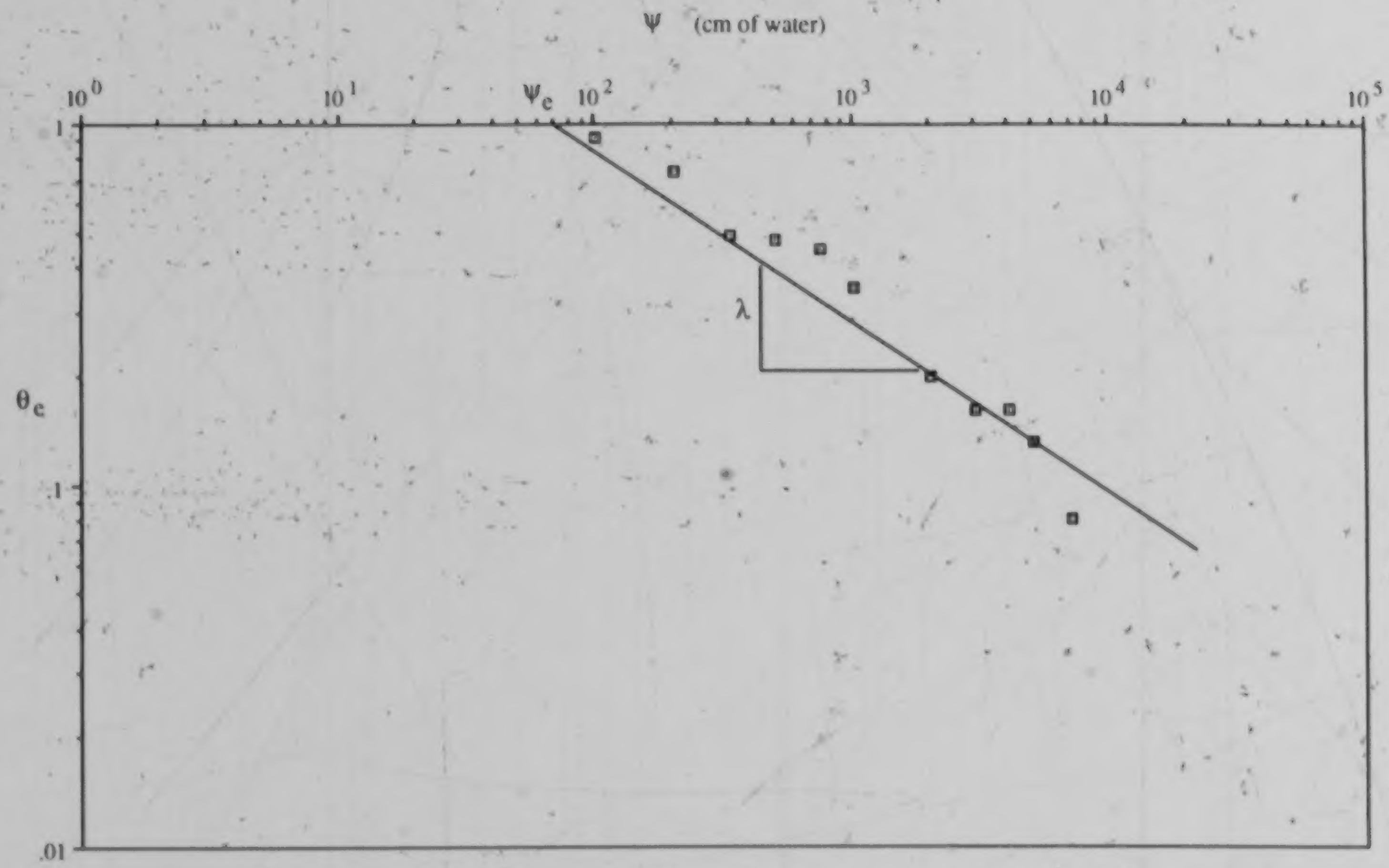

Fig. 7-7. Determination of Brooks-Corey parameters from experimental data (soil-E, Spring Creek).

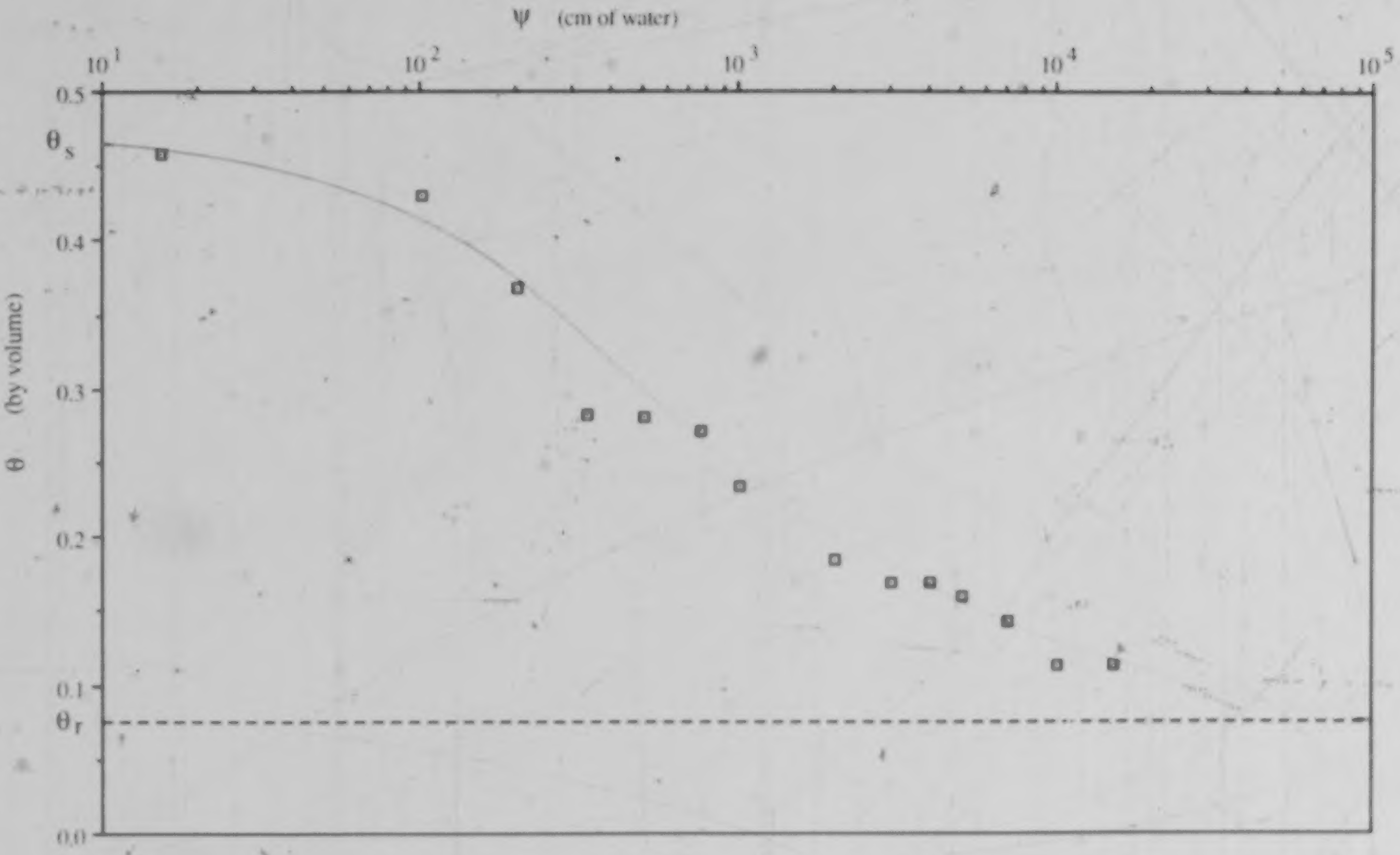

Fig. [illegible]-6. Determination of saturation and residual moisture content (very subjective); soil-E (Spring Creek).

eqn.[2-23] i.e. $\eta = 2+3\lambda$, where η = slope of the $K(\psi)$ curve in logarithmic plotting. Soil curves for the soils in Spring Creek derived in this manner are given in Fig. 7-9. From the figure it seems that a single line could be fitted through these points yielding one $\theta(\psi)$ and one $K(\psi)$ expression typical of the whole Spring Creek basin.

From eqn.[2-22] it is clear that another parameter which must be evaluated is the saturated conductivity, K_s. Considering the complexity and the uncertainties in measurements no attempt was made to obtain it experimentally. However, an estimate or most probable value of K_s could be obtained using the Cozeny-Karman equation (eqn.[2-18]). In all respect this estimate is also subjective. For instance, c, a parameter that accounts for irregularities in the geometry of pore space in eqn.[2-18] can assume any value in the range of 0.1 to 0.8 (Verruijt, 1970). Since there were not many alternatives left, K_s for the soils A, B, C, D, and E, (named after the sampling site as shown in Fig. 7-2) were obtained using eqn.[2-18]. The parameter c was taken as 0.1, d and p (porosity) were approximated by the D_{50} of the soil particles, and the saturation moisture content. Fortunately, for site-B an estimate of K_s was available (Ryckborst and Holecek, 1977). Hence it was possible to adjust K_s for other sites by the ratio (measured K_s at site-B)/(estimated K_s at site-B). The estimated values of K_s for Spring Creek soils, along with K_s values for some similar soils available in the literature, are given in Table 7-3.

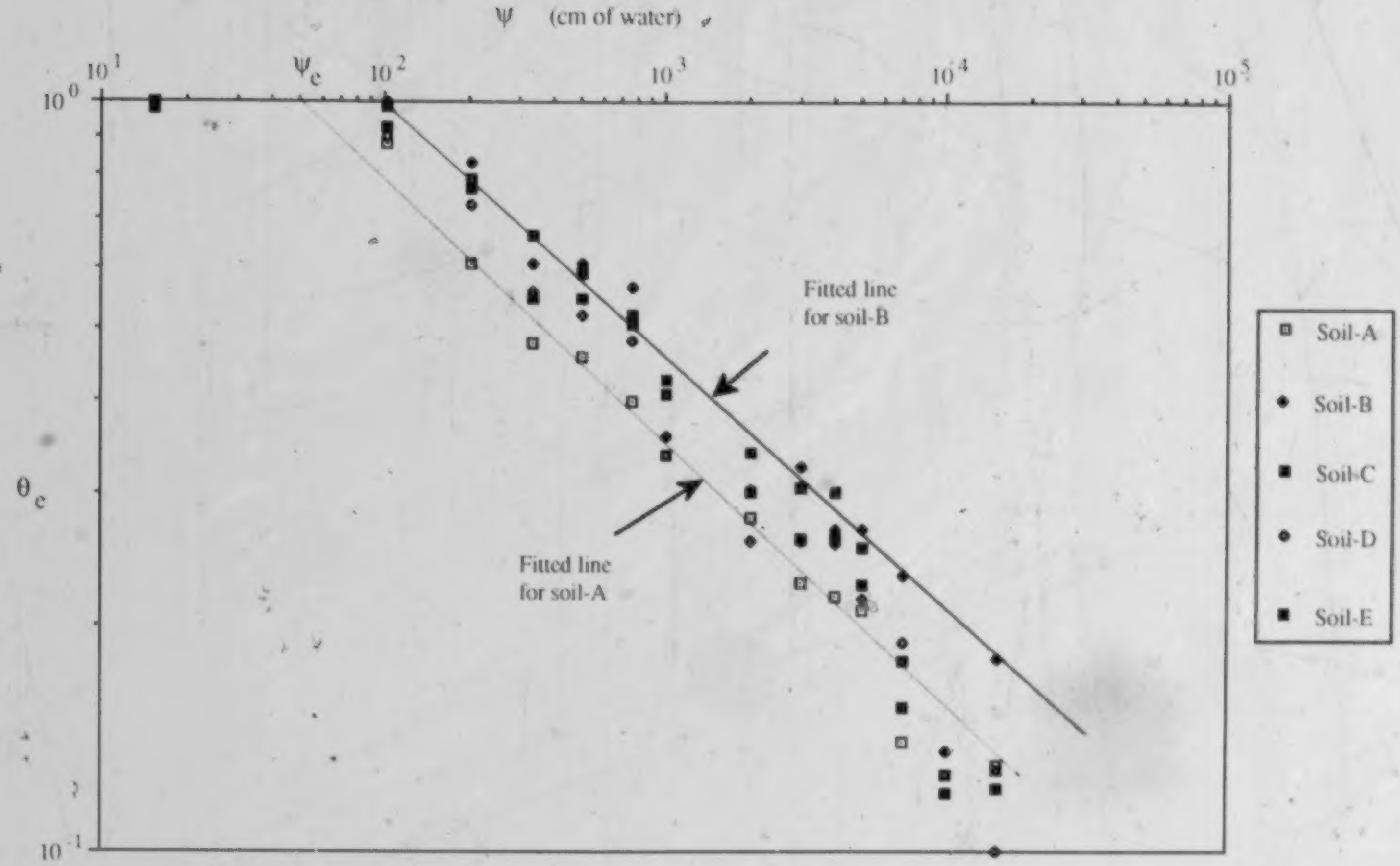

Fig. 7-9. The Brooks-Corey curves of the Spring Creek soils (see Table 7-4 for parameter values).

Table 7-3. Comparison of hydraulic properties of Spring Creek soils with those of soils available in literature.

Soil	K_s cm/min	θ_s m^3/m^3	Source of Data
Soils of Spring Creek			
A (Clay loam)	0.072	0.47	Experiment
B (Clay)	0.001	0.65	Experiment
C (Clay loam)	0.011	0.47	Experiment
D (Silty clay loam)	0.013	0.52	Experiment
E (Silt loam)	0.019	0.42	Experiment
Soils from literature			
Grenville silt loam	0.0210	0.475	Staple (1966)
Colby silt loam	0.0085	0.460	Smith and Woolhiser (1971)
Webster silty clay loam	0.0200	0.500	Kunze et al.(1968)
Pachappa loam	0.0799	0.455	Wesseling (1974)
Yolo light clay	0.0007	0.495	Moore (1939)

The values of θ_s and K_s as derived from the measurements, compare reasonably well with those of the similar group of soils available in the literature. The θ_s values are also in agreement with those of field measurements (Davis, Alberta Environment, 1977). For instance, measurements of soil moisture at site-B on June 6, 1976, may be considered. The day before there was a heavy rainfall and consequently soil moisture status, specially of the surface layer of 30 cm, may be thought to be at saturation. Field measurement using the Neutron prob method shows a moisture content of 0.72 which is not far off from the present estimate of 0.65.

The functional relations of the Spring Creek soils, used in the model, are

$$\theta = (\theta_s - \theta_r)\left(\frac{\psi_e}{\psi}\right)^{\lambda} + \theta_r \qquad [7\text{-}1]$$

and

$$K = K_s\left(\frac{\psi_e}{\psi}\right)^{\eta} \qquad [7\text{-}2]$$

The evaluated parameters are summarized in Table 7-4.

Table 7-4. Soil parameters of the Spring Creek watershed.

Soil	θ_s	K_s	θ_r	ψ_e(cm)	λ	η
A	0.47	0.072	0.16	50	0.36	3.08
B	0.65	0.001	0.22	100	0.35	3.06
C	0.47	0.011	0.15	90	0.36	3.07
D	0.52	0.013	0.25	80	0.37	3.12
E	0.42	0.019	0.14	80	0.35	3.05

As the air entry value, ψ_e, represents, in fact, the height of the so called capillary fringe one would generally expect it to be 10, 20 or so, centimetres. But from Table 7-4, it is apparent that ψ_e's assume values around a 100 cm. However, this is not by any means uncommon in literature (Corey, 1986, Nielsen et al., 1973). According to Corey (1986) "ψ_e may vary over an enormous range, from practically zero to many atmospheres". Although λ is an empirical parameter, sometimes it is thought to be related to pore size distribution which in turn is considered to be influenced by particle size distribution. For uniform graded soil λ should be high and for uniformly graded soil should be minimum. The values of λ obtained in this study is within the range 0.25-0.5 as given by Bresler (1987).

7.3.2 Channel and overland flow parameters

For the channel network a roughness coefficient, Manning's n, is coded from the information given by Niel et al. (1972) in their report "Hydraulic and Geomorphic Characteristics of Rivers in Alberta". Since in that report the estimate of n for the Spring Creek river system is not available, it is taken to be the same as given for the Simonette river, a river in which Spring Creek empties. The channel geometry is assumed trapezoidal with side slope of 1:1. The bed width for the main channel is 5 m and for the tributaries the widths are 3 m on average. The channel length and channel slopes are estimated from the topographic map. The Spring Creek channel network system and its assumed or derived characteristics are summarized in Table 7-5. The network is shown in Fig. 7-2.

Table 7-5. Approximate channel characteristics of the Spring Creek watershed.

Sub-basin	Channel length (m)	Channel slope	[1]Side slope	[2]Bed width (m)
Horse Creek	2700	0.015	1:1	3
Wolverine Creek	5000	0.041	1:1	3
Rockey Creek	9000	0.016	1:1	3
Bridlebit Creek	7600	0.022	1:1	3
Spring Creek-U	14300	0.017	1:1	3
Spring Creek	17000	0.007	1:1	5

During a visit to the watershed, it was observed that the (stream) bank slope and land surface have the same

---

[1] Assumed

2 Assumed

vegetative cover (cf. Plate 7-1). Therefore, Manning's roughness factor n for overland flow was assumed to be the same as that of the channel. The overland flow width, B, depends on the watershed segmentation which in turn is determined by topography. B is measured from element geometry and used as input to the model. Assuming turbulent flow, the exponent, m, of eqn.[4-3] is taken as 0.6667 (Emmett, 1978).

7.3.3 Other parameters

This group includes depth to the impermeable layer, D, specific yield or drainable porosity, S_y, and measures of plant resistance to water flow through the plant biomass. Information concerning S_y is not directly available but can be approximated from the aquifer materials. ~~In the~~ literature (Davis et al., 1964; Jones, 1976) range of values of S_y are often given corresponding to the type of formation materials. So depending on the results of the particle size analysis values of S_y were obtained from Jones (1976). These are provided in Table 7-6.

Table 7-6. Approximate values of available water capacity and drainable porosity.

Soil	[3]AWC	S_y
A (Clay loam)	0.183	0.08
B (Clay)	0.192	0.06
C (Clay loam)	0.183	0.08
D (Silty clay loam	0.183	0.08
E (Silt loam)	0.192	0.11

From the outline, given in section 2.3.2, of the evaporation model it can be realized that estimates of the

---

[3] Available Water Capacity

Plate 7-1. Typical vegetation of the channel system of Spring Creek watershed.

rooting depth and plant resistance to water flow are required. By no means was this possible, in this study, to obtain this information by experiment. Hence, again, recourse is found in the literature. In the past a substantial amount of work towards determining and analyzing theses parameters with different plant species has been done by different workers in plant sciences (Neuman, 1969; Cowan, 1977; Feddes et al., 1978; Stewart, 1988). As a result it is possible to decipher a reasonable value of R_{plant} knowing the type of plants (which is predominantly poplar) in the watershed.

7.4 Application of the Unsaturated Flow Model

Having approximated the required parameters, the unsaturated flow model (infiltration and evaporation) was used to simulate the soil surface processes. These include infiltration, evaporation, runoff and soil moisture status at a particular location (site-B) within the Spring Creek watershed, where some casual field observation of soil moisture were available over a profile of depth 3 m at intervals of 0.30 m. From the measurements it appeared that the moisture content, θ, at depth 3 m remained fairly unchanged over a period of 4 months from Aug 11, 1975 to Oct 14, 1975. Accordingly, during the simulation period the lower boundary was kept at constant measured moisture content of 0.29. The upper boundary was varied depending upon the meteorological events (such as precipitation and dry spells). The surface processes are summarized as follows:

Simulation starts with initial moisture content of 0.4, 0.32, 0.43, and 0.29 at depths of 0.30 m, 0.60 m, 1.20 m, and 3.00 m respectively. It should be noted that as the initial moisture contents are available at only 4 different depths, the intermediate node conditions are obtained through linear interpolation.

During the simulation whenever rainfall is in progress, evaporation is assumed nil. This seemed reasonable as the air mass remains saturated and hence it is very likely that vapour transfer will be negligibly small. At the onset of rainfall and if the initial moisture content of the surface layer is found below saturation, the Neuman boundary condition prevails and eqn.[2-13] is used to solve for moisture content at node-1. As soon as the moisture content of the upper layer or node reached saturation, the boundary condition was changed to the Dirichlet type i.e. node-1 was kept at saturation moisture content of 0.65 (as estimated from measurements, Table 7-4, section 7.2.1). As long as the rainfall continued, this condition remained unaltered. Rainfall in excess to the infiltration was considered as runoff.

When rain ceased, infiltration also stopped in this case. However, in case of basin simulation, as will be seen in the second half of the chapter, the infiltration process is coupled with overland flow, therefore, it is perceived that infiltration will continue as long as water remains on the surface during its journey to the channel. Detail of this treatment is given in the respective section. In this case, it is assumed that the excess precipitation runs off leaving a saturated surface layer. Evaporation takes place at the potential rate. As mentioned previously, this potential evaporation rate is calculated as a function of time using the Penman-Monteith equation. This is considered as upward flux through the surface layer and is treated in the same way as in the case of rainfall but with a negative sign (i.e. PE = -R in eqn.[2-13]). As a consequence moisture storage from the profile depletes. Continuation of this condition makes surface moisture content fall below saturation i.e. the potential at node-1 falls below air entry value, ψ_e (Table 7-4). Then the humidity condition is invoked (derived in section 2.3.6).

The upper boundary conditions such as rainfall, estimates of potential evaporation and leaf water potentials, as calculated using eqn.[2-88], are given in Table 7-7. It is evident that the calculated ψ_{leaf} values are very large numbers. This induced some problems of non-convergence when the humidity condition was invoked at the upper boundary. In order to overcome this problem, the ψ_{leaf} values were imposed gradually over few time steps instead of increasing suddenly.

The simulation results for a period of 4 months are presented graphically in Figs. 7-10a and 7-10b. Fig. 7-10a shows the profile soil moisture content as compared with field measurements. Fig. 7-10b shows cumulative runoff,

Table 7-7. Meteorological elements used to define the upper boundary conditions (for simulation period of Aug 11, 1975 to Oct 14, 1975).

Time (date)	Time (hour)	Temp. (°C)	RH_{max} (%)	RH_{min} (%)	Pot. (ψ) (cm)	Precip (m/hr)	[1]PE (m/hr)
Aug 11	0	11.7	100	50	-3780	0	0.000158
	24	11.1	100	46	-4126	0	0.000158
	48	11.7	100	49	-3868	0	0.000158
	72	12.8	100	38	-4894	0	0.000158
	96	10.6	100	54	-3421	0	0.000158
	120	11.1	100	50	-3772	0	0.000158
	144	8.3	100	86	-942	0	0.000158
	168	10.0	100	86	-948	0.0013	0.000158
	192	11.7	100	75	-1755	0.0010	0.000158
	216	12.2	100	59	-3020	0.0025	0.000158
	240	10.6	100	100	0	0	0.000158
	264	6.7	100	60	-2881	0.0206	0.000113
	288	10.0	100	66	-2434	0.0124	0.000113
	312	8.9	100	53	-3485	0.0015	0.000113
	336	7.8	100	50	-3728	0	0.000113
	360	8.9	100	59	-2985	0	0.000113
	384	12.8	100	65	-2537	0	0.000113
	408	12.2	100	81	-1314	0	0.000113
	432	9.4	100	100	0	0	0.000113
	456	6.7	100	53	-3458	0.0305	0.000113
	480	7.8	100	54	-3387	0	0.000121
	504	8.9	100	50	-3743	0	0.000121
	524	7.8	100	64	-2572	0.0041	0.000121
	552	6.7	100	56	-3207	0.0048	0.000121
	576	6.1	100	50	-3706	0	0.000121
	600	7.8	100	66	-2415	0	0.000121
	624	8.9	100	50	-3743	0	0.000121
	648	8.9	100	52	-3571	0	0.000121
	672	5.6	100	43	-4314	0	0.000121
	696	6.1	100	42	-4412	0	0.000121
	720	5.0	100	54	-3353	0	0.000121
	744	5.0	100	39	-4668	0	0.000121
	768	10.0	100	37	-4941	0	0.000129
	792	11.1	100	35	-5154	0	0.000129
	816	11.1	100	48	-3948	0	0.000129
	840	9.4	100	41	-4556	0	0.000129
	864	7.8	100	45	-4168	0.0010	0.000129
	888	5.6	100	70	-2090	0.0008	0.000129
	912	5.6	100	45	-4135	0	0.000129
	936	7.2	100	44	-4248	0	0.000129
	960	9.4	100	35	-5123	0	0.000129

---

[1] Potential evaporation

Table 7-7. Continued.

Time (date)	Time (hour)	Temp. (°C)	RH_{max} (%)	RH_{min} (%)	Pot. (ψ) (cm)	Precip, (m/hr)	PE (m/hr)
Sep 20	984	10.0	100	35	-5134	0	0.000129
	1008	10.6	100	33	-5340	0	0.000129
	1032	14.4	100	31	-5612	0	0.000100
	1056	12.8	100	33	-5381	0	0.000100
	1080	10.6	100	44	-4300	0	0.000100
	1104	10.0	100	38	-4846	0	0.000100
	1128	10.0	100	55	-3329	0	0.000100
	1152	7.8	100	63	-2651	0.0043	0.000100
	1176	6.1	100	53	-3451	0	0.000100
	1200	9.4	100	41	-4556	0	0.000100
	1224	13.3	100	28	-5897	0	0.000100
	1248	14.4	100	31	-5612	0	0.000100
	1272	14.4	83	48	-5612	0	0.000100
	1296	6.1	100	39	-4687	0	0.000042
	1320	3.3	100	60	-2845	0.0043	0.000042
	1344	0.0	100	98	-127	0.0119	0.000042
	1368	0.0	100	88	-780	0.0023	0.000042
	1392	1.1	100	82	-1193	0	0.000042
	1416	2.8	100	75	-1700	0	0.000042
	1440	4.4	100	89	-724	0	0.000042
	1464	7.2	100	45	-4159	0	0.000042
	1488	8.9	100	43	-4365	0	0.000042
	1512	10.6	100	35	-5144	0	0.000042
	1536	7.2	100	53	-3464	0	0.000042
	1560	6.1	100	56	-3200	0.0089	0.000042
	1584	4.4	100	44	-4206	0.0013	0.000042
	1608	6.1	100	61	-2794	0	0.000042
	1632	4.4	100	40	-4566	0.0130	0.000042
	1656	4.4	93	47	-4566	0	0.000042
	1680	3.9	79	42	-6422	0	0.000042
	1704	0.6	95	54	-3717	0	0.000042
	1728	0.6	92	42	-5057	0	0.000042
	1752	-1.7	100	69	-2109	0.0005	0.000042
	1776	-1.1	100	59	-2879	0.0023	0.000042
	1800	-0.6	100	50	-3617	0.0005	0.000042
	1824	-3.3	100	75	-1662	0	0.000042
	1848	-6.1	100	72	-1858	0	0.000013
	1872	-3.3	100	69	-2096	0	0.000013
	1896	-4.4	100	84	-1034	0	0.000013
	1920	-2.8	100	77	-1523	0	0.000013
	1944	3.9	100	53	-3423	0	0.000013

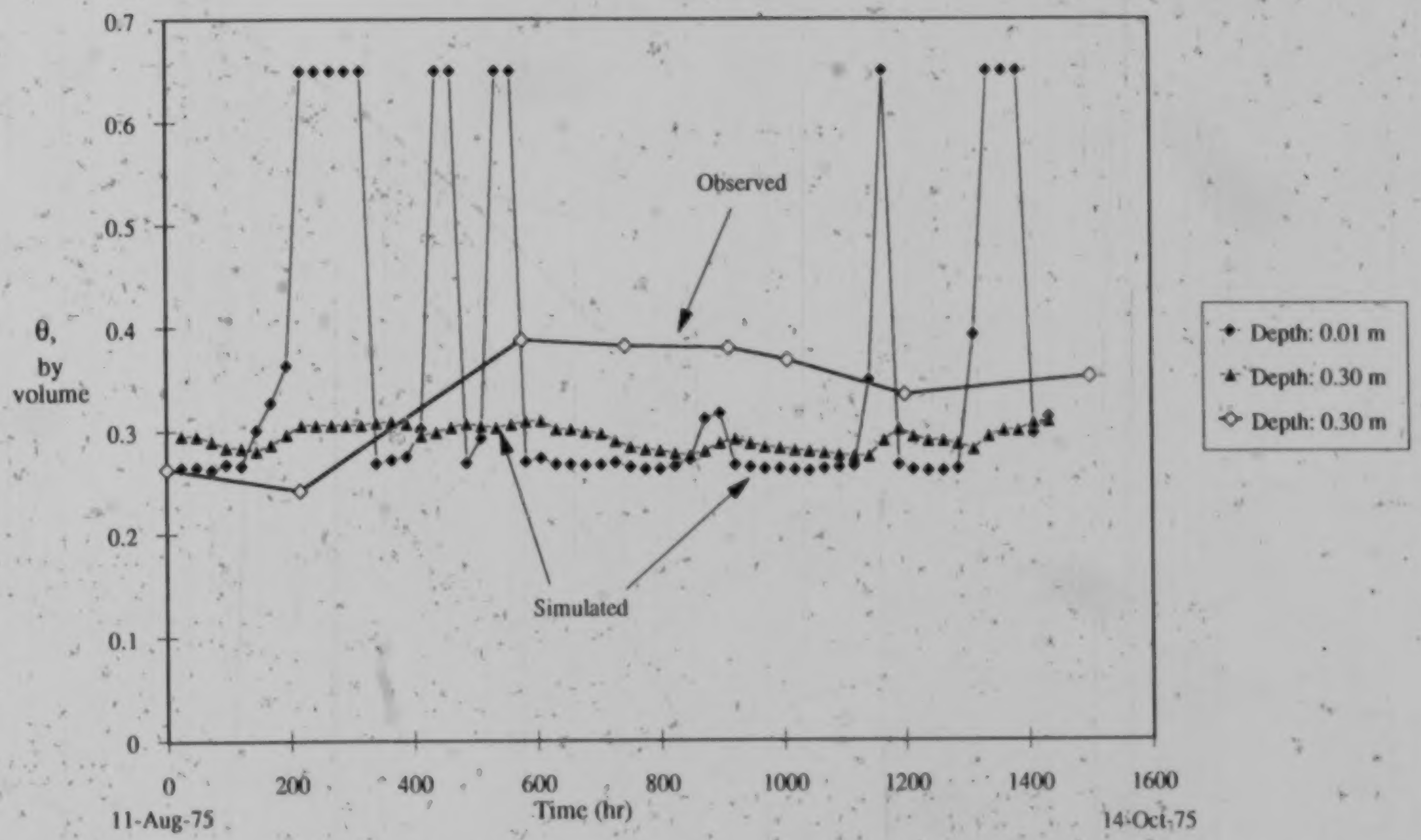

Fig. 7-10a. Simulated and observed (somewhere in the watershed; Alberta Environment, 1975) soil moisture content.

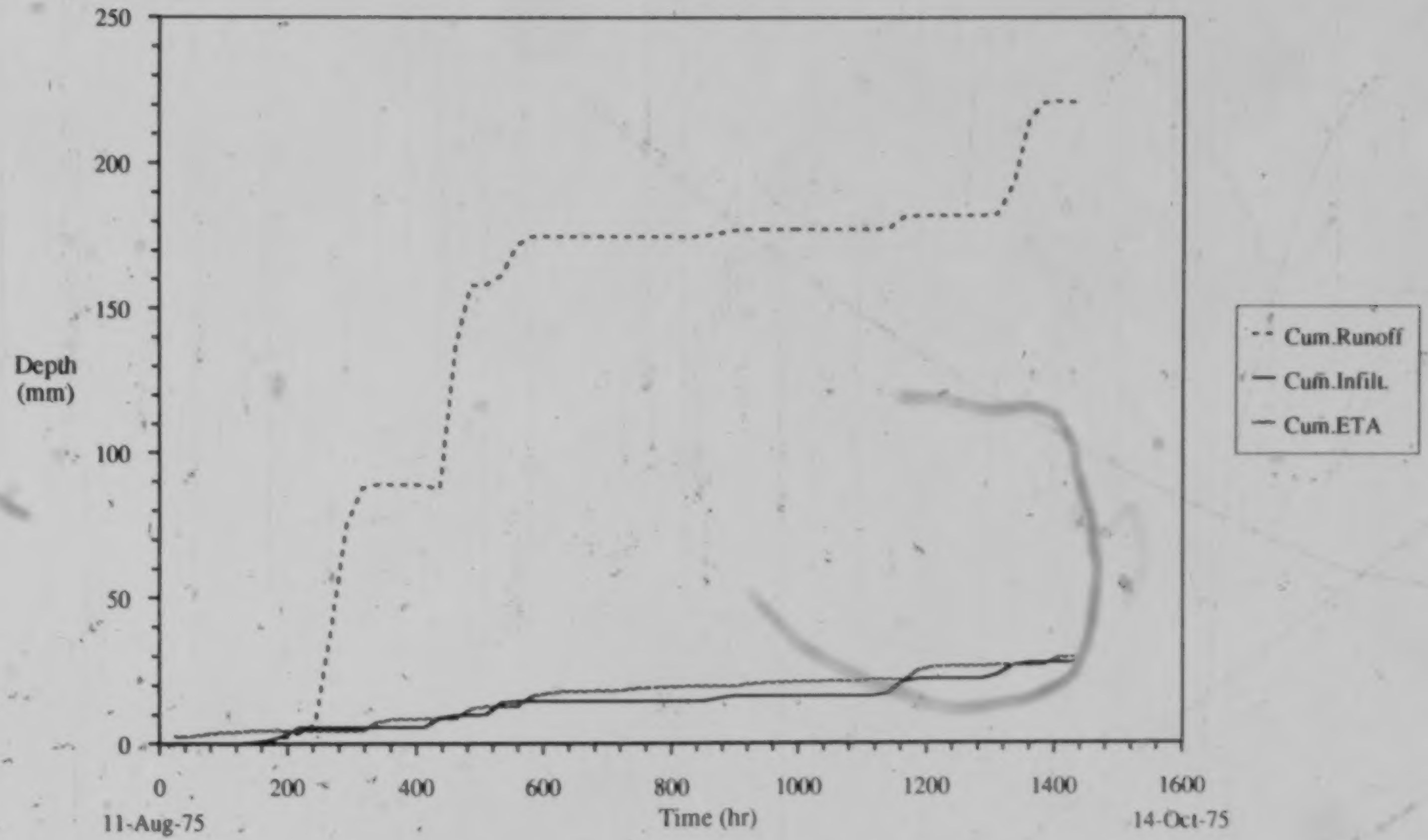

Fig. 7-10b. Simulated runoff, evapotranspiration, and infiltration (at site-B).

evaporation, and infiltration over the simulation time. The agreement between the calculated and measured soil moisture condition of the soil profile is poor. As no measurement of runoff, actual evaporation or infiltration is available, it is not possible to evaluate the accuracy of the calculations of these elements.

7.5 Simulation of Discharge Hydrograph

The discharge hydrograph of a basin is the result of the interaction among input, unsaturated flow, saturated flow, overland flow, channel flow, retention and detention processes. This section deals with the integration of these processes to simulate basin response. Since the input is a part of this system a brief introduction, with special consideration of spatial variability, is given below.

7.5.1 Spatial variability of the inputs

It has been mentioned previously that there are 6 well distributed precipitation gauges in the Spring Creek watershed. Although precipitation is well reputed for its spatial variability (Collinge and Jamieson, 1968; Phien et al., 1980; Osborn, 1983), considering the relatively small size of the basin (111 km^2) the number of existing gauges was taken to be sufficient to provide the mean areal estimate of the precipitation with reasonable accuracy.

Various methods are available for estimating mean areal precipitation. Unweighted mean (UM), grouped area weighted mean (GAAWM), Thiessen polygon (TP) method, isohyetal (IOS) method, trend surface analysis (TSA), modified polygon (MP), and two-axis (TA) method are a few to mention. Comparison of the estimation methods and accuracy of mean areal precipitation estimates can be found in Singh (1989). In this study, the Thiessen polygon method was used for evaluating the areal mean.

As for evaporation, there is only one station within Spring Creek basin that records meteorological variables such as temperature, humidity etc. essential for obtaining estimates of potential evaporation. Variations in some of the dominant factors operating over different surfaces can result in noticeable changes in evaporation rates over small adjacent areas in short time periods (Shaw, 1986). Diurnal fluctuations are considerable since there is no solar radiation during the night. However, evaporation totals over neighbouring areas show relatively smaller differences over periods of a week or a month. For the sake of curiosity, climatological data were gathered from Edson, Slave Lake, and Grand Prairie to obtain monthly potential evaporation estimates using the Penman-Monteith equation. The correlation coefficients among the estimates at different location were calculated and plotted against the corresponding distances of the observation sites (Fig. 7-11). From the plot it appears that the correlation coefficients persist to be close to unity over a substantial distance. This indicates low spatial variability of potential evaporation. Perhaps this stability contributed to restrict the number of meteorological measurement stations to a minimum.

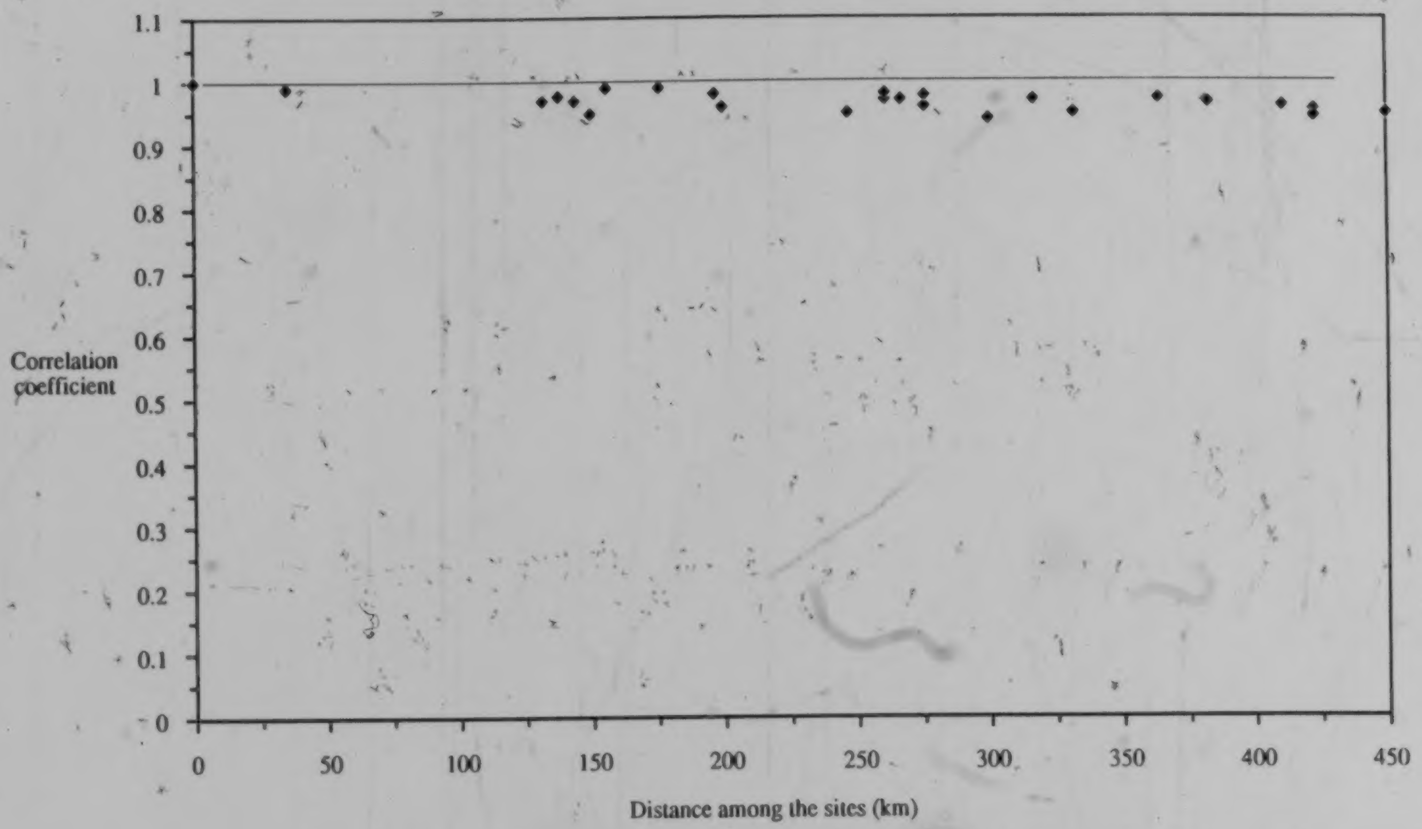

Fig. 7-11. Distance vs correlation coefficients of the potential evaporation estimates at Grand Prairie, Spring Creek, Edson, and Slave Lake.

Thus in this study it was assumed that data available at one station would be sufficient to obtain potential evaporation estimates representative for the whole basin.

7.5.2 Discretization of the watershed

Previously it has been mentioned that the present model is of the distributed type so that spatial variability of input and watershed characteristics can be taken into account. A watershed is a widely variable system, however, because of its extent it is not possible to measure every bit of necessary information at every point in this domain. Some assumptions of uniformity must be made. In this study it is considered that the soil properties and flow parameters are constant over a relatively small area coded here as an element. Accordingly the entire watershed is divided or discretized into such elements of uniform characteristics.

This discretization is performed on a topographic map. The elements are bounded at the top by the drainage divide and at the base by a reach of perennial or intermittent stream. Lateral element boundaries are straight lines drawn normal to the contour lines in an attempt to approximate natural flow separation on the slopes. The shape and number of the elements are determined by the shape and extent of the channel system, the topography, and the soil variability.

In an ideal segmentation, every reach of perennial or intermittent or ephemeral stream is described as the lower boundary of the elements. This calls for a large number of elements and accordingly high simulation costs. The accuracy gained by such fine-grained description of the basin is offset by usually low sampling density of the soils and other physical characteristics and inputs (e.g. precipitation measurements). Accordingly while discretizing the watershed it has been considered that the number of elements be kept to a minimum. Fig. 7-12 shows the compromise reached for this particular simulation.

Furthermore, each element again can be divided into a series of vertical columns (Fig. 7-13), not necessarily of uniform width or properties. Each column can be assumed to consist of homogeneous soil.

7.5.3 Assembling the model

In the model water movement is conceptualized as a series of interacting one-dimensional processes. The lateral extent of the cross section is bounded at the upslope end by the watershed divide and at the downslope end by a channel or stream. The vertical bounds of the system are the soil surface on top and an impervious layer below the soil. So far this continuous system is modeled and discussed in parts and nothing has been said about the way of combining different segments of the model into a complete simulator. This is described here beginning with an outline of the conceived flow processes.

The upper surface receives or loses water according to the prevailing rainfall or evaporative regime. During each rainstorm, water reaching the soil surface is partitioned between infiltration and surface runoff. The runoff is

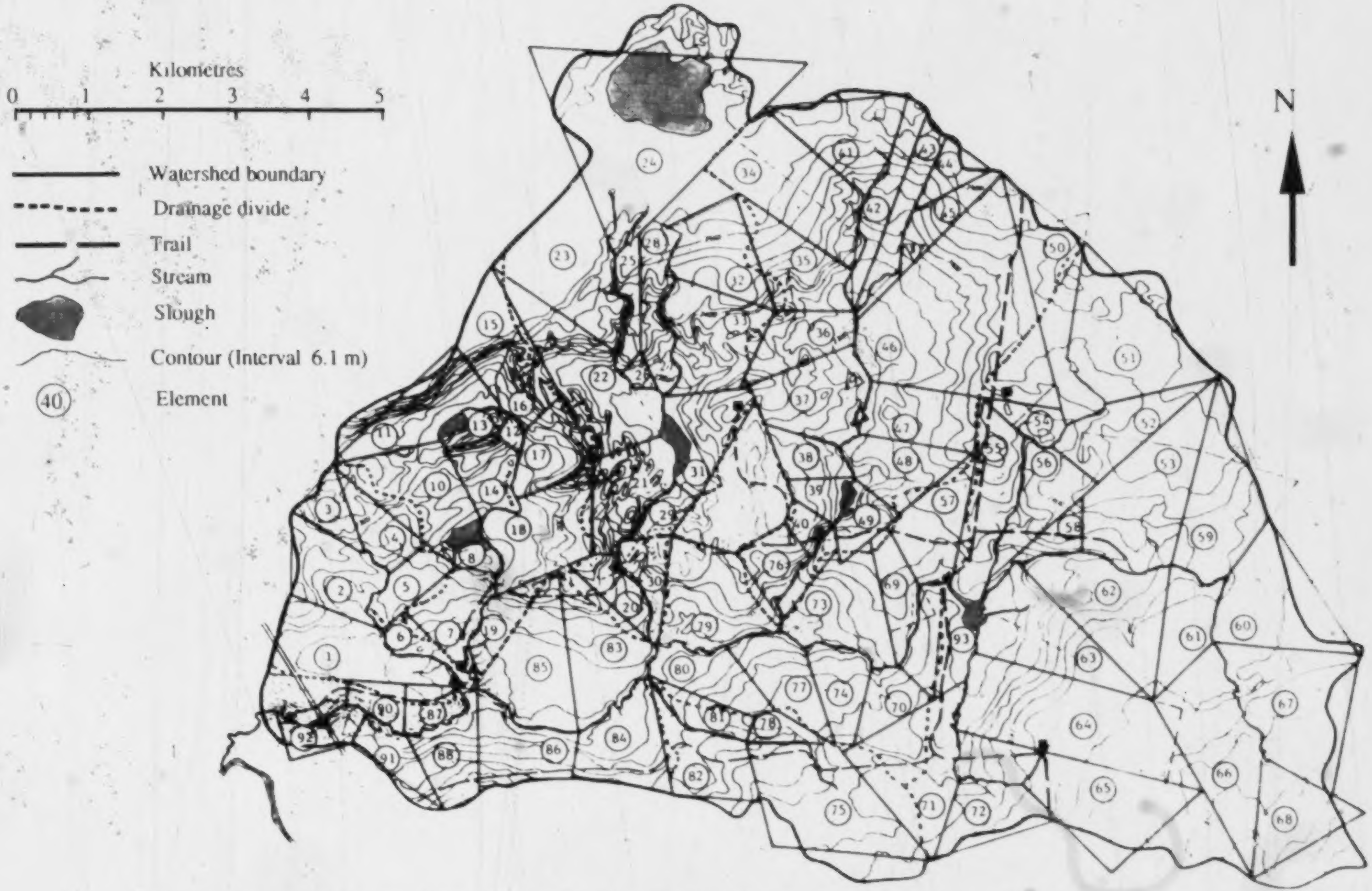
Kilometres
0
1
2
3
4
5
Watershed boundary
Drainage divide
Trail
Stream
Slough
Contour (Interval 6.1 m)
40
Element
N

Fig. 7-12. Discretization of the watershed (map obtained from Alberta Environment, Edmonton).

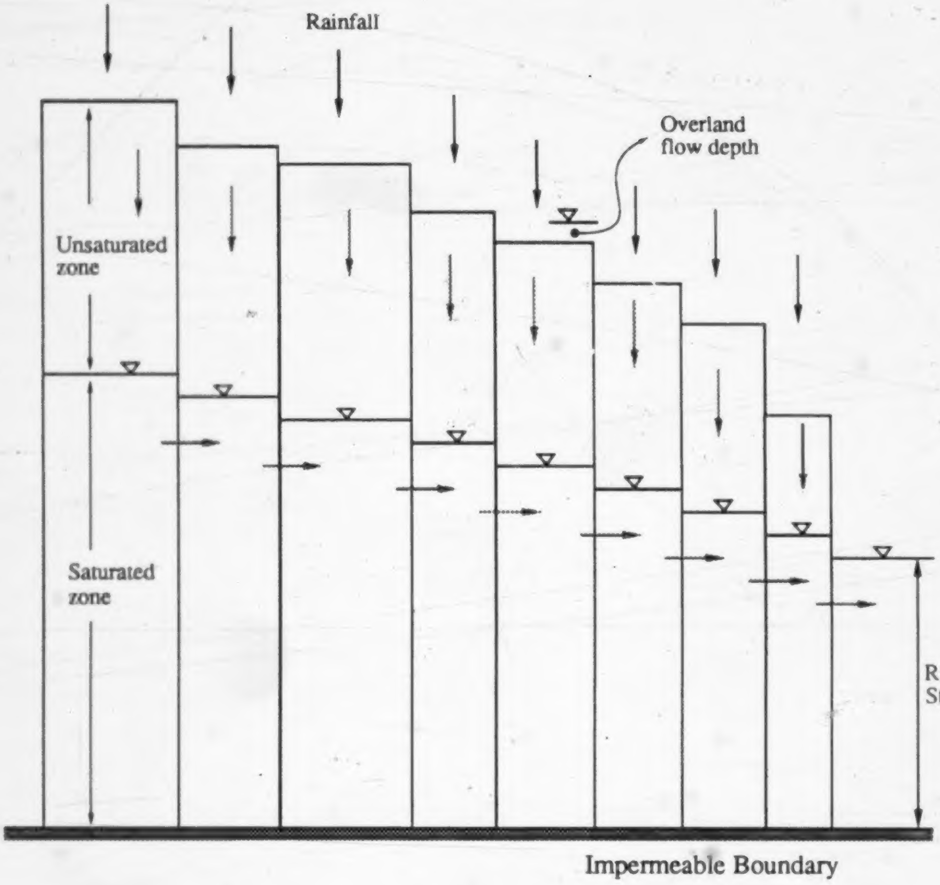
Rainfall
Overland flow depth
Unsaturated zone
Saturated zone
River Stage
Impermeable Boundary

Fig. 7-13. Model representation of the profile of sloping surface divided into columns.

portrayed as a one-dimensional process directed downslope and routed over the upper surface to the streams. Infiltrated water moves vertically through the column. As has been mentioned in section 2.2.2, for the sake of simplicity, it is assumed that the horizontal gradients and fluxes in the unsaturated zone are negligibly small. As the infiltrated water reaches the water table, the water table rises. The water table gradient governs the lateral flow of the groundwater to the stream. The stream network receives lateral inflow from each element as surface or subsurface flows, and eventually transport these waters to the outlet. The following discussion includes the concatenation procedure of these flow systems. It is very difficult to simulate the physics in its entirety. However, in this model an attempt has been made to maintain the gap between real and idealized processes as narrow as possible.

Theoretically it is possible to assemble the equations of unsaturated, saturated, overland and channel flows in finite difference (or finite element) form as one integrated system of equations (to describe the aforementioned continuous physical system). This type of coupling is termed internal coupling. However, this approach has serious practical limitations in that much smaller intervals in both time and space would be required. This would increase the demand of storage and time in the computer, which is already a restriction on the practical application of this type of model.

To avoid this, several workers (Freeze, 1972b, for example) have made use of a less expensive technique called external coupling. Provided that the difference between the time steps for overland flow and subsurface flow is less than the rainfall time increment, this procedure should not lead to excessive errors and has the advantage that some flow subroutines (for instance, overland flow, infiltration or evaporation subroutines etc.) need not be called unless necessary. It is also possible to arrange for smaller space and time discretizations for whichever flow solution is more sensitive. This procedure is adopted here to couple flow processes.

Coupling of the overland, unsaturated and saturated flow processes

(a) Taking initial overland flow depth as zero and initial water table position as known, the unsaturated flow component is solved for the first time step.

(b) The vertical flow rates in the surface layer and the bottom layer are calculated at the end of the time step. These are used to define the quantities $r_j^{n+1/2}$ and $R_j^{n+1/2}$ in eqns.[4-11] and [3-15] for the following time step. If there is any excess rainfall, the overland subroutine is called. However, the saturated flow subroutine is always called because saturated flow takes place depending on the slope of the water table. Depth of overland flow is calculated and a new water table position is found.

(c) In the unsaturated flow solution for this time step, any surface node in the soil at which the calculated depth of overland flow is greater than zero is treated as a fixed head node with capillary pressure equal to the depth of the overland flow. The unsaturated component is solved and the procedure returns to step (b).

Coupling of the overland, saturated and channel flow

The solution of the overland flow component does not depend on the water level in the stream whereas the saturated component does because water level in the stream is used as one of the boundary condition (term d in eqn.[3-21] and Fig. 3-4). For the first time step, taking initial water level in the stream as the required lower boundary condition the saturated flow computations are performed. The groundwater discharge into the stream is calculated. Considering this discharge and the discharge from the overland flow, if any, as the inflow, stream routing is performed and a new water level is obtained. And for the next time step taking this new water level as the lower boundary saturated flow computation is repeated.

The complete model

The outflow from each element becomes inflow to the channel network. To describe the bookkeeping of this inflow reference should be made to Fig. 7-14 which shows a single channel with connected elements from where inflow emanates. The lateral inflow is uniformly distributed over the channel

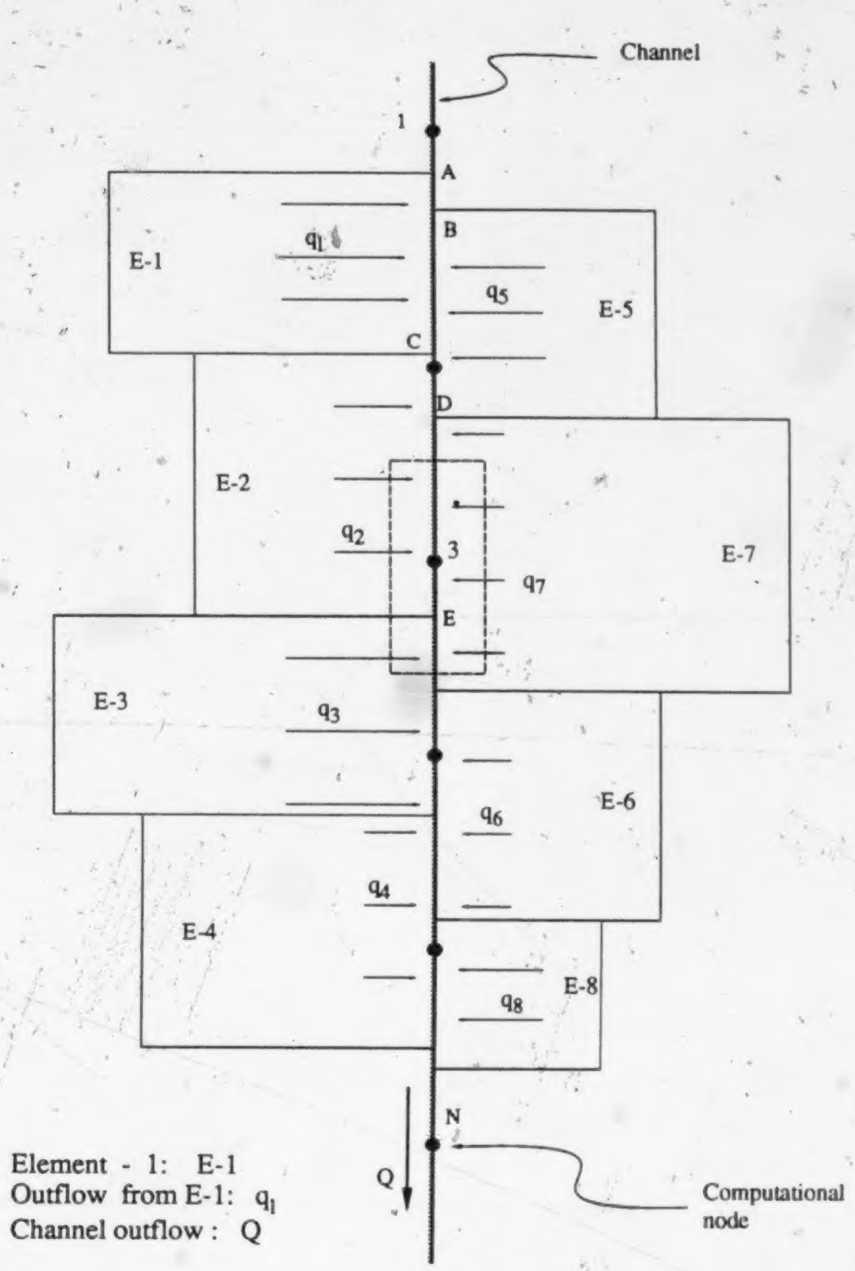
Channel
1
A
B
q1
E-1
q5
E-5
C
D
E-2
q2
3
E-7
q7
E
E-3
q3
E-6
q6
q4
E-4
E-8
q8
N
Q
Element - 1: E-1
Outflow from E-1: q1
Channel outflow : Q
Computational node

Fig. 7-14. Coupling element to the channel.

segments as shown in the figure. Discretization of the channel reach is independent of the connected elements. Total inflow reaching a channel segment between two computational nodes is equally divided to these nodes. Depending on the location relative to the elements a computational node may receive inflow from more than two elements as shown in the figure. Coordinates of the upstream and downstream end of a channel segment connected to a particular element is given as input data in the program with the most upstream channel point as the reference (or origin). For example, elements E-1 and E-5 are connected with channel segments AC and BD respectively. Node-1 is the starting point of the channel, hence $x_1=0$. In order to keep track of the channel segments connected with the above elements, the distances of the points (from node-1) A, C and B, D corresponding to elements E-1 and E-5 are given as input and are remembered throughout the computation. Inflow for node-3, for example, is calculated as $i_3 = (\Delta x/2).(q_7) + (\Delta x).(q_2) + (x_3-D).(q_7) + (\Delta x/2-x_3+D).(q_5)$, which is simply a matter of geometry.

The process of synchronization of the model segments (i.e. the unsaturated, saturated, overland and channel flow processes) in time can be explained with reference to Fig. 7-15. In this figure, the length of the bar represents a solution time step as calculated using Fourier analysis for each of the flow processes. As an example it is shown that the unsaturated flow solution requires the shortest time step. For overland flow the required step is almost twice of

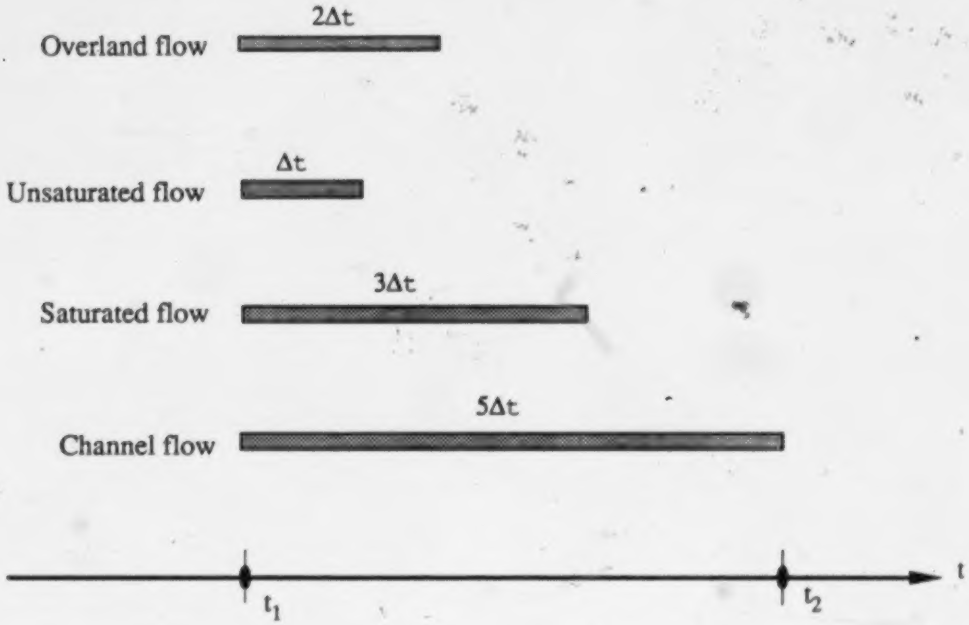
2Δt
Overland flow
Δt
Unsaturated flow
3Δt
Saturated flow
5Δt
Channel flow
t
t_1
t_2

Fig. 7-15. Synchronization of the model segments: Δt - basic time step.

that of unsaturated flow, in case of saturated flow it is about 3 times, and the channel flow solution requires a step approximately 5 times. To obtain a solution, better be termed as the global solution, at time t_2, the overland flow routine is called (if there is any excess rainfall) at every $2\Delta t$, the saturated flow routine is called at every $3\Delta t$, and the channel flow routine is called at $5\Delta t$. Total outflow generated over $5\Delta t$ is used as input to the channel during the solution.

For the next time step of the model (or the global time step), again Fourier analysis is used to calculate the optimum time step of each flow process. The magnitude of the calculated steps will not necessarily follow the same order as before. It may be that the channel flow solution requires the shortest of all the steps. As described in the above paragraph the time steps of the remaining flow processes are set using this shortest step as the basic step.

7.6 Application of the Model to a Sub-basin

It is evident that repeatedly running the model will be rather expensive. Hence to evaluate the model performances it was applied to one of the 5 sub-basins of the Spring Creek watershed prior to extension to the entire basin. The selected sub-basin is the Horse Creek, the smallest of all the sub-basins. It is divided into 6 elements (Fig. 7-16). The channel system consists of a single channel of length 2700 m. The outlet control of the channel consists of a flow measuring weir installed by the Alberta Environment. So the

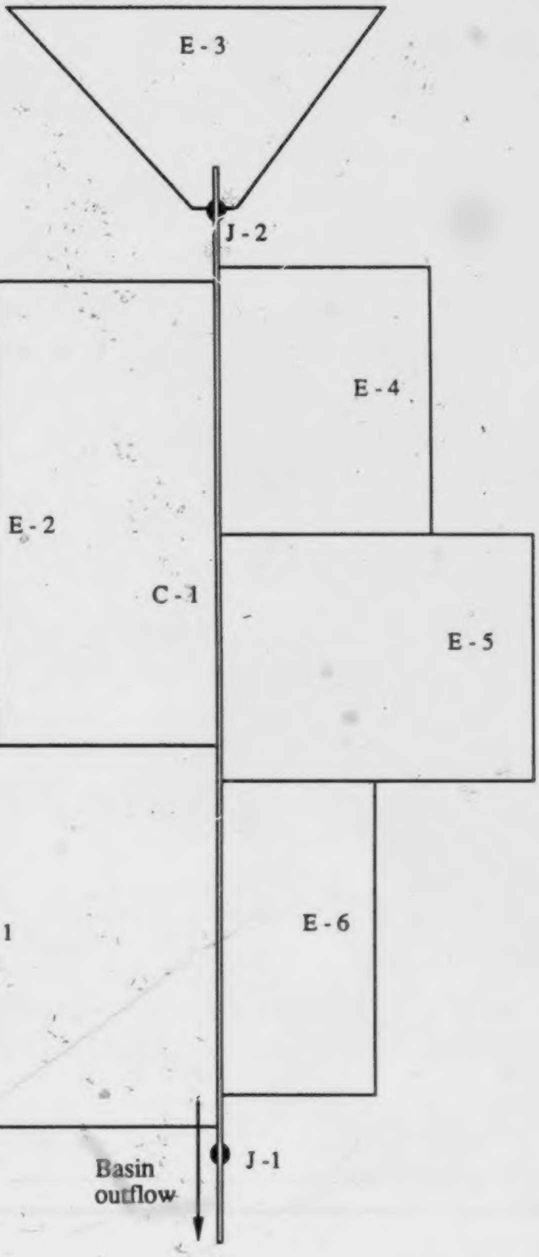
E-3
J-2
E-4
E-2
C-1
E-5
E-1
E-6
J-1
Basin outflow

Fig. 7-16. The Horse Creek sub-basin; E-1: element-1; C-1: channel-1; J-1: junction-1.

boundary condition was the specified rating curve as developed by the Water Survey Branch of Alberta Environment.

The land system of the sub-basin consists of one major class of soils (such as silty clay). The required initial conditions were the water level in the stream, locations of the water table and the soil moisture conditions. The initial water level was estimated from the available records. However, the initial moisture content was very difficult to obtain. Hence several values were assumed to simulate the soil moisture distribution. The other hard to decide on entities were the thickness of the unsaturated zone and the thickness of the unconfined aquifer i.e. the parameter D or d as shown in Fig. 3-4. In a previous study report (Ryckborst and Holecek, 1977) it is indicated that in some locations of the Spring Creek basin the maximum depth to the water table is about 3 m from the ground surface. The thickness of the unsaturated zone was taken as 3 m and the thickness of the unconfined aquifer was arbitrarily assumed to be 30 m.

Previously it was thought that each element would further be divided into several columns (shown in Fig. 7-13) to simulate soil moisture dynamics. However, considering the computational costs it was decided not to do so. Instead the entire element was dealt with, as if it consisted of a single profile (Fig. 7-17a). Recharge calculated at the mid-point of the element is distributed uniformly throughout the element as depicted in Figs. 7-17b and 7-17c. It is not hard to visualize that the flow process through any medium is nothing

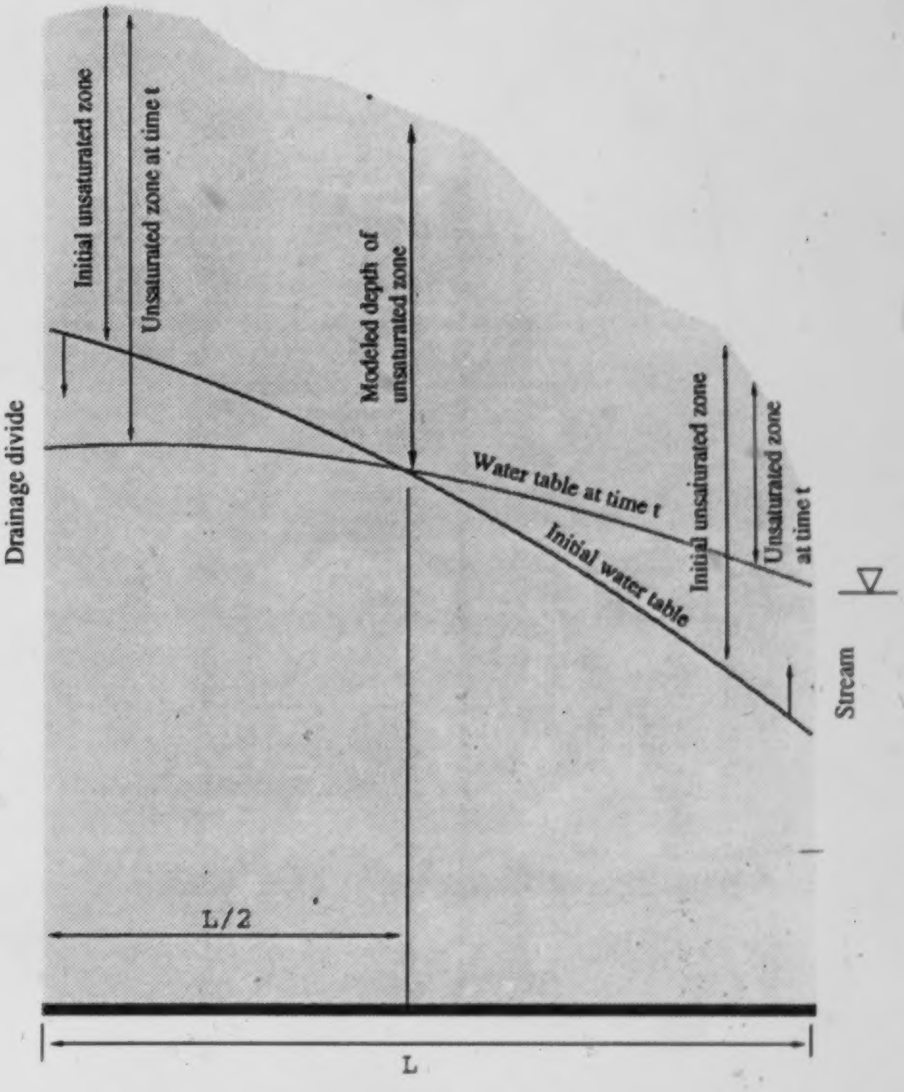
Drainage divide
Initial unsaturated zone
Unsaturated zone at time t
Modeled depth of unsaturated zone
Water table at time t
Initial water table
Initial unsaturated zone
Unsaturated zone at time t
Stream
L/2
L

Fig. 7-17a. Water table movement.

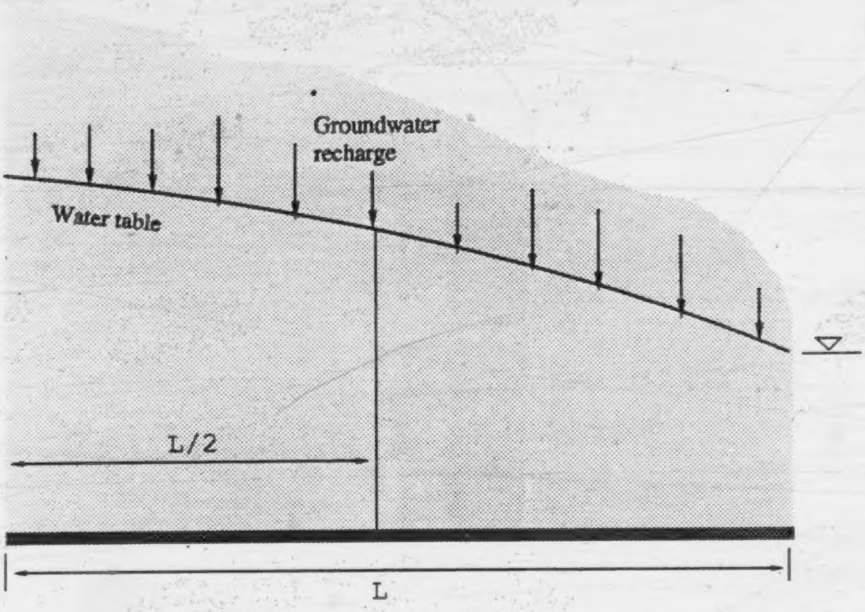
Groundwater recharge
Water table
L/2
L

Fig. 7-17b. Actual nonuniform distribution of grwounwater recharge.

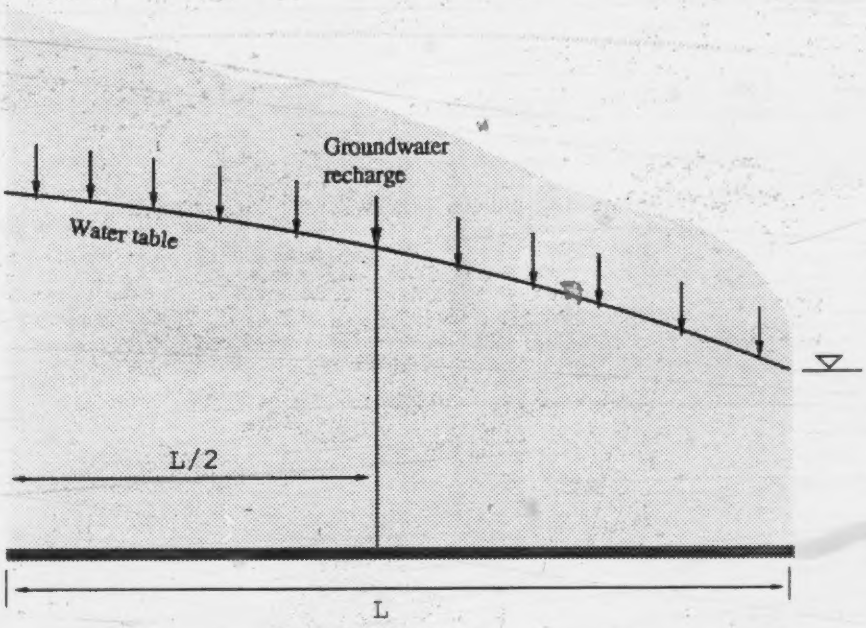
Groundwater recharge
Water table
L/2
L

Fig. 7-17c. Assumed uniform distribution of groundwater recharge.

but the propagation of the boundary conditions. The more apart the boundaries the longer the time it takes before one boundary will feel the effect of the other. From Fig. 7-17a it is evident that the thickness of the unsaturated zone on the left side is more than that on the right side. Accordingly effect of water table on the left side will take longer time to reach surface than what will require on the right side. Hence it is not unreasonable to assume that the effect of lowering the water table on the left side of the mid-point would be offset by the effect of raising the water table on the right side.

Having sized up the initial and boundary conditions, the model was run to simulate a runoff hydrograph from the Horse Creek sub-basin. Since hourly observations of rainfall and discharge hydrograph were available for the storm of May 15-17, 1984, it was selected for the simulation run.

In this part of the simulation three aspects were investigated. These were the computational aspect, the relative significance of the flow processes within the Spring Creek basin, and adjustment of the so called physical parameters.

During the investigation of the computational aspects the unsaturated and saturated flow components were not considered (since these processes did not pose a great deal of difficulties when they were tested separately). With an average abstraction of 40%, the recorded precipitation hyetograph was routed through the surface and channel systems. The parameters were those as indicated in section 7.3.2. As obtained in Chapter 6, for this initial run Δx for the channel and overland flow processes were 275 m and 54 m respectively. The calculated hydrograph from the Horse Creek sub-basin is given in Fig. 7-18.

Total CPU time on MTS computing system (of the University of Alberta) for a simulation period of 80 hours was 15 s. From the CPU-time point of view this is reasonable. The error criteria for overland flow were 0.00000001 m and for channel flow 0.001 m.

From the channel output it is vivid that the solution is contaminated i.e. there are oscillations. This can be accounted for by the coarse discretization. Accordingly using a finer discretization (channel: Δx = 100 m) a smooth hydrograph is obtained (Fig. 7-19). However, this does not seem right either. As it can be noticed that the hydrograph and the hyetograph peaks are almost coincident. This is not the case in the real situation. Usually there is a lag between the precipitation and runoff peaks. The quick rise of the hydrograph peak is due to the quick transport capacity of the basin. In turn this capacity depends on the depth of water and the roughness of the conveyance systems. Here, either the assumed runoff volume is high or the assumed value of the roughness factor too low. These are considered at the end of this section but before that the relative significance of the saturated flow process is discussed in the following paragraphs.

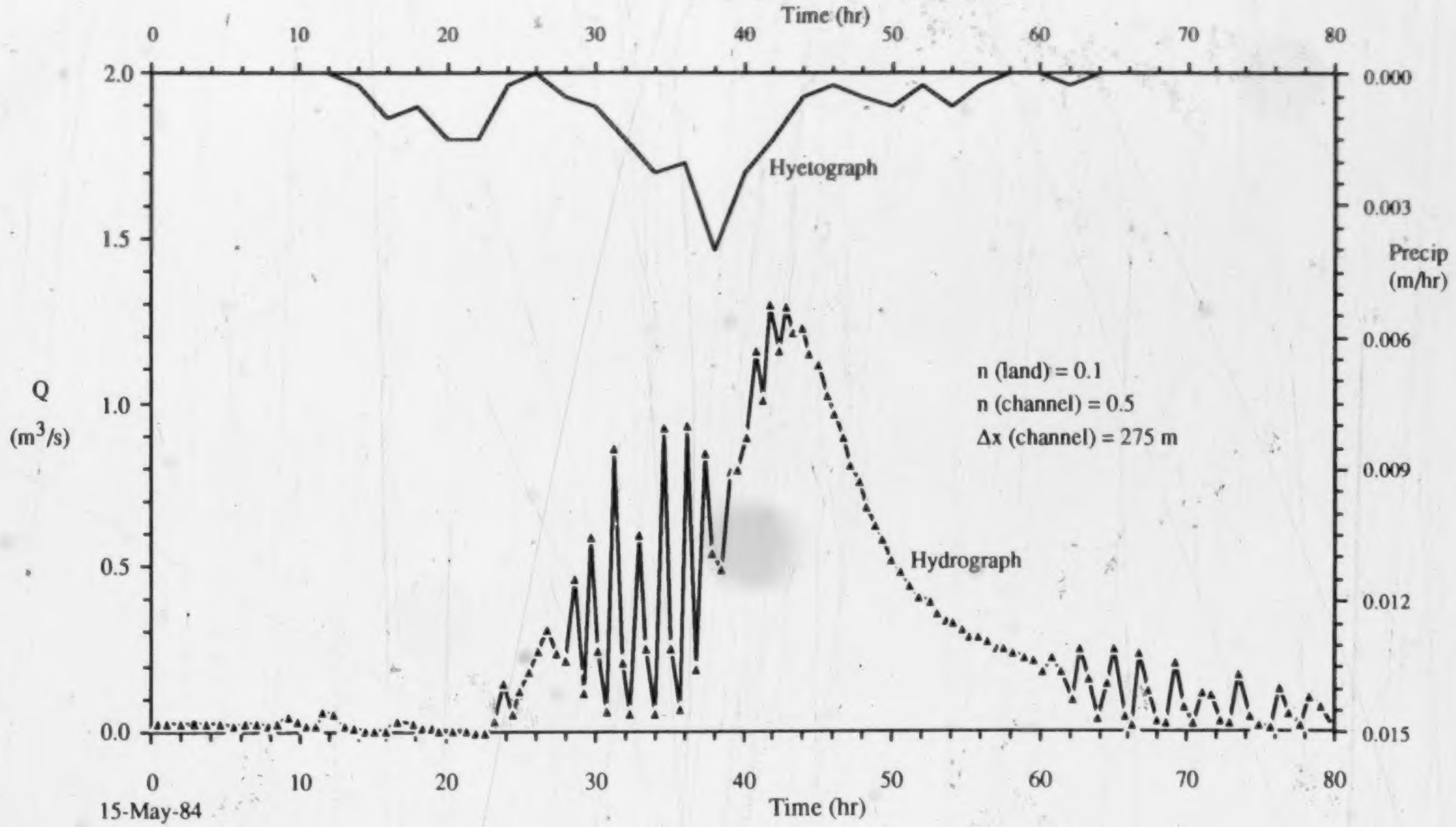

Fig. 7-18. Contaminated solution of outflow hydrograph (Horse Creek).

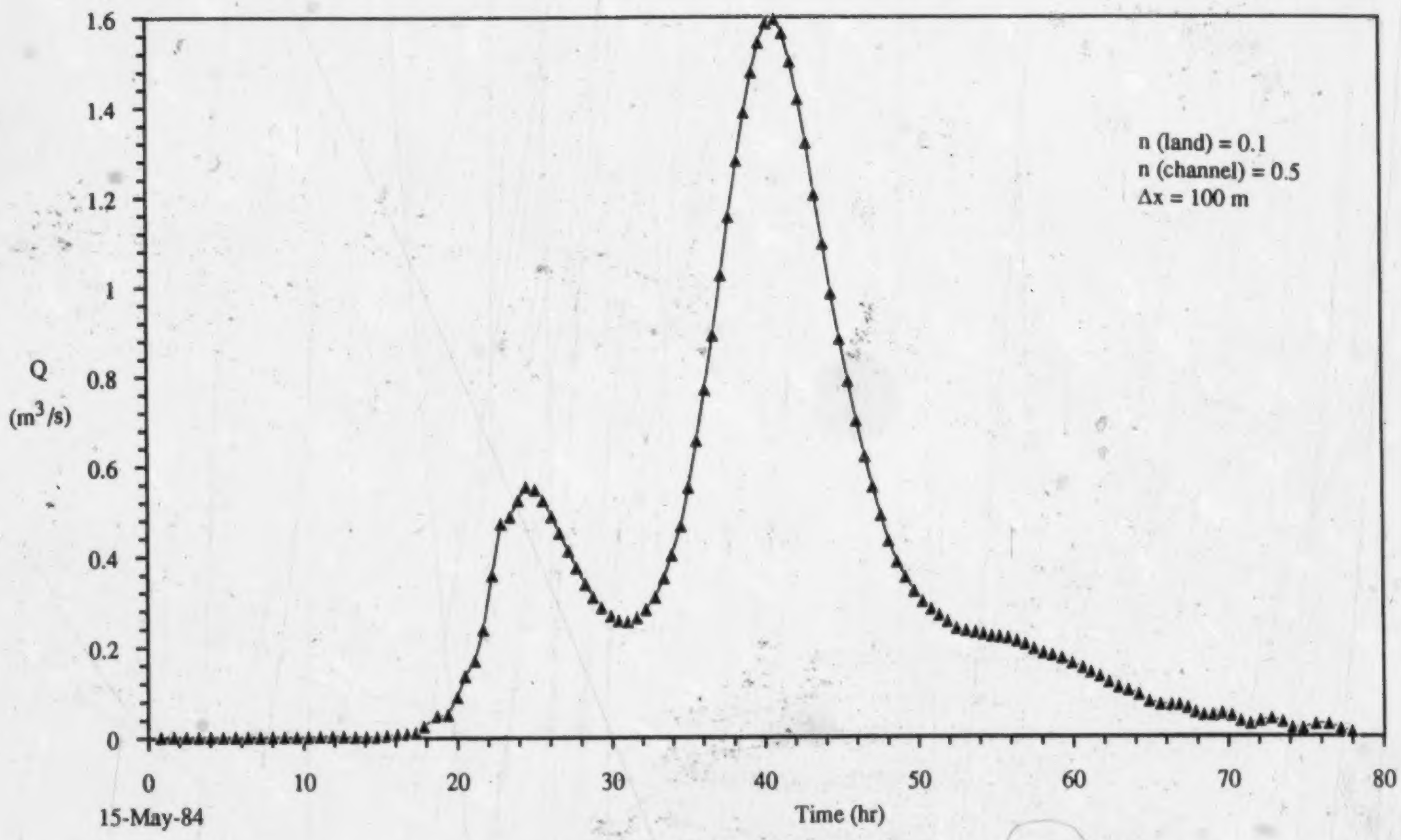

Fig. 7-19. Effect of discretization (on the outflow hydrograph of Horse Creek).

In order to assess the groundwater contribution to the streamflow, the same hyetograph was routed through the saturated flow zone of the sub-basin. The discretization was the same as before. The aquifer thickness and the initial water table position were those as mentioned previously. The results of this run are presented graphically in Figs. 7-20 through 7-22. Fig. 7-20 is an outflow hydrograph from element number-5 and Fig. 7-21 shows the fluctuation of the water table due to the rainfall. The low groundwater outflow corresponds to the low hydraulic conductivity and the low specific yield of the aquifer system. It is noticeable that over a period of 160 hours the drop in water table is small. The outflow from each of the element is so negligible that the computation of channel flow becomes unstable (Fig. 7-22).

Hence, the groundwater component is not considered for simulation of the sub-basin hydrograph. Three runs were given with varying initial (surface) soil moisture conditions such as 0.3, 0.4 and 0.5 (i.e. saturation). As evident from Fig. 7-2 the soil system of the basin consists of soil-C (Table 7-2). Mention has been made that the unsaturated zone was assumed to be 3 m deep. During this short simulation period evaporation has been assumed negligible. In addition it is noticed that the water table fluctuation could be assumed negligible. Therefore the bottom boundary condition was Dirichlet (ψ=0) type. Calculation starts at the inception of the rainfall with an assumed equilibrium soil moisture distribution.

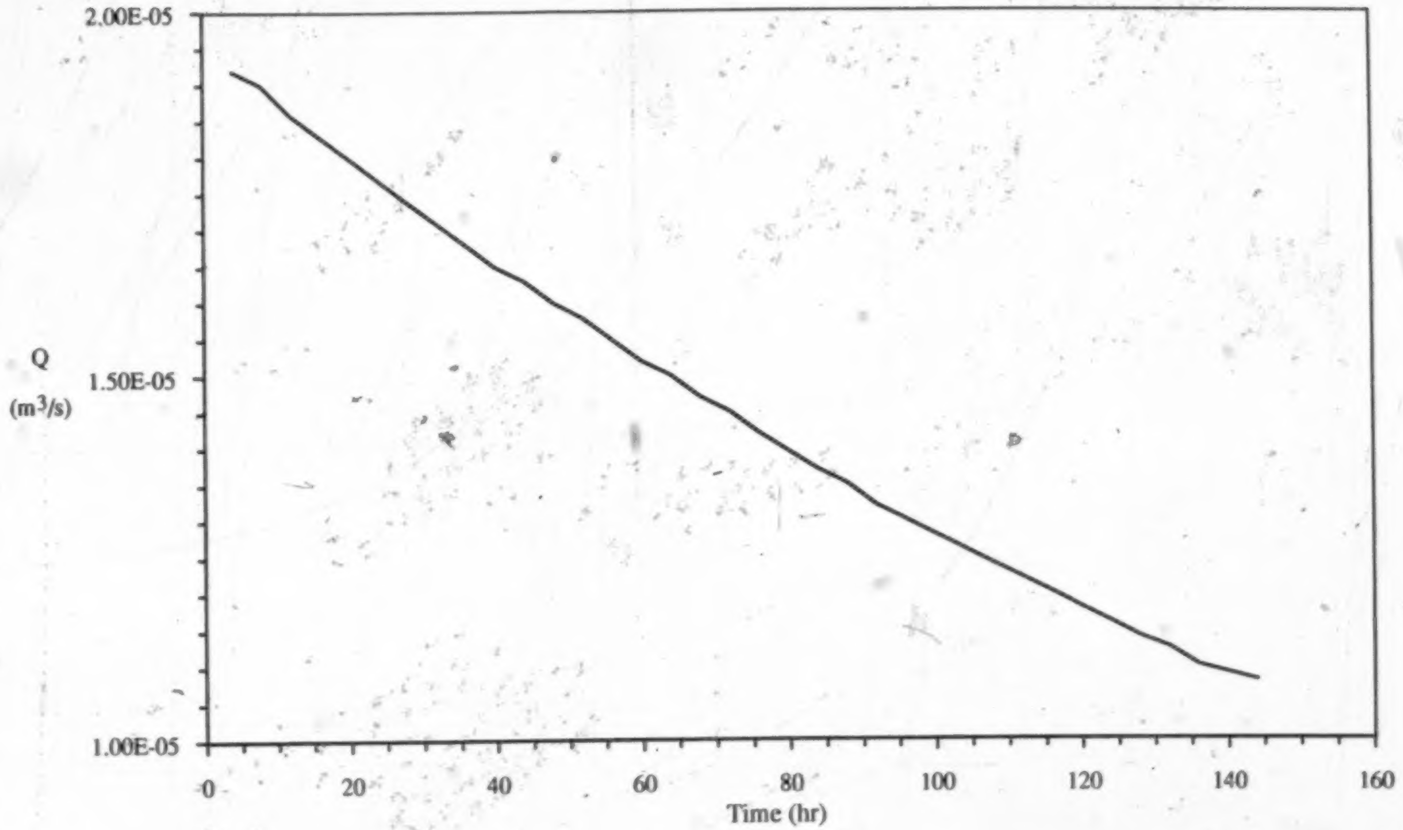

Fig. 7-20. Groundwater discharge from element-5 of Horse Creek sub-basin.

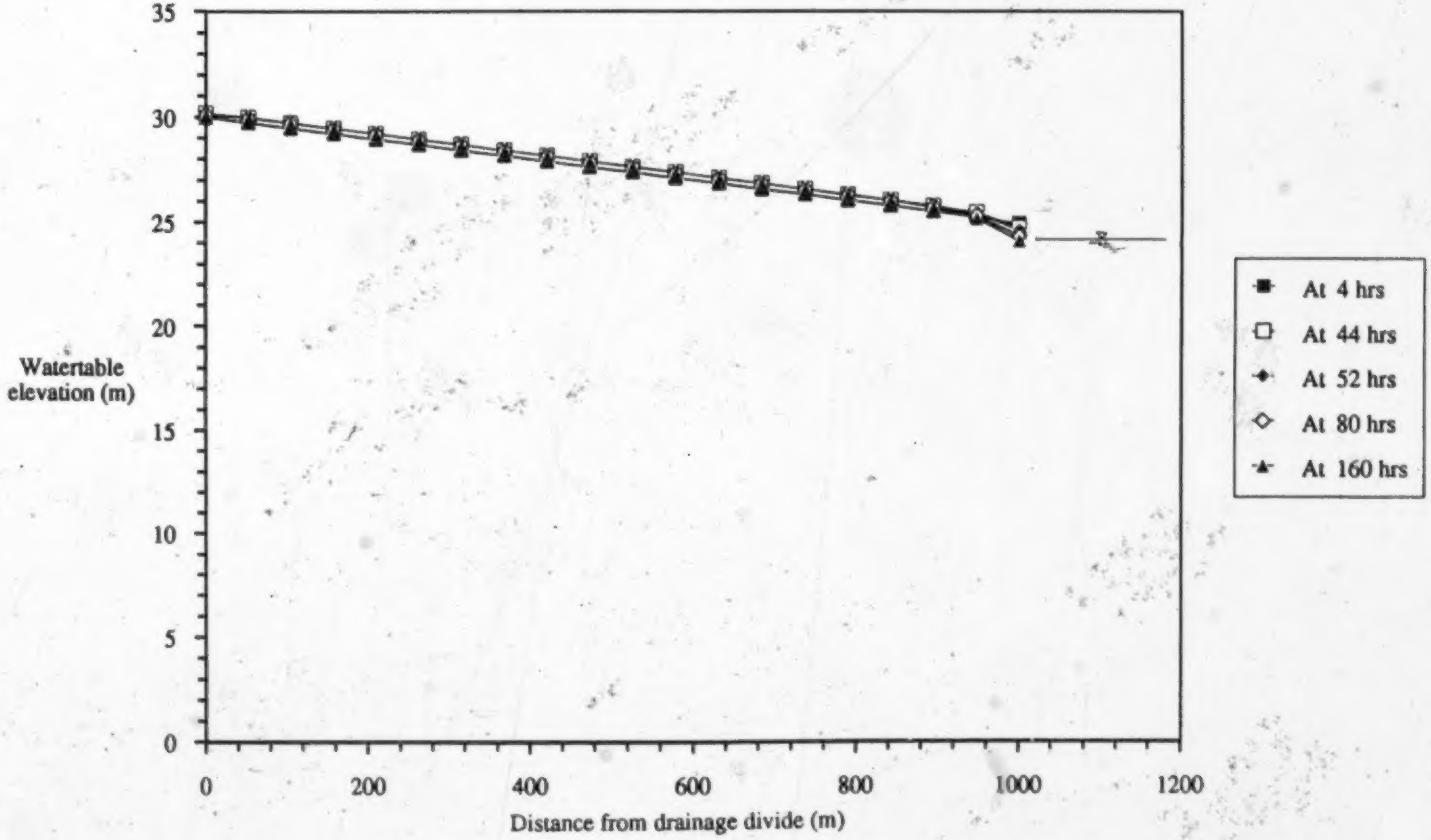

Fig. 7-21. Fluctuation of water table from an initailly assumed position.

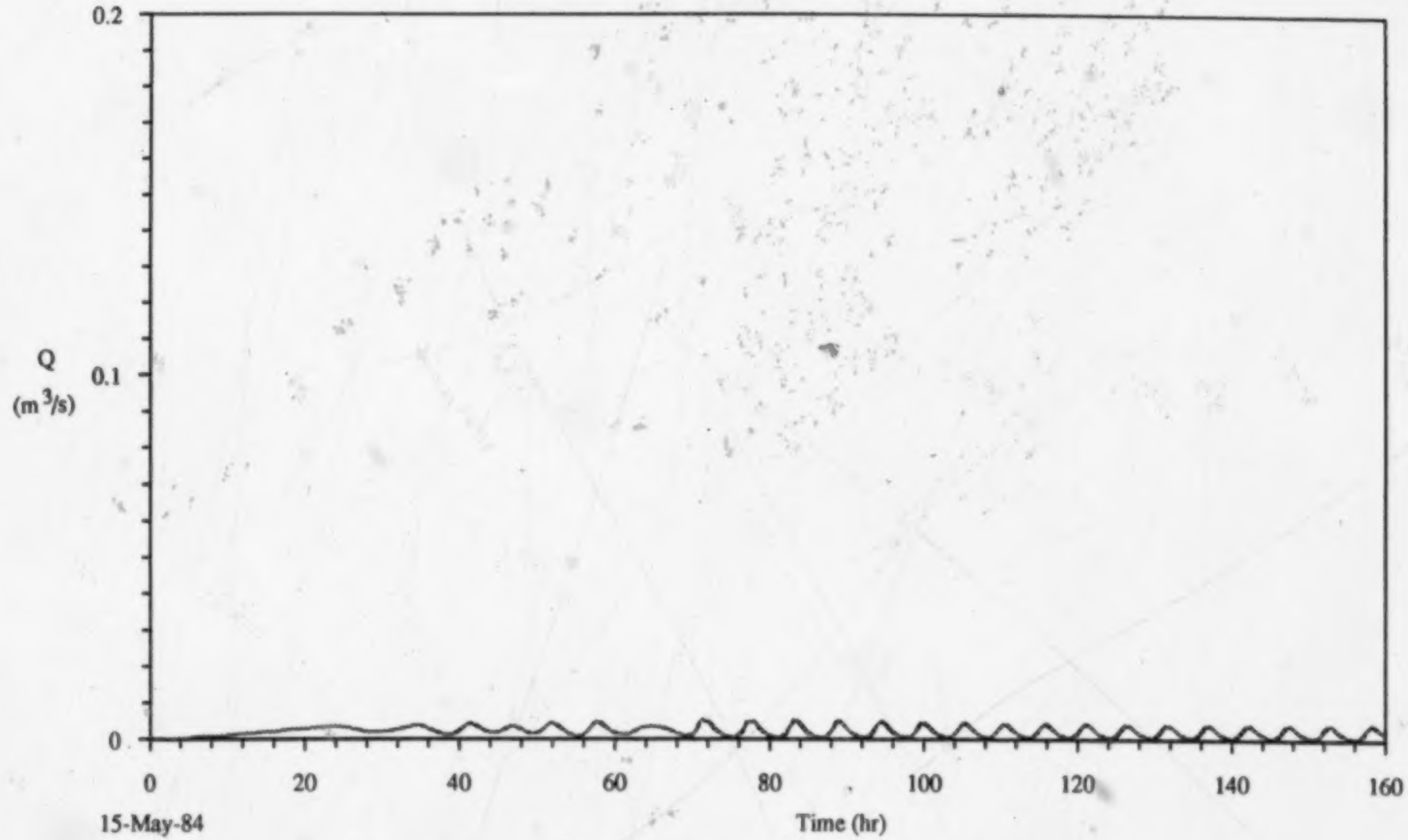

Fig. 7-22. Groundwater outflow from Horse Creek.

Then the generated runoff was routed over the land, and through the channel to obtain the outflow hydrograph. The outlet boundary condition was a rating curve as shown in Fig. 7-23. Initial estimate of the Manning's n was 0.03 for both the overland and the channel flows.

The simulated hydrograph is shown in Fig. 7-24. It appears that the simulated hydrograph reaches its peak relatively fast. This is due, perhaps, to the assumed low values of roughness factors. Increasing n to 0.08 for overland flow and to 2.0 for channel flow it seems possible to push the computed hydrograph peak reasonably close to the observed peak. The adjusted n values are high. However, in literature there are evidences of high n values (Leutheusser and Chishom, 1973). From Plate 7-1 it can be appreciated that the Spring Creek basin is densely vegetated. The channel bed at some locations even supports tree growth. In addition the channel of irregular cross section, occasionally interrupted by beaver dams, is assumed to be represented by a uniform straight channel. To account for these factors high n values are necessary during computation.

A low initial moisture content yields a low runoff volume from the watershed. Similarly a high initial moisture content seems to yield high runoff volume (Fig. 7-25). However, these seem to change the flood peak only. Previously a notion has been developed that the groundwater contribution to the streamflow is negligible. Therefore, the relatively slow recession of the observed hydrograph may be due to the

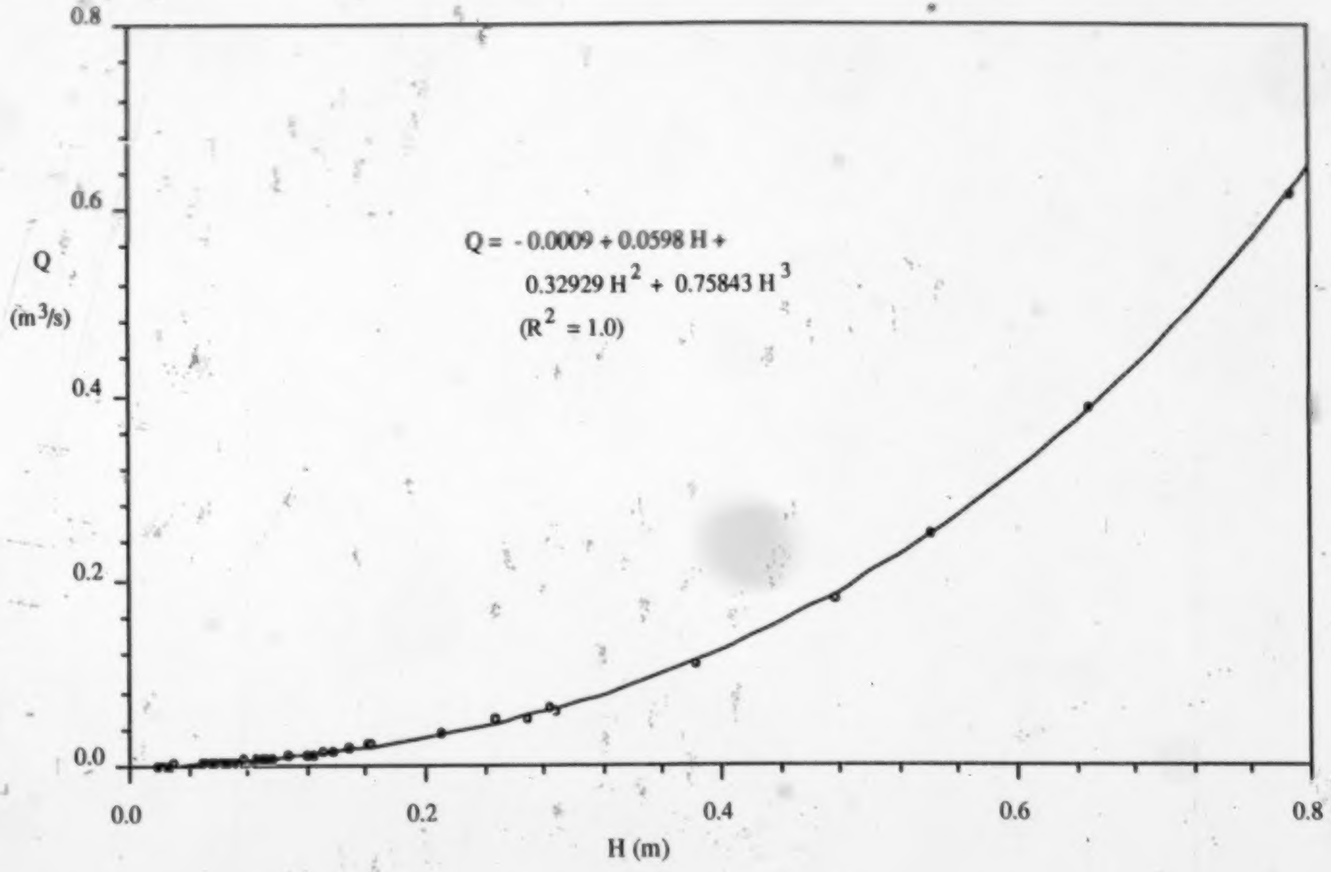

Fig. 7-23. Horse Creek rating curve.

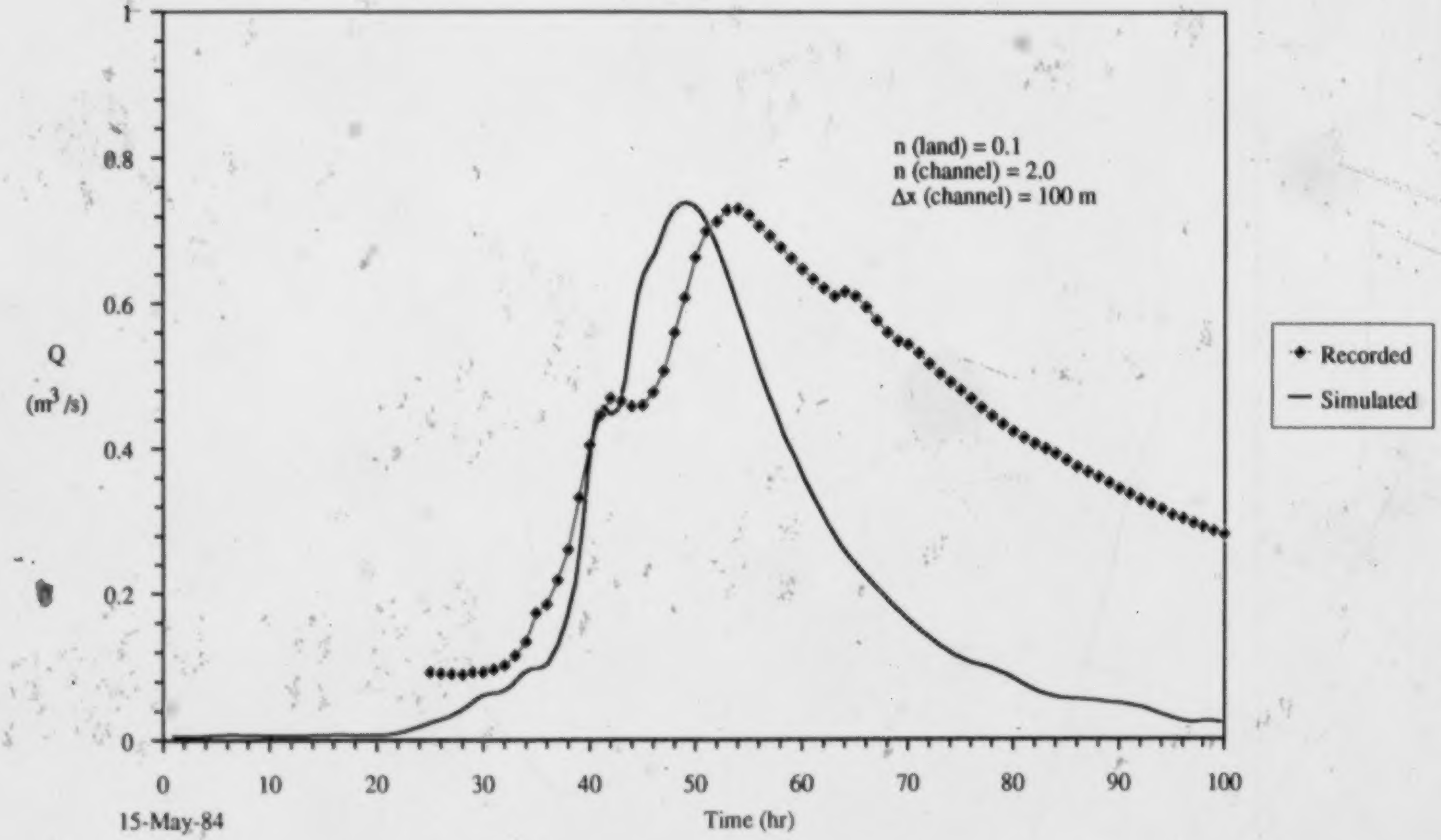

Fig. 7-24. Simulated and recorded hydrograph of Horse Creek.

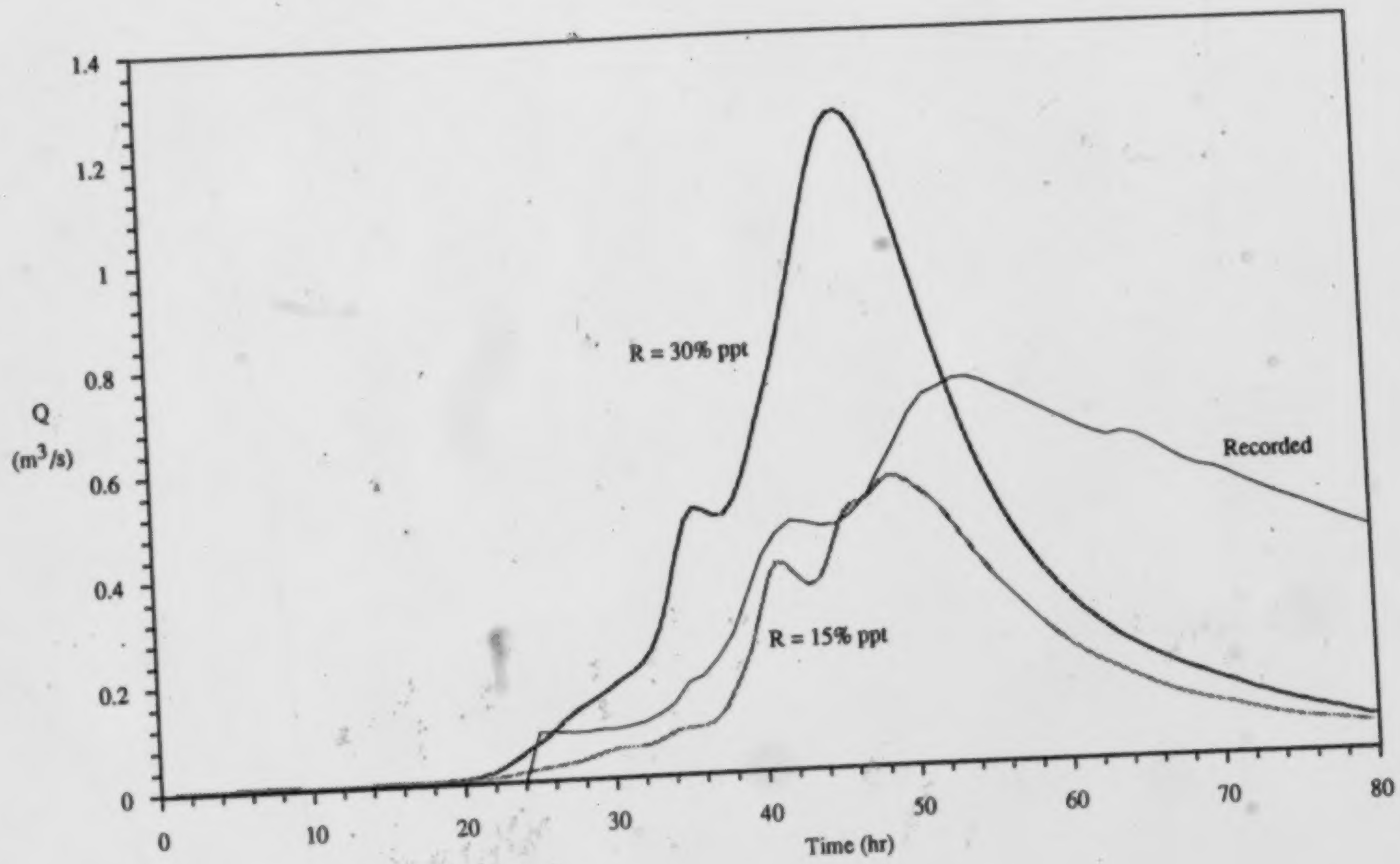

Fig. 7-25. Effect of runoff volume.

presence of some intermediate flow processes such as litter flow, or pipe flow through dead root channels (Whipkey, 1965; Weyman, 1970, 1973; Chanasyk, 1980) or perhaps runoff from the melt water that might have persisted until then.

7.7 Extension of the Model to the Entire Basin

The required initial and the boundary conditions to simulate the entire basin were similar to those of the Horse Creek sub-basin. The rating curves which were used for the constituent sub-basin outlet boundary conditions are shown in Fig. 7-23 and Figs. 7-26 through 7-30. The discretized watershed is shown in Fig. 7-12. From the natural setting of the sub-basin outlet control section and from the nature of the discharge measurement devices (cf. Plates 7-2 and 7-3), installed by Alberta Environment, it appeared that the outflow from the upper sub-basins (such as Horse Creek, Wolverine, Rocky, Bridlebit, and the Spring Creek-upper) were not influenced by the conditions of lower basin (such as the Spring Creek-lower). Hence, the calculations were performed sub-basin wise and the computed hydrographs from the upper sub-basins were stored in the computer to use as input to the lower basin. Thus it was possible to reduce the high computational cost of solving a large matrix. This seems merely a coincidence. If the conditions were not such, it must have been necessary to solve a big matrix.

Here, perhaps, it is worth mentioning that the Spring Creek is a very steep basin (cf. Table 7-2 for mean slope of the existing channel networks). In general this sort of

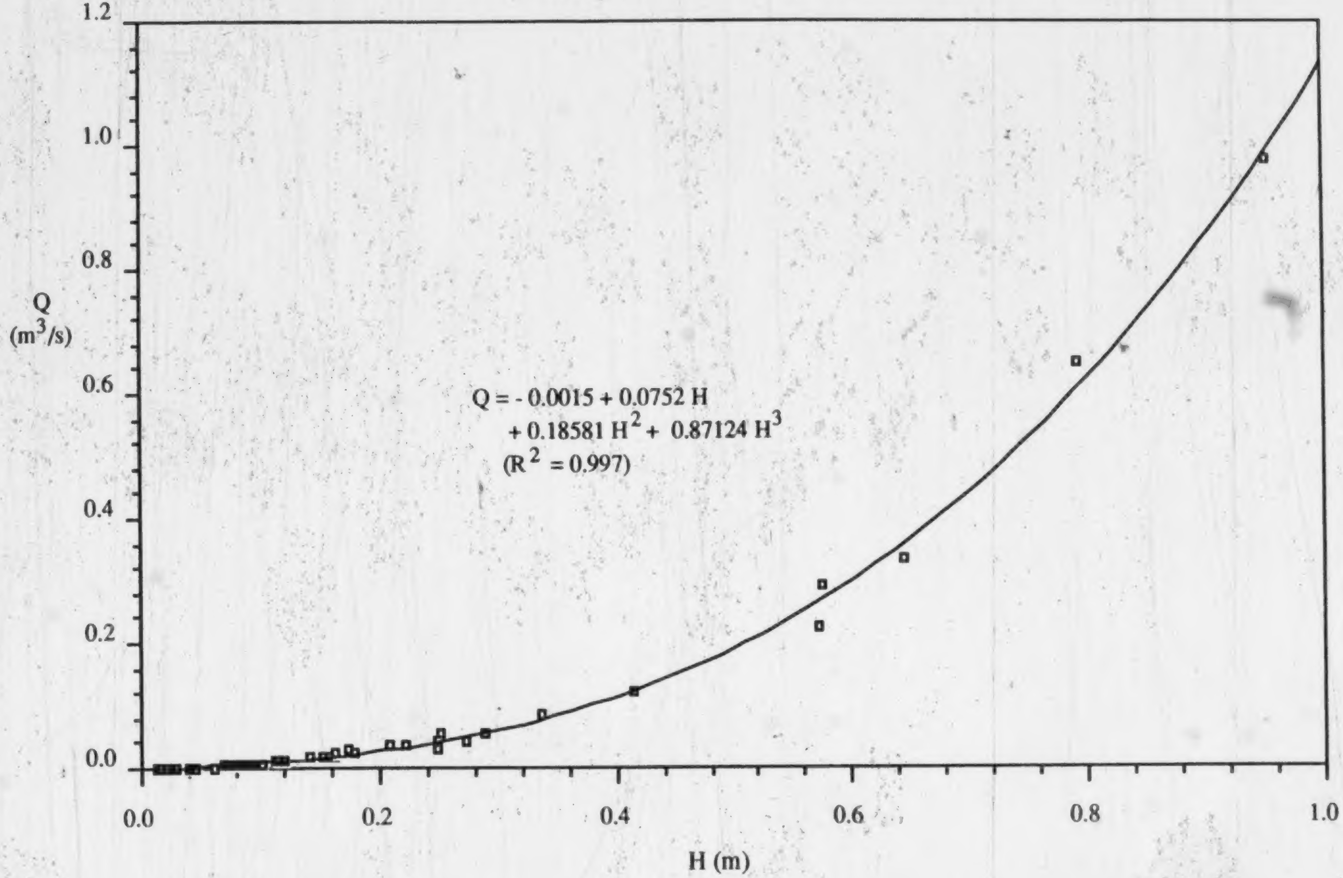

Fig. 7-26. Wolverine Creek rating curve.

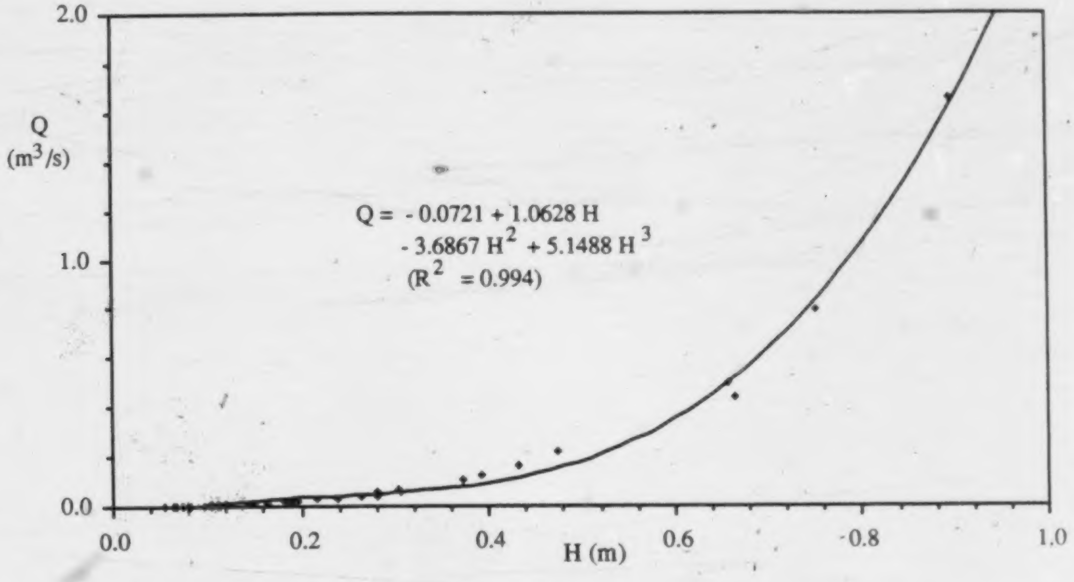

Fig. 7-27. Rocky Creek rating curve.

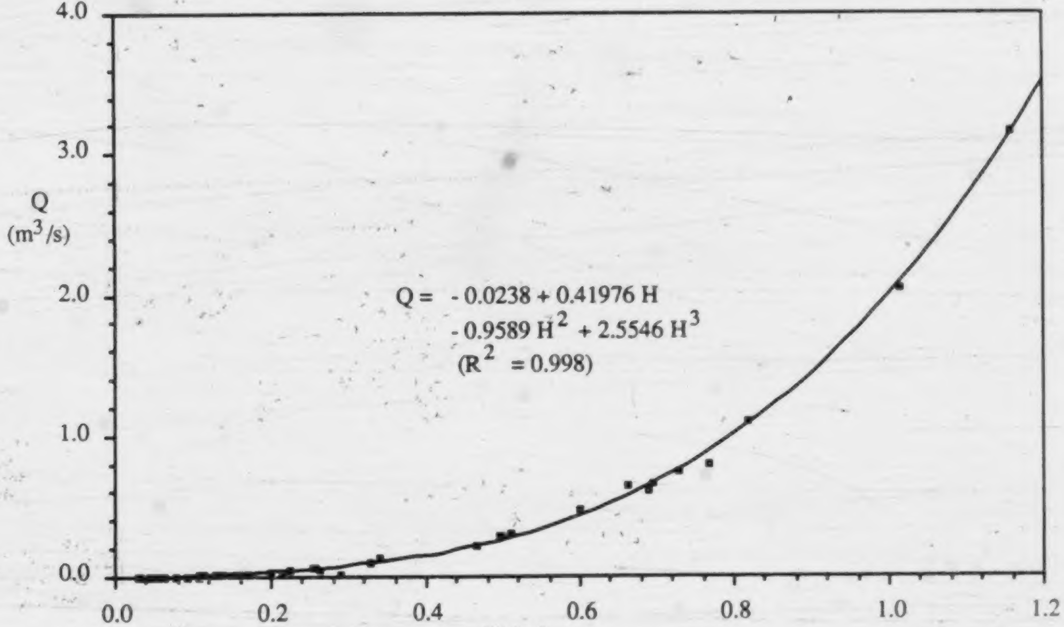

Fig. 7-28. Bridlebit Creek rating curve.

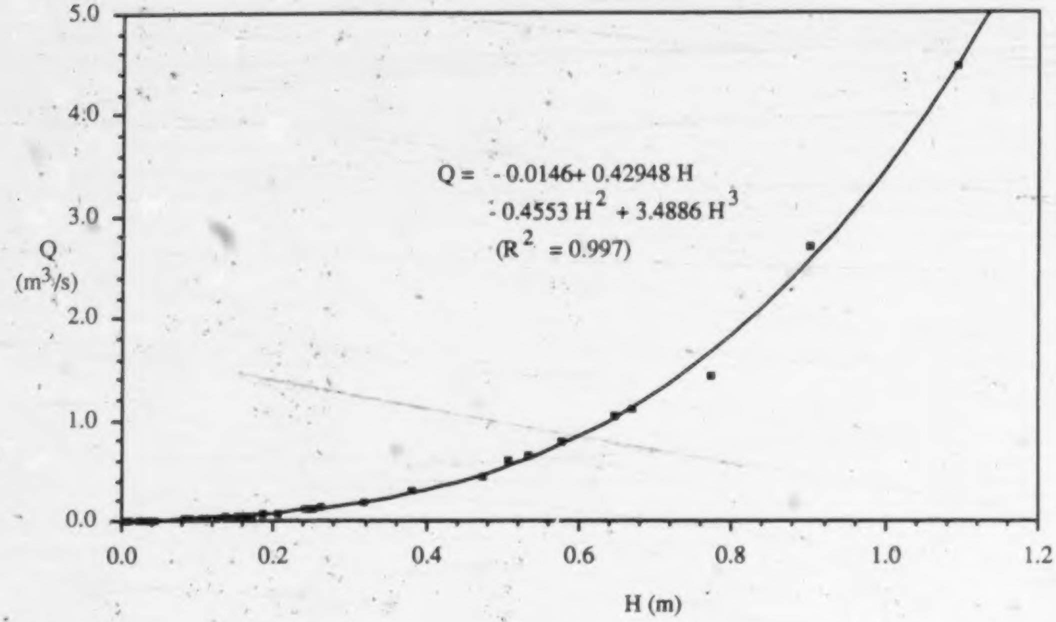

Fig. 7-29. Spring Creek-upper rating curve.

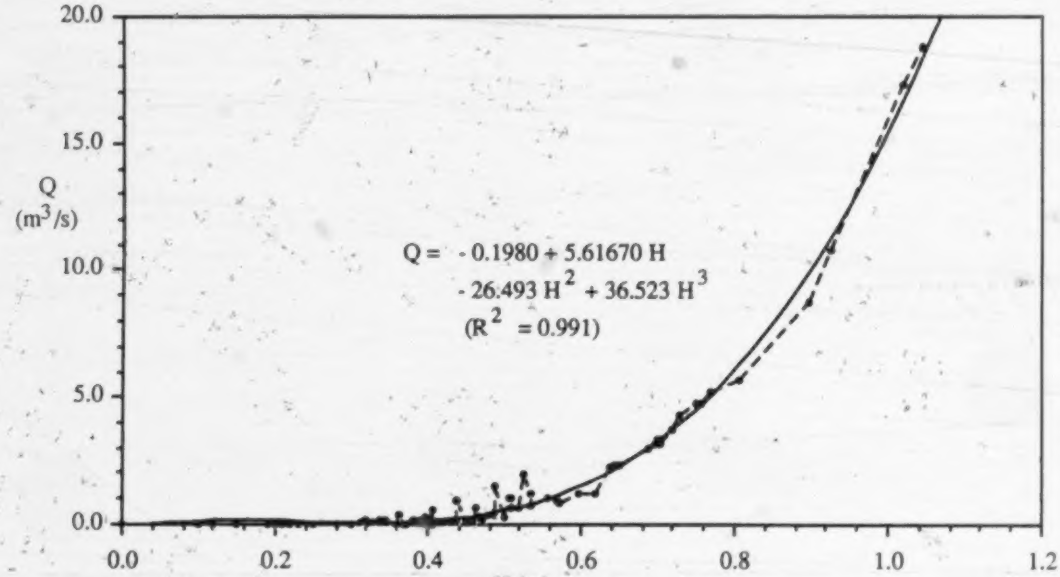

Fig. 7-30. Spring Creek rating curve.

Plate 7-2. Outlet control structure of Bridlebit Creek.

Plate 7-3. Outlet control structure of Spring Creek-upper.

watershed yields sharp peaked hydrographs which require finer discretization thus augmenting the computational costs. However, it is believed that far fewer computational nodes (hence reduced cost) would be required to simulate a basin of low relief of the size of Spring Creek.

Be that as it may, in the present application of the model, the channel network of the Spring Creek sub-basins such as Horse Creek, Wolverine, Rocky, Bridlebit, Spring Creek-upper and the Spring Creek-lower were divided into 25, 76, 61, 50, 95 and 104 computational nodes respectively. Depending on the length of the element a range of node numbers were used when computing the overland and saturated flows. It should be noted that this discretization was obtained following the stability analysis as has been done in Chapter 6.

To obtain an estimate of the maximum computational cost, the model was applied to its entirety. The unsaturated flow computation was performed for all the elements. The saturated flow component was included. Soon, while running the program, it was realized that life is not so simple. The presence of sloughs or storage junctions in the channel networks created problems. Previously it was thought that these storage junctions could be treated according to eqn.[5-7]. But the surface areas, A, of the sloughs are so large, in comparison to the channel top width, that the solution became non-convergent. Eventually these storage junctions were also treated as point junctions. However, storage effects, such as increased time lag and diffused flood peaks, were taken into account by increasing roughness and by using reduced channel slopes.

The required CPU time on MTS computing system of the University of Alberta, was 1500 s for a simulation period of 200 hours. The error criteria for channel, overland, unsaturated and saturated flows were 0.001 m, 0.00000001 m, 0.01 cm and 0.001 m respectively. The simulated and recorded hydrographs of the Spring Creek basin and its constituent sub-basins are given in Figs. 7-31 through 7-35.

The fit is not very good. The two noticeable kinks in the rising limb of the Wolverine Creek hydrograph are most probably due to a mild computational instability which could be fixed at ease. The quick recession and reduced volume (which is persistent in all the simulated hydrographs) is mainly due to some unaccounted water in this simulation. For example, it was thought that the aquifer is a poor conveyor of water to the stream. Most of the infiltrated water would disappear either by deep percolation or would stay in the formation eventually to be depleted by evaporation. This may not be the case. Part of the infiltrated water might be returning to the stream through a moderately slow intermediate route. The other possibility is that in the watershed there might be some additional melt water present.

Explaining all the differences is difficult because hydrographs represent an integration of many distributed effects. How much could be accounted for? Nevertheless, all

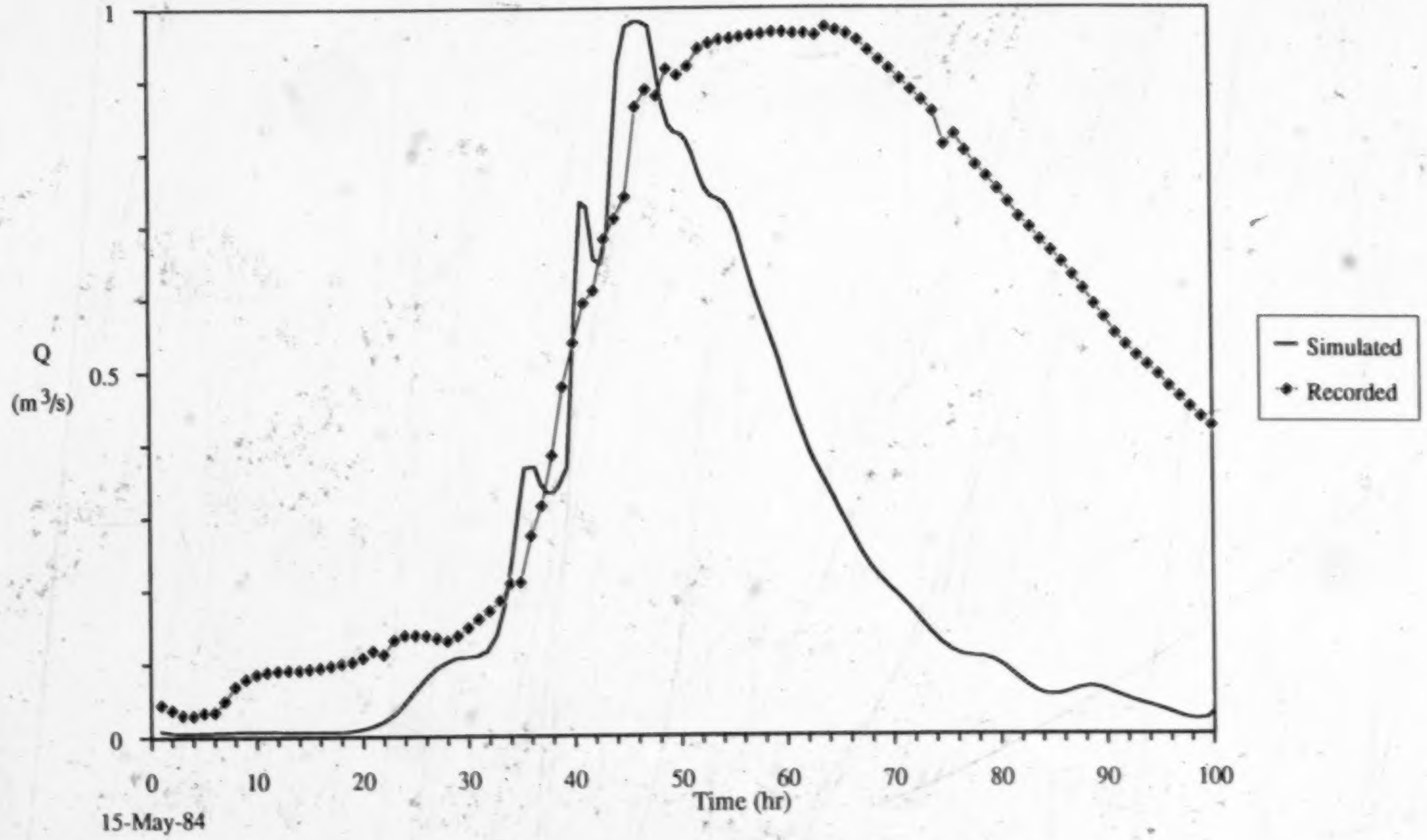

Fig. 7-31. Simulated and recorded hydrographs of Wolverine Creek.

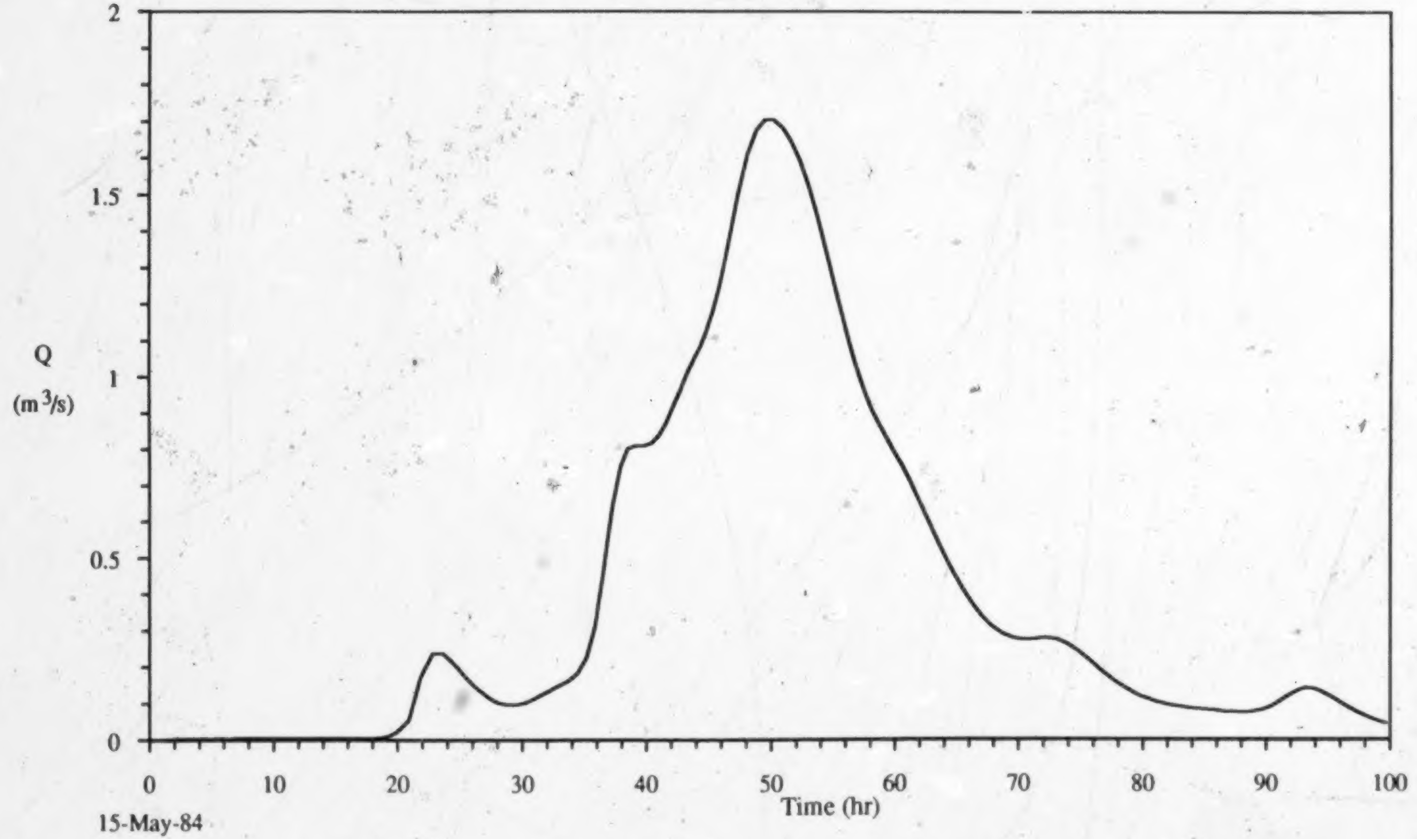

Fig. 7-32. Simulated and recorded hydrographs of Rocky Creek.

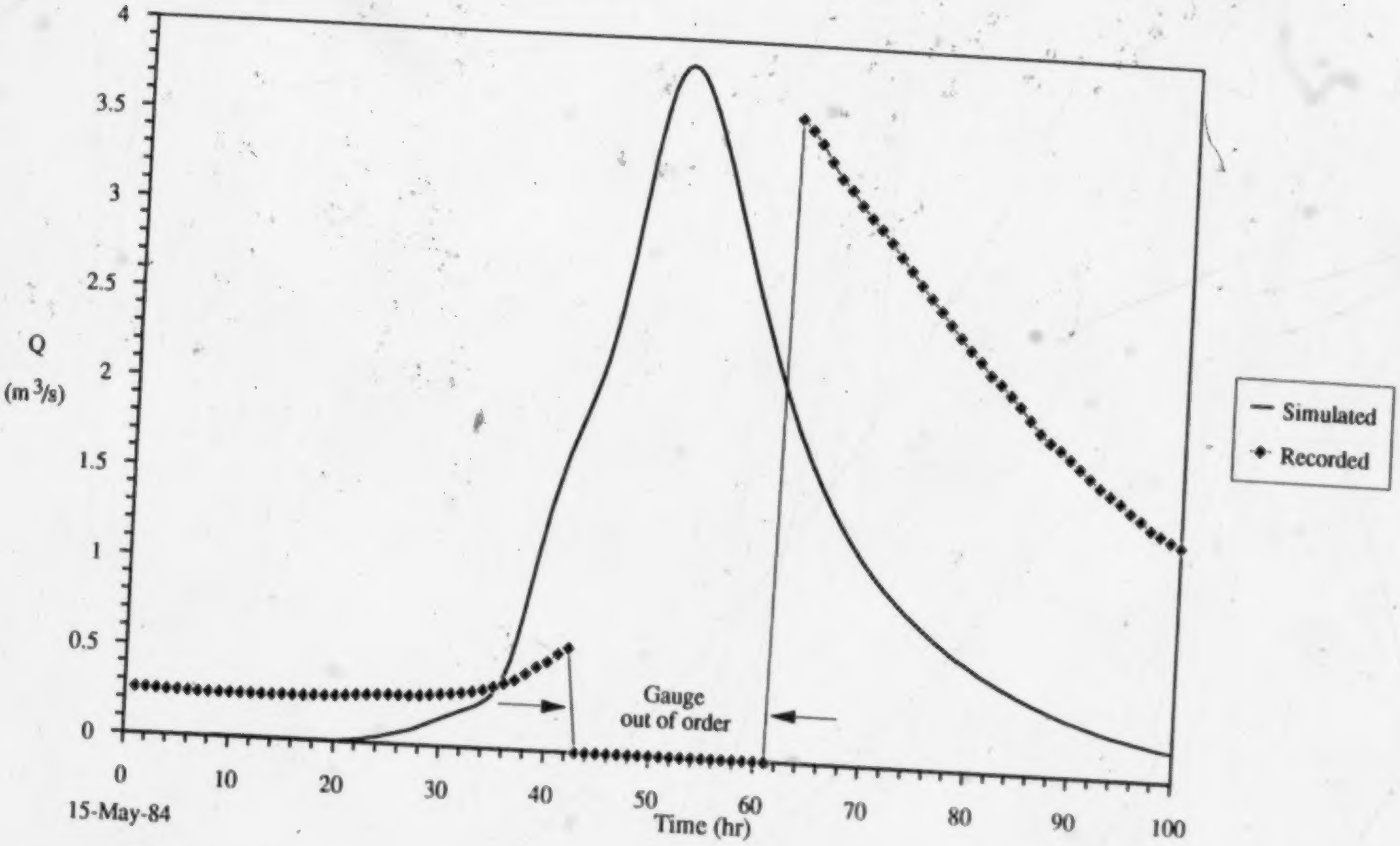

Fig. 7-33. Simulated and recorded hydrographs of Bridlebit Creek.

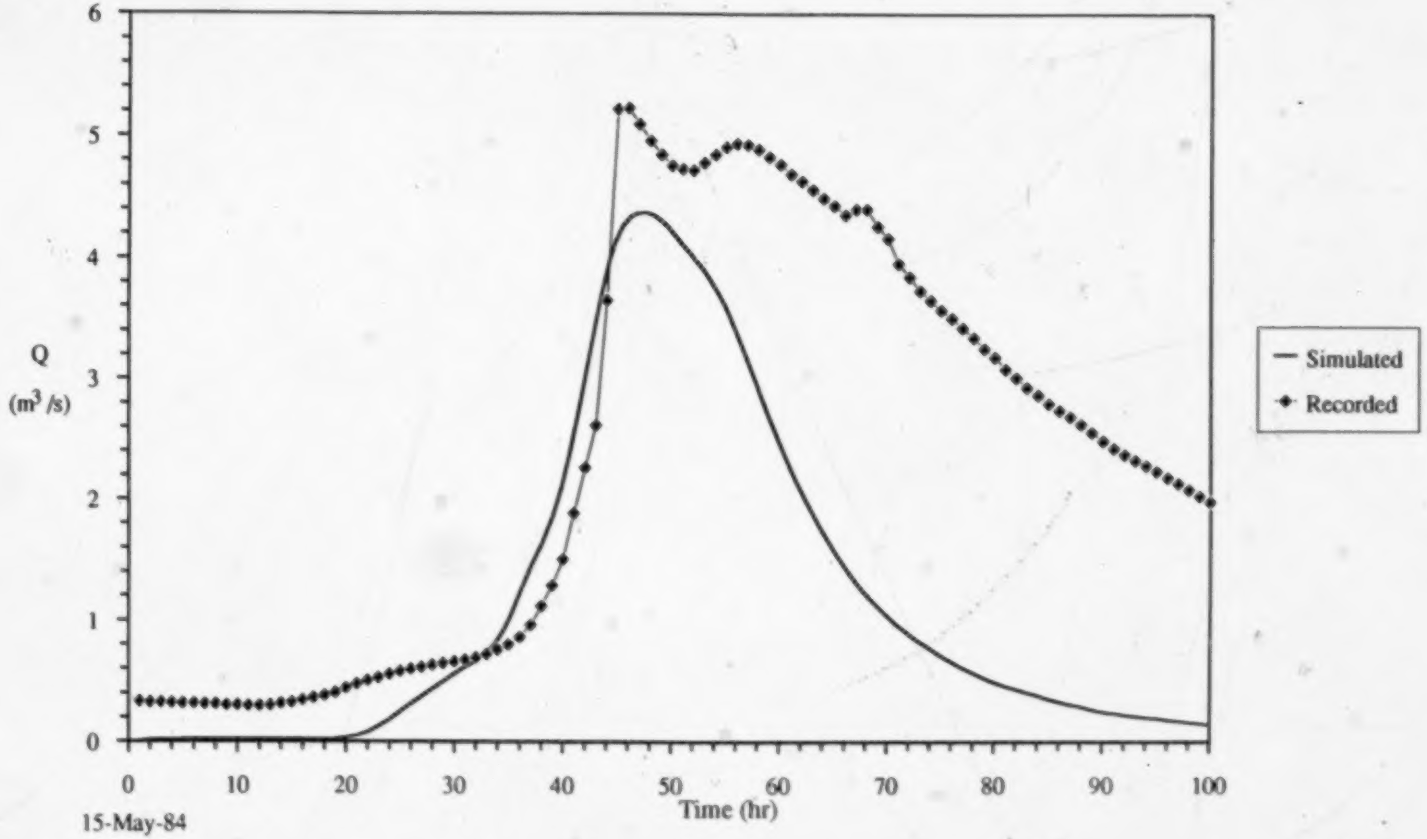

Fig. 7-34. Simulated and recorded hydrographs of Spring Creek-upper.

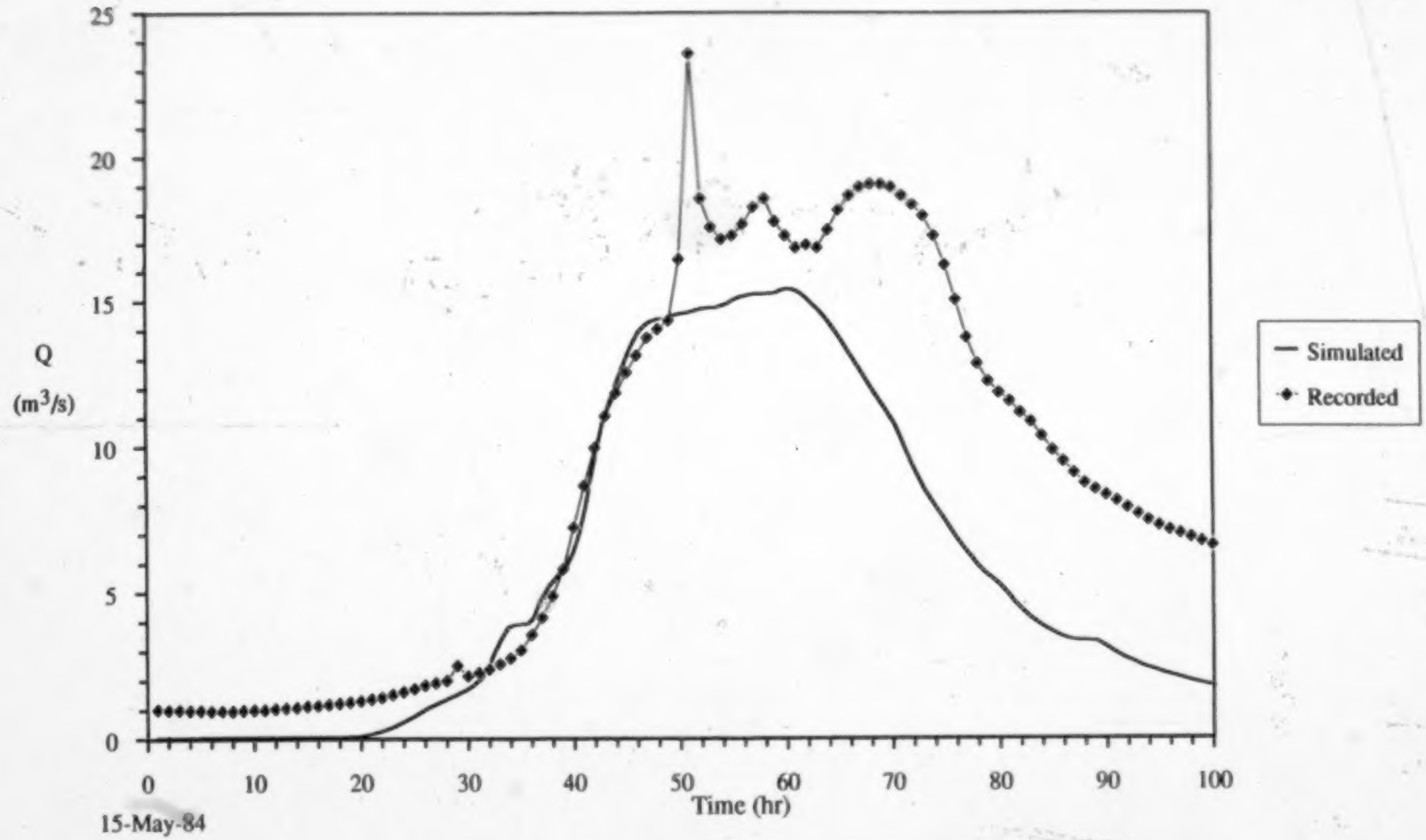

Fig. 7-35. Simulated and recorded hydrographs of Spring Creek watershed.

should not be ended in despair. Except adjustment of Manning's n, no attempt has been made to optimize the parameters. Yet a reasonably good fit is obtained. Fitting between recorded and predicted hydrographs could be improved by the process of calibration or by providing adequate information (such as depth of saturated, unsaturated zones). From this study it is evident that hydrographs can be predicted from known physical and hydrological properties of a basin.

Chapter 8

Finale

8.1 Conclusions

In this study a distributed non-linear model of watershed water yield, infiltration and evaporation (and hence the soil moisture) prediction has been developed. The constitutive equations of the watershed processes are solved using the F-D numerical method. The framework of the model is based on the assumption that the lateral flows (subsurface and surface) are normal to the topographical contours. Thus the watershed relief is incorporated into the model.

The required data are obtained through direct measurement or are estimated from other measured entities. The model was applied to the Spring Creek watershed to simulate catchment response to a single storm. The simulated hydrograph compared favourably with the recorded hydrographs specially in the rising limb. However, there is substantial difference between observed and simulated hydrographs in the recession part.

Watershed models are perceived simplified version of the real system. In addition the information and relationships which used to describe these models are associated with uncertainties. Hence, it can not be expected that models will reproduce the behaviour of the prototype exactly. Furthermore, the present model was applied to only one catchment to simulate a single storm response. Therefore, it difficult to extract definitive conclusions regarding the model and its performances.

Considering the objective of this study which was to develop a model able to predict the hydrological responses of an ungauged catchment using the the informations derived directly from the basin without resort to historical records or regional generalization of model parameters, it can be said that this exercise was not in vein. This is a different approach of modeling hydrological processes in that it can utilize distributed nature of the hydrological variables and the information which was used has physical significance. Traditional lumped and conceptual models can not make use of the physiography of the watershed and the effect of diverse vegetative covers.

In the present application of the model the discrepancies between observed and simulated hydrographs may attributed to the inadequate specification of the subsurface zone. Further tests are necessary to demonstrate the model's capabilities and the means of improvement.

References

Abbott, M. B., 1979. Computational Hydraulics: Elements of the Theory of Free Surface Flows. Pitman.

Abbott, M. B., Bathurst, J. C., Cunge, J. A., O'Connell, P. E., and Rasmussen, J., 1986a. An introduction to the European Hydrologic System - Systeme hydrologique Europeen, 'SHE.' 1. history and philosophy of a physically-based, distributed modelling system. J. Hydrol., **87**, 45-59.

Abbott, M. B., Bathurst, J. C., Cunge, J. A., O'Connell, P. E., and Rasmussen, J., 1986b. An introduction to the European Hydrologic System - Systeme hydrologique Europeen, 'SHE.' 2. structure of a physically-based, distributed modelling system. J. Hydrol., **87**, 61-77.

Abdel-Razaq, A. Y., Viessman Jr., W., and Hernandez, J. W., 1967. A solution to the surface runoff problem. J. Hydraul. Div., Proc. Amer. Soc. Civil Eng., **93**(HY6), 335-352.

Acock, B., and Grange, R. I., 1981. Equilibrium models of leaf water relations. In: Mathematics and Plant Physiology (Eds: D. A. Rose and D. A. Charles-Edwards), Academic Press, 29-47.

Akan, A. O., and Yen, B. C., 1977. A nonlinear diffusion-wave model for unsteady open-channel flow. Proc. Congr. Inter. Assoc. Hydraul. Res., 17th, Baden-Baden, Germany, **2**, 181-190.

Akan, A. O., and Yen, B. C., 1981. Diffusion-wave flood routing in channel networks. J. Hydraul. Div., Proc. Amer. Soc. Civil Eng., **107**(HY6), 719-732.

Amein, M., 1966. Streamflow routing on computer by characteristics. Water Resour. Res., **2**(1), 123-130.

Amein, M., and Fang, C. S., 1970. Implicit flood routing in natural channels. J. Hydraul. Div., Proc. Amer. Soc. Civil Eng., **96**(HY12), 2481-2500.

Amerman, C. R., 1965. The use of unit-source watershed data for runoff prediction. Water Resour. Res., **1**(4), 499-507.

Amerman, C. R., and McGuinness, J. L., 1967. Plot and small watershed runoff: its relation to large areas. Trans. Amer. Soc. Agril. Eng., **10**(4), 464-466.

Ames, W. F., 1969. Numerical methods for Partial Differential Equations. Thomas Nelson and Sons Ltd., 291 p.

Amorocho, J., 1963. Measures of the linearity of hydrologic systems. J. Geophys. Res., **68**(8), 2237-2249.

Amorocho, J., 1967. Role of infiltration in nonlinear watershed analysis processes. Trans. Amer. Soc. Agril. Eng., **10**(3), 396-399, 404.

Anderson, M. G., and Burt, T. P., 1982. The contribution of throughflow to storm runoff: an evaluation of a chemical mixing model. Earth Surface Processes and Landforms, **7**, 565-574.

Arbhabhirama, A., and Kridakorn, C., 1968. Steady downward flow to a water table. Water Resour. Res., **4**(6), 1249-1257.

Army, T. J., and Ostle, B., 1957. The association between free-water evaporation and evapotranspiration of spring wheat under the prevailing climatic conditions of the plains area of Montana. Soil Sci. Soc. Amer. Proc., **21**(5), 469-472.

Aston, M. J., 1970. Changes in internal water status and the gas exchange of leaves in response to ambient evaporative demand. Plant Response to Climatic Factors, Proc. Uppsala Symp., Published by UNESCO in 1973, 243-247.

Baier, W., 1969. Concepts of soil moisture availability and their effect on soil moisture estimates from a meteorological budget. Agril. Meteor., **6**, 165-178.

Balachandra, G., Unny, T. E., and Solomon, S. I., 1975. Potential evaporation as an unsteady process. J. Hydrol., **24**, 291-301.

Ball, J. T., 1987. Calculations related to gas exchange. Stomatal Function (Eds: E. Zeiger, G. D. Farquhar and I. R. Cowan), Stanford University Press, Stanford, California, 445-476.

Baltzer, R. A., and Lai, C., 1968. Computer simulation of unsteady flows in waterways. J. Hydraul. Div., Proc. Amer. Soc. Civil Eng., **94**(HY4), 1083-1117.

Baver, L. D., Gardner, W. H., and Gardner, W. R., 1972. Soil Physics. John Wiley & Sons, 498 p.

Bear, J., Zaslavsky, D., and Irmay, S., 1968. Physical Principles of Water Percolation and Seepage. Published by UNESCO, Paris.

Bear, J., 1988. Dynamics of Fluids in Porous Media. Dover Publications, Inc., NY, Chapter 8.

Becker, L., and Yeh, W. W.-G., 1972. Identification of parameters in unsteady open channel flows. Water Resour. Res., **8**(4), 956-965.

Bernier, P. Y., and Hewlett, J. D., 1982. Test of a revised source area simulator (VSAS2) on a forested basin. Can. Hydrol. Symp:82, Assoc. Committee on Hydrol., Nat. Res. Council Can., Fredericton, N.B., 404-418.

Bernier, P. Y., 1982. VSAS2: a revised source area simulator for small forested basins, Ph.D. dissertation, University of Georgia, Athens, Ga., 143 p.

Best, J. L., and Reid, I., 1984. Separation zone at open channel junctions. J. Hydraul. Eng., Amer. Soc. Civil Eng., **110**(HY11), 1588-1594.

Betson, R. P., 1964. What is watershed runoff? J. Geophys. Res., **69**(8), 1541-1552.

Beven, J. K., 1982. On subsurface stormflow: an analysis of response times. Hydrol. Sci. J., **27**, 505-521.

Beven, J. K., and Kirkby, M. J., 1979. A physically-based, variable contributing area model of basin hydrology. Hydrol. Sci. Bull., **24**, 43-69.

Beven, J. K., and Germann, P. F., 1982. Macropores and water flow in soils. Water Resour. Res., **18**(5), 1311-1325.

Beven, J. K., 1985. Distributed models. In: Hydrological Forecasting (Eds: M. G. Anderson and T. P. Burt), John Wiley and Sons, 405-435.

Bhuiyan, S. I., Hiler, E. A., van Bavel, C. H. M., and Aston, A. R., 1971. Dynamic simulation of vertical infiltration into unsaturated soils. Water Resour. Res., **7**(6), 1597-1606.

Blaney, H. F., and Criddle, W. D., 1950. Determining water requirements in irrigated areas from climatological and irrigation data. U.S. Dept. Agr., Soil Conservation Service Bull., Tech. Pap. 96, 48 p.

Blaney, H. F., 1956. Evaporation from free water surfaces at high altitudes. J. Irrig. Drain. Div., Proc. Amer. Soc. Civil Eng., **82**(IR3), Pap. 1104, 1-15.

Bonnell, M., Hendriks, M. R., Imeson, A. C., and Hazelhoff, L., 1984. The generation of storm runoff in a forested clayey drainage basin in Luxembourg. J. Hydrol., **71**, 53-77.

Borah, D. K., Prasad, S. N., and Alonso, C. V., 1980. Kinematic wave routing incorporating shock fitting. Water Resour. Res., **16**(3), 529-541.

Bouwer, H., 1965. Limitations of the Dupuit-Forhheimer assumption in recharge and seepage. Trans. Amer. Soc. Agril. Eng., **8**(4), 512-515.

Bouwer, H., 1966. Rapid field measurement of air entry value and hydraulic conductivity of soil as significant parameters in flow system analysis. Water Resour. Res., **2**(4), 729-738.

Brakensiek, D. L., 1967. A simulated watershed flow system for hydrograph prediction - a kinematic application. Proc. Inter. Hydrol. Symp., Fort Collins, Colorado.

Brakensiek, K. L., Engleman, R. L., and Rawls, W. J., 1981. Variation within texture classes of soil water parameters. Trans. Amer. Soc. Agril. Eng., **24**(2), 335-339.

Brebbia, C. A., 1978. The Boundary Element Method for Engineers. Pentech Press, London, 189 p.

Brebbia, C. A., and Walker, S., 1980. Boundary Element Techniques in Engineering. 210 p.

Bresler, E., 1973. Simultaneous transport of solutes and water under transient unsaturated flow conditions. Water Resour. Res., **9**(4), 975-986.

Bresler, E., 1987. Modeling of flow, transport and crop yield in spatially variable fields. In: Advances in Soil Science (Ed: B. A. Stewart), **7**, 1-51.

Brooks, R. H., and Corey, A. T., 1964. Hydraulic properties of porous media. Hydrology Pap. No.3, Colorado State University, Fort Collins, Colorado, 27 p.

Brooks, R. H., and Corey, A. T., 1966. Properties of porous media affecting fluid flow. J. Irrig. Drain. Div., Proc. Amer. Soc. Civil Eng., **92**(IR2), 61-68.

Brouwer, R., 1965. Water movement across the root. In: The State and Movement of Water in Living Organisms (Ed: G. E. Fogg), 19th Symp. Soc. Expt. Biol., Cambridge University Press, 131-149.

Brutsaert, W., 1967. Some methods of calculating unsaturated permeability. Trans. Amer. Soc. Agril. Eng., **10**(3), 400-404.

Brutsaert, W. F., 1971. A functional iteration for solving the Richards' equation applied to two-dimensional infiltration problems. Water Resour. Res., **7**(6), 1583-1596.

Brutsaert, W., 1982. Evaporation into the Atmosphere. D. Reidel Publishing Company, London, 300 p.

Budyko, M. I., 1956. The heat balance of the earth surface (translated by N. A. Stepanova). U.S. Dept. of Commerce, Washington.

Burt, T. P., 1986. Runoff process and solutional denudation rates on humid temperate hillslopes. In: Solute Processes (Ed: S. T. Trudgill), John Wiley and Sons, 193-250.

Burt, T. P., 1989. Storm runoff generation in small catchments in relation to the flood response of large basins. In: Floods: Hydrological, Sedimentological and Geomorphological Implications (Eds: J. K. Beven and P. Carling), John Wiley and Sons, 11-35.

Calver, A., Kirkby, M. J., and Weyman, D. R., 1972. Modelling hillslope and channel flow. In: Spatial Analysis in Geomorphology (Ed: R. J. Chorley), Methuen, London, 197-218.

Capece, J. C., Campbell, K. L., and Baldwin, L. B., 1988. Estimating runoff peak rates from flat, high-water-table watersheds. Trans. Amer. Soc. Agril. Eng., **31**(1), 74-81.

Carson, D. J., 1987. An introduction to the parameterization of land-surface processes part I. Radiation and turbulence. The Meteorological Magazine, **116**, 229-242.

Carson, D. J., 1987. An introduction to the parameterization of land-surface processes part II. Soil heat conduction and surface hydrology. The Meteorological Magazine, **116**, 263-279.

Carson, M. A., and Sutton, E. A., 1971. The hydrologic response of the Eaton River Basin, Quebec. Can. J. Earth Sci., **8**, 102-115.

Chanasyk, D. S., 1980. A Model to Evaluate the Hydrologic Response to Land Use Changes. Ph.D. thesis, Dept. of Civil Engineering, University of Alberta, Edmonton, Canada.

Chen, C. L., and Armbruster, J. T., 1980. Dam-break wave model; formulation and verification. J. Hydraul. Div., Proc. Amer. Soc. Civil Eng., **106**(HY5), 747-767.

Chevereau, G., Holly, F. M., and Preissmann, A., 1978. Can detailed hydraulic modeling be worthwhile when hydrologic data is incomplete? In: Urban Storm Drainage (Ed: P. R. Helliwell), Proc. Inter. Conf. 1st., 317-326.

Childs, E. C., 1972. Concepts of soil water phenomena. Soil Sci., **113**(4), 246-253.

Childs, E. C., and Collis-George, N., 1950. The permeability of porous materials. Proc. Roy. Soc., **A 201**, 392-405.

Chorley, R. J., 1978. The hillslope hydrological cycle. In: Hillslope Hydrology (Ed: M. J. Kirkby), John Wiley and Sons, 1-42.

Choudhury, B. J., and Monteith, J. L., 1986. Implications of stomatal response to saturation deficit for the heat balance of vegetation. Agril. Forest Meteor., **36**, 215-225.

Chow, V. T., 1959. Open Channel Hydraulics. McGraw-Hill, NY, 680 p.

Chow, V. T., 1964. Handbook of Applied Hydrology. McGraw-Hill.

Chow, V. T., and Kulandaiswamy, V. C., 1971. General hydrologic system model. J. Hydraul. Div., Proc. Amer. Soc. Civil Eng., **97**(HY6), 791-804.

Clark, C. O., 1945. Storage and the unit hydrograph. Trans. Amer. Soc. Civil Eng., **110**, Pap. 2261, 1419-1446.

Coen, G. M., and Wang, C., 1989. Estimating vertical saturated hydraulic conductivity from soil morphology in Alberta. Can. J. Soil Sci., **69**(1), 1-15.

Coles, N., and Trudgill, S. T., 1985. The movement of nitrate fertilizer from the soil surface to drainage waters by preferential flow in weakly saturated soils, Slapton, south Devon. Agriculture, Ecosystems and Environment, **13**, 241-259.

Collinge, V. K., and Jamieson, D. G., 1968. The spatial distribution of storm rainfall. J. Hydrol., **6**, 45-57.

Committee on Surface-Water Hydrology, 1965. Research needs in surface-water hydrology. J. Hydraul. Div., Proc. Amer. Soc. Civil Eng., **91**(HY1), 75-83.

Corey, A. T., 1986. Mechanics of Immiscible Fluids in Porous Media. Water Resources Publications, Littleton, Colorado, 255 p.

Coskun, E., Claborn, B. T., and Moore, W. L., 1969. Application of continuous accounting techniques to evaluate the effects of small structures on Mukewater Creek, Texas. In: Effects of Watershed Changes on Streamflow (Eds: W. L. Moore and C. W. Morgan), Water Res. Symp. No.2, Center for Res. in Water Resour., University of Texas at Austin, 79-99.

Covey, W., 1963. Mathematical study of the first stage of drying of moist soil. Soil Sci. Soc. Amer. Proc., **27**(2), 130-134.

Cowan, I. R., 1965. Transport of water in the soil-plant-atmosphere system. J. Appl. Ecology, **2**, 221-239.

Cowan, I. R., 1972. Oscillations in stomatal conductance and plant functioning associated with stomatal conductance: observations and a model. Planta (Berlin), **106**, 185-219.

Cowan, I. R., 1972. An electrical analogue of evaporation from, and flow of water in plants. Planta (Berlin), **106**, 221-226.

Cowan, I. R., 1977. Stomatal behaviour and environment. In: Advances in Botanical Research (Eds: R. D. Preston and H. W. Woolhouse), Academic Press, 177-228.

Crawford, N. H., and Linsley, R. K., 1966. Digital simulation in hydrology; Stanford Watershed Model IV. Dept. of Civil Eng., Stanford University, Tech. Rept. No.39.

Crawford, N. H., 1969a. Digital simulation methods for hydrological forecasting. In: Hydrological Forecasting, WMO Tech. Note No.92, 162-171.

Criddle, W. D., 1958. Methods of computing consumptive use of water. J. Irrig. Drain. Div., Proc. Amer. Soc. Civil Eng., **84**(IR1), Pap. 1507, 1-27.

Cunge, J. A., 1969. On the subject of a flood propagation computation method (Muskingum method). J. Hydraul. Res., **7**, 205-230.

Cunge, J. A., Holly, F. M., and Verwey, A., 1981. Practical Aspects of Computational River Hydraulics. Pitman, London.

Cunge, J. A., and Woolhiser, D. A., 1975. Irrigation systems. In: Unsteady Flow in Open-channels (Eds: K. Mahmood and V. Yevjevich), Water Resour. Pub., Littleton, Colorado, 509-537.

Cushman, J. H., Kirkham, D., and Keller, R. F., 1979. A Galerkin in time, linearized finite element model of 2-dimensional unsaturated porous media drainage. Soil Sci. Soc. Amer. J., **43**(4), 638-641.

Dagan, G., 1964. Spacing of drains by an approximate method. J. Irrig. Drain. Div., Proc. Amer. Soc. Civil Eng., **90**(IR1), 41-66.

Dane, J. H., and Wierenga, P. J., 1975. Effect of hysteresis on the prediction of infiltration, redistribution and drainage of water in a layered soil. J. Hydrol., **25**, 229-242.

Dane, J. H., and Mathis, F. H., 1981. An adaptive finite difference scheme for the one-dimensional water flow equation. Soil Sci. Soc. Amer. J., **45**(6), 1048-1054.

Davis, G. H., Lofgren, B. E., and Seymour, M., 1964. Use of ground-water reservoirs for storage of surface water in the San Joaquin Valley, California. U.S. Geol. Survey Water-Supply Pap. No. 1618.

Dawdy, D. R., and O'Donnell, T., 1965. Mathematical models of catchment behavior. J. Hydraul. Div., Proc. Amer. Soc. Civil Eng., **91**(HY4), 123-137.

Dawdy, D. R., and Bergmann, J. M., 1969. Effect of rainfall variability on streamflow simulation. Water Resour. Res., **5**(5), 958-966.

Dawdy, D. R., and Thompson, T. H., 1967. Digital computer simulation in hydrology. J. Amer. Water Works Assoc., **59**(6), 685-688.

Dawdy, D. R., Schaake, J. C., and Alley, W. M., 1978. User's Guide for Distributed Routing Rainfall-runoff Model. U.S. Geol. Survey Water Resour. Investigations, 78-79, 146 p.

de Marsily, G., 1986. Quantitative Hydrology. Academic Press.

Denmead, O. T., and Shaw, R. H., 1962. Availability of soil water to plants as affected by soil moisture content and meteorological conditions. Agronomy Journal, **54**, 385-390.

De Wiest, R. J. M., 1965. History of Dupuit-Forhheimer assumption in groundwater hydraulics. Trans. Amer. Soc. Agril. Eng., **8**, 508-509.

Diskin, M. H., and Boneh, A., 1973. Determination of optimal kernels for second-order stationary surface runoff systems. Water Resour. Res., **9**(2), 311-325.

Dolman, A. J., 1986. Estimates of roughness length and zero plane displacement for a foliated and non-foliated oak canopy. Agril. Forest Meteor., **36**, 241-248.

Dolman, A. J., 1988. Predicting forest transpiration from climatological data. Agril. Forest Meteor., **42**, 339-353.

Dooge, J. C. I., 1959. A general theory of the unit hydrograph. J. Geophys. Res., **64**(2), 241-256.

Dooge, J. C. I., 1968. The hydrologic cycle as a closed system. Inter. Assoc. Sci. Hydrol. Bull., **13**(1), 58-68.

Dooge, J. C. I., 1977. Problems and methods of rainfall-runoff modelling. In: Mathematical Models for Surface Water Hydrology (Eds: T. A. Ciriani, U. Maione, and J. R. Wallis), John Wiley and Sons, NY, 71-108.

Dooge, J. C. I., 1981. Parametrization of hydrologic processes. In: Land Surface Processes in Atmospheric General Circulation Models (Ed: P. S. Eagleson), Cambridge University Press, 243-288.

Doorenbos, J., and Pruitt, W. O., 1977. Crop Water Requirements. FAO Irrig. Drain. Pap. 24.

Dos Santos Jr., A. G., and Youngs, E. G., 1969. A study of the specific yield in land-drainage situations. J. Hydrol., **8**, 59-81.

Drinkwater, W. O., and Janes, B. E., 1957. Relation of potential evapotranspiration to environment and kind of plant. Trans. Amer. Geophys. Union, **38**(4), 524-528.

Dumm, L. D., 1954. New formula for determining depth and spacing of subsurface drains in irrigated lands. Agricultural Engineering, **35**, 726-730.

Dumm, L. D., 1964. Transient-flow concept in subsurface drainage: its validity and use. Trans. Amer. Soc. Agril. Eng., **7**(2), 142-146.

Dumm, L. D. and Winger Jr., R. J., 1964. Subsurface drainage system design for irrigated area using transient-flow concept. Trans. Amer. Soc. Agril. Eng., **7**(2), 147-151.

Dunne, T., and Black, R. G., 1970a. Experimental investigation of runoff production in permeable soils. Water Resour. Res., **6**(2), 478-490.

Dunne, T., 1978. Field studies of hillslope flow processes. In: Hillslope Hydrology (Ed: M. J. Kirkby), John Wiley and Sons, 227-293.

Eagleson, P. S., 1967. A linear distributed model for peak catchment discharge. Proc. Inter. Hydrol. Symp., Fort Collins, Colorado, **1**, 1-8.

Eagleson, P. S., 1970. Dynamic Hydrology. McGraw-Hill, NY, 462 p.

East China College of Hydraulic Engineering, 1977. Flood Forecasting Methods for Humid Regions of China. Nanjing, China.

Edlefsen, N. E., and Anderson, A. B. C., 1943. Thermodynamics of soil moisture. Hilgardia, **15**(2), 31-298.

Edson, C. G., 1951. Parameters for relating unit hydrographs to watershed characteristics. Trans. Amer. Geophys. Union, **32**(4), 591-596.

Emmett, W. W., 1978. Overland flow. In: Hillslope Hydrology (Ed: M. J. Kirkby), John Wiley and Sons., NY, 145-176.

England, C. B., and Stephenson, G. R., 1970. Response units for evaluating the hydrologic performance of rangeland watersheds. J. Hydrol., **11**, 89-97.

England, L. A., and Freeze, R. A., 1988. Finite element simulation of long-term transient regional groundwater flow. Ground Water, **26**(3), 298-308.

Fayer, M. J., and Hillel, D., 1982. Field testing of a two-dimensional soil moisture model simulating water table fluctuations. Soil Sci. Soc. Amer. J., **46**(2), 396-404.

Feddes, R. A., Bresler, E., and Neuman, S. P., 1974. Test of modified numerical model for water uptake by root systems. Water Resour. Res., **10**(6), 1199-1206.

Feddes, R. A., Kowalik, P. J., and Zaradny, H., 1978. Simulation of Field Water Use and Crop Yield. John Wiley and Sons., NY, 188 p.

Finnigan, J. J., and Raupach, M. R., 1987. Transfer processes in plant canopies in relation to stomatal characteristics. In: Stomatal Function (Eds: E. Zeiger, G. D. Farquhar and I. R. Cowan), Stanford University Press, Stanford, California, 383-443.

Fletcher, A. G., and Hamilton, W. S., 1967. Flood routing in an irregular channel. J. Eng. Mech. Div., Proc. Amer. Soc. Civil Eng., **93**(EM3), 45-62.

Fread, D. L., 1973a. Effects of time step size in implicit dynamic routing. Water Resour. Bull., **9**(2), 338-351.

Fread, D. L., 1973b. Technique for implicit dynamic routing in rivers with tributaries. Water Resour. Res., **9**(4), 918-926.

Fread, D. L., 1974. Numerical properties of implicit four-point finite difference equations of unsteady flow. NOAA Tech. Memo. NWS, HYDRO-18, U.S. National Weather Service, Silver Spring, Maryland.

Freeze, R. A., and Witherspoon, P. A., 1966. Theoretical analysis of regional groundwater flow. 1. Analytical and numerical solutions to the mathematical model. Water Resour. Res., **2**(4), 641-656.

Freeze, R. A., and Witherspoon, P. A., 1967. Theoretical analysis of regional groundwater flow. 2. Effect of water-table configuration and subsurface permeability variation. Water Resour. Res., **3**(2), 623-634.

Freeze, R. A., 1969. The mechanism of natural ground-water recharge and discharge. 1. One-dimensional, vertical, unsteady, unsaturated flow above a recharging or discharging ground-water flow system. Water Resour. Res., **5**(1), 153-171.

Freeze, R. A., 1971a. Three-dimensional, transient, saturated-unsaturated flow in a groundwater basin. Water Resour. Res., **7**(2), 347-366.

Freeze, R. A., 1971b. Influence of unsaturated flow domain on seepage through earth dams. Water Resour. Res., **7**(4), 929-941.

Freeze, R. A., 1972a. Role of subsurface flow in generating surface runoff. 1. Baseflow contribution to channel flow. Water Resour. Res., **8**(3), 609-623.

Freeze, R. A., 1972b. Role of subsurface flow in generating surface runoff. 2. Upstream source areas. Water Resour. Res., **8**(5), 1272-1283.

Freeze, R. A., 1978. Mathematical models of hillslope hydrology. In: Hillslope Hydrology (Ed: M. J. Kirkby), John Wiley and Sons, NY, 177-225.

Freeze, R. A., 1986. Modelling interrelationships between climate, hydrology and hydrogeology and the development of slopes. In: Slope Stability (Eds: M. G. Anderson and K. S. Richards), John Wiley and Sons, 381-404.

Freeze, R. A., and Harlan, R. L., 1969. Blueprint for a physically-based, digitally-simulated hydrologic response model. J. Hydrol., **9**, 237-258.

Freeze, R. A., and Cherry, J. A., 1979. Groundwater. Prentice-Hall Inc., NJ, 604 p.

Frind, E. O., and Verge, M. J., 1978. Three-dimensional modeling of groundwater flow systems. Water Resour. Res., **14**(5), 844-856.

Gardner, W. R., 1956. Calculation of capillary conductivity from pressure plate outflow data. Soil Sci. Soc. Amer. Proc., **20**(3), 317-320.

Gardner, W. R., 1958. Some steady-state solutions of the unsaturated moisture flow equation with application to evaporation from a water table. Soil Sci., **85**(4), 228-232.

Garratt, J. R., 1984. The measurements of evaporation by meteorological methods. In: Evapotranspiration from Plant Communities (Ed: M. L. Sharma), Elsevier Sci. Publishers, 99-117.

Gerald, C. F., 1980. Applied Numerical Analysis. 2nd edn., Addison-Wesley Publishing Company, 518 p.

Germann, P. F., 1986. Rapid response to precipitation. Hydrological Processes, **1**, 3-14.

Gilman, K., and Newson, M. D., 1980. Soil pipes and pipeflow: a hydrological study in upland Walse. British Geomorphological Res., Group Res. Monograph No.1, Geobooks, Norwich, 110 p.

Glover, R. E., 1965. Application of Dupuit-Forhheimer assumptions in groundwater hydraulics. Trans. Amer. Soc. Agril. Eng., **8**(4), 510-512.

Glover, R. E., 1974. Transient Groundwater Hydraulics. Fort Collins, Colorado.

Gollan, T., Turner, N. C., and Schulze, E.-D., 1985. The response of stomata and leaf gas exchange to vapour pressure deficits and soil water content III. In the sclerophyllous woody species *Nerium oleander*. Oecologia (Berlin), **65**, 356-362.

Gray, W. G., 1982. Comparison of finite difference and finite element methods. In: Fundamental of Transport Phenomena in Porous Media (Ed: J. Bear), NATO ASI Series No.82, 899-952.

Green, W. H., and Ampt, G. A., 1911. Studies on soil physics. Part 1. The flow of air and water through soils. J. Agril. Sci., **4**(1), 1-24.

Green, H. W., and Ampt, G. A., 1912. Studies on soil physics. Part 2. The permeability of an ideal soil to air and water. J. Agril. Sci., **5**(1), 1-26.

Green, R. E., Hanks, R. J., and Larson, W. E., 1964. Estimates of field infiltration by numerical solution of the moisture flow equation. Soil Sci. Soc. Amer. Proc., **28**(1), 15-19.

Greminger, P. J., Sud, Y. K., and Nielsen, D. R., 1985. Spatial variability of field measured soil-water characteristics. Soil Sci. Soc. Amer. J., **49**(5), 1075-1081.

Grindley, J., 1969: The calculation of actual evaporation and soil moisture deficit over specific catchment areas. Hydrol. Mem. No.38, Meteorological Office, Bracknell, Berkshire, U.K.

Gupta, S. K., and Tanji, K. K., 1977. Computer program for solution of large, sparse, unsymmetric systems of linear equations. Inter. J. Num. Meth. Eng., **11**, 1251-1259.

Haan, C. T., 1972a. A water yield model for small watersheds. Water Resour. Res., **8**(1), 58-69.

Haan, C. T., 1972b. Adequacy of hydrologic records for parameter estimation. J. Hydraul. Div., Proc. Amer. Soc. Civil Eng., **98**(HY8), 1387-1393.

Halstead, M. H., and Covey, W., 1957. Some meteorological aspects of evapotranspiration. Soil Sci. Soc. Amer. Proc., **21**(5), 461-464.

Hamon, W. R., 1966. Evapotranspiration and water yield predictions. Amer. Soc. Agril. Eng., Conf. Proc.13, 8-9.

Hanks, R. J., and Bowers, S. A., 1962. Numerical solution of the moisture flow equation for infiltration into layered soils. Soil Sci. Soc. Amer. Proc., **26**(6), 530-534.

Hanks, R. J. and Bowers, S. A., 1963. Influence of variations in the diffusivity-water content relation on infiltration. Soil Sci. Soc. Amer. Porc., **27**(3), 263-265.

Hansen, S., 1984. Estimation of potential and actual evapotranspiration. Nordic Hydrology, **15**, 205-212.

Harr, M. E., 1962. Groundwater and Seepage. McGraw-Hill, NY.

Haverkamp, R., Vauclin, M., Touma, J., Wierenga, P. J., and Vachaud, G., 1977. A comparison of numerical simulation models for one-dimensional infiltration. Soil Sci. Soc. Amer. J., **41**(2), 285-294.

Hayhoe, H. N., 1978. Numerical study of quasi-analytic and finite difference solutions of the soil-water transfer equation. Soil Sci., **125**(2), 68-74.

Henderson, F. M., 1963. Flood waves in prismatic channels. J. Hydraul. Div., Proc. Amer. Soc. Civil Eng., **89**(HY4), 39-67.

Henderson, F. M., 1966. Open-channel Flow. McMillan Co., NY, 522 p.

Henderson, F. M., and Wooding, R. A., 1964. Overland flow and groundwater flow from a steady rainfall of finite duration. J. Geophys. Res., **69**(8), 1531-1540.

Hewlett, J. D., 1961. Soil moisture as a source of base flow from steep mountain watershed. U.S. Forestry Service, Southeastern Forest, Expt. Sta. Res. Pap. SE132, 11 p.

Hewlett, J. D., and Hibbert, A. R., 1967. Factors affecting the response of small watersheds to precipitation in humid areas. In: International Symposium on Forest Hydrology (Eds: W. E. Sopper and H. W. Lull), Pergamon Press, 275-290.

Hewlett, J. D., and Troendle, C. A., 1975. Non-point and diffused water sources: A variable source area problem. In: Watershed Management, Symp. Proc., Amer. Soc. Civil Eng., Irrig. Drain. Div., Logan, Utah, 21-46.

Hewlett, J. D., Fortson, J. C., and Cunningham, G. B., 1977. The effect of rainfall intensity on storm flow and peak discharge from forest land. Water Resour. Res., **13**(2), 259-266.

Hewlett, J. D., 1982. Principle of Forest Hydrology. University of Georgia Press, Athens, Ga.

Higgins, D. T., 1980. Unsteady drawdown in 2-D water table aquifer. J. Irrig. Drain. Div., Proc. Amer. Soc. Civil Eng., **106**(IR3), 237-251.

Hillel, D., and van Bavel, C. H. M., 1976. Simulation of profile water storage as related to soil hydraulic properties. Soil Sci. Soc. Amer. J., **40**(6), 807-815.

Hillel, D., 1977. Computer Simulation of Soil Water Dynamics: A Compendium of Recent Works. Ottawa, IDRC.

Hillel, D., 1982. Soil Physics. Academic Press.

Hillman, G. R., 1983. SUBFEM: A Subsurface Flow Model for a Forest Environment. Ph.D. thesis, Dept. of Civil Engineering, University of Alberta, Edmonton, Canada.

Hitchon, B., 1969. Fluid flow in the Western Canada sedimentary basin. 1. Effect of topography. Water Resour. Res., **5**(1), 186-195.

Holecek, G. R., 1967. Spring Creek Watershed Investigation. Annual Report No.1, Alberta Dept. of Agriculture, Water Resour. Div., Hydrology Branch.

Holtan, H. N., 1961. A concept for infiltration estimates in watershed engineering. U.S. Dept. Agric., Agril. Res. Service pub., 41-51.

Holtan, H. N., and Creitz, N. R., 1967. Influence of soils, vegetation and geomorphology on elements of the flood hydrograph. In: Floods and their Computation, Proc. of the Leningrad Symp. (IASH-Unesco-WMO), **2**, 755-766.

Holtan, H. N., England, C. B., and Shanholtz, V. O., 1967. Concepts in hydrologic soil grouping. Trans. Amer. Soc. Agril. Eng., **10**(3), 407-410.

Holtan, H. N., 1970. Representative and experimental basins as dispersed system. Proc. of a Symp. on Representative and Experimental Basins, Wellington, N.Z., Inter. Assoc. Sci. Hydrol. Pub. No. 96, **1**, 112.

Hornberger, G. M., and Remson, I., and Fungaroli, A. A., 1969. Numerical studies of a composite soil moisture ground-water system. Water Resour. Res., **5**(4), 797-802.

Hornung, U., 1977. A numerical method for the simulation of unsteady groundwater flow in both saturated and unsaturated soils. Soil Sci., **124**(3), 140-144.

Horton, R. E., 1933. The role of infiltration in the hydrologic cycle. Trans. Amer. Geophys. Union, **14**, 446-460.

Horton, R. E., 1939. Analysis of runoff-plat experiments with varying infiltration-capacity. Trans. Amer. Geophys. Union, **20**, 693-711.

Horton, R. E., 1940. An approach toward a physical interpretation of infiltration-capacity. Soil Sci. Soc. Amer. Proc., **5**, 399-417.

Hubbert, M. K., 1940. The theory of ground-water motion. J. Geol., **48**(8), pt.1, 785-944.

Hudlow, M. D., and Clark, R. A., 1969. Hydrograph synthesis by digital computer. J. Hydraul. Div., Proc. Amer. Soc. Civil Eng., **95**(HY3), 839-860.

Hursh, G. R., 1944. Appendix-B Report of sub-committee on subsurface-flow. Trans. Amer. Geophys. Union. **25**(5), 743-746.

Ibbitt, R. P., 1972. Effects of random data errors on the parameter values for a conceptual model. Water Resour. Res., **8**(1), 70-78.

Ibbitt, R. P., 1972b. Report on symposium on uncertainties in hydrologic and water resources systems. Tuscon, J. Hydrol. (New Zealand), **11**, 140-143.

Ibrahim, H. A., and Brutsaert, W., 1968. Intermittent infiltration into soils with hysteresis. J. Hydraul. Div., Proc. Amer. Soc. Civil Eng., **94**(HY1), 113-137.

Jackson, R. D., Reginato, R. J., and van Bavel, C. H. M., 1965. Comaprison of measured and calculated hydraulic conductivities of unsaturated soils. Water Resour. Res., **1**(3), 375-380.

Jackson, R. D., Pinter Jr., P. J., and Reginato, R. J., 1985. Net radiation calculated from remote multispectral and ground station meteorological data. Agril. Forest Meteor., **35**, 153-164.

James, L. D., 1972. Hydrologic modelling, parameter estimation, and watershed characteristics. J. Hydrol., **17**, 283-307.

Jamieson, D. G., and Wilkinson, J. C., 1972. River Dee Research Program 3. A short-term control strategy for multipurpose reservoir systems. Water Resour. Res., **8**(4), 911-920.

Jarboe, J. E., and Haan, C. T., 1974. Calibrating a water yield model for small ungaged watersheds. Water Resour. Res., **10**(2), 256-262.

Jarvis, P. G., Edwards, W. R. N., and Talbot, H., 1981. Models of plant and crop water use. In: Mathematics and Plant Physiology (Eds: D. A. Rose and D. A. Edwards), Academic Press, 151-194.

Javandel, I., and Witherspoon, P. A., 1969. A method of analyzing transient fluid flow in multilayered aquifers. Water Resour. Res., **5**(4), 856-869.

Jensen, K. H., 1981. Application of soil water flow theory in field situation. Nordic Hydrology, **12**, 167-184.

Jensen, M. E., and Haise, H. R., 1963. Estimating evapotranspiration from solar radiation. J. Irrig. Drain. Div., Proc. Amer. Soc. Civil Eng., **89**(IR4), 15-41.

Joliffe, I. B., 1982. Comparison of Implicit Finite Difference Methods to Solve the Unsteady Open Channel Flow Equations. Water Resources Engineering Report, WRE 82-1, Department of Civil Engineering, University of Alberta, Edmonton, 134 p.

Joliffe, I. B., 1984b. Computation of dynamic waves in channel networks. J. Hydraul. Eng., Amer. Soc. Civil Eng., **110**(HY10), 1358-1370.

Jonch-Causen, T., 1979. Systeme Hydrologique Europeen: a short description. Danish Hydraulics Institute, Horsholm, Denmark.

Jones, A., 1971. Soil piping and stream channel initiation. Water Resour. Res., **7**(3), 602-610.

Jones, H. E., and Kohnke, H., 1952. The influence of soil moisture tension on vapor movement of soil water. Soil Sci. Soc. Amer. Proc., **16**(3), 245-248.

Jones, J. A. A., 1981. The nature of soil piping: a review of research. British Geomorphological Res. Group Res. Monograph No.3, Geo Books, Norwich.

Jones, J. R., 1976. Physical data for catchment models. Nordic Hydrol., **7**, 245-264.

Katopodes, N. D., 1982. On zero-inertia and kinematic waves. J. Hydraul. Div., Proc. Amer. Soc. Civil Eng., **108**(HY11), 1380-1387.

Katopodes, N. D., 1984. Fourier analysis of dissipative Finite Element Method channel flow model. J. Hydraul. Eng., Amer. Soc. Civil Eng., **110**(7), 927-944.

Keey, R. B., 1972. Drying Principles and Practices. First edition, Pergamon Press, 358 p.

Kempthorne, O., and Allmaras, R. R., 1965. Errors of observation. In: Methods of Soil Analysis, pt.1 (Ed.-in-Chief: C. A. Black), 1-23.

Kibler, D. F., and Woolhiser, D. A., 1970. The kinematic cascade as a hydrologic model. Hydrol. Pap. No.39, Fort Collins, Colorado, 28 p.

Kirkby, M. J., and Chorley, R. J., 1967. Throughflow, overland flow and erosion. Inter. Assoc. Sci. Hydrol. Bull., **12**(3), 5-21.

Kirkby, M. J., 1969. Infiltration, throughflow and overland flow. In: Water, Earth and Man (Ed: R. J. Chorley), 215-228.

Kirkby, M. J., and Weyman, D. R., 1974. Measurements of contributing area in very small drainage basins. University Of Bristol, Department of Geography, Seminar Paper, Series B, No.3.

Kirkham, D., 1967. Explanation of paradoxes in Dupuit-Forchheimer seepage theory. Water Resour. Res., **3**(2), 609-622.

Kirkham, D., and Powers, W. L., 1972. Advanced Soil Physics. Wiley-Interscience, Chapter 7.

Klute, A., 1952. A numerical method for solving the flow equation for water in unsaturated materials. Soil Sci., **73**(2), 105-116.

Klute, A., 1965. Laboratory measurement of hydraulic conductivity of unsaturated soil. In: Methods of Soil Analysis, pt.1 (Ed.-in-Chief: C. A. Black), 253-261.

Klute, A., 1965. Water diffusivity. In: Methods of Soil Analysis, pt.1 (Ed.-in-Chief: C. A. Black), 262-272.

Klute, A., 1965. Water capacity. In: Methods of Soil Analysis, pt.1 (Ed.-in-Chief: C. A. Black), 273-278.

Klute, A., 1972. The determination of the hydraulic conductivity and diffusivity of unsaturated soils. Soil Sci., **113**(4), 264-276.

Klute, A., and Whisler, F. D., and Scott, E. J., 1965. Numerical solution of the nonlinear diffusion equation for water flow in a horizontal soil column of finite length. Soil Sci. Soc. Amer. Proc., **29**(4), 353-358.

Kohnke, H., and Werkhoven, C. H., 1963. Soil temperature and soil freezing as affected by an organic mulch. Soil Sci. Soc. Amer. Proc., **27**(1), 13-17.

Korzun, V. I., 1978. World Water Balance and Water Resources of the Earth. Published by UNESCO.

Kostiakov, A. N., 1932. On the dynamics of the coefficient of water percolation in soils and on the necessity of studying it from a dynamic point of view for purposes of amelioration. Moscow: Trans. 6th Com. Inter. Soc. Soil Sci., pt.A, 17-21.

Koussis, A. D., 1980. Comparison of Muskingum method difference schemes. J. Hydraul. Div., Proc. Amer. Soc. Civil Eng., **108**(HY5), 925-929.

Kozeny, J., 1927. Uber Kapillare leitun des wassers im l boden, sitzungsber akad. wiss, wein 136, 271-306. (Citation is from a translation by W. F. Striedieck and C. M. Davis, published by the Petroleum Branch of AIME).

Kraijenhoff van de Leur, D. A., 1958. A study of nonsteady groundwater flow with special reference to a reservoir-coefficient. De Ingenieur, **70B**, 87-94.

Kunze, R. J., Uehara, G., and Graham, K., 1968. Factors important in the calculation of hydraulic conductivity. Soil Sci. Soc. Amer. Proc., **32**(6), 760-765.

Lai, C., 1969. A computer simulation study of traveltimes of injected particles and tide-wave in well-mixed estuaries. Proc. Congr. Inter. Assoc. Hydraul. Res., 13th, Kyoto, Japan, **3**, 123-130.

Lai, C., 1986. Numerical modeling of unsteady open channel flow. In: Advances in Hydroscience (Ed. B. C. Yen), **14**, 161-333.

Laliberte, G. E., Corey, A. T., and Brooks, R. H., 1966. Properties of unsaturated porous media. Hydrol. Pap. No.17, Fort Collins, Colorado.

Lemon, E. R., Glaser, A. H., and Satterwhite, L. E., 1957. Some aspects of the relationship of soil, plant, and meteorological factors to evapotranspiration. Soil Sci. Soc. Amer. Proc., **21**(5), 464-468.

Leutheusser, H. J., and Chishom, W. O., 1973. Extreme roughness of natural channels. J. Hydraul. Div., Proc. Amer. Soc. Civil Eng., **99**(HY7), 1027-1042.

Liggett, J. A., 1968. Mathematical flow determination in open channels. J. Eng. Mech. Div., Proc. Amer. Soc. Civil Eng., **94**(EM4), 947-963.

Liggett, J. A., and Woolhiser, D. A., 1967. Difference solutions of shallow-water equation. J. Eng. Mech. Div., Proc. Amer. Soc. Civil Eng., **93**(EM2), 39-71.

Liggett, J. A., and Woolhiser, D. A., 1969. Closure to discussion of 'Difference solutions of the shallow-water equation'. J. Eng. Mech. Div., Proc. Amer. Soc. Civil Eng., **95**(EM1), 303-311.

Liggett, J. A., 1975. Basic equations of unsteady flow. In: Unsteady Flow in Open-channels (Eds: K. Mahmood and V. Yevjevich), Water Resour. Pub., Littleton, Colorado, 29-62.

Liggett, J. A., and Cunge, J. A., 1975. Numerical methods of solution of the unsteady flow equation. In: Unsteady Flow in Open Channels (Eds: K. Mahmood and V. Yevjevich), **1**, Water Resour. Pub., Littleton, Colorado.

Liggett, J. A., and Taigbenu, A. E., 1986. Calculation of diffusion, advection-diffusion and Boussinesq flow by integral methods. In: Finite Elements in Water Resources

(Eds: A. S. Costa, A. M. Baptista, W. G. Gray, C. A. Brebbia and G. F. Pinder), Proc. 6th Inter. Conf., Lisboa, Portugal, 723-733.

Lighthill, M. J., and Whitham, G. B., 1955. On kinematic waves. I. Flood movements in long rivers. Proc. Roy. Soc., London, **229 A** (1178), 281-316.

Lin, J. D., and Soong, H. K., 1979. Junction losses in open channel flows. Water Resour. Res., **15**(2), 414-418.

Linsley, R. K., Kohler, M. A., and Paulhus, J. L. H., 1958. Hydrology for Engineers. McGraw-Hill, NY.

Linsley, R. K., Kohler, M. A., and Paulhus, J. L. H., 1975. Hydrology for Engineers. 2nd edn., McGraw-Hill.

Maasland, M., 1959. Water table fluctuations induced by intermittent recharge. J. Geophys. Res., **64**(5), 549-559.

Maddaus, W. O., and Eagleson, P. S., 1969. A distributed linear representation of surface runoff. Rept. 115, Hydrodynamics Laboratory, MIT, Cambridge, Massachusetts.

Makkink, G. F., and van Heemst, H. D. J., 1956. The actual evapotranspiration as a function of the potential evapotranspiration and the soil moisture tension. Neth. J. Agril. Sci., **4**, 67-72.

Mandeville, A. N., O'Donnell, T., 1973. Introduction of time variance to linear conceptual catchment models. Water Resour. Res., **9**(2), 298-310.

Markar, M. S., and Mein, R. G., 1987. Modeling of evapotranspiration from homogeneous soils. Water Resour. Res., **23**(10), 2001-2007.

Marshall, T. J., 1958. A relation between permeability and size distribution of pores. J. Soil Sci., **9**(1), 1-8.

Marshall, T. J., and Holmes, J. W., 1979. Soil Physics. Cambridge University Press, NY.

Martz, L. W., 1978. The Sediment Yield of Spring Creek Watershed. Report no.1978/3, Research Secretariat, Alberta Environment, Edmonton.

Masch, F. D., and Denny, K. J., 1966. Grain size distribution and its effect on the permeability of unconsolidated sands. Water Resour. Res., **2**(4), 665-677.

McIlroy, I. C., 1984. Terminology and concepts in natural evaporation. In: Evapotranspiration from Plant Communities (Ed: M. L. Sharma), Elsevier Sci. Publishers, 77-98.

McIntosh, D. H., and Thom, A. S., 1983. Essentials of Meteoroloy. The Wykeham Sci. Series, Taylor and Francis Ltd., London, 240 p.

Meidner, H., 1965. Stomatal control of transpirational water loss. In: The State and Movement of Water in Living Organisms (Ed: G. E. Fogg), 19th Symp. Soc. Expt. Biol., Cambridge University Press, 185-203.

Mein, R. G., and Larson, C. L., 1973. Modeling infiltration during a steady rain. Water Resour. Res., **9**(2), 384-394.

Meyer, W. S., 1985. Enclosing leaves for water potential measurement and its effect on interpreting soil-induced water stress. Agril. Forest Meteor., **35**, 187-192.

Miller, R. D., and Richard, F., 1952. Hydraulic gradients during infiltration in soils. Soil Sci. Sco. Amer. Proc., **16**(1), 33-38.

Millington, R. J., and Quirk, J. P., 1961. Permeability of porous solids. Trans. Faraday Soc., **57**, 1200-1207.

Milly, P. C. D., 1987. Estimation of Brooks-Corey parameters from water retention data. Water Resour. Res., **23**(6), 1085-1089.

Monteith, J. L., 1965. Evaporation and environment. In: The State and Movement of Water in Living Organisms (Ed: G. E. Fogg), 19th Symp. Soc. Expt. Biol., Cambridge University Press, 205-234.

Monteith, J. L., 1973. Principles of Environmental Physics. Edward Arnold, London, 241p.

Monteith, J. L., 1980. The development and extension of Penman's evaporation formula. In: Application of Soil Physics (Ed: D, Hillel), Academic Press, NY, 247-252.

Monteith, J. L., 1981. Evaporation and surface temperature. Quart. J. Roy. Meteor. Soc., **107**(451), 1-27.

Moore, C. J., 1976. Eddy flux measurements above a pine forest. Quart. J. Roy. Meteor. Soc., **102**(434), 913-918.

Moore, R. E., 1939. Water conduction from shallow water tables. Hilgardia, **12**(6), 383-426.

Morgali, J. R., and Linsley, R. K., 1965. Computer analysis of overland flow. J. Hydraul. Div., Proc. Amer. Soc. Civil Eng., **91**(HY5), 81-100.

Morris, E. M., and Woolhiser, D. A., 1980. Unsteady one-dimensional flow over a plane: partial equilibrium and recession hydrographs. Water Resour. Res., **16**(2), 355-360.

Mosley, M. P., 1979. Streamflow generation in a forested watershed, New Zealand. Water Resour. Res., **15**(4), 795-806.

Muskat, M., 1946. The Flow of Homogeneous Fluids Through Porous Media. J. W. Edwards Inc., Michigan.

Narasimhan, T. N., and Witherspoon, P. A., 1976. An integrated difference method for analysing fluid flow in porous media. Water Resour. Res., **12**(1), 57-64.

Nash, J. E., 1957. The form of the instantaneous unit hydrograph. Inter. Assoc. Sci. Hydrol. Pub. No.45, **3**, 114-121.

Nash, J. E., 1959. Systematic determination of unit hydrograph parameters. J. Geophys. Res., **64**(1), 111-115.

Nash, J. E., 1960. A unit hydrograph study with particular reference to British catchments. Proc. Inst. Civil Eng., **17**, 249-282.

Nash, J. E. and Sutcliffe, J. V., 1970. River flow forecasting through conceptual models. I. A discussion of principles. J. Hydrol., **10**, 282-290.

Nash, J. E., and Sutcliffe, J. V., 1971. Reply to comment by G. Fleming on 'River flow forecasting through conceptual models'. J. Hydrol., **13**, 357-359.

Nash, J. E., 1983. Applied Hydrology-1 (deterministic). Unpublished Lecture Notes, Dept. of Engineering Hydrology, University College Galway, Ireland.

Neil, C. R., Kellerhals, R., and Bray, D. I., 1972. Hydraulic and Geomorphic Characteristics of Rivers in Alberta. A publication of the Alberta Cooperative Research Program in Highway and River Engineering. Department of the Environment - Water Resources Division, Research Council of Alberta.

Neuman, S. P., Feddes, R. A., and Bresler, E., 1975. Finite element analysis of two-dimensional flow in soils considering water uptake by roots. I. Theory and II. field applications. Soil Sci. Soc. Amer. Proc., **39**(2), 224-237.

Newman, E. I., 1969. Resistance to water flow in soil and plant. I. Soil resistance in relation to amounts of root: theoretical estimates. J. Appl. Ecology, **6**, 1-12.

Newman, E. I., 1969. Resistance to water flow in soil and plant. II. A review of experimental evidence on the rhizosphere resistance. J. Appl. Ecology, **6**, 261-272.

Nielsen, D. R., Kirkham, D., and Perrier, E. R., 1960. Soil capillary conductivity: comparison of measured and calculated values. Soil Sci. Soc. Amer. Proc., **24**(3), 157-160.

Nielsen, D. R., Kirkham, D., and van Wijk, W. R., 1961. Diffusion equation calculations of field soil water infiltration profiles. Soil Sci. Soc. Amer. Proc., **25**(3), 165-168.

Nielsen, D. R., Davidson, J. M., Bigger, J. W., and Miller, R. J., 1964. Water movement through Panoche clay loam soil. Hilgardia, **35**(17), 491-505.

Nielsen, D. R., Bigger, J. W., and Miller, R. J., 1967. Field observations of infiltration and soil-water redistribution. Trans. Amer. Soc. Agril. Eng., **10**(3), 382-387, 410..

Nielsen, D. R., Bigger, J. W., and Erh, K. T., 1973. Spatial variability of field-measured soil-water properties. Hilgardia, **42**(7), 215-259.

Nimah, M. N., and Hanks, R. J., 1973. Model for estimating soil water, plant, and atmospheric interrelations. I. Description and sensitivity. Soil Sci. Soc. Amer. Proc., **37**(4), 522-527.

Nimah, M. N., and Hanks, R. J., 1973. Model for estimating soil water, plant, and atmospheric interrelations. II. Field test of model. Soil Sci. Soc. Amer. Proc., **37**(4), 528-532

Norman, J. M., and Campbell, G., 1983. Application of a plant-environment model to problems in irrigation. In: Advances in Irrigation (Ed: D. Hillel), Academic Press, **2**, 155-188.

O'Brien, G. G., Hyman, M. A., and Sidney, K., 1950. A study of numerical solution of partial differential equations. J. Math. Physic., **29**, 223-251.

O'Connel, P. E., 1988. Hydrological systems modelling: a historical perspective. NATO ASI Lecture Series, Sintra, Portugal.

O'Loughlin, E. M., 1981. Saturation regions in catchments and their relations to soil and topographic properties. J. Hydrol., **53**, 229-246.

O'Loughlin, E. M., 1986. Prediction of surface and saturated zones in natural catchments by topographic analysis. Water Resour. Res., **22**(5), 794-804.

Onstad, C. A., and Brakensiek, D. L., 1968. Watershed simulation by stream path analogy. Water Resour. Res., **4**(5), 965-971.

Onstad, C. A., and Jamieson, D. G., 1970. Modeling the effects of land use modifications of runoff. Water Resour. Res., **6**(5), 1287-1295.

Ophori, D. U., and To'th, J., 1989. Characterization of groundwater flow by field mapping and numerical simulation, Ross Creek basin, Alberta, Canada. Ground Water, **27**(2), 193-201.

Osborn, H. B., 1983. Precipitation characteristics affecting hydrologic response of southwestern rangelands. Agril. Rev. and Mannuals, ARM-W-34, Agril. Res. Service, U.S. Dept. of Agriculture, Western Region, California.

Overton, D. E., 1966. Hydraulics in synthesis of upland runoff hydrographs. Trans. Amer. Soc. Agril. Eng., **9**(4), 543-545, 549.

Parlange, J.-Y., 1971. Theory of water-movement in soils: 1. One-dimensional absorption. Soil Sci., **111**(2), 134-137.

Parlange, J.-Y., 1971. Theory of water movement in soils: 2. One-dimensional infiltration. Soil Sci., **111**(3), 170-174.

Parlange, J.-Y., and Brutsaert, W., 1987. A capillary correction of free surface flow of groundwater. Water Resour. Res., **23**(5), 805-808.

Parr, J. F., and Papendick, R. I., 1971. Interactions of microbial metabolism and soil physical properties and heir significance in some hydrologic processes. Proc. 3rd Inter. Seminar for Hydrol. Professors, 82-102.

Patankar, S. V., 1980. Numerical Heat Transfer and Fluid Flow. McGraw-Hill Book Co., NY.

Penman, H. L., 1948. Natural evaporation from open water, bare soil and grass. Proc. Roy. Soc., **A 193**, 120-146.

Penman, H. L, 1955. Evaporation over parts of Europe. Pub. no.38.

Penman, H. L., 1956. Evaporation: an introductory survey. Neth. J. Agril. Sci., **4**, 9-29.

Penman, H. L., 1961. Weather, plant and soil factors in hydrology. Weather, **16**, 207-219.

Penman, H. L., 1967. Evaporation from forests: a comparison of theory and observation. In: Forest Hydrology (Eds: W. L. Sopper and H. W. Lull), Pergamon Press, 373-380.

Penman, H. L., and Long, I. F., 1960. Weather in wheat: an essay in micro-meteorology. Quart. J. Roy. Meteor. Soc., **86**(367), 16-50.

Petersen, R. G., and Calvin., L. D., 1964. Sampling. In: Methods of Soil Analysis, pt.1 (Ed. C. A. Black), 54-72.

Phien, H. N., Arbhabhirama, A., and Sunchindah, A., 1980. Rainfall distribution in northeastern Thailand. Hydrol. Sci. Bull., **25**(2/6), 167-182.

Philip, J. R., 1957. The theory of infiltration. 1. The infiltration equation and its solution. Soil Sci., **83**(5), 345-357.

Philip, J. R., 1957. Theory of infiltration: 4. Sorptivity and algebraic infiltration equations. Soil Sci., **84**(3), 257-264.

Philip, J. R., 1957. Evaporation, and moisture and heat fields in the soil. J. Meteor., **14**, 354-366.

Philip. J. R., 1964. Sources and transfer processes in air layers occupied by vegetation. J. Appl. Meteor., **3**, 390-395.

Philip, J. R., 1966. Plant water relations: some physical aspects. Annu. Rev. Plant Physiol., **17**, 245-268.

Philip, J. R., 1967. Sorption and infiltration in heterogeneous media. Australian J. Soil Res., **5**, 1-10.

Philip, J. R., 1969: Theory of infiltration. In: Advances in Hydroscince (Ed: V. T. Chow), **5**, 215-296.

Philip, J. R., and Knight, J. H., 1974. On solving unsaturated flow equation: 3. New quasi-analytical technique. Soil Sci., **117**(1), 1-13.

Pilgrim, D. H., 1966. Radio active tracing of storm runoff on a small catchment. J. Hydrol., **4**, 289-326.

Pinder, G. F., and Gray, W. G., 1977. Finite Element Simulation in Surface and Subsurface Hydrology. Academic Press.

Place, R. E., and Brown, D. M., 1987. Modelling corn yields from soil moisture estimates: description, sensitivity analysis and validation. Agril. Forest Meteor., **41**, 31-56.

Polubarinova-Kochina, P. Ya., 1962. Theory of Ground Water Movement (translated by J. M. R. De Wiest). Princeton University Press, Princeton, NJ.

Ponce, V. M., and Simons, D. B., 1977. Shallow wave propagation in open channel flow. J. Hydraul. Div., Proc. Amer. Soc. Civil Eng., **103**(HY2), 1461-1476.

Ponce, V. M., Li, R. M., and Simons, D. B., 1978. Applicability of kinematic and diffusion models. J. Hydraul. Div., Proc. Amer. Soc. Civil Eng., **104**(HY3), 353-360.

Ponce, V. M., and Theurer, F. D., 1982. Accuracy criteria in diffusion routing. J. Hydraul. Div., Proc. Amer. Soc. Civil Eng., **108**(HY6), 747-757.

Ponce, V. M., 1989. Engineering Hydrology: Principles and Practices. Prentice Hall, NJ, 640 p.

Prasad, R., 1967. A nonlinear hydrologic system response model. J. Hydraul. Div., Proc. Amer. Soc. Civil Eng., **93**(HY4), 201-221.

Price, R. K., 1974. Comparison of four numerical methods for flood routing. J. Hydraul. Div., Proc. Amer. Soc. Civil Eng., **100**(HY7), 879-899.

Pruitt, W. O., 1971. Factors affecting potential evapotranspiration. Biological Effects in the Hydrological Cycle, Proc. 3rd Inter. Seminar for Hydrol. Professors, 82-102.

Puri, A. N., Crowther, E. M., and Keen, B. A., 1925. The relation between the vapour pressure and water content of soils. J. Agril. Sci., **15**(1), 68-88.

Ragan, R. M., 1967. An experimental investigation of partial area contributions. Inter. Assoc. Sci. Hydrol., General assembly of Bern, Pub. No.76, 241-249.

Rawlins, S. L., Gardner, W. R., and Dalton, F. N., 1968. *In-situ* measurement of soil and plant leaf water potential. Soil Sci. Soc. Amer. Proc., **32**(4), 468-470.

Remson, I., Drake, R. L., McNeary, S. S., and Wallo, E. M., 1965. Vertical drainage of an unsaturated soil. J. Hydraul. Div., Proc. Amer. Soc. Civil Eng., **91**(HY1), 55-74.

Remson, I., Hornberger, G. M., and Molz, F. J., 1971. Numerical Methods in Subsurface Hydrology. John Wiley and Sons, NY.

Richard, L. A., 1931. Capillary conduction of liquids through porous mediums. Physics, **1**, 318-333.

Richardson, L. F., 1910. The approximate arithmetical solution by finite differences of physical problems involving differential equations, with an application to the stresses in a masonry dam. Phil. Trans. Roy. Soc. Series-A, **210**, 307-357.

Richtmyer, R. D., and Morton, K. W., 1967. Difference Methods for Initial-value Problems. 2nd edn., John Wiley & Sons, 450 p.

Rider, N. E., 1954. Eddy diffusion of momentum, water vapour, and heat near the ground. Phil. Trans. Roy. Soc. (London) Series-A, **246**, 481-501.

Rijtema, P. E., 1965. An analysis of actual evapotranspiration. Agric. Res. Rep. 659, Wageningen, The Netherlands, 107 p.

Ritchie, J. T., 1981. Water dynamics in the soil-plant-atmosphere system. Plant and Soil, **58**, 81-96.

Rogowski, A. S., 1971. Watershed physics: model of the soil moisture characteristic. Water Resour. Res., **7**(6), 1575-1582.

Rose, C. W., 1984. Modelling evapotranspiration: an approach to heterogeneous communities. In: Evapotranspiration from Plant Communities (Ed: M. L. Sharma), Elsevier Sci. Publishers, 203-221.

Rose, D. A., 1981. Gas exchange in leaves. In: Mathematics and Plant Physiology (Eds: D. A. Rose and D. A. Charles-Edwards), Academic Press, 67-78.

Rose, W. D., 1959. Calculations based on the Kozeny-Carman theory. J. Geophys. Res., **64**(1), 103-109.

Ross, G. A., 1970. The Stanford watershed model: the correlation of parameter values selected by a computerized procedure with measurable physical characteristics of the watershed. Res. Rept. No.35, Water Resour. Inst., Univ. of Kentucky, Lexington.

Rovey, C. E. K., 1975. Numerical model of flow in a stream-aquifer system. Hydrol. Pap. No.74, Fort Collins, Colorado, 73 p.

Rubin, J., and Steinhardt, R., 1963. Soil water relations during rain infiltration: I. Theory. Soil Sci. Soc. Amer. Proc., **27**(3), 246-251.

Rubin, J., 1967. Numerical method for analyzing hysteresis-affected post-infiltration redistribution of soil moisture. Soil Sci. Soc. Amer. Proc., **31**(1), 13-20.

Rubin, J., 1968. Theoretical analysis of two-dimensional transient flow of water in unsaturated and partly unsaturated soils. Soil Sci. Soc. Amer. Proc., **32**(5), 607-615.

Russell, G., 1980. Crop evaporation, surface resistance and soil water status. Agril. Meteor., **21**, 213-226.

Russo, D., and Bresler, E., 1980. Field determinations of soil hydraulic properties for statistical analyses. Soil Sci. Soc. Amer. J., **44**(4), 697-702.

Ryckborst, H., and Holecek, G. R., 1977. Spring Creek Groundwater Study. Unpublished Research Report, Alberta Environment, Edmonton.

Salter, P. J., and Williams, J. B., 1965. The influence of texture on the moisture characteristics of soils. I. A critical comparison of techniques for determining the available-water capacity and moisture characteristic curve of a soil. J. Soil Sci., **16**(1), 1-15.

Salter, P. J., and Williams, J. B., 1965. The influence of texture on the moisture characteristics of soils. II. Available-water capacity and moisture release characteristic. J. Soil Sci., **16**(2), 310-317.

Savage, J. M., Cass, A., and de Jager, J. M., 1983. Statistical assessment of some errors in thermocouple hygrometric water potential measurement. Agril. Meteor., **30**, 83-97.

Schaake, J. C., 1965. Synthesis of Inlet Hydrograph. Ph.D. dissertation, John Hopkins University.

Schaake, J. C., 1970. Modeling urban runoff as a deterministic process. In: Treatise on Urban Water Systems, Proc. Inst. Urban Water System, Fort Collins, Colorado.

Scheidegger, A. E., 1974. The Physics of Flow through Porous Media. 3rd edn., University of Toronto Press, 353 p.

Schermerhorn, V. P., and Kuehl, D. W., 1968. Operational streamflow forecasting with the SSARR model. Symp. on 'The use of analog and digital computers in hydrology', Tucson, Arizona, USA, Inter. Assoc. Sci. Hydrol./UNESCO Pub. No.80, 317-328.

Schulze, E.-D., 1986. Whole-plant responses to drought. Australian J. Plant Physiology, **13**, 127-141.

Schulze, E.-D., Turner, N. C., Gollan, T., and Shackel, K. A., 1987. Stomatal responses to air humidity and to soil drought. In: Stomatal Function (Eds: E. Zeiger, G. D. Farquhar and I. R. Cowan), Stanford University Press, Stanford, California, 311-321.

Scott, V. H., and Corey, A. T., 1961. Pressure distribution during steady flow in unsaturated sands. Soil Sci. Soc. Amer. Proc., **25**(4), 270-274.

Seginer, I., 1969. The effect of albedo on the evapotranspiration rate. Agril. Meteorol., **6**, 5-31.

Selim, H. M., Selim, M. S., Kirkham, D., 1975. Mathematical analysis of saturated flow through a multilayered soil with a sloping surface. Soil Sci. Soc. Amer. Proc., **39**(3), 445-453.

Selim, H. M., 1978. Transport of reactive solutes during transient, unsaturated water flow in multilayered soils. Soil Sci., **126**(3), 127-135.

Sharman, R. A., 1968. A Mathematical Simulation Model for Water Flow in Stream Catchments. Ph.D. thesis, Dept. of Geography, University of Wales, Aberystwth.

Sharon, D., 1970. Topography conditioned variations in rainfall as related to the runoff contributing area in a small watershed. Israel J. Earth Sci., **19**, 85-89.

Shaw, E. M., 1986. Hydrology in Practice. Nostrand Reinhold (U.K.) Co. Ltd.

Shaw, F. S., and Southwell, R. V., 1941. Relaxation methods applied to engineering problems. VII. Problems relating to the percolation of fluids through porous materials. Proc. Roy. Soc., Series-A, 178.

Shepherd, R. G., 1989. Correlation of permeability and grain size. Ground Water, **27**(5), 633-638.

Sherman, L. K., 1932. Streamflow from rainfall by the unit graph method. Eng. News Rec., **108**, 501-505.

Singh, V. P., 1989. Hydrologic Systems; Rainfall-Runoff Modeling, **1&2**. Prentice Hall, NJ.

Sklash, M. G., and Farvolden, R. N., 1979. The role of groundwater in storm runoff. J. Hydrol., **43**, 45-65.

Slatyer, R. O., 1956. Evapotranspiration in relation to soil moisture. Neth. J. Agril. Sci., **4**, 73-76.

Slatyer, R. O., and Gardner, W. R., 1965. Overall aspects of water movement in plants and soils. In: The State and Movement of Water in Living Organisms (Ed: G. E. Fogg), 19th Symp. Soc. Expt. Biol., Cambridge University Press, 113-129.

Smith, A. A., 1980. A generalized approach to kinematic flood routing. J. Hydrol., **45**, 71-89.

Smith, R. E., and Woolhiser, D. A., 1971. Mathematical Simulation of Infiltrating Watersheds. Hydrology Pap. No.47, Fort Collins, Colorado.

Smith, R. E., 1973. Comments on 'Modeling infiltration during a steady rain' by Russel G. Mein and Curtis L. Larson. Water Resour. Res., **9**(5), 1475-1477.

Smith, R. E., and Hebbert, R. N. B., 1983. Mathematical simulation of interdependent surface and subsurface hydrologic processes. Water Resour. Res., **19**(4), 987-1001.

Snyder, F. F., 1938. Synthetic unit-hydrographs. Trans. Amer. Geophys. Union, **19**(1), 447-454.

Snyder, W. M., Stall, J. B., 1965. Men, models, methods and machines in hydrologic analysis. J. Hydraul. Div., Proc. Amer. Soc. Civil Eng., **91**(HY2), 85-99.

Staple, W. J., 1965. Moisture tension, diffusivity, and conductivity of a loam soil during wetting and drying. Can. J. Soil Sci., **45**(1), 78-86.

Staple, W. J., 1966. Infiltration and redistribution of water in vertical columns of loam soil. Soil Sci. Soc. Amer. Proc., **30**(5), 553-558.

Staple, W. J., 1969. Comparison of computed and measured moisture redistribution following infiltration. Soil Sci. Soc. Amer. Proc., **33**(6), 840-847.

Staple, W. J., 1971. Boundary conditions and conductivities used in isothermal model of evaporation from soil. Soil Sci. Soc. Amer. Proc., **35**(6), 853-855.

Staple, W. J., 1974. Modified Penman equation to provide the upper boundary condition in computing evaporation from soil. Soil Sci. Soc. Amer. Proc., **38**(5), 837-839.

Steffler, P. M., 1989. Introduction to Computational Fluid Dynamics. Unpublished Lecture Notes, Department of Civil Engineering, University of Alberta.

Stegman, E. C., 1983. Irrigation scheduling: applied timing criteria. In: Advances in Irrigation (Ed: D. Hillel), **2**, 1-59.

Stephenson, G. R., and Freeze, R. A., 1974. Mathematical simulation of subsurface flow contributions to snowmelt runoff, Reynolds Creek Watershed, Idaho. Water Resour. Res., **10**(2), 284-298.

Stewart, J. B., 1983. A discussion of the relationships between the principal forms of the combination equation for estimating crop evaporation. Agril. Meteor., **30**, 111-127.

Stewart, J. B., 1984. Measurements and prediction of evaporation from forested and agricultural catchments. In: Evapotranspiration from Plant Communities (Ed: M. L. Sharma), Elsevier Sci. Publishers, 1-28.

Stewart, J. B., 1989. On the use of Penman-Monteith equation for determining areal evapotranspiration. In: Estimation of Areal Evapotranspiration (Eds: T. A. Black, D. L. Spittlehouse, M. D. Novak and D. T. Price), Inter. Assoc. Hydro. Sci., Pub. No.177, 3-12.

Stoertz, W., and Bradbury, R., 1989. Mapping recharge area using groundwater flow model - A Case Study. Ground Water, **27**(2), 220-228.

Stoker, J. J., 1957. Water Waves. Interscience Press.

Storm, B., 1988. The state of the art in modelling components of the hydrological cycle: saturated flow. NATO ASI Lecture Series, July 11-21, Sintra, Portugal.

Strelkoff, T., 1969. One-dimensional equations of open-channel flow. J. Hydraul. Div., Proc. Amer. Soc. Civil Eng., **95**(HY3), 861-876.

Strelkoff, T., 1970. Numerical solution of Saint-Venant equation. J. Hydraul. Div., Proc. Amer. Soc. Civil Eng., **96**(HY1), 223-252.

Su, C., and Brooks, R. H., 1975. Soil hydraulic properties from infiltration tests. Watershed Management Proceedings, Irrig. Drain. Div., Amer. Soc. Civil Eng., Logan, Utah, Aug. 11-17, 516-542.

Sugawara, M., 1970. Difficult problems about small experimental basins and the necessity of collecting information on large basins. Inter. Assoc. Sci. Hydrol., Pub. No.96, 393.

Surkan, A. J., 1974. Simulation of storm velocity effects on flow from distributed channel networks. Water Resour. Res., **10**(6), 1149-1160.

Taigbenu, A. E., and Liggett, J. A., 1985. Boundary element calculations of diffusion equation. J. Eng. Mech., Amer. Soc. Civil Eng., **111**(EM2), 311-328.

Tanner, C. B., 1968. Evaporation of water from plants and soil. In: Water Deficit and Plant Growth (Ed: T. T. Kozlowski), **1**, Academic Press, NY, 73-106.

Taylor, G. S., and Luthin, J. N., 1969. Computer methods for transient analysis of water table aquifers. Water Resour. Res., **5**(1), 144-152.

Taylor, A. B., and Schwarz, H. E., 1952. Unit-hydrograph lag and peak flow related to basin characteristics. Trans. Amer. Geophys. Union, **33**(2), 235-246.

Tenhunen, J. D., Pearcy, R. W., and Lange, O. L., 1987. Diurnal variations in leaf conductance and gas exchange in natural environments. In: Stomatal Function (Eds: E. Zeiger, G. D. Farquhar and I. R. Cowan), Stanford University Press, Stanford, California, 323-351.

Tennesse Valley Authority, 1965. Area-stream factor correlation: a pilot study in the Elk River Basin. Inter. Assoc. Hydrol. Bull., **10**(2), 22-37.

Terzaghi, C., 1925. Eng. News Rec., 832 p.

Thom, A. S., 1972. Momentum, mass and heat exchange of vegetation. Quart. J. Roy. Meteorol. Soc., **98**(415), 124-134.

Thom, A. S., and Oliver, H. R., 1977. On Penman's equation for estimating regional evaporation. Quart. J. Roy. Meteor. Soc., **103**(436), 345-357.

Thornthwaite, C. W., 1948. An approach toward a rational classification of climate. Geog. Rev., **38**, 55-94.

Thornthwaite, C. W., and Mather, J. R., 1955a. The water budget and its use in irrigation. In: Water, U.S. Dept. Agril. Yearbook, 346-357.

Thornthwaite, C. W., and Mather, J. R., 1955b. The water balance. Pub. in Climatology, **8**, 1-104.

To'th, J., 1963. A theoretical analysis of groundwater flow in small drainage basins. J. Geophys. Res., **68**(16), 4795-4812.

Turner, N. C., Schulze, E.-D., Gollan, T., 1984. The responses of stomata and leaf gas exchange to vapour pressure deficits and soil water content. I. Species comparisons at high soil water contents. Oecologia (Berlin), **63**, 338-342.

U.S. Army Corps of Engineers, 1972. Program Description and User's Mannual for SSARR. Program 724-K5-G0010.

van Bavel, C. H. M., 1966. Potential evaporation: the combination concept and its experimental verification. Water Resour. Res., **2**(3), 455-467.

van Bavel, C. H. M., Stirk, G. B., and Brust, K. J., 1968a. Hydraulic properties of clay loam and the field measurement of water uptake by roots: I. Interpretation of water content and pressure profiles. Soil Sci. Soc. Amer. Proc., **32**(3), 310-317.

van Bavel, C. H. M., Brust, K. J., and Stirk, G. B., 1968b. Hydraulic properties of clay loam and the field measurement of water uptake by roots: II. The water balance of the root zone. Soil Sci. Soc. Amer. Proc., **32**(3), 317-321.

van Genuchten, M. T., and Nielsen, D. R., 1985. On describing and predicting the hydraulic properties of unsaturated soils. Ann. Geophys., **3**(5), 615-628.

van Schielfgaarde, J., 1963. Design of tile drainage for falling water tables. J. Irrig. Drain. Div., Proc. Amer. Soc. Civil Eng., **89**(IR2), 1-11.

van Schielfgaarde, J., 1965. Limitations of Dupuit-Forhheimer theory in drainage. Trans. Amer. Soc. Agril. Eng., **8**(4), 515-516, 519.

van't Woudt, B. D., 1954. On factors governing subsurface storm flow in volcanic ash soils, New Zealand. Trans. Amer. Geophys. Union, **35**(1), 136-144.

van Zyl, W. H., and de Jager, J. M., 1987. Accuracy of the Penman-Monteith equation adjusted for atmospheric stability. Agril. Forest Meteor., **41**, 57-64.

Vauclin, M., Vachaud, G., and Khanji, J., 1975. Two dimensional numerical analysis of transient water transfer in saturated-unsaturated soils. In: Computer Simulation of Water Resources Systems (Ed: G. C. Vansteenkiste), North Holland Publishing Company, Amsterdam, 299-323.

Vemuri, V., and Vemuri, N., 1970. On the systems approach in hydrology. Inter. Assoc. Sci. Hydrol. Bull., **15**(2), 17-38.

Verma, R. D., and Brutsaert, W., 1970. Unconfined aquifer seepage by capillary flow theory. J. Hydraul. Div., Proc. Amer. Soc. Civil Eng., **96**(HY6), 1331-1334.

Verma, R. D., and Brutsaert, W., 1971. Similitude criteria for flow from unconfined aquifers. J. Hydraul. Div., Proc. Amer. Soc. Civil Eng., **97**(HY9), 1493-1509.

Verruijt, A., 1970. Theory of Groundwater Flow. McMillan and Co. Ltd., London, 190 p.

Viessman, W., Knapp, J. W., Lewis, G. L., and Harbough, T. E., 1988. Introduction to Hydrology, 2nd edn., Harper and Rowe, NY.

von Neuman, J., and Goldstein, H. H., 1947. Numerical inverting of matrices of higher order. Bull. Amer. Math. Soc., **53**, 1021-1099.

Wang, F. C., and Lakshminarayana, V., 1968. Mathematical simulation of water movement through unsaturated nonhomogeneous soils. Soil Sci. Soc. Amer. Proc., **32**(3), 329-334.

Wartena, L., 1974. Basic difficulties in predicting evaporation. J. Hydrol., **23**, 159-177.

Watson, K. K., 1965. Infiltration: the physical process. Hydrology Symposium, Pap. No. 2000, Melbourne, Australia.

Watson, K. K., 1971. Numerical analysis of finite depth problems in soil-water hydrology. Nordic Hydrol., **11**, 1-22.

Weatherley, P. E., 1965. The state and movement of water in the leaf. In: The State and Movement of Water in Living Organisms (Ed: G. E. Fogg), 19th Symp. Soc. Expt. Biol., Cambridge University Press, 157-184.

Webb, E. K., 1975. Evaporation from catchments. In: Predictions in Catchment Hydrology (Eds: T. G. Chapman and F. X. Dunin), Aust. Academy of Sci., Canberra, 203-236.

Webb, E. K., Pearman, G. I., and Leuning, R., 1980. Correction of flux measurements for density effect due to heat and water vapour transfer. Quart. J. Roy. Meteor. Soc., **106**, 85-100.

Weinmann, P. E., and Laurenson, E. M., 1979. Approximate flood routing methods: a review. J. Hydraul. Div., Proc. Amer. Soc. Civil Eng., **105**(HY12), 1521-1536.

Werner, P. W., 1957. Some problems in non-artesian groundwater flow. Trans. Amer. Geophys. Union, **38**(4), 511-518.

Wesseling, J., 1972. Subsurface flow into drains. In: Theories of Field Drainage and Watershed Runoff, **16**, Inter. Inst. Land. Water Management Res., Wageningen, The Netherlands, 1-56.

Wesseling, J., 1974. Hydraulic conductivity of natural Pachappa soil columns. Soil Sci., **118**(1), 6-10.

Weyman, D. R., 1971. Surface and subsurface runoff in small basin. Ph.D. thesis, Dept. of Geography, University of Bristol.

Weyman, D. R., 1973. Measurements of the downslope flow of water in a soil. J. Hydrol., **20**, 267-288.

Whipkey, R. Z., 1969. Storm runoff from forested catchments by subsurface routes. In. Floods and their computations, Inter. Assoc. Sci. Hydrol., Pub. No.85, **2**, 773-779.

Whisler, F. D., and Klute, A., 1967. Rainfall infiltration into a vertical soil column. Trans. Amer. Soc. Agril. Eng., **10**(3), 391-395.

Whisler, F, D., Watson, K. K., and Perrens, S. J., 1972. The numerical analysis of infiltration into heterogeneous porous media. Soil Sci. Soc. Amer. Proc., **36**(6), 868-874.

Wiggert, D. C., and Wylie, E. B., 1976. Numerical predictions of two-dimensional transient groundwater flow by the method of characteristics. Water Resour. Res., **12**(5), 971-977.

Williams, T. A., and Williamson, A. K., 1989. Estimating water table altitudes for regional groundwater flow modeling, U.S. Gulf Coast. Ground Water, **27**(3), 333-340.

Wilson, B. N., and Ruffini, J. R., 1988. Comparison of physically-based Muskingum methods. Trans. Amer. Soc. Agril. Eng., **31**(1), 91-97.

Wilson, J. D., 1989. Turbulent transport within the plant canopy. In: Estimation of Areal Evapotranspiration (Eds: T. A. Black, D. L. Spittlehouse, M. D. Novak and D. T. Price), Inter. Assoc. Hydro. Sci., Pub. No.177, 43-80.

Wilson, T. V., and Ligon, J. T., 1973. The interflow process on sloping watershed areas. Water Resour. Res. Inst., Clemson University, South Carolina, Rept. No.38.

Wolfram, S., 1988. Mathematica: a System for Doing Mathematics by Computer. Addison-Wesley Publishing Company, Inc.

Wood, N. L. H., 1977. A field study on the representativeness of turbulent fluxes of heat and water vapour at various sites in southern England. Quart. J. Roy. Meteor. Soc., **103**(438), 617-624.

Wooding, R. A., 1966. Groundwater flow over a sloping impermeable layer. 2. Exact solutions by conformal mapping. J. Geophys. Res., **71**(12), 2903-2910.

Wooding, R. A., and Chapman, T. G., 1966. Groundwater flow over a sloping impermeable layer. 1. Application of the Dupuit-Forhheimer assumption. J. Geophys. Res., **71**(12), 2895-2902.

Woolhiser, D. A., and Liggett, J. A., 1967. Unsteady, one-dimensional flow over a plane - the rising hydrograph. Water Resour. Res., **3**(3), 753-771.

Yen. B. C., 1973b. Open-channel flow equations revisited. J. Eng. Mech. Div., Proc. Amer. Soc. Civil Eng., **99**(EM5), 979-1009.

Yen, B. C., and Akan, A. O., 1976. Flood routing through river junctions. Rivers'76, **1**, 212-231.

Yen, B. C., 1982. Some measures for evaluation and comparison of simulation models. In: Urban Stormwater Hydraulics and Hydrology (Ed: B. C. Yen), Water Resour. Pub., Littleton, Colorado, 341-349.

Yevjevich, V., and Barnes, A. H., 1970. Flood routing through storm drains. Hydrol. Pap. No.43 to 46, Fort Collins, Colorado.

Youngs, E. G., 1965. Water movement in soils. In: The State and Movement of Water in Living Organisms (Ed: G. E. Fogg), 19th Symp. Soc. Expt. Biol., Cambridge University Press, 89-112.

Youngs, E. G., 1968. Horizontal seepage through unconfined aquifers taking into account flow in the capillary fringe. In: Water in the Unsaturated Zone; Effect of Capillary Fringe on Groundwater Flow (Eds: P.E. Rijtema and H. Wassink), Symp. Proc., **2**, IASH-Unesco, 897-905.

Youngs, E. G., and Aggelides, S., 1976. Drainage to a water table analysed by the Green-Ampt approach. J. Hydrol., **31**, 67-79.

Zaslavsky, D., and Sinai, G., 1981. Surface hydrology: 5 parts. J. Hydraul. Div., Proc. Amer. Soc. Civil Eng., **107**(HY1), 1-93.

Zimmermann, M. H., 1965. Water movement in stems of tall plants. In: The State and Movement of Water in Living Organisms (Ed: G. E. Fogg), 19th Symp. Soc. Expt. Biol., Cambridge University Press, 151-155.

Zunker, F., 1933. Trans. 6th Com. Inter. Soc. Soil Sci.B, 18.